1974

The Petrology, Geochemistry And Genesis Of Sulphide-related Alteration At The Temagami Mine, Ontario

Alexander Combe Colvine

THE PETROLOGY, GEOCHEMISTRY AND GENESIS OF SULPHIDE-RELATED ALTERATION AT THE TEMAGAMI MINE, ONTARIO

by

Alexander Combe Colvine

Department of Geology

Submitted in partial fulfillment

of the requirements for the degree of

Doctor of Philosophy

Faculty of Graduate Studies

The University of Western Ontario

London, Ontario

June, 1974

ABSTRACT

The Temagami Mine occurs within a sequence of metamorphosed volcanic rocks of Archean age. Two distinct parallel zones of sulphide concentration are present: a stratiform, massive to disseminated pyritic zone of wide lateral extent, and a less extensive planar zone containing over 40 discrete lenses of massive chalcopyrite and pyrite; only the latter concentration has been economically extracted. The orebodies lie approximately 200' stratigraphically below the pyritic zone which lies at the top of the intermediate-felsic portion of the volcanic pile and beneath a thick doleritic unit.

The purpose of this study is to interpret the cause of sulphide localization and concentration and the relationship between the two sulphide zones. The study was concerned largely with the petrography and chemistry of the volcanic rocks in an attempt to define alteration associated with sulphide concentration.

Sixty samples of the volcanic rocks outside the mine were studied and shown to form a well defined differentiation trend; these results were used as a standard in the study of the mine rocks. In addition the study showed that the volcanic rocks have undergone extensive hydration, carbonatization, albitization and chemical redistribution which may be indicative of burial metamorphism, in the presence of a mobile hydrous

phase, shortly following their deposition and prior to more uniform regional metamorphism to greenschist facies assemblage.

One hundred and ten samples were chosen for similar study of the volcanic sequence from drill core cross-sections through two orebodies, including the pyritic zone and the base of the dolerite. Two orebody types are represented: the "pod-type" which occurs within a rhyodacitic-rhyolitic unit, and the "vein-type" at the contact between an underlying breccia and an overlying massive dacitic unit.

The rocks around the pod-type orebody are significantly enriched in FeO, Cu, Pb, Zn, Co, Ni, Ba and B and depleted in CaO, Na_2O and CO_2 which is reflected in the quartz-sericite-tourmaline-sulphide mineral assemblage. The alteration zone transects the volcanic units and widens towards the base of the pyritic zone but does not continue into the overlying dolerite. MgO, FeO and Fe_2O_3 contents increase towards the pyritic zone, as reflected in the increasing chlorite content of the volcanic rocks and in the chloritic matrix of the pyritic zone.

The alteration zone is interpreted as one of several channelways of hydrothermal fluid ascent. Discharge of the hydrothermal fluid on the sea floor resulted in deposition of the pyritic zone, while the pod-type orebodies were formed as subsurface cavity fillings during cooling of the fluid along the ascent channelways. The vein-type orebodies, which are not associated with zones of intense alteration, were deposited from more dispersed ascending fluid delayed at the base of the less permeable dacitic unit. Deposition or emplacement of the dolerite above the pyritic zone during renewed volcanic activity caused melting and remobilization of the pyritic zone.

The hydrothermal fluid was probably derived from both magmatic and sea-connate water sources. A model of convective sea water circulation is proposed, in which metals are concentrated by leaching of the volcanic rocks, consistent with the observed alteration within both the mine and the surrounding volcanic rocks.

The exact form and composition of the sulphide concentrations are the result of interaction of several factors, including volcanic rock composition, extent, intensity and composition of hydrothermal activity and localized structural and permeability conditions.

ACKNOWLEDGEMENTS

The writer wishes to express his sincere gratitude to all those involved in the preparation of this thesis, and particularly to the members of his advisory committee, Dr. R. W. Hutchinson, Dr. N. D. MacRae and Dr. A. Dreimanis. Special thanks go to Dr. Hutchinson whose interest in massive sulphide deposits led to this study and to Dr. MacRae for extensive discussion and editing work during Dr. Hutchinson's absence on sabbatical leave. Dr. A. D. Edgar also acted as advisor during Dr. Hutchinson's absence and Dr. G. G. Suffel reviewed and critically edited the thesis. Dr. W. S. Fyfe and Dr. R. W. Hodder also assisted with constructive criticism.

The writer wishes to acknowledge the co-operation of the Teck Mining Group, in all stages of this thesis, and specifically the assistance of several of its personnel. Mr. H. Jones provided liaison with the company and also many hours of fruitful discussion. During two field seasons Mr. R. J. Graham added greatly to the writer's knowledge of the area. All of the staff at the mine were most helpful, particularly mine geologist Mr. A. Amos.

Whole rock analyses were performed by Mr. K. Ramlal of the University of Manitoba and by the Mineral Research Branch of the Ontario

Division of Mines. Sulphur isotope analyses were provided by Dr. H. Schwarcz of McMaster University. Microprobe analyses were performed by Mr. R. L. Barnett and some x-ray diffraction work by Miss Y. C. Cheng, both of the University of Western Ontario. Ms. S. Watt typed all drafts of the thesis.

Extensive financial assistance for analytical work was provided by the Teck Mining Group for which the writer is most grateful. Additional financial assistance was provided in the form of research assistantships from funds made available to Dr. R. W. Hutchinson and Dr. N. D. MacRae by the National Research Council of Canada. Receipt of Province of Ontario Graduate Fellowships for the years 1970-1971 and 1972-1973 is gratefully acknowledged.

TABLE OF CONTENTS

LIST OF PHOTOGRAPHIC PLATES

Plate		Page
13	Dacitic breccia. Large andesitic fragments in dacitic matrix. Approximately 600' stratigraphically below the No. 4 orebody.	135

LIST OF TABLES

LIST OF FIGURES

LIST OF APPENDIX FIGURES

CHAPTER I

INTRODUCTION

The Temagami Mine lies within the intermediate-felsic portion of metamorphosed volcanic and pyroclastic rocks of Archean age. The geology has been documented and genesis proposed for numerous massive sulphide deposits associated with volcanic rocks of similar age. The geology of the Temagami Mine is significantly different in several respects from that described as "typical" for such deposits. Firstly, two distinct zones of sulphide concentrations are present closely related spatially but somewhat different in form and mineral content. In previous studies of specific aspects of the mine one or both of these zones have been considered genetically related to an overlying mafic sill and not to the volcanic rocks. Secondly, one sulphide zone consists, not of a single unit, but of over forty lenses of massive, chalcopyritic sulphide. Thirdly, some of the lenses are associated with tourmaline mineralization, more typical of alteration associated with porphyry deposits, and not the chloritic alteration of massive sulphide deposits. Fourthly, the dominant sulphide mineral assemblage is chalcopyrite-pyrite. Zinc is present but its content is significantly lower than normal for massive sulphide deposits of felsic volcanic association. Although the nickel content is minor it is significantly higher than normal for these deposits.

The purpose of this study is to investigate the nature of the ore-

bodies at the Temagami Mine - specifically their relationships with their host rocks - and to interpret the cause of sulphide localization and concentration. As part of this study it is necessary to explain the differences between this deposit and others of similar association.

The approach to the study was principally through a detailed geochemical and petrographic investigation of the nature of wallrock alteration associated with the concentrations of sulphide. The aspects of the geology which appear to be most significant and which were investigated in greatest detail are the nature of the volcanic activity within the Temagami greenstone belt and the conditions under which it took place. In addition, the processes of synvolcanic alteration are important, but evidence for this must be distinguished from the effects of subsequent regional metamorphism. These results were then used in the detailed study of the rocks near the sulphide zones thereby allowing the definition of the effects of alteration present here.

Discussion and interpretation of the immediate cause of sulphide localization and concentration is largely substantiated by the evidence presented. A discussion is also included of the implications of this study in the broader context of mineral deposits geology, specifically the relationship between sulphide mineral deposits and volcanic activity. Although interpretations in this section are largely speculative, their consideration is necessary if such studies are to go beyond detailed description of specific deposits and contribute to a more general understanding of the processes and implications of metallogenesis.

The writer's experience in the local geology proved most useful in all stages of the study, particularly in the formulation and the assessment of the feasibility of the proposed models. This experience

was gained over a ten month period, including two field seasons, working both within the greenstone belt and the mine.

CHAPTER II

GENERAL GEOLOGY OF THE TEMAGAMI AREA, AND MINE

A. Regional Geology

The Archean metamorphosed volcanic and sedimentary rocks of the Temagami greenstone belt and the granites that intrude them are exposed in an erosional window through the overlying Huronian sedimentary sequences. The belt was mapped by Moorhouse (1942), and sections of it by Grant (1964), Simony (1964) and Bennett (1970, 1971). The following description is based largely on these reports and on additional observations made during the writer's mapping of parts of this area.

All of the Archean rocks of the Temagami greenstone belt have been metamorphosed to greenschist facies mineralogy and for the most part would be classified as chlorite, sericite schists. To avoid confusion, igneous terminology consistent with government and mine reports will be used. Qualification of this nomenclature will follow in subsequent chapters.

1. Archean

The Archean rocks of the Temagami area fall into three groups (Table 1): firstly, the metamorphosed volcanic and sedimentary sequences of the greenstone belt, secondly, a variety of intrusions which appear to have undergone the same metamorphism as the rocks of the previous group,

TABLE 1

TABLE OF FORMATIONS

PHANEROZOIC

RECENT: swamp, lake, and stream deposits

PLEISTOCENE: glacial and glaciofluvial deposits

———————————unconformity———————————

PROTEROZOIC

olivine diabase dykes (Sudbury type)

———————————intrusive contact———————————

quartz diabase sills and dykes, granophyre (Nipissing type)

———————————intrusive contact———————————

HURONIAN:

COBALT GROUP: Lorrain formation: feldspathic quartzite, arkose
Gowganda formation: argillite, slate, greywacke, breccia, conglomerate, quartzite

———————————unconformity———————————

ARCHEAN

lamprophyres, amphibolite, carbonate, diorite, greenstone dykes

———————————intrusive contact———————————

quartz porphyry, feldspar porphyry, felsite dykes, granite, granodiorite, albite granite, aplite dykes (Algoman type)

———————————intrusive contact———————————

diorite, quartz diorite

———————————intrusive contact———————————

diorite, quartz diorite, peridotite

———————————intrusive contact———————————

GREENSTONE SEQUENCE: (Keewatin type)

metasedimentary rocks: lithic greywacke, siltstone, slate, tuffaceous sandstone

iron formation: banded silicate-oxide facies, sulphide facies.

mafic and intermediate lavas: massive, pillowed, amygdaloidal, pyroclastic tuff and metamorphosed equivalents

felsic lavas: quartz and feldspar porphyry, tuff, agglomerate, breccia, rhyolite, rhyodacite, dacite

and thirdly, the large batholiths and associated smaller intrusions emplaced during the Kenoran Orogeny.

Greenstone sequence

The Temagami greenstone belt is in the shape of a 'Y' opening westwards and has been folded synclinally about the axis of the 'Y' (Fig. 1). A complete differentiation sequence from basalt to rhyolite is found in the volcanic rocks of the area, although the two end members are scarce. Pyroclastic rocks are common throughout. The field evidence for distinction between felsic and mafic-intermediate categories is tenuous, the dominant rock types being dacite and andesite.

Felsic volcanic rocks are exposed along the south shore of the Northeast Arm of Lake Temagami, and over large areas of Chambers and Strathy townships (Fig. 1). Considerable textural and compositional variations are present, and no single unit is mappable for long distances along strike before grading, lensing or changing abruptly into a different unit.

Mafic-intermediate volcanic rocks are also varied in composition but form larger and more consistently mappable units. Most of their exposures are of a uniform, dark grey, fine grained andesite. Considerable recrystallization of the andesites has taken place around the granite intrusion of Strathy township. Small occurrences of basalt are found in the southwestern and northern portions of the area.

All these rocks are now schistose, with chlorite and sericite developed in them, and fracturing is common. A detailed petrographic description follows in Chapter III.

Iron formations, found on both north and south limbs of the syncline

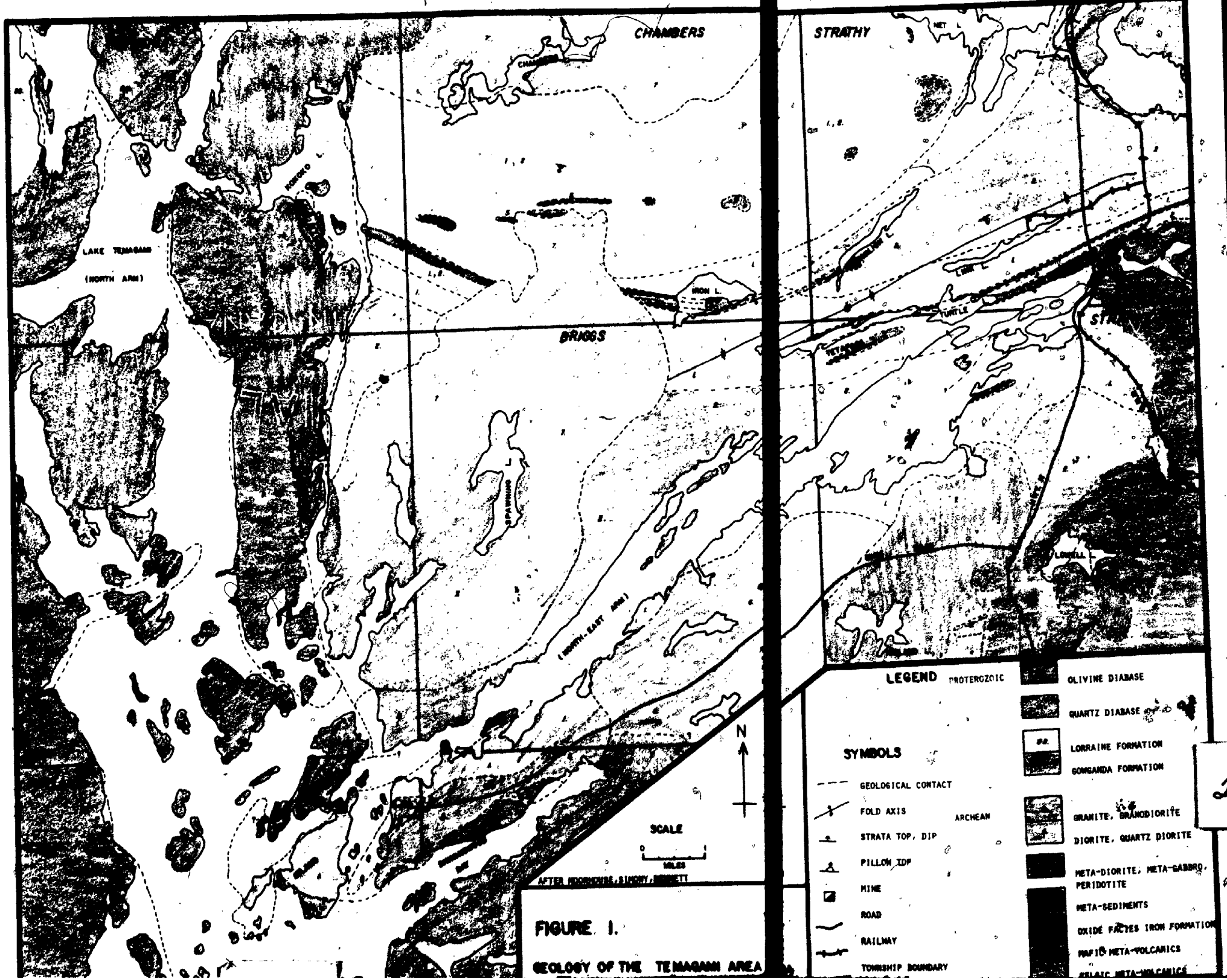

FIGURE 1.

GEOLOGY OF THE TEMAGAMI AREA

Boyum and Hartviksen, 1970), are the only continuous stratigraphic horizon markers. They range in thickness from five feet to over six hundred feet consisting of alternating bands of magnetite and sugary white quartz, jasper or grey cherty quartz, jasper being most abundant in the western Kokoko section. "Chloritic and tremolitic tuff" (Moorhouse, 1942, p. 9) is also associated with the iron formation. The variation in silicate mineralogy appears to be a result of both primary facies change along strike and change in degree of metamorphism. Fracturing and minor faulting cut the thinly bedded iron formation. The iron formation is mined by open pit method on both north and south limbs, south of Iron Lake and west of Turtle Lake, at the Sherman Mine.

Thin bands of metasedimentary rocks have been mapped by Bennett (1970, 1971) close to - both above and below - both iron formations, but these have not been described in detail.

Pre-Kenoran intrusions

The pre-Kenoran intrusions include diorites, gabbros and peridotites. They are grouped together here due to their common highly altered and deformed nature and their intrusive relationships.

The "metadiorite", locally important at the Temagami Mine, extends up the length of the Northeast Arm of Lake Temagami and is the largest of these bodies. A series of diorites, gabbros and peridotites occur in the northern section (Fig. 1). Ultramafic lenses are found on the margins of two intrusions and appear to be formed by differentiation from a gabbroic source. Some of the diorites mapped by Bennett (1971) in this northern section are fresh hornblende, plagioclase diorites and probably belong in the next group.

Kenoran intrusions

This group includes all intrusions which do not appear to have undergone significant metamorphism and do not cut the Huronian sedimentary rocks.

A large mass of quartz diorite is exposed south of the Northeast Arm of Lake Temagami. It is composed of plagioclase, interstitial quartz, biotite, hornblende and chlorite. Sections are sheared and cut by quartz veins.

Three large granitic stocks of Algoman type are present at Chambers, Spawning and Iceland lakes (Fig. 1). The Chambers Lake stock is coarse, equigranular pink granite with euhedral plagioclase, anhedral microcline, perthite, quartz and biotite. A recrystallization halo in the intruded volcanic rocks is more evident around this stock than the other two. The Spawning Lake stock is a massive, fresh, porphyritic granite with large oligoclase phenocrysts and matrix similar to the Chambers Lake stock.

The Iceland Lake intrusion is white or greenish-pink granite and is more albitic and chloritic than the other two intrusions. Gneissosity and schistosity are locally developed. Sections of this body, its satellitic bodies and the small body to the east of Temagami Island are fine grained with small feldspar and/or quartz phenocrysts and resemble the surrounding volcanic rocks in mineralogy and apparent grade of metamorphism. All of the Iceland Lake intrusion has been mapped as Algoman-type granite (Moorhouse, 1942), but the above evidence suggests that parts of it are synvolcanic hypabyssal intrusions.

Numerous felsite dykes are found throughout the area and appear to be related to the granitic intrusions.

The various mafic dykes (Table 1) are grouped together because they clearly post-date the granite, but predate the Huronian sedimentary rocks.

2. Proterozoic

Huronian

The erosional unconformity between the Archean rocks and the overlying Huronian sedimentary rocks is well exposed around Temagami Island (Fig. 1). The erosional surface appears to have had considerably relief at the time of Huronian sedimentation. Where the basal Gowganda conglomerate overlies volcanic agglomerate, the two appear almost identical in structure and composition, except for occasional granodioritic fragments in the Gowganda. The Lorrain Formation has a transitional conformable contact with the Gowganda Formation (Simony, 1964).

Quartz diabase

The coarse- to fine-grained diabase bodies consist of andesine-labradorite and albite plagioclase, quartz, pyroxene altered to uralitic hornblende and chlorite, with pyrite, magnetite, leucoxene and apatite. Where exposed cuttings the Archean, they are dyke-like with moderate to steep dips. Within the Cobalt Group sedimentary rocks, they are generally conformable and therefore basin shaped. It has, however, been suggested that some may be cone-shaped ring intrusions (Lovell, 1970).

Olivine diabase

Fresh olivine, labradorite, augite diabases intrude all consolidated formations in the Temagami area. There is a wide range of possible ages for these intrusions and they have been equated both with the "Sudbury type" (Fahrig et al., 1965; Gates and Hurley, 1973) and with the younger

"Keweenawan type" (Moorhouse, 1942; Simony, 1964).

3. Phanerozoic

The area has an extensive cover of Pleistocene glacial drift, including eskers which were deposited by southward moving glaciers (Simony, 1964). Much of this material has been re-worked by recent lake and stream action to form beach and gravel deposits.

4. Structure

Folding

The major folding of the Archean rocks is represented by the syncline whose axis passes through Link and Tetapaga lakes approximately parallel to the Northeast Arm and is truncated by the Spawning Lake granite (Fig. 1). The numerous evidences of this major structure include graded bedding in tuffaceous bands within the iron formation, minor drag folds, pillow-indicated tops and fragments of iron formation in overlying units (Moorhouse, 1942). There appears to be no additional folding affecting only the Archean rocks, but the lack of mappable stratigraphic horizons makes it impossible to determine this with certainty.

The Cobalt Group rocks are folded into a series of broad, open anticlines and synclines, plunging at 5° to the north and dipping at an average of 20°.

Faulting, fracturing and shearing

The major fault-shear zone in the area follows the Northeast Arm of Lake Temagami from Temagami Townsite to, but not into, Temagami Island. The shear zone consists of highly deformed schists commonly carbonatised, and is up to half a mile in width. Moorhouse (1942) notes a complimentary zone of shearing and tension fracturing striking at

300°-310°. Numerous smaller shear zones are present, commonly trending parallel to the major zone. The felsic portions of the greenstone rocks in particular are highly jointed and, in areas where offset can be measured, faulting is common.

The northeast trending Grenville Front is about ten miles southeast of Temagami Mine (Johnston, 1954), where the sharp contact between the Cobalt Group and the Grenville high-grade metamorphic rocks has been mapped in detail by Grant (1964).

5. Economic Geology

The only currently producing mine of the area is Sherman Iron Mine. In addition, there are numerous mineralized showings which have undergone varying degrees of development and production. Nickel-copper-platinum group showings have been found associated with the meta-intrusive rocks of central Strathy township, the largest being the Cuniptau property in a small lens of peridotite on the margin of a meta-diorite. A showing of molybdenite-chalcopyrite in quartz-carbonate veins occurs within mafic volcanic rocks near Goward. Many gold showings are present throughout the area, either closely associated with iron formation or in quartz-carbonate veins within volcanic rocks.

B. General Geology of the Temagami Mine

The first orebody at the Temagami Mine of the Copperfields Mining Corporation was discovered in 1954 by diamond drilling that followed self potential and resistivity geophysical surveys (Bergey et al., 1957). Outcroppings of a pyritic zone had been noted by Miller and Hoffman in 1901 and by Moorhouse in 1942 in the central part of Temagami Island. Investigation of this pyritic zone led to the discovery of a second

zone of chalcopyrite-rich sulphides stratigraphically below and paralleling the pyritic zone. This second sulphide zone constitutes the mined ore zone, which until the mine's closure in 1972, produced more than 800,000 tons of ore containing over 6% copper.

Figure 2 shows the surface geology near the Temagami Mine. The deposit lies near the top of the northward-dipping sequence of felsic volcanic rocks which forms the southern half of Temagami Island. Overlying the volcanic pile is a metadiorite sill with the pyritic sulphide zone at its base. The sill is in turn unconformably overlain by Gowganda conglomerate to the north, such that its north (i.e. top) contact is not exposed. The faulting is complex and difficult to define except where displacement of the pyritic zone can be measured. Additional faulting close to, or paralleling, the plane of the stratigraphy has been shown by underground mapping.

Figure 3 is a typical section through the mine showing the relative position of the chalcopyrite orebodies, lying from 50 to 300 feet stratigraphically below the pyritic zone. Over forty small, separate, lenticular chalcopyritic orebodies have been mined, the majority lying at, or close to, the contact between the rhyolite and the rhyolite breccia. In the eastern part of the mine the underlying rhyolite fragmental (Fig. 3) is thicker and is closer to, or in contact with, the pyritic zone. The orebodies lie within it at 200 feet from the base of the pyritic zone.

Interpretations of the genesis of these sulphide deposits have been made in several theses, published papers and mine reports. The main aspects of concern to these writers are the source and nature of

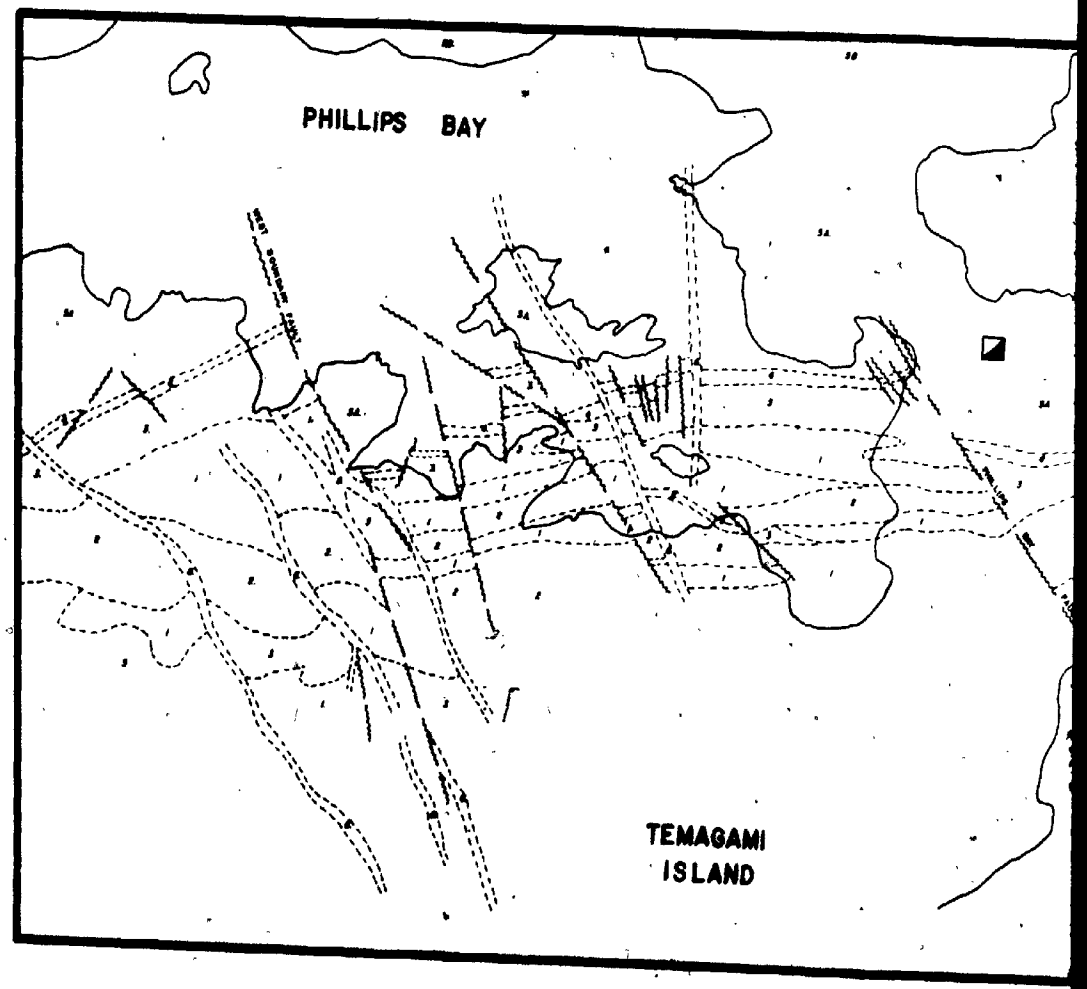
PHILLIPS BAY
TEMAGAMI ISLAND

1 of 2

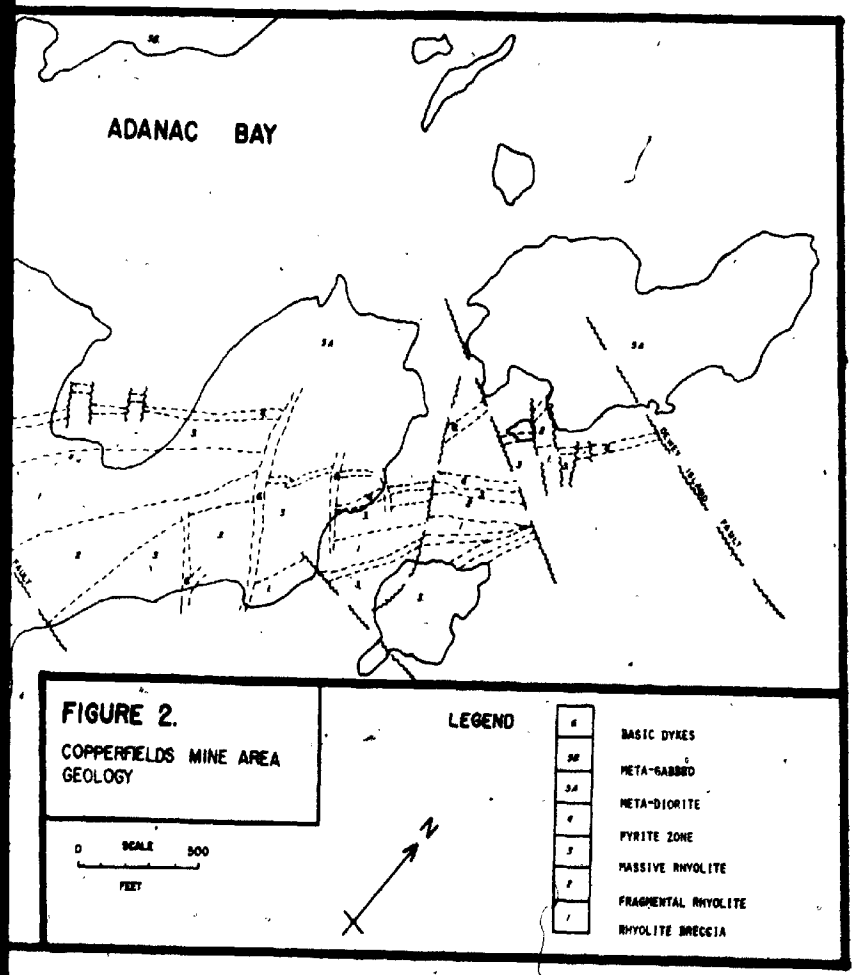
ADANAC BAY
FIGURE 2.
COPPERFIELDS MINE AREA
GEOLOGY
LEGEND
BASIC DYKES
META-GABBRO
META-DIORITE
PYRITE ZONE
MASSIVE RHYOLITE
FRAGMENTAL RHYOLITE
RHYOLITE BRECCIA
SCALE
500
FEET
N

2 of 2

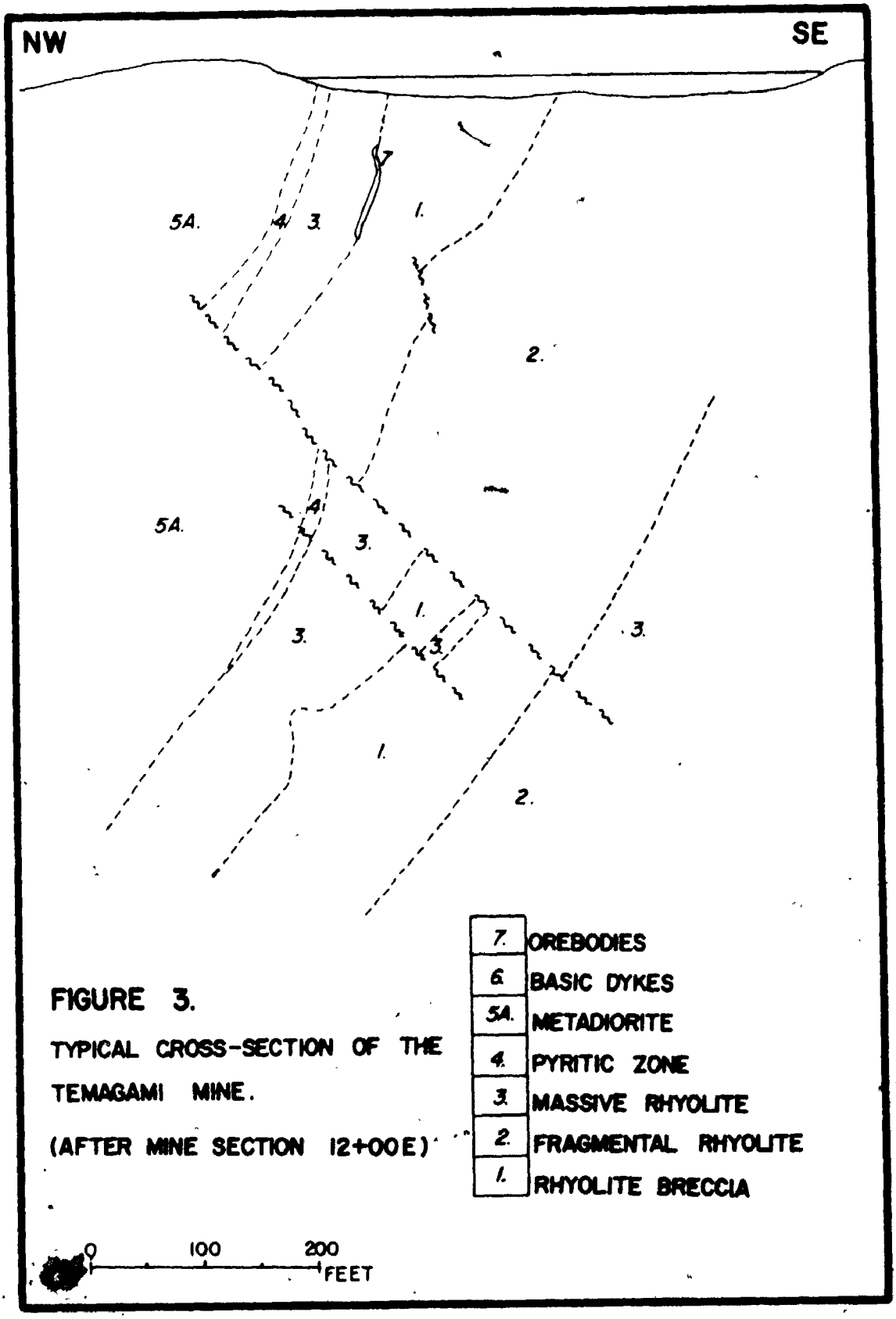

FIGURE 3.

TYPICAL CROSS-SECTION OF THE TEMAGAMI MINE.

(AFTER MINE SECTION 12+00E)

the sulphide-depositing fluids, the age of sulphide deposition and the time and genetic relationships between the two sulphide zones.

Smith (1957) considered the orebodies to have formed by an "injection of sulphide melt into the underlying lavas" from a segregation in the "Post-Huronian (Nipissing) gabbroic intrusive", metadiorite. Rose (1966A, 1966B) considered the orebodies to have been derived from the pyritic zone, deposited by a hot fluid of magmatic origin. Although Scott (1969) also considered the orebodies to be derived from the pyritic zone, she suggested that the depositing fluid was a post-metamorphic hydrous emanation.

Franklin (1967) hypothesised that the pyritic zone was formed by liquid immiscibility in the sill and that the chalcopyrite orebodies were not genetically related to it. Patrick (1966) agreed with this source for the pyritic zone, and also suggested that the chalcopyrite orebodies were deposited during the volcanism and that the sill was emplaced shortly after the deposition of the volcanic rocks. Patrick also suggested that the sill could have been a thick basaltic flow.

CHAPTER III

PETROLOGY AND GEOCHEMISTRY OF THE SOUTHWESTERN PORTION OF THE TEMAGAMI GREENSTONE BELT

A. Introduction

The approach to this work was threefold: firstly, to define the mineralogy and chemistry of the rocks of the southwestern portion of the greenstone belt; secondly, to interpret the original nature of the volcanic rocks; and thirdly, to hypothesise the effects of alteration and metamorphism on these original volcanic rocks. The purpose of this work was to show to what extent these rocks may be used as a standard to define as normal or anomalous the mineralogy and chemistry of the rocks within the Temagami Mine.

An attempt was made to sample the full range of meta-volcanic rock types. Ideally, samples should be taken sufficiently far from the mine that the rocks are unaffected by localized alteration associated with the concentrations of sulphides, yet close enough that they are derived from the same centre of volcanism as the mine rocks. The principal factors which controlled sample location were, however, the extensive Huronian sedimentary cover around the mine (Fig. 1), and water and glacial drift coverage. Figure 4 shows the location of the sixty samples collected for this study. The large number was necessary to minimize

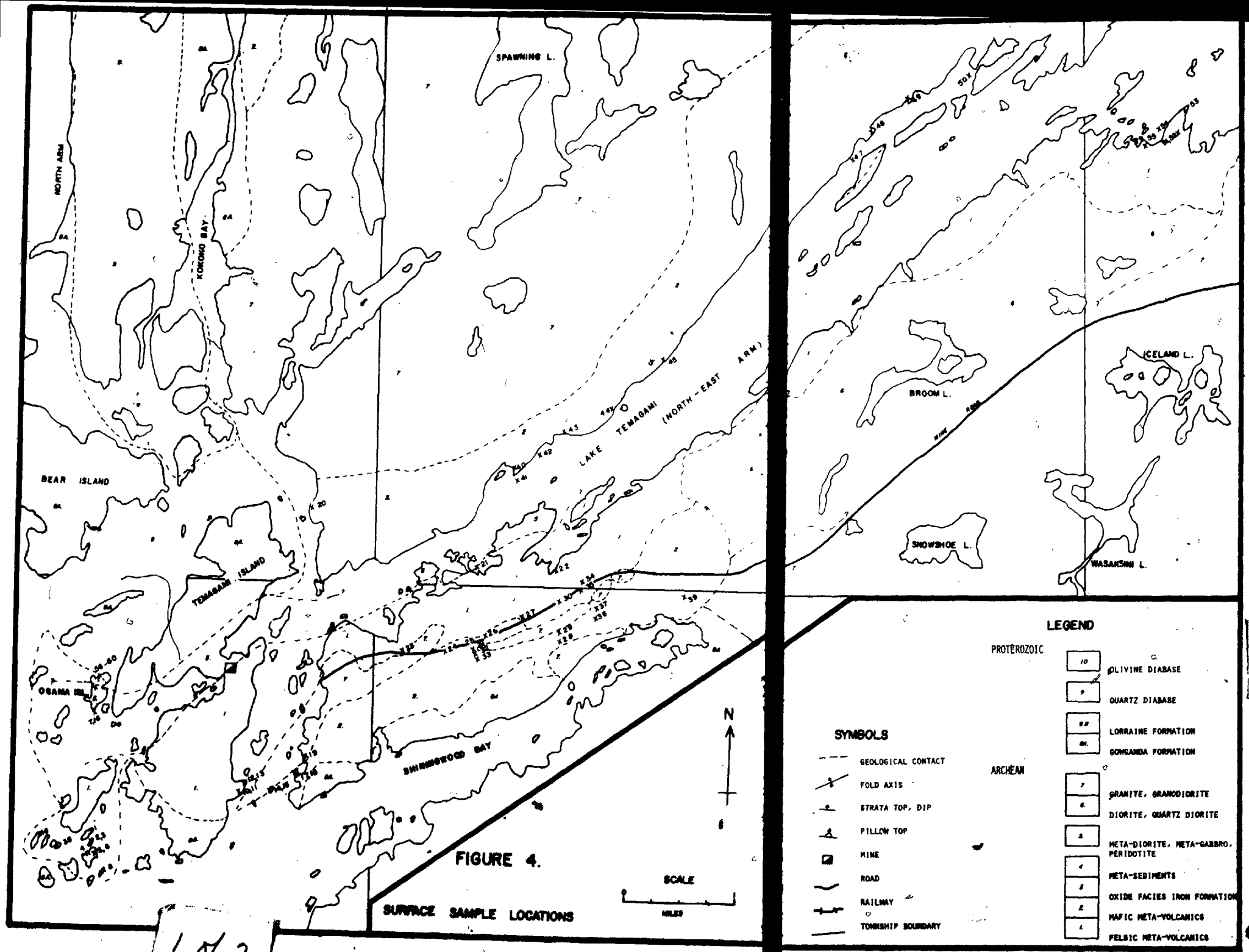

FIGURE 4.

SURFACE SAMPLE LOCATIONS

1 of 2

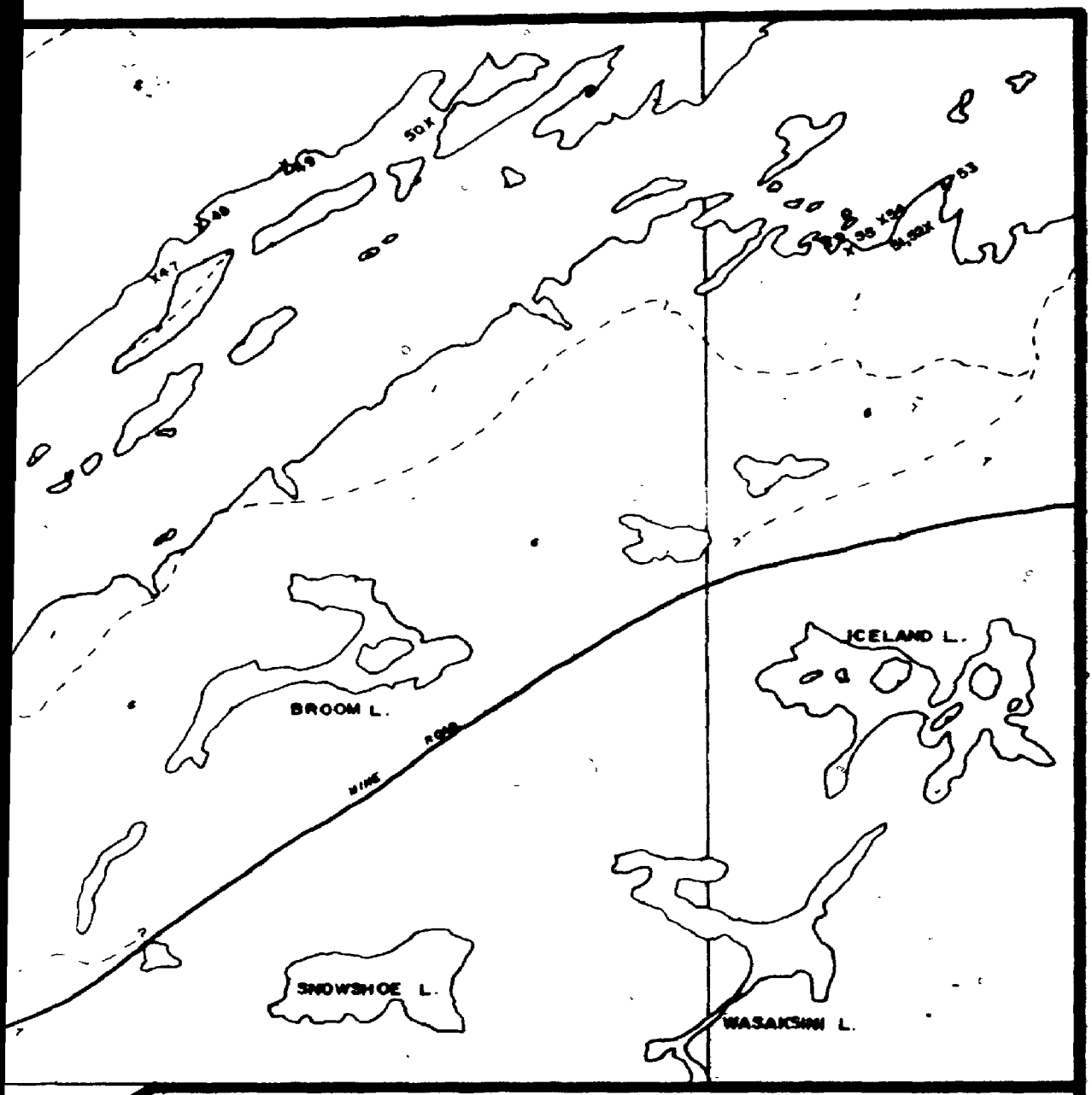

LEGEND

PROTEROZOIC

- 10 — OLIVINE DIABASE
- 9 — QUARTZ DIABASE
- 8a — LORRAINE FORMATION
- 8a — GOWGANDA FORMATION

ARCHEAN

- 7 — GRANITE, GRANODIORITE
- 6 — DIORITE, QUARTZ DIORITE
- 5 — META-DIORITE, META-GABBRO, PERIDOTITE
- 4 — META-SEDIMENTS
- 3 — OXIDE FACIES IRON FORMATION
- 2 — MAFIC META-VOLCANICS
- 1 — FELSIC META-VOLCANICS

SYMBOLS

- GEOLOGICAL CONTACT
- FOLD AXIS
- STRATA TOP, DIP
- PILLOW TOP
- MINE
- ROAD
- RAILWAY
- TOWNSHIP BOUNDARY

2 of 2

the effects of local alteration.

B. Petrography

A grouping of the samples based on their present mineralogy and texture is shown in Table 2. Recrystallization during alteration and metamorphism has masked or destroyed most of the original volcanic textures. A more detailed description of some of the minerals present is given in Appendix I.

Common metamorphic nomenclature would categorise virtually all of the samples as various types of albite, epidote, chlorite, sericite schists of the greenschist facies (Turner and Verhoogen, 1960). An attempt is made in Table 2 to interpret - using the present mineralogy and texture - the original rock type from which each group is derived. Igneous terminology is used principally to distinguish between rock types, and to compare these with other meta-volcanic rock suites in which igneous terminology is used almost exclusively. Such usage of igneous terminology for these metamorphic rocks is subject to errors in interpretation.

Groups 7, 6, 2 and 1 appear to form a continuous basalt-rhyolite differentiation suite. The number of samples within each group is principally the result of non-systematic sampling, rather than being indicative of the relative volumes of each rock type. Groups 3, 4 and 5 are samples of recognisable fragmental and tuffaceous units within the volcanic sequence. Their compositions are similar to the surrounding more massive rocks and they were probably formed by pyroclastic volcanic activity.

The original nature of Group 8 rocks is more difficult to interpret.

SAMPLE NUMBERS	FIELD AND HAND SPECIMEN	THIN SECTION	
		TEXTURE	PHENOCRYST-METACRYST MINERALOGY
Group: 1 2,10,38,44,4.	massive or fractured. 2,4: coarse agglomerate, 3' diameter fragments. light coloured, hard, fine fracturing, buff coloured fragments to 1". 44: darker.	fine grd. equigranular. occasional rounded qtz. cavity fillings to 1 mm. carb. & ser. rich patches.	Qtz. cavity filling, interlocking anhedral grains to 2 mm.
Group: 2 11,12,13,24,26, 29,34,46,51,52,43.	massive. 43: strongly sheared. appearance dominated by numerous qtz. grains.	fine grd. equigranular matrix. large qtz. grains evenly distributed.	Qtz. grains anhedral to 1 mm., some ser. & carb. inclusions. 20-40% of rock. Ab. few eroded laths replaced by carb. & ser.
Group: 3 1,3,9,22,23,25.	massive. coarse grd. mottled appearance, dark coloured fragment patches in lighter matrix.	dark angular fragments to 10 mm. 20-40% of rock. light fine grd. equigranular matrix.	
Group: 4 8.	massive. mottled light and dark patches.	closely packed rounded fragments 80% of rock.	FRAGMENTS: Ab. small highly eroded laths. 5-10% of rock. Qtz. few small rounded grains.
Group: 5 20.	1-4 mm. banding. alternating colour bands, dark-light-buff.	mineral banding and elongation of minerals parallel to banding, fine to medium grd.	Epid. small metacrysts in patches to 1 mm.
Group: 6 21,35,37,48.	massive or fractured. uniformly fine grd., dark green.	fine to medium grd. equigranular.	
Group: 7 14,15,17,18,19,28, 36,39,40,41,42,45, 47,49,60.	massive or fractured. dark green, fine grd.	fine to medium grd. equigranular.	
Group: 8 5,6,27,30,31,32,33, 50,53,54,55.	massive. light coloured phenocrysts in darker matrix.	ab. and few qtz. pheno-metacrysts in fine grd. equigranular matrix.	Ab. margins regular or eroded, ser. & carb. alteration, epid. & ser. inclusions. 20-40% of rock. Qtz. few anhedral grains.
Group: 9 7,16,56,57,58,59	massive or fractured, highly weathered. large phenocrysts in dark green matrix.	assorted phenocrysts in dark green fine grd. equigranular chloritic matrix.	Lc. large skeletal grains, remnant exsolution lamellae. Qtz. 16: large anhedral grains. 56: grains to 1 mm. less common in others. Ab. highly altered, fractured.

ABBREVIATIONS

n: sample representative of group
grd: grained
Qtz.: quartz
Ab. : albite
Ser.: sericitic mica
Carb.: carbonate
Chl. : chlorite
Lc. : leucoxene
Py. : pyrite
Epid.: epidote
To. : tourmaline
Cp.: chalcopyrite
Mt.: magnetite

GROUNDMASS MINERALOGY		INTERPRETIVE IGNEOUS NAME	COMPARATIVE MINE NAME
Qtz. fine grd. anhedral.	45-55%	Massive rhyolite. Rhyolitic agglomerate. Brecciated rhyolite.	Rhyolite fragmental.
Ab. fine grd. within matrix.	5-15%		
Ser. fine grd. laths.	20-25%		
Carb. fine grd., to 0.5 mm in patches	10-15%		
Chl. rare except in patches	5%		
Lc. small grains.			
Pt.,Mt. small grains.			
Qtz. fine grd. anhedral or subhedral.	35-40%	Rhyodacite-dacite. Dacitic quartz porphyry	Rhyolite. Rhyolite breccia.
Ab. very small subhedral laths.	5-10%		
Ser. fine grd. laths, elongate patches.	20-30%		
Carb. fine grd., coarser grd. patches.	10-15%		
Chl. fine grd., patches to 1 mm. of small laths.	10-15%		
Lc. small grains.			
Py.,Mt. small grains.			
FRAGMENTS:		Fragments: Andesite-basalt. Matrix: Rhyolite. Rock: Rhyolite breccia.	Rhyolite breccia. Tuffaceous rhyolite breccia.
Qtz. fine grd, subhedral.	15-25%		
Ab. fine grd. laths.	15-20%		
Ser. very fine grd. laths.	5%		
Carb. fine grd., coarser grd. patches.	10-20%		
Chl. fine grd., coarser grd. segregations.	25-50%		
MATRIX: similar to Group 1.			
FRAGMENTS:		Dacite breccia.	Rhyolite breccia.
Qtz. fine grd. subhedral.	30%		
Ab. not recognised.			
Ser. fine grd. laths	20%		
Carb. fine grd., coarser grd. patches.	25%		
Chl. fine grd.	20%		
MATRIX: similar to Group 2.			
Qtz. fine grd. equigranular.	40%	Dacitic tuff.	Rhyolitic tuff.
Ab. small laths.	15%		
Ser. fine grd., patches elongate, parallel to banding.	15%		
Carb. elongate patches.	10%		
Chl. small laths in elongate patches.	20%		
Qtz. fine interlocking grains.	20-30%	Dacite-andesite	Rhyolite
Ab. small laths.	15-20%		
Ser. very fine elongate laths, fracture filling	5-10%		
Carb. small patches.	10-20%		
Chl. fine grd., rimming other grains.	20-30%		
Lc. small grains.			
Py.,Mt. small grains.			
Epid. small dispersed grains.			
Qtz. fine grd.	10-20%	Andesite-basalt.	Not present.
Ab. small laths.	15-25%		
Ser. very fine grd., rare.	1- 5%		
Carb. fine and coarser grd.	15-20%		
Chl. fine grd., rimming other grains.	20-35%		
Lc. small grains.			
Py.,Mt. few large grains.			
Epid. small rounded grains, in patches with chl. & carb.	5-15%		
Qtz. fine grd.	30-40%	Rhyodacite-dacite porphyry	Not present.
Ab. fine laths.	15-25%		
Ser. very fine laths.	3- 8%		
Carb. fine and coarser grd.	10-15%		
Chl. fine grd., rimming other grains.	5-15%		
Lc. small grains.			
Epid. small rounded grains.			
Qtz. fine grd. anhedral or subhedral.	5-30%	Dolerite.	Metadiorite.
Ab. not recognised.			
Ser. very fine laths, rare.			
Chl. fine and medium grd. laths.	30-60%		
Carb. medium grd.	15-30%		
Py.,Mt. small grains and aggregates			
Epid. small grains and patches.	0-30%		

TABLE 2. PETROGRAPHY OF SURFACE SAMPLES

1 of 2

The size and euhedral shape of the albite phenocrysts (Plate 1) indicates that they were original plagioclase phenocrysts, albitised during metamorphism (Spooner and Fyfe, 1973). Since groundmass mineralogy is the same as surrounding felsic rocks, the Group 8 rocks have been subjected to similar alteration and metamorphic conditions. This group may include both porphyritic extrusive and hypabyssal intrusive rocks.

The Northeast Arm metadiorite has been mapped as a single unit and therefore the samples taken from it are grouped together (Table 2, Group 9) although they vary considerably in composition. This group will be considered in more detail in the discussion of the nature of the mine rocks.

C. Chemistry

The study of the rock analyses was carried out primarily to show if chemical trends characteristic of the Temagami metavolcanic rocks existed. Appendix II contains details of sample collection and preparation, and analytical techniques.

Unmodified data, containing both CO_2 and H_2O, is used in this section. As the analyses sum to 100% and the CO_2 and H_2O content varies between samples, the relative ratios of other oxides between samples are affected although oxide ratios within individual samples are not affected. It is, however, considered more valuable in this section to include both CO_2 and H_2O, treating them as variable constituents within the system, rather than exclude them from it.

Graphical representation is in the form of oxide vs. SiO_2 diagrams. In addition to inherent errors in all weight percent oxide diagrams (Chayes, 1964c, Pearce, 1968) validity of such representation, in this

case, is dependent on SiO_2 being a relatively fixed, non-mobile constituent. SiO_2 is considered here to be immobile, because presentation of the data in this form produced the most well defined distribution of all methods investigated. SiO_2 mobility will be considered further in Section E of this chapter. Complete diagrams are presented in Appendix Figures 1 a-p. Where possible to generalise their overall trend into a single line, these are shown in Figures 5 a-c. (Table 2, Group 9 dolerite is represented by black squares in Appendix Figures 1, and not included in calculation of the best-fit line).

MnO, MgO, FeO, Fe_2O_3 (Fig. 5a) show well defined trends with a small spread of values, particularly within the more felsic rock samples. Fe_2O_3 shows a wider spread within the mafic rocks, indicative of more variable oxidation particularly within iron rich rocks. Dolerite samples lie close to the average trend, generally lower than it.

CaO, Na_2O and K_2O generalized in Figure 5b do not exhibit such well defined trends, and have a wider spread of values. Because of the wide variation of its values in the felsic rocks (Appendix Fig. 1j), Na_2O cannot be represented by a single line, but combined with K_2O it can be represented in Figure 5b as a single line. Combination of all three oxides gives a fairly tightly grouped, well defined pattern. The dolerite is noticeably higher in both Na_2O and K_2O.

The remaining major element oxides are shown in Figure 5c. CO_2 is variable, but Appendix Figure 1o shows that the generally high CO_2 values are not restricted to the higher CaO bearing mafic rocks. Similarly, H_2O is generally high throughout the whole range of rock types (Appendix Fig. 1p).

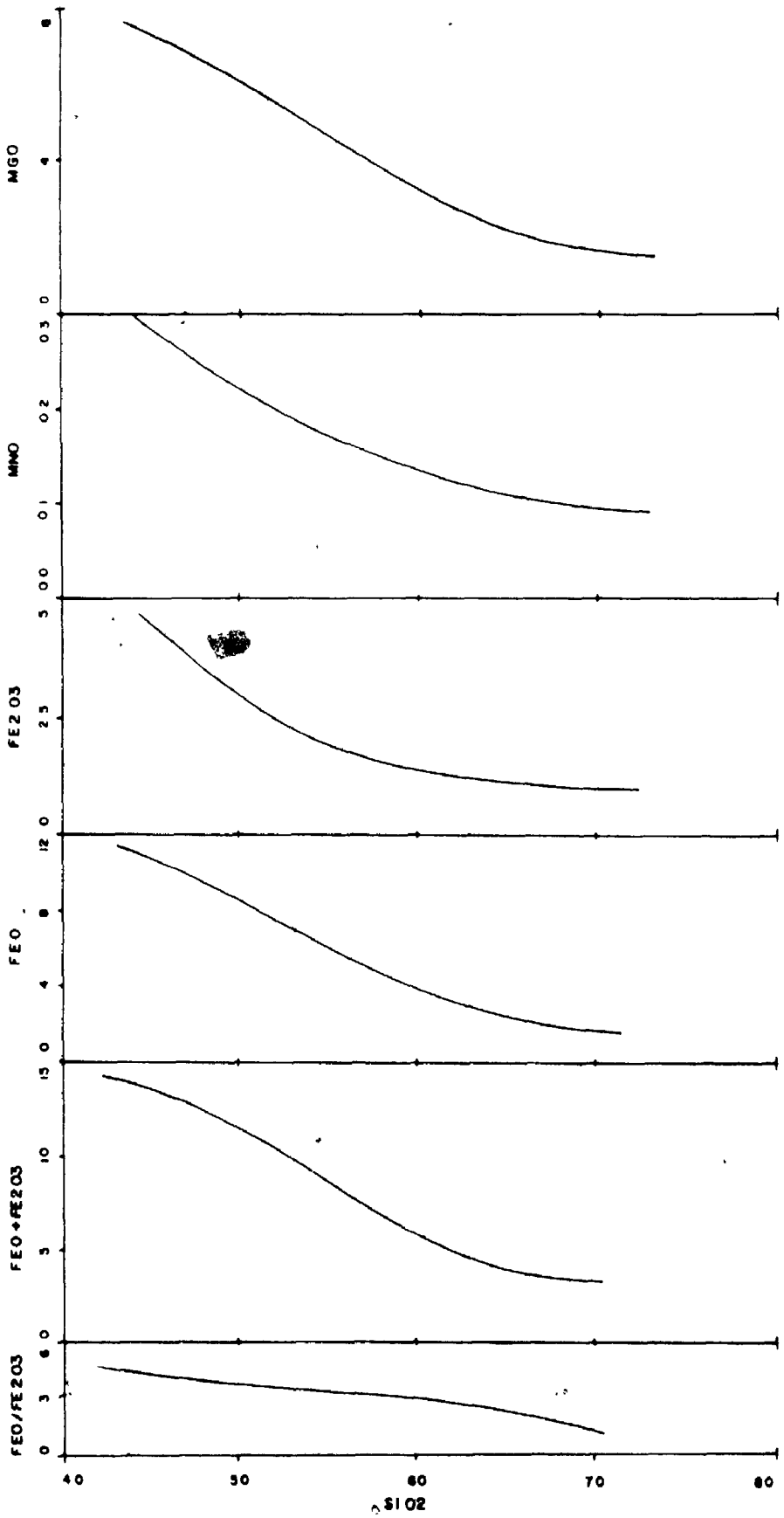

FIGURE 5A · SURFACE MAJOR OXIDES VS. SIO2. GENERALIZED AFTER APPENDIX FIGS. 1A-P.

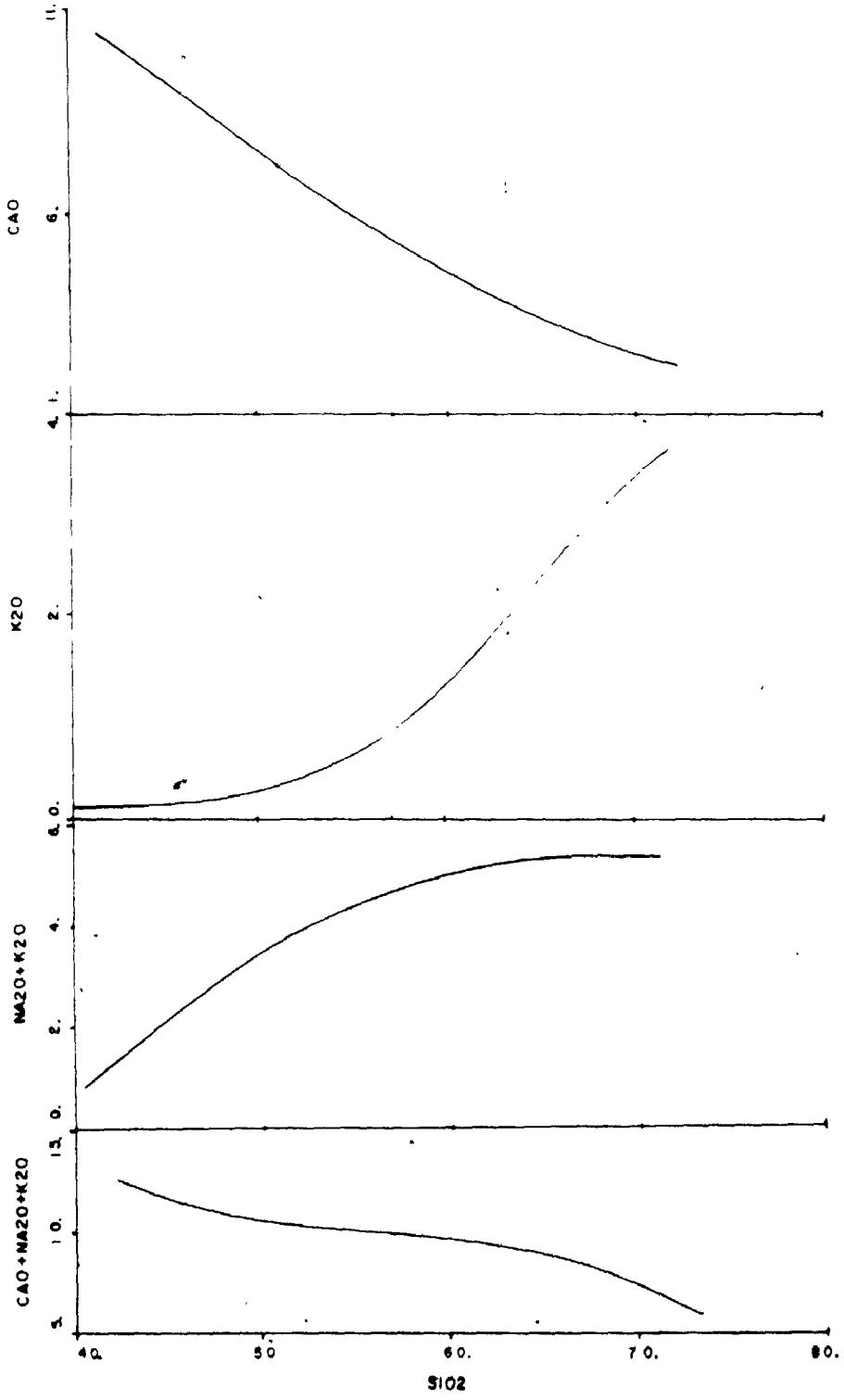
CAO
11.
6.
4.1.
K2O
2.
0.0.
NA2O+K2O
4.
2.
0.
CAO+NA2O+K2O
15.
10.
5.
40.
50.
60.
70.
80.
SIO2

FIGURE 5B.

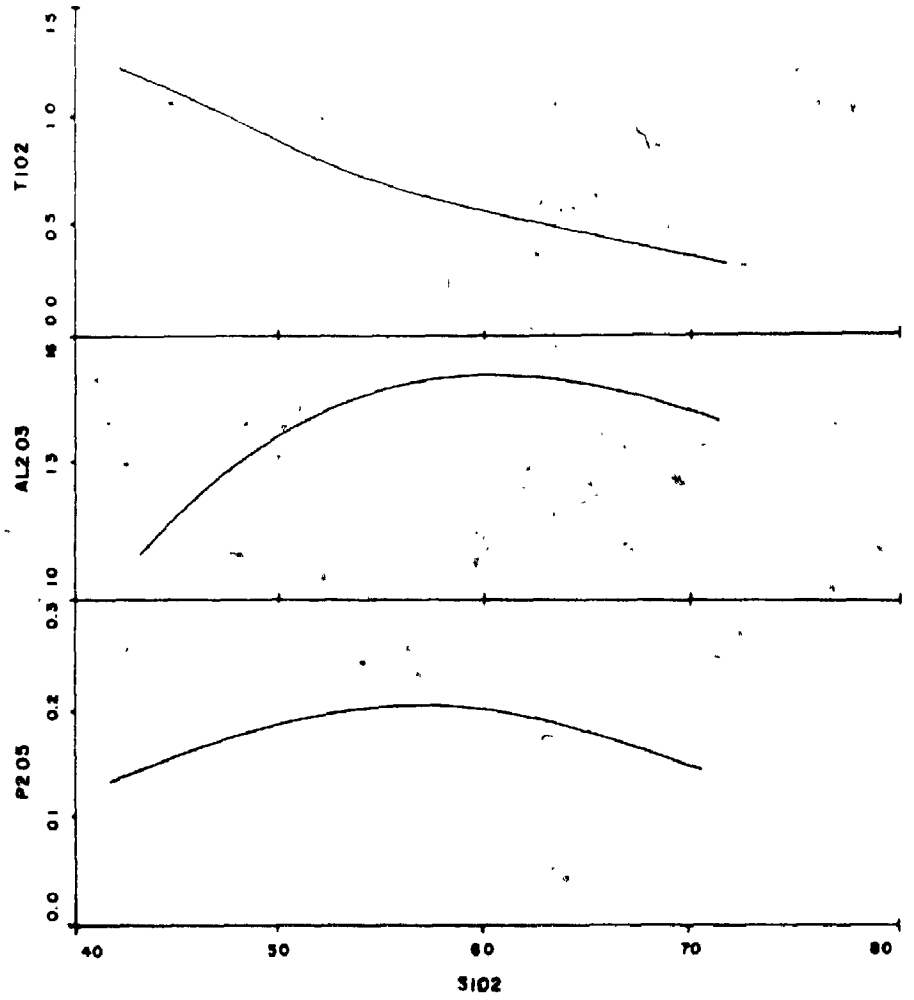

FIGURE 5C.

Sample D14 is the only one to lie consistently outside the normal ranges (Appendix Fig. 1), partially explainable by its high CO_2 content of 15%.

Metallic elements show a fairly regular distribution, with average values of: 50 ppm. Cu, 25 ppm. Pb, 80 ppm. Zn, 80 ppm. Ni, 20 ppm. Co. Relatively higher values are found within the more mafic samples, most marked in the case of nickel. The dolerite is generally higher in these elements.

Lithium is generally low throughout, averaging 10 ppm. Both barium and boron, averaging 220 and 17 ppm. respectively, are noticeably higher in the felsic rock samples.

D. Igneous Interpretation

In this section an attempt is made to interpret the original nature of the volcanic rocks from which the metamorphic rocks were derived. This requires assumptions as to the effects of alteration and metamorphism. These effects are not accurately known and are not considered in detail until Section E of this chapter.

If it is at all valid to 'unmetamorphose' these rocks, justification of the system used must be made. Igneous petrologists either assume fresh, unaltered samples and use raw data (Kuno, 1967) or define their own limits of acceptability, particularly for volatile content (Manson, 1967). Chayes (1964a) shows that 1% H_2O within a sample makes its classification less accurate. Many other writers do not include reference to limits of acceptability or treatment of their data.

Workers in metamorphosed igneous rocks have conflicting views as to the validity of geochemical interpretation. Goodwin (1968) considers

Archean greenstone rocks to consist almost entirely of secondary minerals and therefore hesitates to use more than SiO_2 content of fresh samples as an igneous indicator. Apart from excluding the more altered samples - for example, excluding those containing 4% normative calcite (Wilson et al., 1965), other writers have used chemical data to make extensive conclusions. Descarreaux (1973) apparently uses all samples, excludes H_2O and recalculates to 100%.

Irvine and Baragar (1971) have presented a system for recalculating analyses of metamorphosed volcanic rocks, such that they might be compared with fresh volcanic suites. The basis of their treatment is to exclude CO_2 and H_2O and recalculate to 100%, principally basing the classification thereafter on normative mineralogy.

The writer not only has misgivings as to the validity of treating metamorphic rocks in general in this manner, because the method assumes isochemical metamorphism apart from volatile introduction, but also has serious doubts as to whether such a system can be applied to rocks as altered as those of the Temagami greenstone belt. Extensive conclusions made on the basis of a normative mineralogy could not be justified for these rocks because the calculations involved require further assumptions and modifications of the data. Comparison diagrams used are therefore simple oxide plots in which variation from trends in fresh volcanic rocks can be more readily explained. Any conclusions made from this part of the study are made in general terms, with the qualification that the present chemistry of the rocks may be the result of extensive modification.

Analyses from the Temagami rocks were first recalculated to 100%

excluding CO_2 and H_2O. This initially assumes simple introduction of these two constituents by assigning their values on an equal weighted average basis to all other major oxides. Recalculation of Fe_2O_3 on the basis of TiO_2 content (Irvine and Baragar, 1971) was not considered necessary as Fe_2O_3 is already within the range of values produced by this calculation. The samples were then grouped together on the basis of SiO_2 content and an average calculated for each group (Table 3). This grouping is solely for convenience in data presentation and is not a proposed classification, although the groups correspond roughly with those in Table 2. The averaging process clarifies the main trends but by the use of it information is lost on the variation of individual samples.

Three sets of published average data, two from the Archean of Canada (Wilson et al., 1965; Baragar and Goodwin, 1969) and one for volcanic rocks (Nockolds, 1954), were recalculated on the same basis.

Normative mineralogy was calculated for all averages (Table 3) and the more interesting variation diagrams plotted (Figs. 6-11).

The Temagami averages are significantly lower in alkalies than Nockold's averages (Fig. 6), particularly the more felsic ones, which are themselves lower than the two Archean averages. All points lie within the subalkaline field below the dividing line of Irvine and Baragar (1971), which is slightly modified from the tholeiitic/alkaline dividing line of McDonald (1968).

As might be expected, all samples are hypersthene normative (Table 3) and are also quartz normative, with the exception of the Temagami dolerite. Four individual dolerite samples plotted separately lie above

TABLE 3. CHEMISTRY AND NORMATIVE MINERALOGY OF VOLCANIC ROCK AVERAGES

	A1	A2	B1	C1	D1	A3	B2	C2	D2	A4	C3	D3	A5	B3	C4	D4	A6	C5	C6	C7	D5
SiO_2	51.13	50.43	52.07	51.01	51.33	53.63	59.95	53.09	54.67	61.04	63.38	63.94	67.80	69.12	68.38	66.72	72.75	75.55	74.07	77.03	74.24
TiO_2	.88	1.35	1.05	.96	2.05	1.06	1.04	1.14	1.32	.73	1.25	.64	.52	.52	.47	.66	.39	.14	.18	.11	.22
Al_2O_3	16.93	13.35	15.61	14.99	14.21	14.20	16.03	14.88	17.32	16.14	15.57	16.76	15.49	15.31	17.03	15.50	14.21	13.85	14.55	13.16	13.56
Fe_2O_3	2.72	4.13	2.69	3.10	2.91	2.88	1.89	3.03	3.51	1.69	1.92	2.25	1.29	1.13	.91	2.15	.96	.65	.86	.45	1.26
FeO	10.20	11.45	9.19	8.98	9.09	9.13	6.20	8.67	5.54	5.98	5.89	3.02	2.84	3.11	2.82	2.25	2.01	1.29	1.57	1.01	.76
MnO	.14	.31	.20	.21	.18	.22	.16	.18	.15	.12	.14	.11	.12	.10	.02	.07	.13	.02	.02	.02	.03
MgO	4.55	7.48	6.61	7.53	6.40	6.62	3.90	6.37	4.40	5.28	2.36	2.13	2.60	1.84	1.89	1.58	1.85	1.06	1.50	.63	.82
CaO	9.22	9.54	9.84	10.71	10.52	8.40	5.87	8.63	7.99	3.81	4.93	5.56	3.81	2.64	3.35	3.71	3.11	.61	.90	.32	1.14
Na_2O	3.19	1.99	2.21	2.07	2.25	3.35	3.85	3.48	3.70	3.78	3.66	4.00	3.13	4.20	3.68	4.16	1.60	2.79	4.78	.82	3.01
K_2O	.86	.19	.34	.24	.83	.35	.87	.30	1.12	1.17	.55	1.41	2.21	1.84	1.33	3.03	2.79	3.89	1.35	6.40	5.39
P_2O_5	.18	.18	.19	.19	.23	.16	.23	.23	.28	.26	.33	.17	.19	.19	.12	.17	.18	.12	.20	.03	.07
Qtz.	--	5.9	4.9	3.2	3.8	3.3	13.5	2.7	5.8	13.0	22.7	20.0	26.8	26.1	27.3	21.0	40.4	38.1	33.4	42.7	32.7
Or.	5.1	1.1	2.0	1.4	4.9	2.1	5.1	1.8	6.6	7.1	3.3	8.3	13.3	11.1	8.2	17.9	17.2	24.2	8.4	39.9	32.2
Ab.	27.0	13.5	18.7	17.5	19.0	28.3	32.6	29.4	31.3	32.9	31.3	33.8	26.9	36.4	32.6	35.2	14.1	24.9	42.5	7.3	25.7
An.	29.3	28.7	31.7	30.9	26.2	22.7	23.9	24.1	27.3	17.7	22.5	23.6	18.0	12.1	16.6	14.7	14.8	2.4	3.3	1.5	5.3
Wo.	6.4	7.3	6.6	8.8	10.2	7.5	1.6	7.2	4.4	--	--	1.2	--	--	--	1.1	--	--	--	--	--
En.	10.6	18.6	15.6	18.7	15.9	16.4	9.7	15.9	11.0	13.5	5.9	5.3	6.6	4.7	4.9	3.9	4.8	2.8	3.9	1.7	.8
Fs.	14.3	16.0	13.3	12.7	14.2	13.0	8.4	11.9	7.1	8.8	7.5	2.8	3.6	4.2	3.9	1.4	2.6	1.7	2.0	1.4	.1
Fo.	.5	--	--	--	--	--	--	--	--	--	--	--	--	--	--	--	--	--	--	--	--
Fa.	.7	--	--	--	--	--	--	--	--	--	--	--	--	--	--	--	--	--	--	--	--
Mt.	3.9	6.0	3.9	4.5	4.2	4.2	2.7	4.4	5.1	2.5	2.8	3.2	1.9	1.7	1.4	3.1	1.4	1.0	1.3	.7	1.8
Il.	1.7	2.6	2.0	1.9	3.9	2.0	2.0	2.2	2.5	1.4	2.4	1.2	1.0	1.0	.9	1.3	.8	.3	.4	.2	.4
Ap.	.4	.4	.4	.4	.5	.4	.5	.5	.7	.6	.8	.4	.5	.5	.3	.4	.4	.3	.5	.1	.2
C.	--	--	--	--	--	--	--	--	--	2.4	.8	--	1.5	2.1	3.9	--	3.5	4.5	4.3	4.6	.9

A. Temagami Averages:
1. Table II Group 9
2. Basalt < 52% SiO_2
3. Andesite 52-58%
4. Dacite 58-64%
5. Rhyodacite 64-71%
6. Andesite > 71%

B. Baragar and Goodwin (1969)
1. Basalt
2. Andesite
3. Salic

C. Wilson et al. (1965):
1. Basalt
2. Andesite
3. Dacite
4. Rhyodacite
5. Rhyolite
6. Sodic Rhyolite
7. Potassic Rhyolite

D. Nockolds (1954)
1. Basalt
2. Andesite
3. Dacite
4. Calc-alkaline Rhyodacite
5. Calc-alkaline Rhyolite

FIGURE 6.

NA2O+K2O VS. SIO2 PLOTS

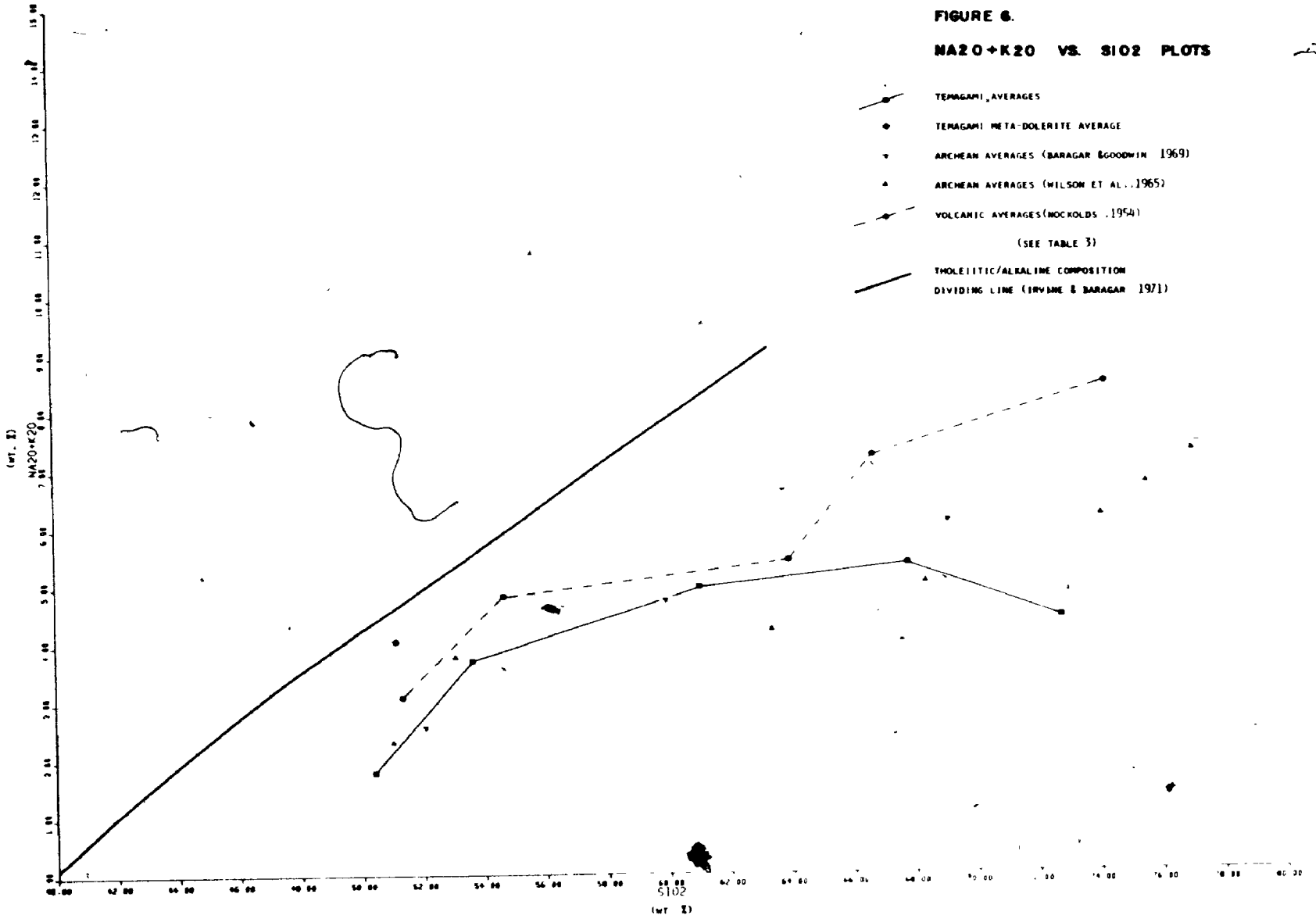

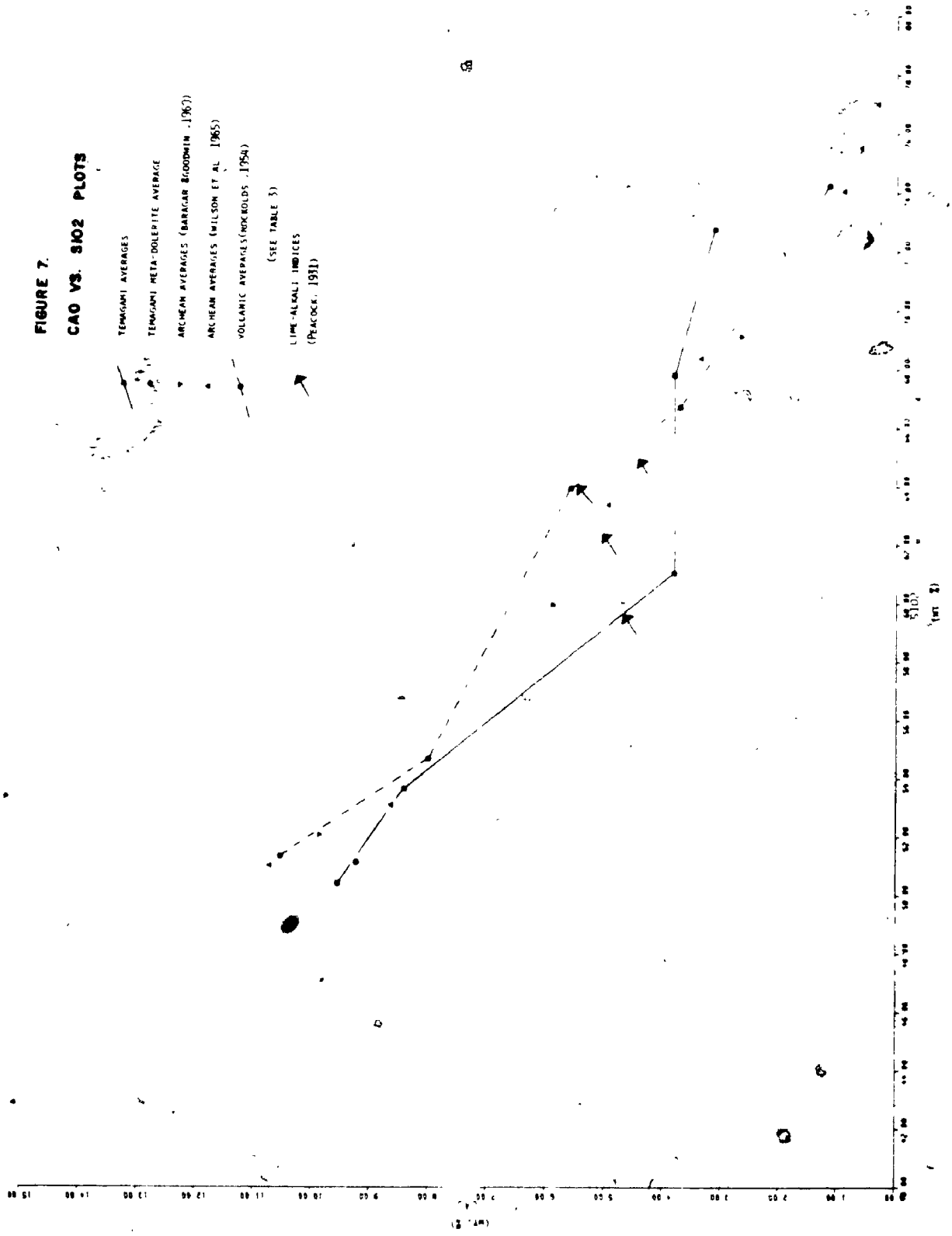
FIGURE 7.
CAO VS. SIO2 PLOTS
TEMAGAMI AVERAGES
TEMAGAMI META-DOLERITE AVERAGE
ARCHEAN AVERAGES (BARAGAR & GOODWIN, 1967)
ARCHEAN AVERAGES (WILSON ET AL, 1965)
VOLCANIC AVERAGES (NOCKOLDS, 1954)
(SEE TABLE 3)
LIME-ALKALI INDICES
(PEACOCK, 1931)

FIGURE 8.

N - K - C PLOTS

TEMAGAMI AVERAGES

TEMAGAMI META-DOLERITE AVERAGE

ARCHEAN AVERAGES (BARAGAR &GOODWIN ,1969)

ARCHEAN AVERAGES (WILSON ET.AL..1965)

VOLCANIC AVERAGES(NOCKOLDS ,1954)

(SEE TABLE 3)

N = NA2O

K = K2O

C = CAO (WT.%)

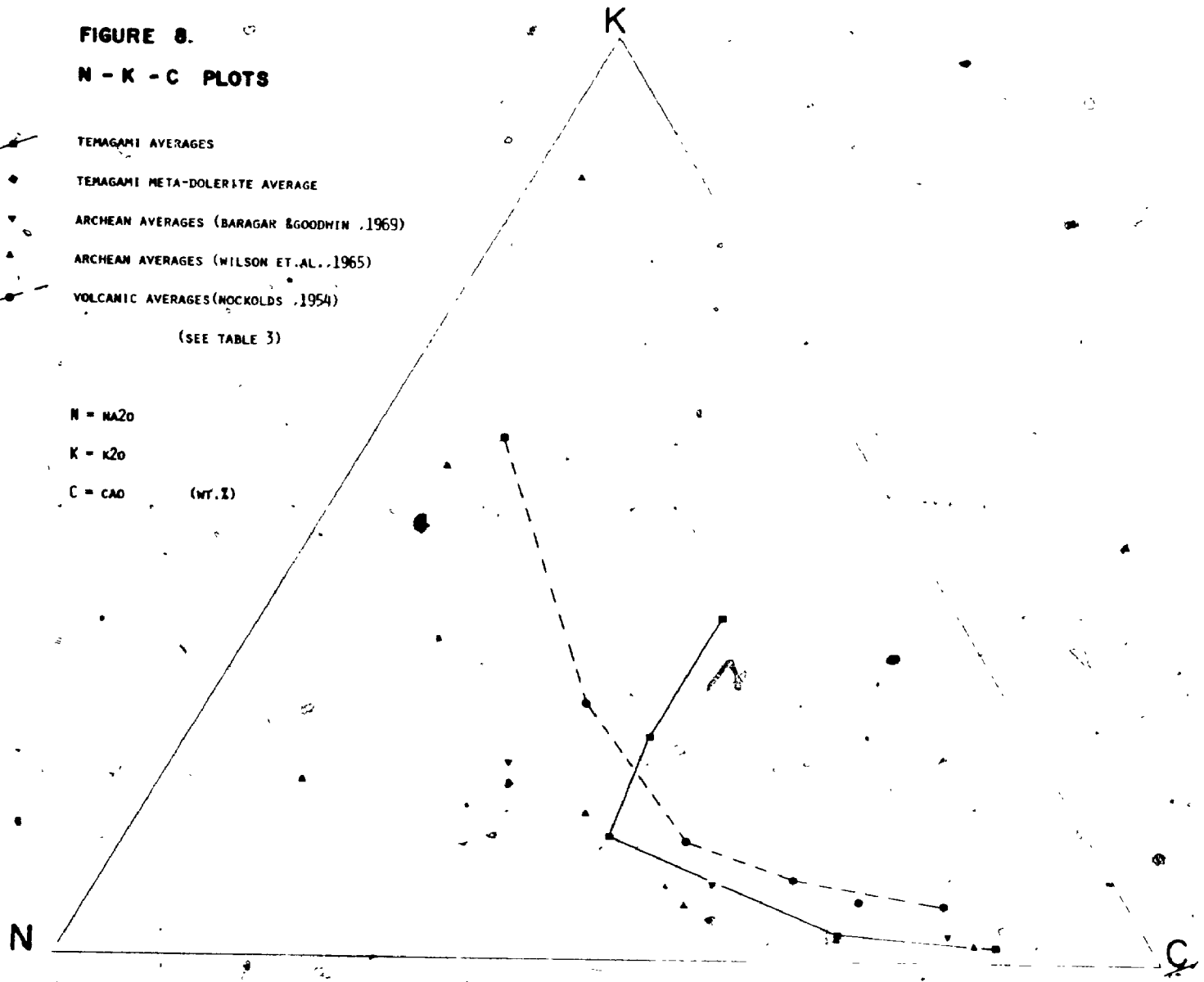

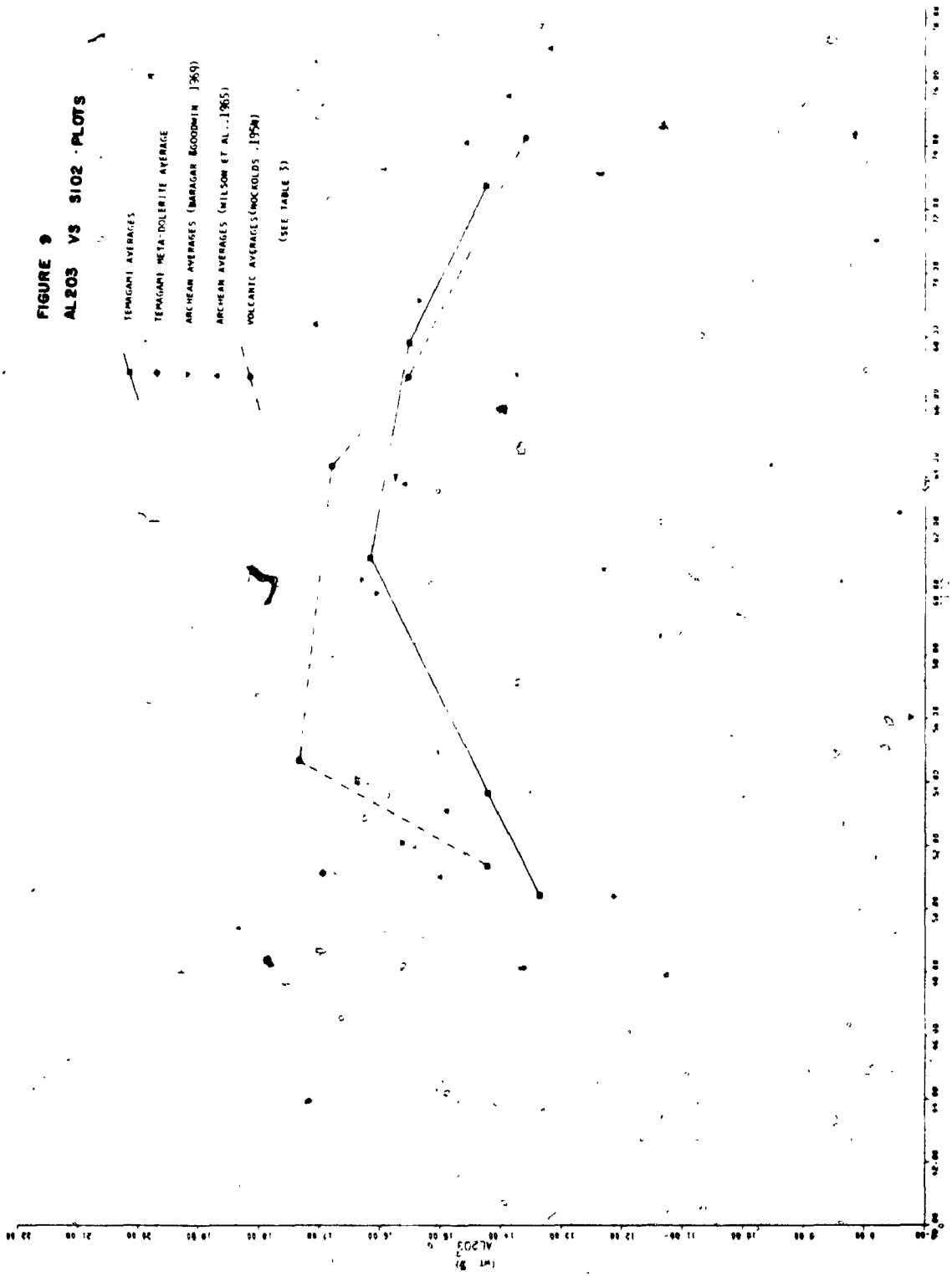
FIGURE 9
AL203 VS SIO2 - PLOTS
TEMAGAMI AVERAGES
TEMAGAMI META-DOLERITE AVERAGE
ARCHEAN AVERAGES (BARAGAR &GOODWIN 1969)
ARCHEAN AVERAGES (WILSON ET AL.,1965)
VOLCANIC AVERAGES(NOCKOLDS ,1954)
(SEE TABLE 3)

FIGURE 10

A - F - M PLOTS

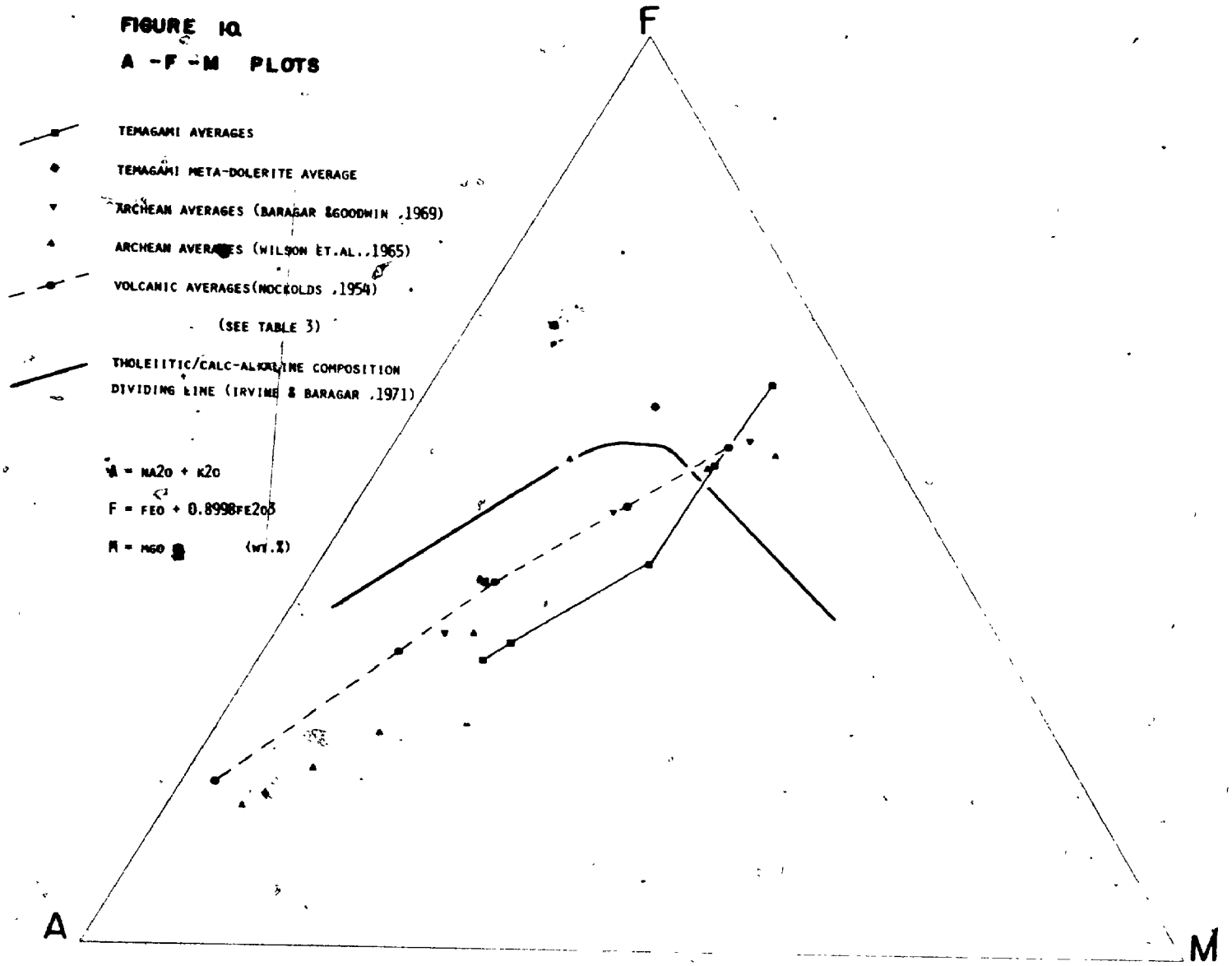

TEMAGAMI AVERAGES

TEMAGAMI META-DOLERITE AVERAGE

ARCHEAN AVERAGES (BARAGAR &GOODWIN ,1969)

ARCHEAN AVERAGES (WILSON ET.AL.,1965)

VOLCANIC AVERAGES(NOCKOLDS ,1954)

(SEE TABLE 3)

THOLEIITIC/CALC-ALKALINE COMPOSITION DIVIDING LINE (IRVINE & BARAGAR ,1971)

A = $Na_2O + K_2O$

F = $FeO + 0.8998Fe_2O_3$

M = MgO (wt.%)

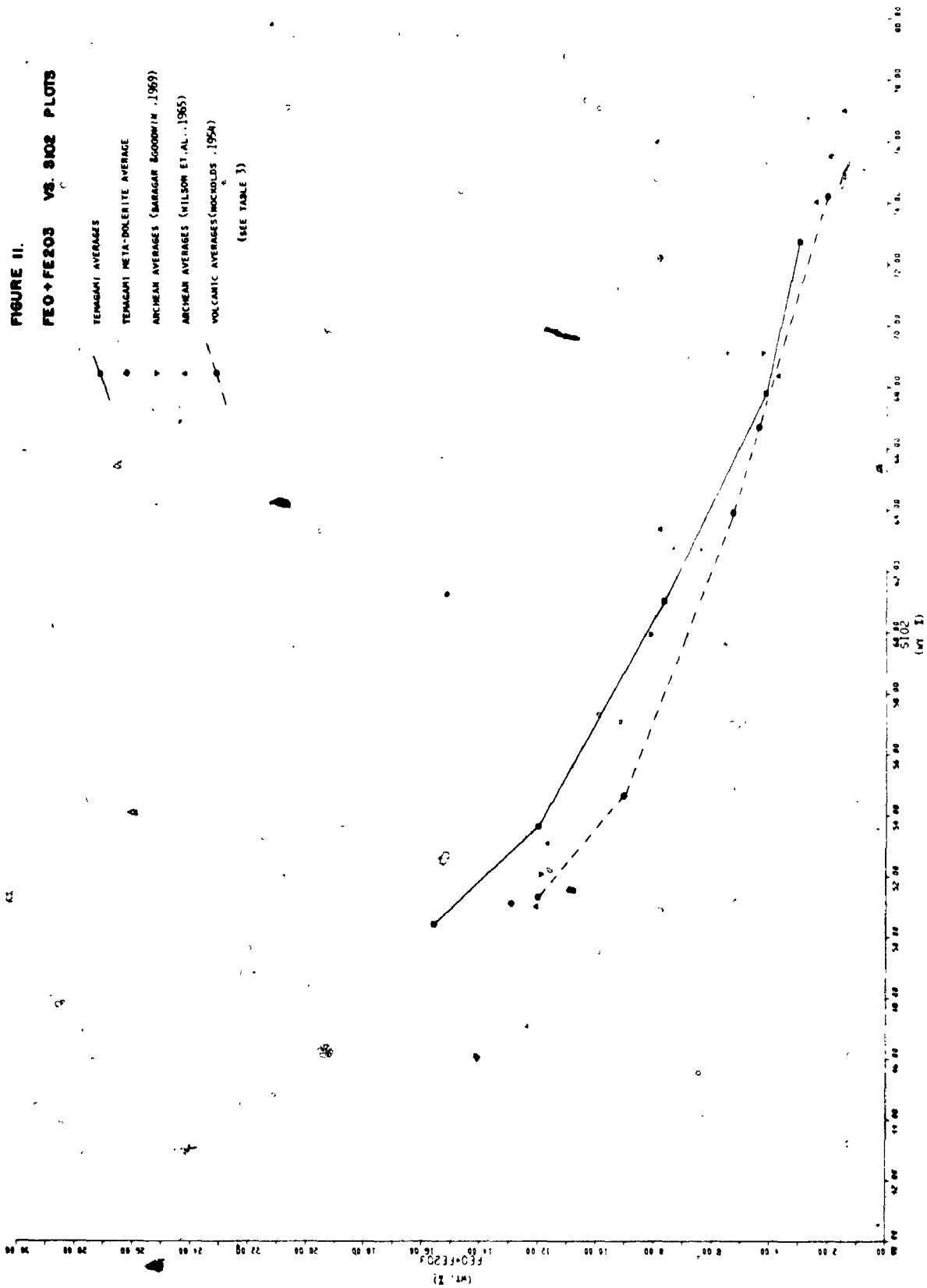

FIGURE 11.

FEO + FE2O3 VS. SIO2 PLOTS

the dividing line, within the alkaline field and are nepheline normative.

All the Archean basalt averages have K_2O values typical of oceanic tholeiites as opposed to continental tholeiites (Engel et al., 1965), Nockold's average being of the continental type. These Archean averages are not characteristic of Engel's Archean metatholeiitic category.

The Temagami intermediate averages are lower and the felsic averages higher in CaO than the other averages (Fig. 7). The lime-alkali index (Peacock, 1931) of the Temagami averages lies within the calc-alkaline field, the indices of the other averages being above 61% SiO_2 and therefore within the calcic field. The Temagami average lines for alkalies and CaO do not diverge, but parallel each other for SiO_2 values above the lime-alkali index point. The Na_2O:K_2O:CaO diagram (Fig. 8) shows that the mafic-intermediate Temagami averages follow the trend of the other averages, but that the felsic averages are significantly richer in CaO and poorer in Na_2O; K_2O is relatively normal throughout.

Although the Al_2O_3 values of the Temagami averages are generally lower, their trend parallels closely those of the other suites (Fig. 9). The normative feldspars of the Temagami averages are not typical of the other averages (Table 3), their values being controlled principally by Na_2O, K_2O and CaO content. They are also controlled to a lesser extent by Al_2O_3 in the mafic rocks, where excess CaO over Al_2O_3 after the formation of anorthite allows the formation of normative wollastonite.

In the felsic rocks excess Al_2O_3 after the calculation of feldspars appears as corundum in the normative calculation (Table 3); other normative minerals are not affected by its presence. Corundum is not a normal modal mineral in these rocks and therefore its normative presence

requires explanation. Exsolution of an aluminous spinel within plagioclase is possible (Wass, 1973), but unlikely within sub-alkaline felsic rocks. In Nockolds'[18] calc-alkaline rhyolite (Table 3) the low excess Al_2O_3 can be readily explained by Al_2O_3-bearing modal mafic minerals, amphibole and biotite. These minerals are typical of felsic volcanic rocks, but not considered in the anhydrous C.I.P.W. normative calculation. The Archean felsic averages show a higher excess of Al_2O_3 than Nockolds' averages. The excess Al_2O_3 in the Temagami averages would be considerably higher were it not for the unusually high CaO content allowing the formation of more anorthite than is normal (Table 3). This excess cannot be explained solely on the basis of Al_2O_3-bearing modal volcanic minerals. The explanation may lie within the processes of alteration which have produced the present metamorphic mineralogy. This possibility will be considered in Section E of this chapter.

The A-F-M trends for all suites are from a high iron tholeiitic basalt, crossing Irvine and Baragar's (1971) dividing line into the field of a calc-alkaline differentiation suite (Fig. 10). The Temagami andesite average also lies within the tholeiitic field. This is due to the high iron content of the Temagami mafic rocks (Fig. 11); MgO is within the normal range (Table 3). The low alkalies of the Temagami felsic averages show on this figure as low final alkali enrichment.

TiO_2 values of the Archean average basalts (Table 3) are low, typical of circum-oceanic as opposed to oceanic suites (Chayes, 1964b); Nockolds' average basalt is higher, closer to either oceanic or continental type (Engel et al., 1965).

In general terms the chemistry of the Temagami rocks is similar to

other Archean meta-volcanic suites and to those more recent volcanic rocks which are considered to be sub-alkaline tholeiitic-calc-alkaline and typical of recent circum-oceanic volcanic activity.

E. Alteration and Metamorphism

The present mineralogy of the Temagami rocks is consistent with lower greenschist facies metamorphism. This has been attributed to regional metamorphism associated with the Kenoran Orogeny, affecting large areas of the Superior Province of Canada. These rocks, however, appear to have been extensively altered from their original igneous state. In addition to Na_2O and CaO redistribution CO_2 and H_2O have been extensively added to these rocks (Appendix Figs. 1 o-p). Regional metamorphism cannot be considered as being strictly isochemical, but it is difficult to envisage its being responsible for bulk addition or removal of these constituents. It is possible that large scale alteration in the composition of these rocks took place during hydrothermal activity affecting the freshly deposited, hot, submarine volcanic rocks. Temperatures attained in some of these rocks during hydrothermal activity may well have been in excess of 300°C (Browne and Ellis, 1970) and therefore sufficient to cause metamorphism to greenschist mineralogy. A discussion of hydrothermal alteration and the feasibility of such a system having developed within the rocks of the Temagami area is included in Chapter V.

The present metamorphic mineralogy and chemistry is known and an approximation of the original chemistry and mineralogy has been made (Table 3). It is, therefore, possible to outline in qualitative terms the processes of mineral alteration. Quantitative calculations are not

possible as the original chemistry and mineralogy are only assumed, and the compositions of the variable composition metamorphic minerals have not been determined accurately (Appendix I).

Feldspar Group: Potassic alkali feldspars are altered to muscovite, upon addition of alumina and water.

1. $KAlSi_3O_8 + Al_2O_3 + H_2O \longrightarrow KAl_3Si_3O_{10}(OH)_2$
   orthoclase (sanidine) — muscovite

Within felsic rocks where K_2O content is high, muscovite contains up to 70% of the Al_2O_3 content of the rocks.

The high CO_2 content of the felsic rocks requires complete breakdown of the anorthitic feldspar component to form calcite.

2. $CaAl_2Si_2O_8 + CO_2 \longrightarrow CaCO_3 + Al_2O_3 + SiO_2$
   anorthite — calcite

Pyrophyllite could be formed with the addition of silica and water, but it is more likely that the Al_2O_3 is used in the formation of muscovite, the excess silica forming quartz. Muscovite inclusions in albite phenocrysts are common, suggesting simultaneous formation of both muscovite and albite.

Carbonates of the felsic rocks are dolomites and ferruginous dolomites, with little calcite, indicating that the partial pressure of CO_2 in the hydrothermal fluids was sufficiently high to cause carbonatization of ferromagnesian silicates.

Due to the higher CaO content of the mafic rocks, more calcite is present and in addition to carbonatization, epidotization of anorthite occurs.

3. $4CaAl_2Si_2O_8 + H_2O \longrightarrow 2Ca_2Al_2Si_3O_{12}(OH) + Al_2O_3 + 2SiO_2$
anorthite → zoisite

In the mafic and intermediate rocks, where phenocrysts or microphenocrysts of albite occur, the Na_2O content of the rocks is normal (Fig. 6, Appendix Fig. 1j). In these rocks albite is formed by replacement of andesine and labradorite grains (Plate 2). In the more felsic rocks, where albite occurs within the groundmass, Na_2O is lower than normal (Fig. 6). In felsic rocks Na_2O would be contained in alkali feldspars or within volcanic glass. Muscovite formed, upon alteration of the feldspar or devitrification of the glass, using up Al_2O_3 at the expense of albite formation. Excess Na_2O appears to have been mobile and removed from the system. Paragonite is certainly unlikely to form in competition with muscovite for Al_2O_3 (Grunier, 1942).

Ferromagnesian Group: The main ferromagnesian mineral present is chlorite, formed by the breakdown of all other ferromagnesian minerals. The formation of actinolite is suppressed due to the high partial pressure of CO_2 (Turner, 1958, p. 220).

In the felsic rocks the minor ferromagnesian minerals were probably in the form of amphibole and biotite, which were readily altered to form chlorite, carbonate and muscovite. In the mafic rocks, where ferromagnesian mineral content is high, a quantitative expression of alteration cannot be given without an exact knowledge of igneous and metamorphic mineral compositions.

4. $CaMgFe^{2+}$ Pyroxene + Alumina + Water + Carbon dioxide $\longrightarrow$ $Fe^{2+}Al(Mg)$ Chlorite + $CaMg(Fe^{2+})$ carbonate + quartz

A balance appears to have been set in each sample, dependent on hydrothermal fluid composition and temperature and degree of alteration for the relative progression of the reactions:

Anorthite ⟶ calcite-zoisite

Pyroxene ⟶ carbonate-chlorite (Plate 4)

Spinel Group: TiO_2 was probably originally present in the form of titanomagnetite or ulvospinel, as suggested by remnant ilmenite exsolution lamellae in larger leucoxene grains in the dolerite. Alteration to leucoxene involved the formation of finely crystalline rutile, the excess iron (both Fe^{2+} and Fe^{3+}) forming chlorite, hematite or magnetite (Plate 6).

Sulphides: Where present, the sulphide minerals are pyrite, and occasional chalcopyrite and sphalerite, probably being original or recrystallized.

It is possible to calculate the approximate normative metamorphic mineralogy on the basis of those minerals present, showing that the present chemistry is consistent with the proposed scheme of alteration and metamorphism. Table 4 shows the results of such a calculation for rhyolite and basalt samples.

Consideration in this manner of the behaviour of major element oxides in each reaction summarises the processes of alteration and metamorphism (Table 5).

Original quartz may be recrystallized, but appears fixed. SiO_2 released in three reactions appears to form additional quartz. In the mafic rocks sufficient Al_2O_3 is released from the breakdown of anorthite for the formation of chlorite. In the more felsic rocks, however, anorthite is low, producing insufficient Al_2O_3 for muscovite formation.

TABLE 4

HYDROUS METAMORPHIC NORMATIVE MINERALOGY

	Molecular %
Sample D4: Rhyolite	
Ferruginous dolomite / calcite ($Ca:Mg:Fe^{2+}$=4.5:2.6:1.2)	15
Muscovite	23
Albite	10
Chlorite (Fe,Al)	6
Quartz	44
	98%
Sample D17: Basalt	
Dolomite / calcite (Ca:Mg=2.1)	17
Muscovite	1
Albite	27
Zoisite	12
Chlorite (Fe,Mg,(Al))	28.5
Quartz	14.5
	100%

TABLE 5

RELATIVE CHANGES OF MAJOR OXIDES IN METAMORPHIC REACTIONS

OXIDE \ REACTION	orthoclase-muscovite	anorthitic plagioclase-calcite	anorthitic plagioclase-albite	albitic feldspar-albite	pyroxene-chlorite+dolomite	titanomagnetite-leucoxene
SiO_2	0	+	+	0	+	
TiO_2						0
Al_2O_3	-	+	+	0	-	
Fe_2O_3						+
FeO					0	+
MnO					0	
MgO					0	
CaO		0	0		0	
Na_2O				0		
K_2O	0					
CO_2		-			-	
H_2O	-		-		-	

\+ Released by reaction

0 No change in reaction

\- Required for reaction

Not involved in reaction

Muscovite appears to form in preference to albite recrystallization allowing Na^+ to be removed from the system. This explains in part the Al_2O_3 excess in felsic average normative calculations (Table 3) (cf. Chapter III, Section D). CaO is now present in the form of carbonate. Solution and precipitation of Ca^{++} ion would have been dependent on variable chemistry in the hydrothermal fluid. Ca^{++} mobility within the system involving relative removal from the intermediate rocks and addition to the felsic rocks would explain the values found in Figure 7.

The above reactions could all occur within the physical and chemical conditions of hydrothermal activity. Hydrothermal activity does not normally affect rocks uniformly. Permeable rocks such as pyroclastics are more susceptible to intense alteration than massive impermeable rocks. In areas of highly altered rocks the effect of later regional metamorphism may only have been to recrystallize the greenschist mineralogy already present. In areas of less altered rocks its effect may have been to produce greenschist mineralogy in relatively fresh volcanic rocks.

The overall effect of the regional metamorphism has been to superimpose a uniform metamorphic grade on the Temagami Archean volcanic rocks; this would have had the effect of evening out the irregularities produced by a previous hydrothermal alteration which may have affected these rocks.

F. Summary and Conclusions

Mineralogically the rocks of the southwestern portion of the Temagami greenstone belt conform to a regular pattern characteristic of lower greenschist facies metamorphism. Variations in mineralogy appear to be the result of variations in the rock bulk chemistry.

Major element oxides, when plotted on simple variation diagrams,

in most instances form well defined trends within narrow limits. These trends can be considered as characteristic of this suite of meta-volcanic rocks without any genetic implications, and therefore may be used as standards to compare with the trends of the mine rocks. When recalculated, the chemical composition of these rocks appears similar to that of other differentiated volcanic suites, particularly recent circum-oceanic volcanics.

Much of the present mineralogy can be explained by synvolcanic hydrothermal alteration. The abnormal content of some chemical constituents can be explained by their mobility during this hydrothermal alteration. Subsequent regional metamorphism has superimposed a uniform grade of metamorphism throughout the area.

CHAPTER IV

THE GEOLOGY AND GEOCHEMISTRY OF THE TEMAGAMI MINE

A. Detailed Geology of the Temagami Mine

1. Structure and Stratigraphy

The extent of underground workings at the Temagami Mine is shown in projection in figure 12. Extensive diamond drilling is restricted to a zone approximately 600' in width about this plane, from which three million feet of diamond drill core has been extracted and examined. It is only within this zone, which includes the upper felsic volcanic rock sequences, the pyritic zone and the lower part of the metadiorite (Figure 2), that a detailed structural and stratigraphic interpretation is possible. Outside this zone knowledge of the geology is restricted to that gained from surface mapping and sparsely distributed diamond drilling.

Also projected onto the section of figure 12 are the outlines of the mined orebodies. Fault gaps or overlaps are produced on this projection, dependent on attitude and displacement of faulting. The plane of projection is the rhyolite-rhyolite breccia contact (Fig. 3) or its lateral equivalent. The two orebodies chosen for detailed study, the No. 4 and E. No. 3, are marked on figure 12.

The rocks of the mine strike at 50° and dip to the northwest at

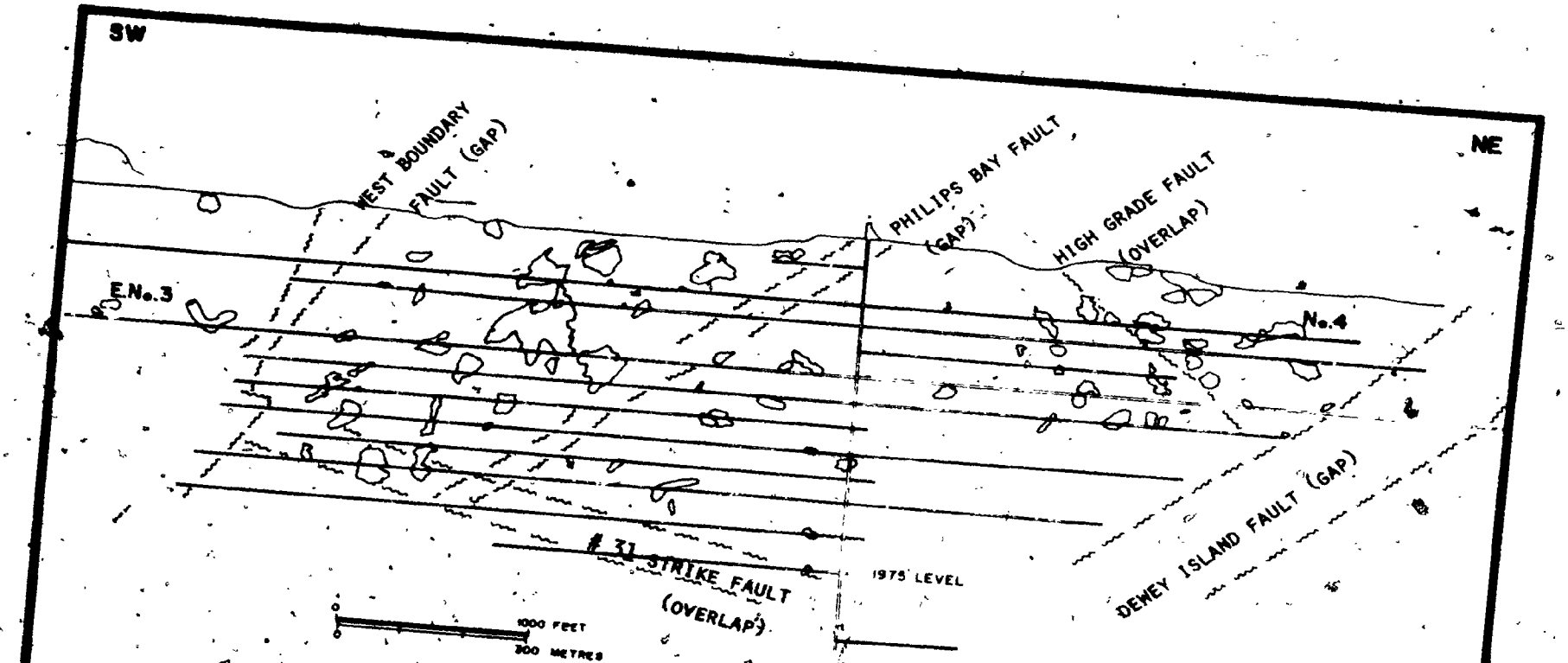

FIGURE 12.

TEMAGAMI MINE WORKINGS AND OREBODIES.
(PROJECTION INTO PLANE OF OREBODIES)

67-72° consistent with their location on the south limb of the Temagami syncline (Fig. 1). No top determinations have been made within the mine. The contacts between volcanic rock units appear to dip slightly more steeply than the 67° average of the rhyolite-metadiorite contact, but are generally more variable and are difficult to measure accurately. The rhyolite-metadiorite contact itself appears to dip less steeply at depths greater than 2000' below surface. Insufficient information is available to determine if this is due to faulting, folding or lensing out of the metadiorite unit; the volcanic rock units have not been mapped in detail at this depth.

There is no evidence of local folding of the mine rocks. The rocks are normally massive, without extensive development of schistosity. The large shear zone associated with the Northeast Arm of Lake Temagami does not continue into the central part of Temagami Island (Fig. 1); the shear zone may be offset by faulting to the east of the island. Extensive faulting occurs throughout the mine, displacing all units except some lamprophyre and diorite dykes which appear to have intruded along fault planes. Joint planes with no apparent offsets are common. The mine rocks appear to have behaved as a competent block during regional deformation; the majority of the stress during folding may have been absorbed by the more mafic rocks to the north and south of the mine.

Scott (1969) has attempted to relate ore emplacement to a system of compression-tension faulting. Beyond the observation that orebodies are found in areas of concentration of cross faulting and fault controlled dykes, no general rule of fault control of orebodies is consistent throughout the mine (Mine staff, personal communication, 1971).

A series of sections showing the relative thicknesses of the upper three volcanic rock units of the mine are shown in figure 13a-c (after sections compiled under the supervision of H. Jones, Geophysical Engineering and Surveys Limited, 1971). The units were identified by underground mapping; distances were measured within individual fault blocks and contours projected to the plane of the base of the pyritic zone. Difficulty was encountered delineating the contacts consistently between measured drill cores as alternations of rock type occurs within each of the major units. The plane of section is that of figure 12. A detailed description of the volcanic rock types is given in sections B and C of this chapter.

The upper unit is rhyolite which has an average thickness of less than 200', but is absent in the northeast of the mine (Fig. 13a). By combining figures 13a and 13b it can be seen that the rhyolite breccia is thickest in the central part of the mine and thins laterally and with depth. The rhyolite fragmental averages less than 200' in the southwest, but thickens considerably to over 600' in the northeast of the mine and is in contact with the pyritic zone (Fig. 13c).

If the assumption is made that the contact between the pyritic zone and the underlying volcanic rocks represented an original stratigraphic horizon of the volcanic rocks it is possible to draw a hypothetical cross section through the mine rocks, reconstructing their original geometry prior to folding and faulting (Fig. 14). The volcanic rock-pyritic zone contact is drawn as an original, regular volcanic surface. The thickening of the rhyolite fragmental and the rhyolite breccia underlying it in the northeast of the mine suggests that this area may represent

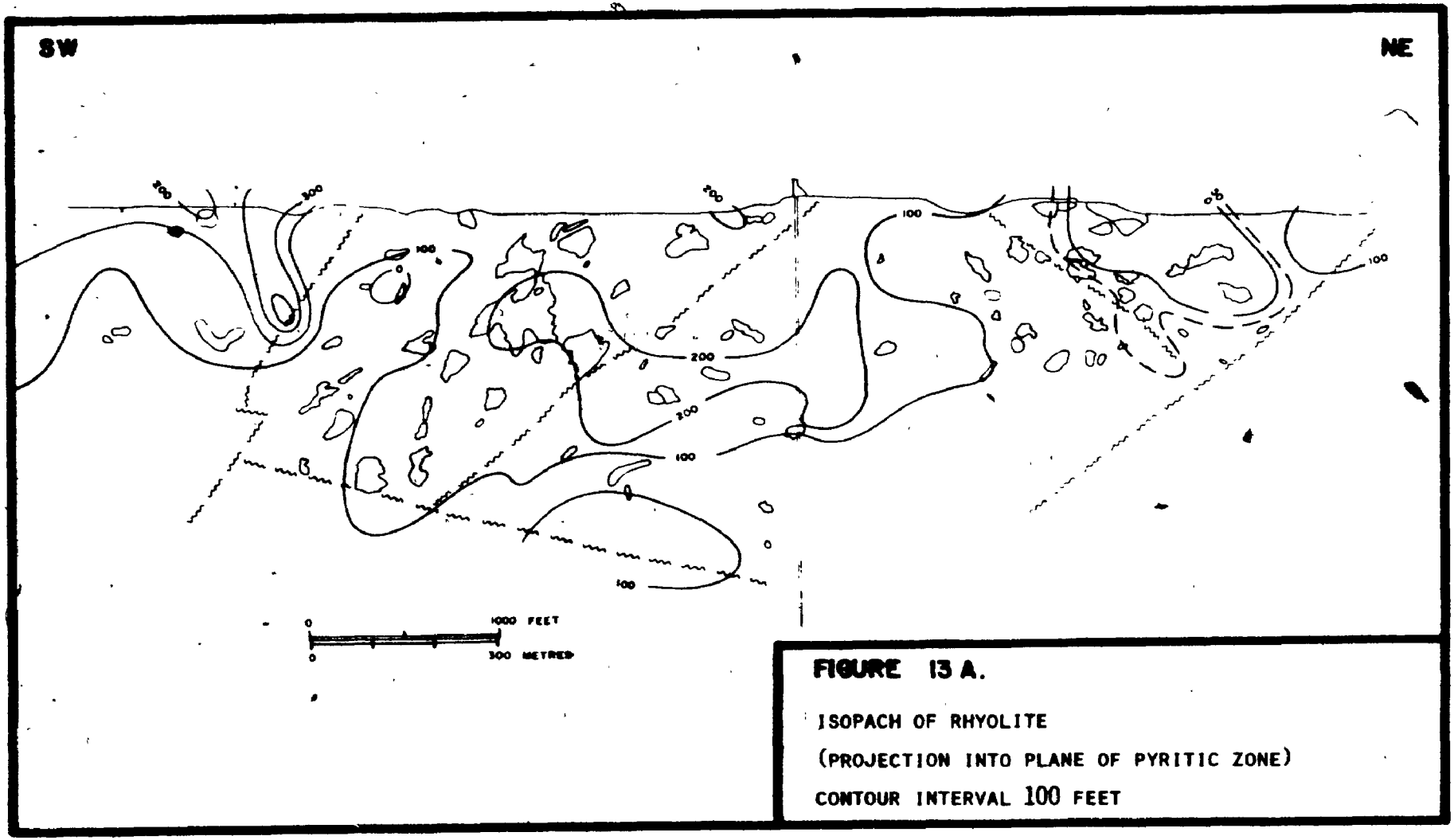

FIGURE 13 A.

ISOPACH OF RHYOLITE

(PROJECTION INTO PLANE OF PYRITIC ZONE)

CONTOUR INTERVAL 100 FEET

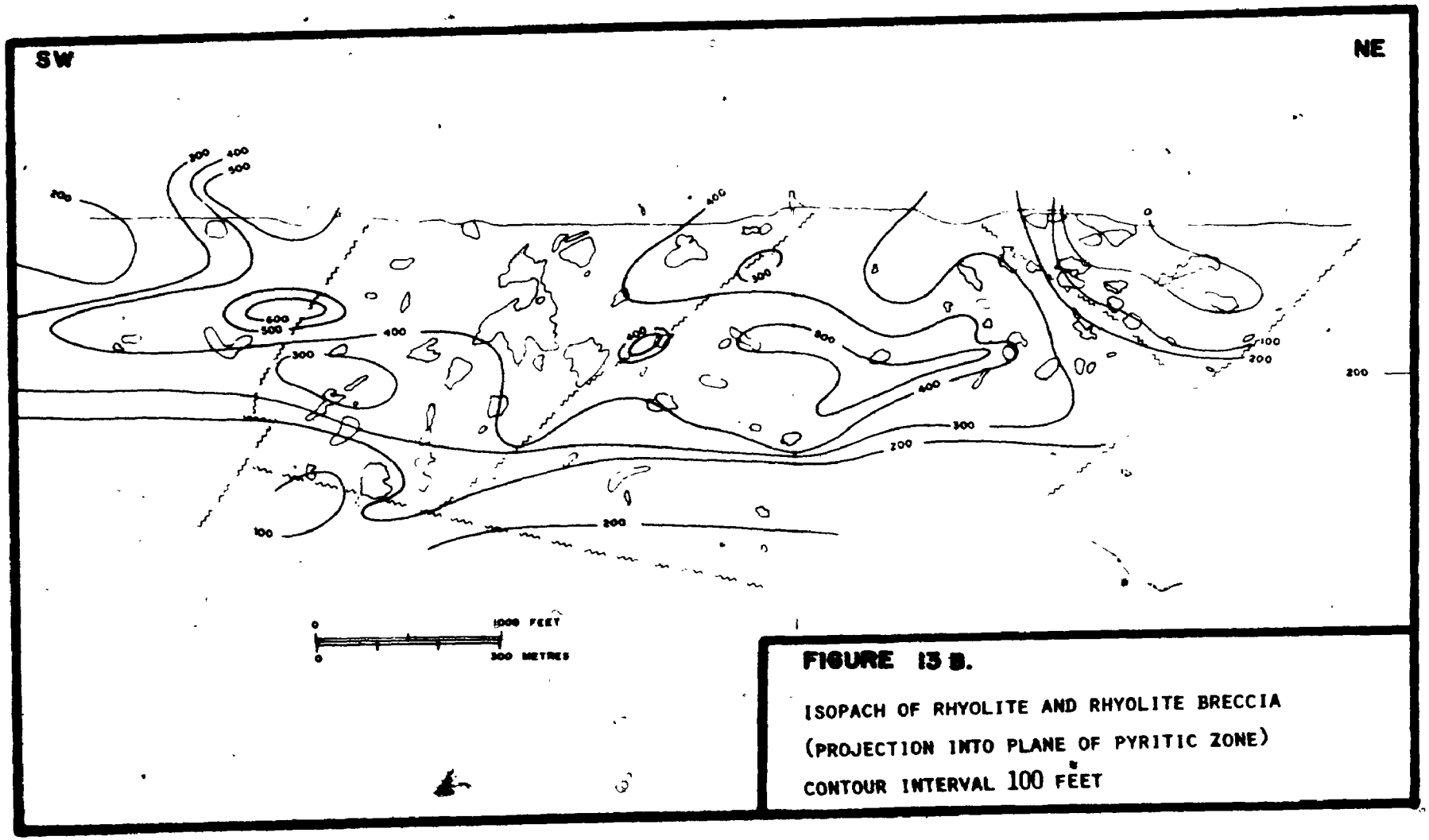

FIGURE 13 B.

ISOPACH OF RHYOLITE AND RHYOLITE BRECCIA
(PROJECTION INTO PLANE OF PYRITIC ZONE)
CONTOUR INTERVAL 100 FEET

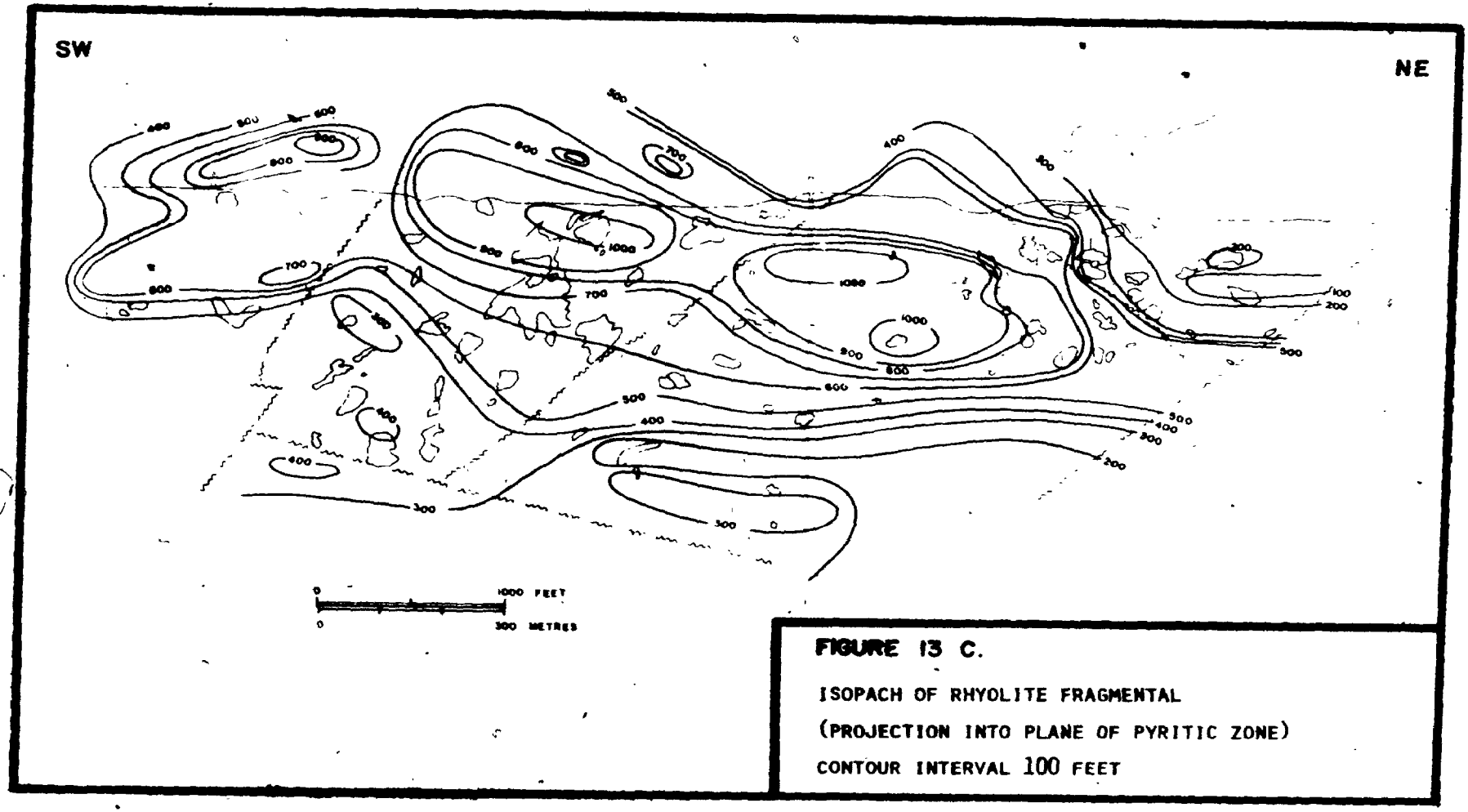

FIGURE 13 C.

ISOPACH OF RHYOLITE FRAGMENTAL
(PROJECTION INTO PLANE OF PYRITIC ZONE)
CONTOUR INTERVAL 100 FEET

FIGURE 14.

RECONSTRUCTION OF MINE VOLCANIC ROCK UNITS

HORIZONTAL SCALE 0 500 1000 FEET

VERTICAL SCALE 0 100 200 300 FEET

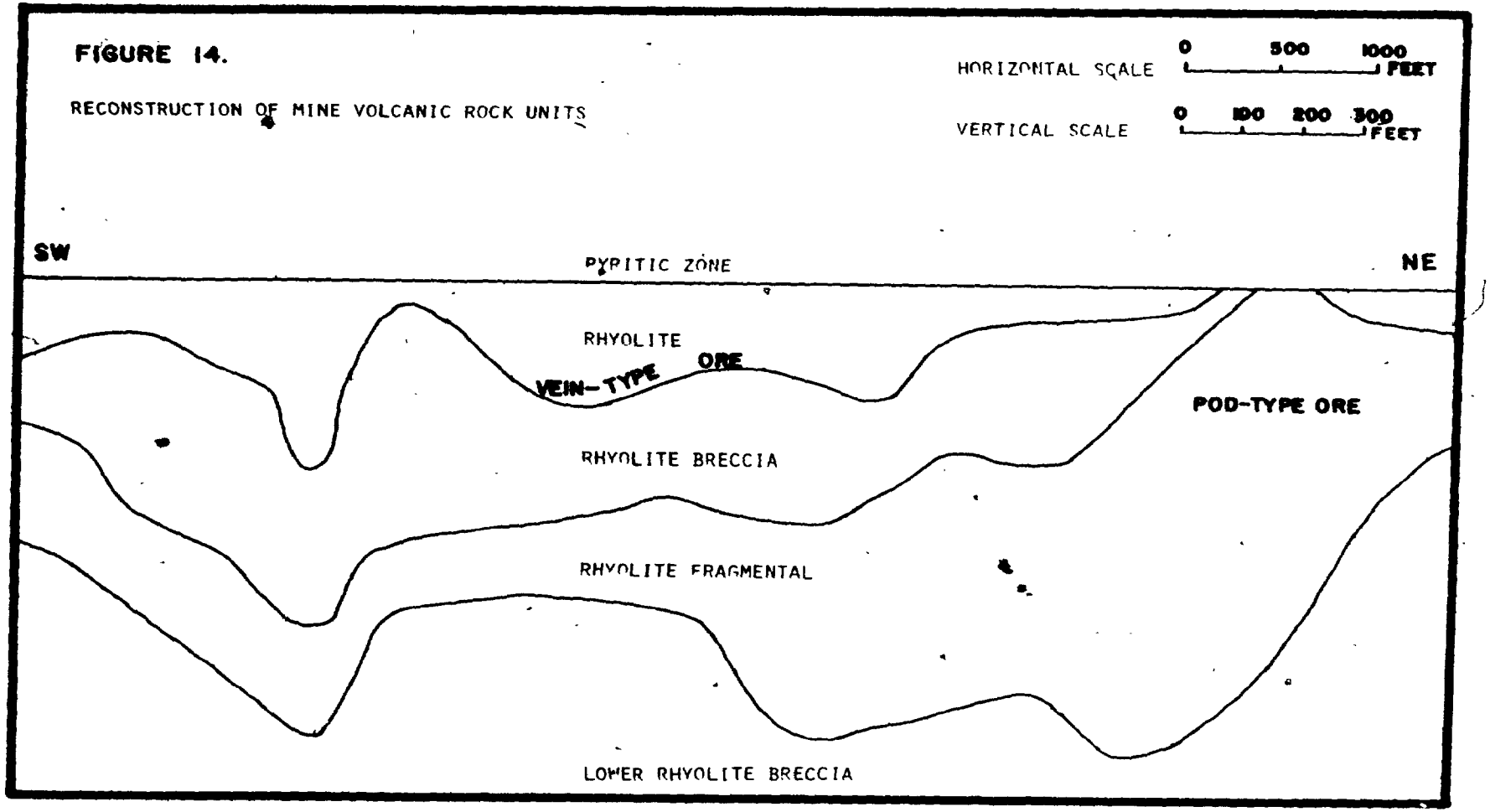

an original topographic high as a centre of volcanic activity during extrusion of the mine rocks. The overlying rhyolite breccia was therefore deposited round the margins of this volcanic centre; fragment size and thickness of the unit decrease with distance from this centre. The overlying rhyolite may have been a more mobile, less viscous flow which filled irregularities in the rhyolite breccia surface and had itself a relatively flat, regular top surface. This subject will be discussed further in Chapter V.

2. Orebodies

The original mine classification of the orebodies subdivided them into two groups on the basis of their thickness: the pod-type with a maximum thickness of 50', the vein-type 25'. This classification was later modified to one based on host rock of the orebodies (Patrick, 1966): the pod-type within the rhyolite fragmental, the vein type at or adjacent to the rhyolite-rhyolite breccia contact (Fig. 14). The general thickness relationship is however still valid. The pod-type is restricted to the northeastern part of the mine, where the rhyolite fragmental lies close to, or is in contact with, the pyritic zone. All orebodies lie between 50 and 300' below the base of the pyritic zone, and most lie close to the average distance of 200'.

The mineralogy of pod- and vein-type orebodies is similar, consisting of chalcopyrite, pyrite, millerite, sphalerite, gersdorffite, magnetite and gangue. The following description of the mineralogy is based partially on the work of Franklin (1967).

Chalcopyrite ($CuFeS_2$) constitutes between 65 and 85% of the orebodies. It occurs as equant, tightly interlocking grains averaging 0.4 mm; grains may be twinned but show no cleavage.

Pyrite (FeS_2) constitutes up to 25% of the orebodies. It occurs in the form of euhedral grains within chalcopyrite masses, either randomly distributed or aligned in trains. Pyrite-rich masses or lenses occur within some orebodies, commonly in the lower portion of vein-type orebodies as a pyritic "keel" (Patrick, 1966). Pyritic nodules up to 25 cm in diameter occur in smooth walled voids within chalcopyrite (Plate 11). They consist of platy ribs of pyrite which form a cellular structure (Rose, 1966b). These nodules appear to be more common in thicker veins and pods (Patrick, 1966).

Sphalerite (ZnS) is present as an accessory mineral within carbonate-rich portions of the orebodies. The anhedral grains average 0.1 mm and may contain minute chalcopyrite inclusions. Millerite (NiS) occurs in twinned euhedral bladed crystals up to 3 cm in length. It is found predominantly in pod-type orebodies, associated with relative concentrations of gersdorffite (NiAsS). Millerite is generally scarce, but no quantitative estimate of nickel concentration in the orebodies has been made. Small grains of gersdorffite are present, normally located near gangue-chalcopyrite boundaries. Magnetite grains averaging 0.15 mm in diameter are present, either randomly distributed or in narrow bands of concentration. Galena, silver, sperrylite and gold have also been identified in trace quantities within the orebodies (Franklin, 1967).

The gangue minerals are predominantly quartz and carbonate, which constitute up to 20% of the orebodies. They occur as blebs, stringers, veins and intricate network structures within the sulphides.

Sulphide-wallrock contacts are normally sharp (Plates 9 and 10). The pod-type orebodies may be surrounded by a zone of disseminated chalcopyrite. The vein-type orebodies normally thin laterally into narrow stringers; the orebody boundaries as shown (Fig. 12) are the limits

of economic mining. Stringers may widen out again, typical of the irregular shape of the vein-type orebodies, attenuated parallel to the rhyolite-rhyolite breccia contact. Adjacent to some vein-type orebodies "breccia ore" (Patrick, 1966) occurs, in which chalcopyrite fills fractures and voids in the rhyolite breccia.

Concentrations of sulphides occur in two other environments within the felsic volcanic rocks. The first occurrence is that of chalcopyrite with pyrite and rarely bornite in quartz-carbonate veins up to two feet in width. These veins transect the volcanic units and the orebodies and may occupy fault zones. A high concentration of veins appears to occur transecting the rocks close to orebodies; a higher concentration of chalcopyrite is found within the veins immediately adjacent to the orebodies (Patrick, 1966). These veins run parallel to the dominant drilling direction in the mine and are therefore intersected infrequently, thus their distribution is not mapped in detail. The second sulphide occurrence is that of chalcopyrite within rhyolite breccia approximately 1000' stratigraphically below the pyritic zone in the northeast of the mine. Chalcopyrite occurs as small grains around the margins of large andesite fragments in a more felsic matrix. Copper content of 1% has been found in a volume of rock with a thickness of up to 100' and a lateral extent of several hundred feet.

3. Pyritic Zone

The pyritic zone is the largest concentration of sulphides within the Temagami greenstone belt. It lies at the base of the metadiorite which is traceable intermittently from its unconformable contact with the Gowganda conglomerate to the southwest of the mine, along most of

the Northeast Arm of Lake Temagami (Fig. 1). About two miles from Temagami townsite it narrows and appears to terminate in a faulted contact. Aeromagnetic surveys indicate that it continues for several miles to the southwest of the mine under the sedimentary rock cover. Sulphide concentrations in the mine at the base of the metadiorite vary from disseminated pyrite to massive pyrite over 50' in thickness.

The pyritic zone mineralogy within the mine is pyrite with chalcopyrite, millerite, siegenite, gersdorffite, hematite, magnetite, leucoxene and gangue minerals. Concentration of the minor sulphide minerals is not necessarily directly proportional to the amount of pyrite present (Patrick, 1966).

Pyrite constitutes up to 80% of the total volume of the pyritic zone and up to 98% of the sulphide volume. It is anhedral with average grain size of 0.5 mm. Franklin (1967) recognised two distinct pyrite species; one has low relief containing "up to 6% nickel", the other higher relief and low nickel content. Similar nickeloan pyrite has been recognised in association with the Sudbury nickel deposits (Hawley, 1962). It occurs in the Temagami Mine in areas of concentration of other nickel sulphides.

Chalcopyrite occurs both in pyrite masses and within the gangue. In pyrite masses it occurs interstitially as fracture fillings and as minute inclusions within pyrite grains. Small euhedral grains of chalcopyrite are distributed throughout the chloritic gangue. Concentrations of chalcopyrite within the gangue are normally highest where the massive pyrite portion of the pyritic zone is absent.

Millerite occurs interstitially within pyrite aggregates, and co-

exists with chalcopyrite. Individual grains within a small area have parallel optic orientation. Small euhedral grains of millerite occur with siegenite grains. Siegenite occurs throughout the pyritic zone, both in pyritic masses and within the silicate gangue. The composition within the polydymite (Ni_3S_4)-linnaeite (Co_3S_4) solid solution series has not been accurately determined. Textural relationships suggest contemporaneous crystallization of siegenite, millerite and chalcopyrite (Franklin, 1967).

Gersdorffite is present in minor quantities and is found either close to the base of the pyritic zone or in areas of disseminated sulphides. Magnetite and hematite pseudomorphs after magnetite occur as disseminated grains throughout the pyritic zone. Magnetite also occurs in zones of concentration sufficiently large to be depicted as "magnetite veins" in underground mapping. Coarse grained skeletal leucoxene is present in the upper part of the pyritic zone.

The gangue mineralogy in two sections through the pyritic zone will be described in sections B and C of this chapter. The lower contact of the pyritic zone has been described as sharp (Franklin, 1967). The lower contact of massive sulphide is normally sharp - not with fresh volcanic rocks, but with a chloritized volcanic rock containing disseminated sulphides. These rocks grade into fresher volcanic rocks over a few feet. Similarly the host rock to the massive sulphide has normally been equated with the metadiorite because of its chloritic, mafic nature. It does not however have any features which allow its positive identification as fine grained metadiorite. Only in the upper part of the pyritic zone are distinguishing features encountered which

are typical of the metadiorite: altered feldspar and leucoxene phenocrysts and large quartz eyes. The upper contact of the pyritic zone is gradational, sulphide content decreasing upwards; the contact is delineated in the mine at the level where sulphide volume constitutes less than 5% of the rock. The average mapped thickness of the pyritic zone decreases westwards and at depths below 800', and is normally represented in these areas by a zone of disseminated sulphides. A few large angular blocks of rhyolite have been mapped within the pyritic zone.

4. Trace Element Content of Sulphides

Scott (1969) studied the trace element content of coexisting pyrite and chalcopyrite in sulphide concentrations, the vein-type orebodies in the southwest and also northeast of the mine, and the pod-type orebodies. She also sampled from the pyritic zone immediately adjacent to each orebody sample. The main observation from this geochemical study was that there is a significant difference in trace element sulphide content between orebody and adjacent pyritic zone samples (Table 6). Scott concluded from this that the sulphides of the two zones had a different history, although not necessarily a different origin.

Scott also studied variations in trace element content of sulphides with depth from surface, but found no obvious relationships. She did not study lateral variations in trace elements. It is considered worthwhile to present her data in a format in which lateral variations can be more readily seen. Table 6 shows the mean values of each of Scott's three sample groupings in their relative geographic locations. Lateral variations within the pyritic zone are most distinctive. Gold, manganese and nickel within chalcopyrite and to a lesser extent cobalt and nickel

TABLE 6

MEAN TRACE ELEMENT DISTRIBUTIONS IN SULPHIDES OF TEMAGAMI MINE

(after Scott, 1969)

		West Vein-Type		East Vein-Type		Pod-Type	
		Py.	Cp.	Py.	Cp.	Py.	Cp.
GOLD (ppm)	Py. Zone	76	28	85	50	70	63
	Ore Zone	78	41	136	45	95	47
MANGANESE (ppm)	Py. Zone	21	36	26	55	24	115
	Ore Zone	4	10	6	16	5	15
SILVER (ppm)	Py. Zone	160	65	120	85	400	78
	Ore Zone	65	65	200	83	115	82
ZINC (ppm)	Py. Zone	30	500	50	400	45	830
	Ore Zone	380	280	700	360	1,625	350
COBALT (ppm)	Py. Zone	1,950	460	1,900	500	1,350	380
	Ore Zone	1,700	80	1,900	220	1,300	240
NICKEL (ppm)	Py. Zone	5,200	1,700	10,500	2,200	11,600	3,400
	Ore Zone	6,000	600	5,000	1,400	5,000	7,500
COBALT/NICKEL	Py. Zone	.37		.18		.12	
	Ore Zone	.28		.38		.26	

in pyrite show a distinctive regular variation. If the northeastern part of the mine can be considered to have been an original centre of volcanism, then this variation may be related to distance from this centre. Insufficient experimental work has been done, however, to explain whether this variation is related to variations in temperature, pressure or partial pressure of volatile components.

The most important results of Scott's work relating to the genesis of the sulphide deposits is her study of cobalt and nickel content and ratios. A considerable amount of work has been performed concerning cobalt and nickel content of pyrites from different geological environments throughout the world (Loftus-Hills and Solomon, 1967). Two distinctive categories of massive sulphide deposits have been outlined in the Precambrian of Canada, in terms of cobalt and nickel content of associated pyrites. The Sudbury nickel ores are associated with mafic intrusive rocks; their pyrites have high cobalt and nickel content and low Co:Ni ratios. Copper and copper-zinc deposits associated with felsic volcanic rocks have lower cobalt and nickel content and high Co:Ni.

The data from several Canadian mines, including the Temagami Mine, are summarized in Table 7 (after Scott, 1969). Most noticeable is the exceptionally high nickel content of the Temagami pyrite relative to other dominantly copper deposits, whereas cobalt values are similar to these. Co:Ni ratios are therefore low, closer to the Sudbury values. These results show that the Temagami pyrites have features similar to those of both mafic intrusive and felsic volcanic association; this evidence indicates that the Temagami pyrites may have been derived by a process intermediate between these two types.

TABLE 7

MEAN CONCENTRATION OF COBALT AND NICKEL IN PYRITES FROM VARIOUS CANADIAN MINES (after Scott, 1969)

Deposit		Co ppm	Ni ppm	Co:Ni
Nickel ores -				
Sudbury	1)	13,300	2,500	5.3
	1)	10,300	1,000	10.3
	1)	1,800	2,000	0.9
Sudbury (early)	4)	5,600	500	11.2
Sudbury (late)	4)	4,000	38,000 - 52,000	0.11 - 0.08
Copper ores -				
Temagami ore	3)	1,700	5,500	0.31
Temagami pyritic zone	3)	1,800	8,400	0.22
Chibougamau	1)	3,000	110	27.3
	2)	4,500	570	7.9
Noranda	1)	1,160	41	28.3
Quemont	1)	840	22	38.2
Quemont, Vauze (disseminated Cu ore)	2)	400	100	4.0
Horne (massive Cu-Au ore)	2)	900	70	12.9
Massive Zn-Cu ores -				
Matagami	2)	600	70	8.6
Noranda	2)	500	130	3.8
Gold ores -				
McIntyre	1)	790	410	1.9

1) Hawley and Nichol, 1961
2) Roscoe, 1965
3) Scott, 1969
4) Hawley, 1962

5. Sulphur Isotopes

Isotopic sulphur content (S^{32} and S^{34}) of chalcopyrite and/or pyrite was measured in ten samples, taken from vein and pod type orebodies and adjacent pyritic zone. In all instances S^{32}:S^{34} ratios were close to those of the Canyon Diablo meteorite (Jensen and Nakai, 1963). This indicates that the sulphur has been derived directly from a magmatic source, probably of mantle origin, and has not undergone biogenic fractionation (Jensen, 1967).

Ohmoto (1972) has demonstrated that numerous variables affect isotopic sulphur fractionation. At least three equally plausible explanations can be put forward to explain the observed isotopic sulphur contents, assuming these are representative of isotopic equilibrium. The sulphur was derived from a mantle source; the sulphur was derived from Archean sea water which had itself not undergone significant bacterial fractionation to produce S^{34} enrichment; the sulphur was derived from S^{34} enriched sea water, which had undergone reduction and sulphate deposition causing S^{34} depletion, prior to sulphide deposition in the orebodies and pyritic zone.

S^{34} fractionation between samples of coexisting chalcopyrite and pyrite indicates temperatures of crystallization of 300-500°C (Kajiwara and Krouse, 1971). This temperature range is consistent with assumed temperatures attained during regional metamorphism, and may reflect sulphide recrystallization during metamorphism. Details of sample collection and preparation, analytical techniques and results are presented in Appendix 5.

B. Mineralogy, Chemistry and Alteration Around the No. 4 Orebody

The presence of tourmaline associated with the No. 4 and other pod-type orebodies has been cited by Patrick (1966) as evidence of wallrock alteration associated with these orebodies. The present study was carried out to define variations in mineralogy and chemistry of the rocks around the No. 4 orebody, which might be related to the presence of the sulphide concentration.

The cross section through the orebody chosen for study is shown in figure 15. This section appears to lie within a single major fault block and is sufficiently far distant from other orebodies that localized alteration zones might not interfere. The area of diamond drill coverage was the largest for a single cross-section; all core was available for study apart from the upper sections, within metadiorite (Fig. 15), which had been discarded after examination by mine geologists.

An interpretation of the geological units in this cross section, compiled by mine geologists from drill core and underground exposure examination, is also shown in figure 15. The area depicted as orebody in this figure is the outline of the mined area. The orebody itself had variable thickness, up to 25' in the centre with two 5' wide veins on the margins. The orebody was up to 300' in length extending 150' on either side of this cross section.

1. Petrography

Drill core from the cross section was split lengthwise using a diamond saw and re-examined. Thin sections made from samples distributed down the length of the cores were also examined. A description and interpretive classification of these rocks is shown in table 8. An interpretation of the geology of the cross-section using drill core and thin

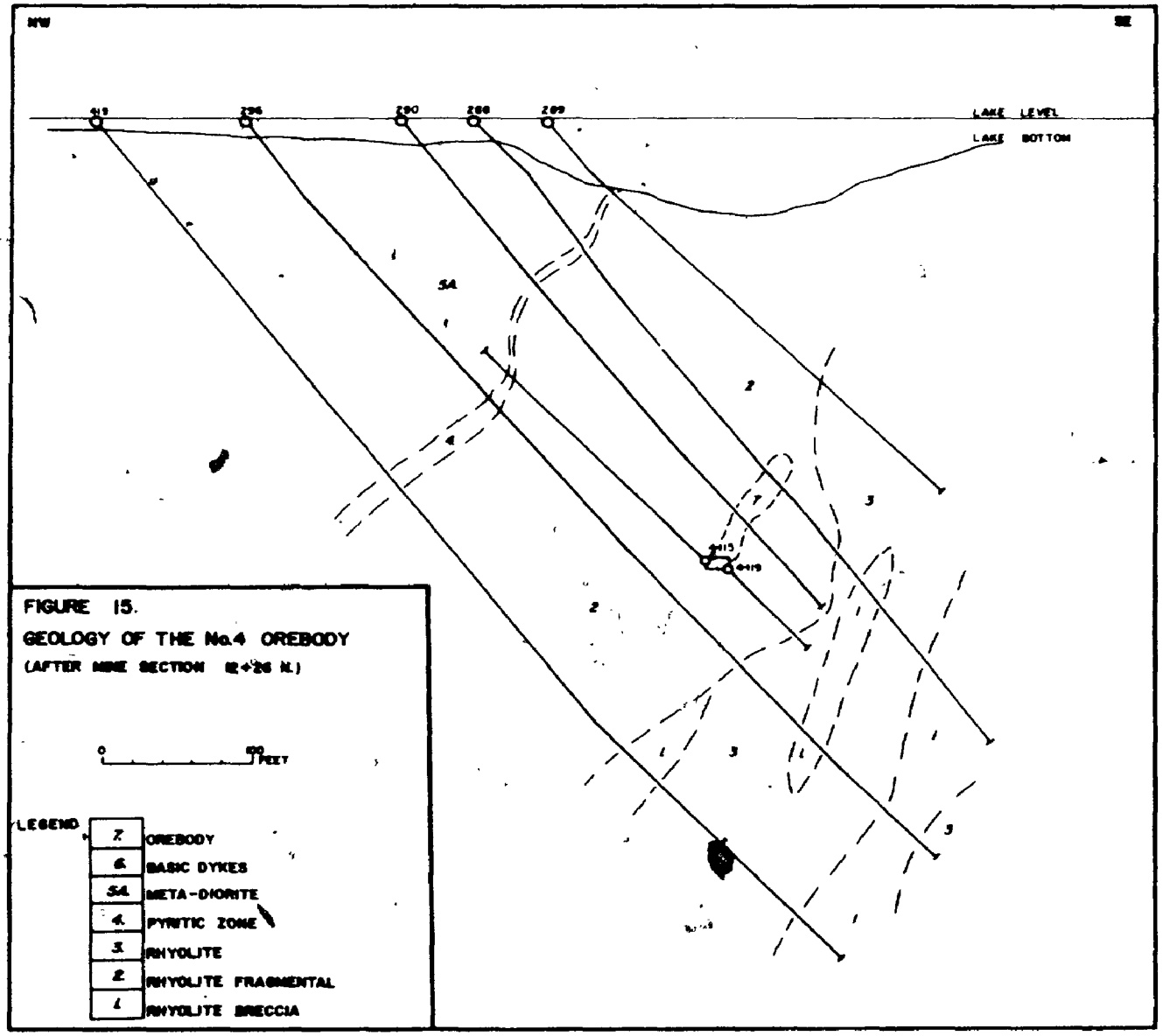

FIGURE 15.
GEOLOGY OF THE No.4 OREBODY
(AFTER MINE SECTION 12+26 N.)

SAMPLE NUMBERS	HAND SPECIMEN	THIN SECTION				INTERPRETIVE IGNEOUS NAME
		TEXTURE	PHENOCRYST-METACRYST MINERALOGY		GROUNDMASS MINERALOGY	
Group: 1 43,30,25,52,59,104,272,276,154,157,164,215.	massive or fractured. light coloured qtz. rich aggregates to 10 mm., light grey finer grd. lower in sequence.	qtz. equigranular to 0.1 mm., micas rimming qtz. grains and aggregates.	To.	1-3 mm. euhedral to subhedral grains or larger aggregates or veinlets, irregular distribution, poikiloblastically enclosing qtz. grains. 1-20% of rock.	Qtz. anhedral equigranular. 50-60% Ab. very fine grd. 3-10% Ser. fine grd. matrix to qtz. grains, coarser grd. patches rimming qtz. aggregates. 15-30% Carb. rare, fine grd. 1-10% Chl. rare, fine grd., outside qtz. aggregates. 3- 8% Py.-Cp. individual grains.	Rhyolite.
Group: 2 50,101,201,200,279.	massive or fractured. green grey fine grd., buff coloured lc. patches. 279: highly chloritized, within pyritic zone.	similar to group: 1.	To.	similar to group: 1. 1-20% of rock.	Qtz. anhedral to subhedral, medium grd. 30-50% Ab. not recognised Ser. fine grd. with chl. 5-15% Carb. fine grd. throughout matrix. 2-15% Chl. fine grd. matrix to qtz. grains 15-35% Lc. few small to medium grains. 2- 3% Py.-Cp. individual grains. 0- 5%	Altered rhyolite. gradational contact with group: 1.
Group: 3 14,55,60,121,255,170,178,187,205,220,225,79.	fractured. light grey coloured mottled with darker green patches.	fine grd. equigranular qtz. in chl. & ser. matrix, coarser grd. qtz. aggregates and patches to 2 mm.	Ab. To.	euhedral to anhedral laths to 1 mm., strongly ser. & chl. rare.	Qtz. fine grd. throughout matrix, 0.05 mm. anhedral grains in aggregates. 35-40% Ab. fine grd. in matrix. 5-10% Ser. very fine laths in matrix. 15-25% Carb. fine grd. throughout matrix. 5-15% Chl. fine grd., in matrix and patches. 10-20% Py. individual grains. 0- 3%	Rhyodacite-dacite. gradational contact with group: 1.
Group: 4 10,8,1,3,5,116,250,261.	highly fractured and veined. qtz., carb., chl., cp. within fracture and vein network.	highly veined and altered, margins of some qtz. grains eroded, patches similar to groups: 1 & 3.	To.	similar to group: 1, mainly within veinlets. 1-20% of rock.	Qtz. anhedral to subhedral to 1 mm., fine grd. in matrix. 25-50% Ab. fine grd. in matrix. 5-10% Ser. variable in matrix and patches. 10-20% Carb. in matrix, patches and veinlets. 3-25% Chl. in matrix, patches and fractures fillings to 1 mm. 5-25% Cp. individual grains and veinlets. 0-15%	Altered rhyolite-dacite. gradational contact with groups: 1 & 3.
Group: 5 16,19,38,41,65,70,73,126,259,181,182,229,232.	massive or fractured, coarse breccia in places. dark green fine grd., chl. patches and fragments.	fine medium grd. equigranular, chl. patches to 1 mm.	Ab.	very highly altered to ser. & carb.	Qtz. anhedral grains to 0.2 mm., fine grd. in matrix. 20-30% Ab. not recognised. Ser. very fine laths. 2-10% Carb. fine grd. throughout matrix. 5-20% Chl. fine grd. in matrix and patches. 15-30% Py.,Mt. individual grains.	Massive or brecciated dacite-andesite.
Group: 6 48,128,188.	massive. dark grey-green coloured, large lighter lc., qtz., ab. grains.	highly altered pheno-metacryst in finer grd. chloritic matrix.	Qtz. Ab. Lc.	large euhedral grains to 4 mm. 10% of rock. remnant lath shaped grains highly cracked and altered to ser. & carb. 10%. large skeletal grains, remnant ilmenite exsolution	Qtz. fine grd. 5-10% Ab. fine grd. 3- 6% Carb. fine to medium grd. throughout matrix. 15-25% Chl. fine grd. 25-60% Epid. small individual grains. 5-15% Mt.-Py. individual grains.	Dolerite.

TABLE 8. PETROGRAPHY OF No.4 OREBODY SAMPLES

(ABBREVIATIONS SEE TABLE 2)

section data is shown in figure 16. A more detailed description of some of the minerals present is given in Appendix I. Also included in figure 16 are the locations of samples collected for chemical analysis and thin section. Additional thin sections were examined where necessary to better define the units. Further reference to the rock types of the section will use the interpretative igneous nomenclature of table 8.

The basal unit on the cross section is dacitic-andesitic in composition (Table 8, Group 5). Although large fragments are difficult to define in drill core, it appears to be made up in part of a coarse breccia, consisting of andesitic fragments up to 10 cm in length in a more felsic matrix. Several lenses of breccia and rhyodacite-dacite are present within this unit. A cross cut extending 800' southeastwards into the footwall rocks from this section shows considerably variation of rock types, the dominant one being a coarse breccia possibly equivalent to Group 5 (Plate 13).

Overlying the breccia is a fine grained, highly fractured rhyodacite-dacite (Group 3). This unit has a gradational contact with the overlying rhyolite unit (Group 1). The quartz content and grain size of the rhyolite unit increase upwards; it is possible that the transition between this unit and the underlying unit represents a progressive change in original magma composition.

The highly fractured rocks around the orebody are strongly veined such that original composition is modified (Group 4). Patches of this unit are less altered and retain the mineralogy and textures of the surrounding units.

The contact between rhyolite and altered rhyolite (Group 2) is

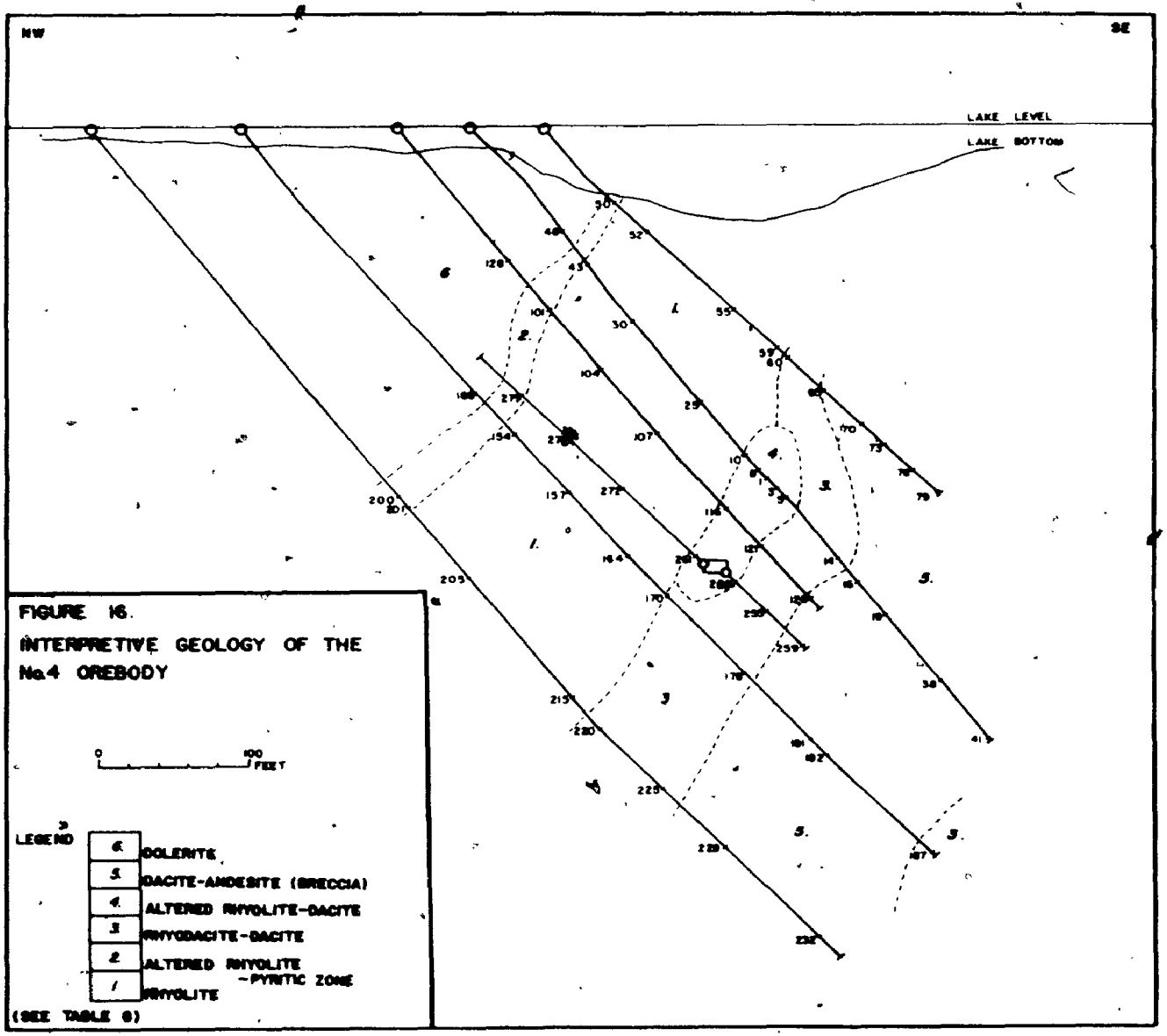
NW
SE
LAKE LEVEL
LAKE BOTTOM
FIGURE 16.
INTERPRETIVE GEOLOGY OF THE
No.4 OREBODY
0
100
FEET
LEGEND
6. DOLERITE
5. DACITE-ANDESITE (BRECCIA)
4. ALTERED RHYOLITE-DACITE
3. RHYODACITE-DACITE
2. ALTERED RHYOLITE
-PYRITIC ZONE
1. RHYOLITE
(SEE TABLE 6)

gradational. The quartz aggregate texture, typical of the rhyolite, is retained as the pyritic zone is approached. A section through the pyritic zone from samples 43 to 48 (Fig. 16), has been examined in detail. The quartz content of the rhyolite decreases and chlorite content increases as the pyritic zone is approached (Plate 6). Stringers of pyrite occur within this rock. The wallrock to the massive pyrite is a fine grained chloritic rock with quartz, sericite and carbonate; massive pyrite may be in contact with altered rhyolite, which is recognizable by its texture. In this drill core the massive pyrite is narrow with a thickness of less than 3'. Pyrite occurs in stringers and veins within the highly chloritized rock above this. Approximately 10' above the base of the massive pyrite the rock type changes and skeletal leucoxene (Plate 8) and altered plagioclase phenocrysts are present in a chlorite, carbonate and epidote-rich groundmass; these features are typical of the overlying dolerite (Group 6). The wallrock to the pyritic zone could not be recognized as either rhyolite or dolerite.

The volcanic rock units in this cross section appear to form a conformable sequence similar to that derived previously from core logging. Contacts between units are gradational and are the result of change in volcanic style or localized alteration. These units are similar to some of those previously described from the southwestern portion of the greenstone belt (Table 2); they were probably derived during the same phase of volcanic activity, many of them from the same centre of volcanism. Coarse breccias and siliceous rhyolites appear to be more common in this part of the mine.

2. Chemistry and Alteration

Variations in mineralogy and texture can be recognized optically

in the rocks in the immediate vicinity of the orebody and the pyritic zone. Abnormally high concentrations of tourmaline (Plate 7) spatially related to but more distant from the two sulphide zones may be indicative of more extensive wallrock alteration; other effects of this alteration may be masked from optical identification by the present complex metamorphic mineralogy. A study was therefore made of the wholerock chemistry in an attempt to define in quantitative terms more extensive alteration features within these rocks. A listing of the analytical data is presented in Appendix IV.

The chemical data were plotted in oxide-SiO_2 diagrams and compared with similarly plotted data from the surface samples collected from the southwestern portion of the greenstone belt (Appendix Fig. 1). Individual oxides and elements and combinations and ratios of these were plotted in their relative positions on cross sections; value contouring was performed using a standard system for all data. A large number of diagrams and graphs were examined; only those few considered of greatest significance are included and are presented in appendix IV as appendix figures 2-15.

The cross-section distribution patterns for the 13 major oxides and the 13 minor and metallic elements and the combinations of these show a wide range of variation. To simplify discussion they are divided into two categories: first, those in which the distribution appears to be controlled principally by the stratigraphic location of each sample and second, those in which the distribution cannot be explained solely on this basis.

Plotted against SiO_2 the oxides of the first category normally have tightly grouped distribution trends, similar to the trends of the surface samples. In cross-section, values within each stratigraphic unit (Fig. 16)

are similar and changes in values take place across geological contacts; contour lines therefore tend to run across section paralleling the contacts. Abnormal values may be found in the immediate proximity of the orebody or the pyritic zone.

One of the most significant patterns is that of SiO_2 (Appendix fig. 2) in which the stratigraphic sequence of figure 16 is clearly delineated. Only the most highly veined sample around the orebody (116) has an SiO_2 value significantly lower than the surrounding rocks. SiO_2 values decrease as the pyritic zone is approached, consistent with the decrease in quartz and increase in chlorite. This pattern substantiates the hypothesis that SiO_2 is relatively immobile within these rocks; it must be remembered however that free quartz content is itself one of the criteria used in optical classification. The validity of comparison of oxide-SiO_2 graphs is dependent on SiO_2 being immobile relative to the other oxides.

Plotted against SiO_2 the TiO_2 values show a wider range than the surface samples and consequently the distribution pattern on section is not well defined. TiO_2 is relatively low around and above the orebody.

Both FeO and Fe_2O_3 values show distribution patterns generally consistent with the stratigraphy; their combination produces a well defined pattern (Appendix Fig. 3). Values are generally high around the orebody, but this increase is exaggerated by the exceptionally high value of sample 116. The gradual increase in iron content of the rhyolite as the pyritic zone is approached is consistent with the increase of chlorite content. Plotted against SiO_2 the $FeO:Fe_2O_3$ ratios show a generally wider range than the surface samples; on section these values are low in the rhyolite and also around and below the orebody (Appendix Fig. 4). MnO values

have a wide range similar to the surface samples, and on section produce a poorly defined pattern generally consistent with the stratigraphy; values increase as the pyritic zone is approached. The more mafic samples have a lower MgO content than equivalent surface samples; plotted against SiO_2 all samples lie in a well defined trend with a low range of values. In section the distribution pattern is closely related to the stratigraphy, with little effect around the orebody; there is a gradual increase of MgO values as the pyritic zone is approached.

P_2O_5 values have a wide range similar to the surface samples; these values can be correlated roughly with the stratigraphy. Lithium values are close to the surface sample average and on section are stratigraphically distributed. Barium values, generally higher than the surface samples, on section show a general stratigraphic distribution; values are high around the orebody and decrease through the pyritic zone. Chromium and vanadium were not measured for the surface samples. They have average values of 50 and 30 ppm. respectively in the felsic rocks and 150 and 75 ppm. in the mafic rocks. Both are generally stratigraphically distributed.

The remaining oxides and elements belong to the second category. Plotted against SiO_2 the oxides tend to show a wider range of values than the surface samples. Distribution patterns on cross section are variable and appear to be partially controlled by factors other than stratigraphic location of samples.

Figure 17 shows an idealized alteration pattern around the orebody. This figure will be discussed later within this chapter; it is presented at this stage solely for ease of reference to specific areas of the cross section.

FIGURE 17

IDEALIZED ALTERATION ZONES AROUND THE No.4 OREBODY

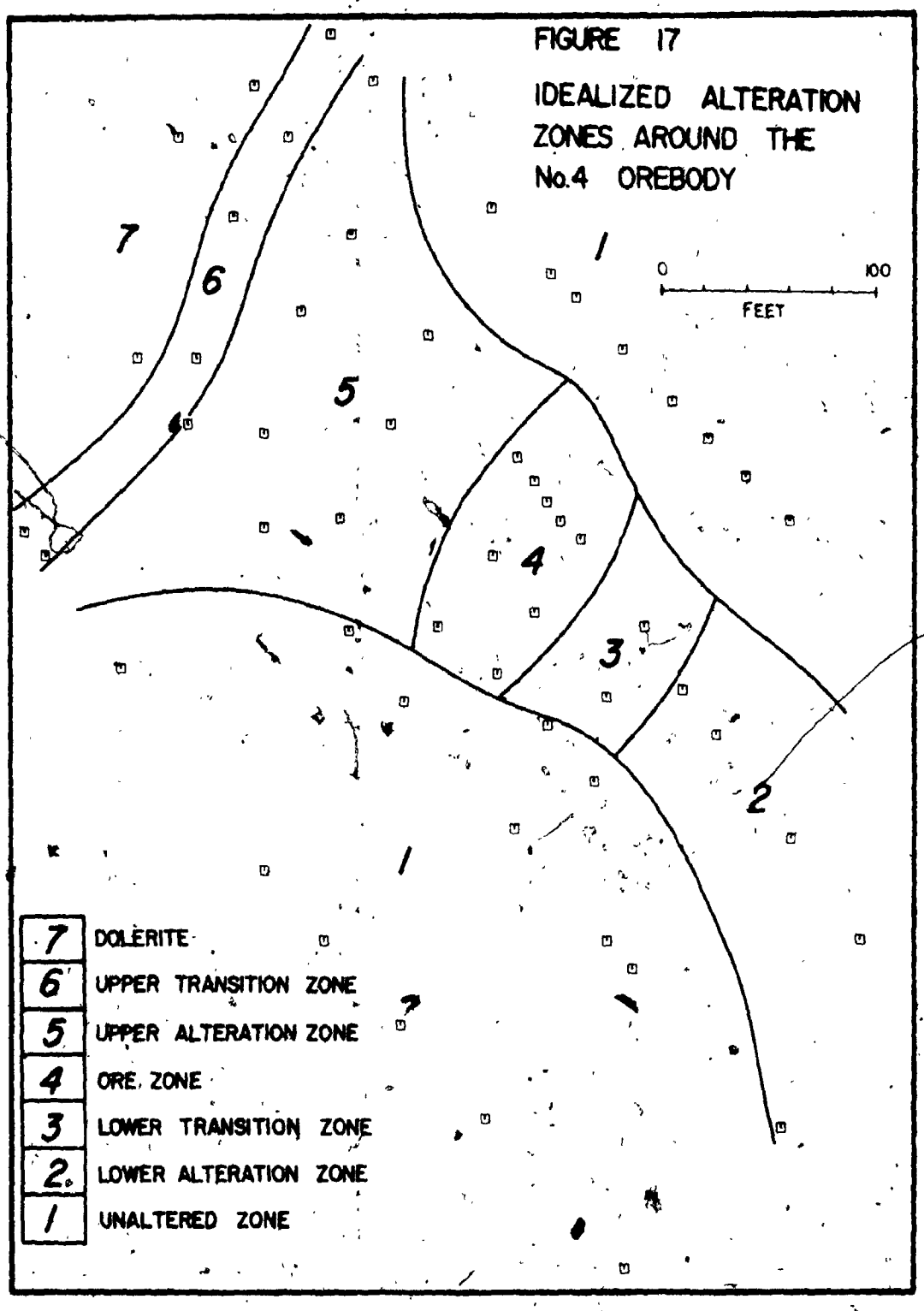

2 3

OF/DE

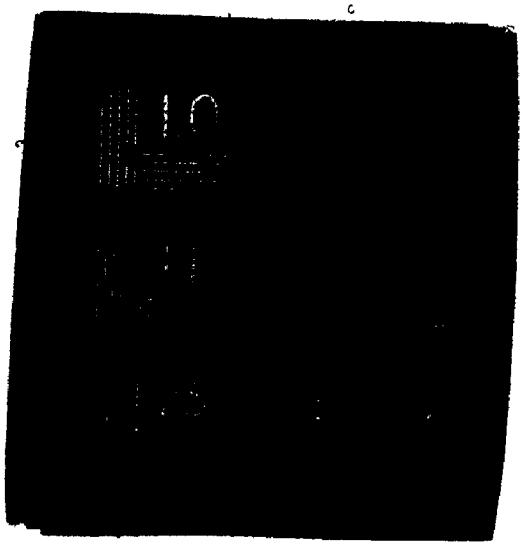

A quantitative estimate of tourmaline concentration is difficult to obtain in core or thin section as it occurs in patches and veinlets. A more accurate estimate of its concentration might be derived from boron analyses of the 5' sections of drill core. All samples have boron values higher than the 17 ppm. average for the surface samples, with the exception of those taken in the dolerite (Appendix Fig. 6). Concentrations are greatest in the ore zone; values are high in the upper alteration zone and decrease through the upper transition zone, although high values are present in samples 50 and 52. Values in the lower alteration zone are also slightly higher than surrounding samples, but are low within the lower transition zone.

Copper, lead, zinc, cobalt and nickel are all relatively higher around the orebody and close to the pyritic zone. Copper values are generally higher than the surface sample average of 40 ppm. although some values lower than this are present in the unaltered zones (Appendix Fig. 7). Highest values are found in the ore zone; their extent is exaggerated by the contouring technique. High values are present throughout the upper alteration zone and increase to the base of the pyritic zone; dolerite values are generally high. The high values of the lower alteration zone are separated from the ore zone by low values in a narrow transition zone.

Lead values are generally low or below detectable limits except in and below the ore zone and in the upper transition zone; they decrease from the base of the pyritic zone into the dolerite. Zinc values are generally higher than the 80 ppm. average for the surface samples (Appendix Fig. 8). Values are highest in and laterally from the ore zone,

a narrow upper alteration zone and in the upper transition zone; the dolerite has moderately high values.

Nickel values are generally close to the 80 ppm. average for the surface samples. Higher values are present only in and below the ore zone and in the upper transition zone and dolerite (Appendix fig. 9). Cobalt values are highest in the lower alteration zone but also increase through the upper transition zone into the dolerite. Elsewhere cobalt values are close to the surface sample average of 20 ppm. except for slightly higher values in the ore zone. Co:Ni ratios are therefore average in the unaltered and lower transition zones, high in the lower alteration zone, and low in all other zones (Appendix fig. 10).

Plotted against SiO_2, K_2O values appear to show a well defined distribution similar to that of the surface samples. On section their distribution pattern appears to be stratigraphically controlled. Low values are present in the ore zone and decrease through the upper transition zone. Na_2O and CaO however show a considerably wider range of values than the surface samples. Their distribution patterns on section are not well defined and show erratic changes of values (Appendix figs. 11, 12). Generally higher values are found in the unaltered zones (Fig. 17). The distribution pattern of CO_2 is almost identical to that of CaO, further confirming their relationship and the probability of CO_2 controlled CaO mobility.

The distribution of Na_2O and CaO in relation to the surface samples was investigated further in an attempt to better define their variation. Average Na_2O and CaO values were calculated for the surface samples using the same groupings as in Table 3, but using unmodified data containing

both H_2O and CO_2 (Appendix fig. 13). The No. 4 orebody samples were plotted on a similar diagram (Appendix fig. 14) in which it can be seen that all but two samples lie below the surface average join. Distance of each sample from the average join was measured relative to the vertical axis such that a quantitative estimate of relative Na_2O+CaO enrichment or depletion could be obtained. Values of ±1% are within the normal range of values of the surface samples and those up to ±2% cannot be considered anomalous. Greater than ±2% is well outside the range of values of the surface samples. Plotted on section these values form a distribution pattern similar to that of figure 17 (Appendix fig. 15). Greatest removal has taken place in the lower alteration zone, the ore zone and the upper alteration zone to the base of the pyritic zone. The dolerite does not appear to be affected by this alteration and is therefore assigned values of zero, but insufficient samples of it are available to make an accurate estimate of its variation. The nature of the dolerite will be discussed in section D of this chapter. Both Na_2O and CaO treated separately show a similar, though not so well defined removal pattern.

Plotted against SiO_2, Al_2O_3 values have a much wider distribution range than the surface samples. A narrow zone of low Al_2O_3 values is present around and above the orebody. Zirconium, strontium and gallium values are less easy to evaluate as these elements were not analysed in the surface samples. On section strontium and gallium have relatively lower values and zirconium relatively higher values in a narrow zone around and above the orebody.

The segments of the alteration zone shown in figure 17 are characterised

by relative enrichment or depletion of various oxides and elements. The characteristics of each zone are summarized in table 9. An interpretation of alteration zone and its relationship to the sulphide concentration is presented in Chapter V.

C. Mineralogy, Chemistry and Alteration Around the Empire No. 3 Orebody

No optically recognizable alteration features have been described either in the immediate vicinity of the vein-type orebodies or more distant from them. Vague references have been made to chloritic "haloes" (Franklin, 1967) around some vein-type orebodies, but these have not been described in detail. A cross-section through a vein-type orebody was therefore chosen for detailed study, similar to the study around the No. 4 orebody.

The cross-section investigated is shown in figure 18. The orebody is of small lateral extent and therefore the drill core available for study gave complete coverage around its margins. Although the cross section does not lie within a single fault block, the offsets due to faulting appeared to be small. None of the larger vein-type orebodies could be covered by a single cross-section in a similar manner.

Also shown in figure 18 is the interpretation of the geological sequences compiled by mine geologists. The geological sequences are generalized in the immediate vicinity of the orebody because of conflict between drill logs of adjacent cores. The orebody is considerably smaller than the No. 4 orebody; it is less than 300' in length and a maximum of 150' in width. Its thickness is variable, typical of vein-type orebodies, in some places consisting of 5' of massive chalcopyrite; in other places it is represented by several narrower veins of massive sulphide over

TABLE 9

RELATIVE CHANGE IN OXIDES AND ELEMENTS AROUND THE NO. 4 OREBODY
(for alteration zones see Fig. 17)

	lower alteration zone	lower transition zone	ore zone	upper alteration zone	upper transition zone	dolerite
SiO_2	0	0	-	0	-?	0
TiO_2	0	+	-?	-?	0	0
Al_2O_3	0	+	-	-	0	0
Fe_2O_3	0	-?	+	0	+	0
FeO	0	0	++	0	+	0
MnO	0	0	-	-	0	0
MgO	0	0	-	0	+	0
CaO	--	-	--	-	--	0?
Na_2O	--	-	--	--	-	0?
K_2O	0	0	-	0	0	0
P_2O_5	0	0	0	0	0	0
CO_2	-	+	-	-	-	0+
H_2O	0	+?	+	0	+	0
Cu	+	0	++	+	++	+?
Pb	0	+	+	0	+	0?
Zn	0	0	+	+	+	+?
Ni	0	+?	++	0	++	+?
Co	+	0	+	0	+	0?
Co:Ni	+	0	-	-	-	0?
Li	0	0	0	0	0	0
Ba	0	0	+	0	-?	0
B	+	0	++	++	+	0
Cr	0	+	0	0	0	n.a.
Ga	0	0	-	-	0	n.a.
Sr	0	0	-?	-	-?	n.a.
V	0	+	+?	0	+?	n.a.
Zr	0	0	+	+	+	n.a.

+ relative increase
- relative decrease
0 no change
n.a. not analysed

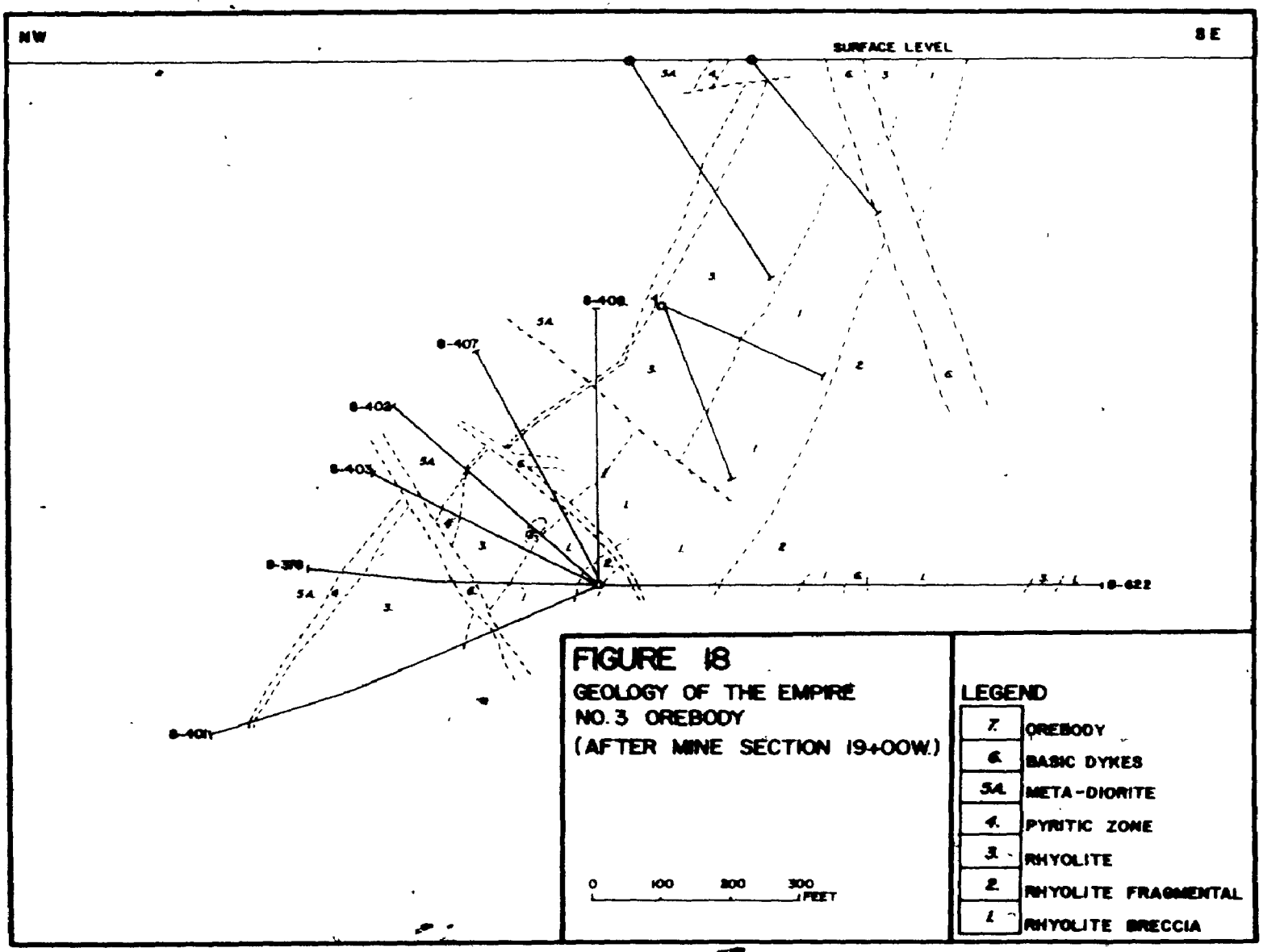
NW
SE
SURFACE LEVEL
B-408
B-407
B-402
B-403
B-379
B-401
B-622
FIGURE 18
GEOLOGY OF THE EMPIRE
NO. 3 OREBODY
(AFTER MINE SECTION 19+00W.)
0 100 200 300
FEET
LEGEND
7. OREBODY
6. BASIC DYKES
5A. META-DIORITE
4. PYRITIC ZONE
3. RHYOLITE
2. RHYOLITE FRAGMENTAL
1. RHYOLITE BRECCIA

a thickness of 20'.

1.--Petrography

The drill core was re-examined in a similar manner to that of the No. 4 orebody. A description of the thin sections is presented in Table 10. An interpretation of the geological units from drill core and thin section data is shown in figure 19. Also included in this figure are the locations of samples collected for thin section and chemical analysis. Further reference to the rock types of this section will use the interpretive igneous nomenclature of Table 10.

A thick breccia sequence underlies the upper volcanic units within this section (Table 10, Group 4) similar to the thick breccia unit underlying the No. 4 orebody section. This unit includes lenses of rhyolite-rhyodacite (Group 1). A thick rhyolite unit (Group 1) overlies the breccia, occurring between 300 and 400' from the base of the pyritic zone. This rhyolite is the lateral stratigraphic equivalent of the No. 4 orebody rhyolite (Fig. 14). The rhyolite is in turn overlain by another breccia unit which forms the footwall to most of the vein-type orebodies.

The breccia is overlain by a dacitic unit (Group 3) which forms the hanging wall to the vein-type orebodies and is in contact with the pyritic zone. Although this unit was initially less felsic than the rhyolite of the No. 4 orebody which is in contact with the pyritic zone, increasing chlorite content as the pyritic zone is approached is also recognizable within it (Group 3). Traversing the pyritic zone, porphyritic dolerite is not encountered until the zone of high sulphide concentration is crossed; a highly chloritic rock forms the wallrock to the massive sulphide.

SAMPLE NUMBERS	HAND SPECIMEN	THIN SECTION			
		TEXTURE	PHENOCRYST-METACRYST MINERALOGY	GROUNDMASS MINERALOGY	INTERPRETIVE IGNEOUS NAME
Group: 1 1,20,22,23,24,50, 51,52,60,61,62,63.	massive, fractured or brecciated. light coloured qtz. rich aggregates rimmed by chl. & ser., chl. stringers and patches.	fine to medium grd. equigranular, irregular chl. patches.	Qtz. few anhedral grains to 2 m Ab. highly altered to ser. & chl., remnant laths to 1.5 mm.	Qtz. anhedral equigranular. 45-60% Ab. very fine grd. 5-20% Ser. fine grd. euhedral, coarser grd. patches and stringers. 10-25% Carb. scarce, fine grd. 1-10% Chl. fine grd. patches and veinlets. 5-15% Lc.,Mt.,Py. & Cp. grains.	Rhyolite.
Group: 2 4,5,12,13,14,32, 33,34,44,53	massive. medium green coloured with small light patches.	fine to medium grd. equigranular.	Ab. laths to 3 mm., highly altered to ser. carb. to 10% of rock. Carb. euhedral rhombs to 1 mm.	Qtz. fine grd. anhedral. 25-35% Ab. fine grd. euhedral to anhedral. 5-15% Ser. fine grd. laths throughout. 10-20% Carb. fine grd. 5-15% Chl. very fine grd., some larger grains in patches. 10-25% Mt. & Lc. grains 13: small cp. stringers.	Dacite.
Group: 3 6,15,16,25,35,55.	massive or fractured. light grey-green coloured, chl. & carb. patches.	variable, fine to medium grd., anhedral to subhedral.	Ab. altered laths to 2 mm. 0-15% of rock. Qtz. anhedral grains to 1 mm.	Qtz. fine to medium grd. anhedral. 20-30% Ab. fine grd. 2-10% Ser. fine grd. scarce, small stringers. 5-15% Carb. fine grd. throughout and coarser grd. patches. 10-20% Chl. very fine grd., some larger grains in patches. 20-30% Py. grains and patches to 8 mm. 0- 5% Lc. small grains. Mt. small euhedral grains.	Altered dacite.
Group: 4 2,3,10,11,21,30,31, 40,41,42,43,64,65.	fine to coarse breccia, massive or fractured, fragments 3-30 mm. sharp to gradational margins. 10-70% of rock 64 & 65: fragments more siliceous than matrix.	fine and medium grd. patches.	FRAGMENTS: Ab. small laths highly altered Carb. euhedral rhombs to 2 mm. MATRIX: To. in sample 2, small grains.	FRAGMENTS: Qtz. fine grd. 20-25% Ab. very fine grd. anhedral. 5-10% Ser. fine wisps. 5% Carb. fine grd. throughout. 10-25% Chl. fine grd. throughout and coarser grd. patches. 20-30% Mt.,Lc. & Py. grains. MATRIX: similar to or more siliceous than group: 3.	Fragments: Andesite Matrix: Rhyodacite-dacite. Rock: Dacite breccia.
Group: 5 17,36,54.	massive. dark to light green coloured mottled appearance, remnant feldspar and lc. phenocrysts.	large highly altered phenometacrysts in fine grd. chloritic matrix.	Qtz. large anhedral grains. 0-10% of rock. Ab. laths highly altered to chl., ser., epid., & carb. 10-20%. Lc. large skeletal grains.	Qtz. fine grd. 5-10% Ab. fine grd. 5% Carb. fine to medium grd. throughout. 10-30% Chl. fine grd. 20-50% Epid. small grains. 5-15% Mt. & Py. grains.	Dolerite.

TABLE 10. PETROGRAPHY OF EMPIRE No.3 OREBODY SAMPLES

(ABBREVIATIONS SEE TABLE 2)

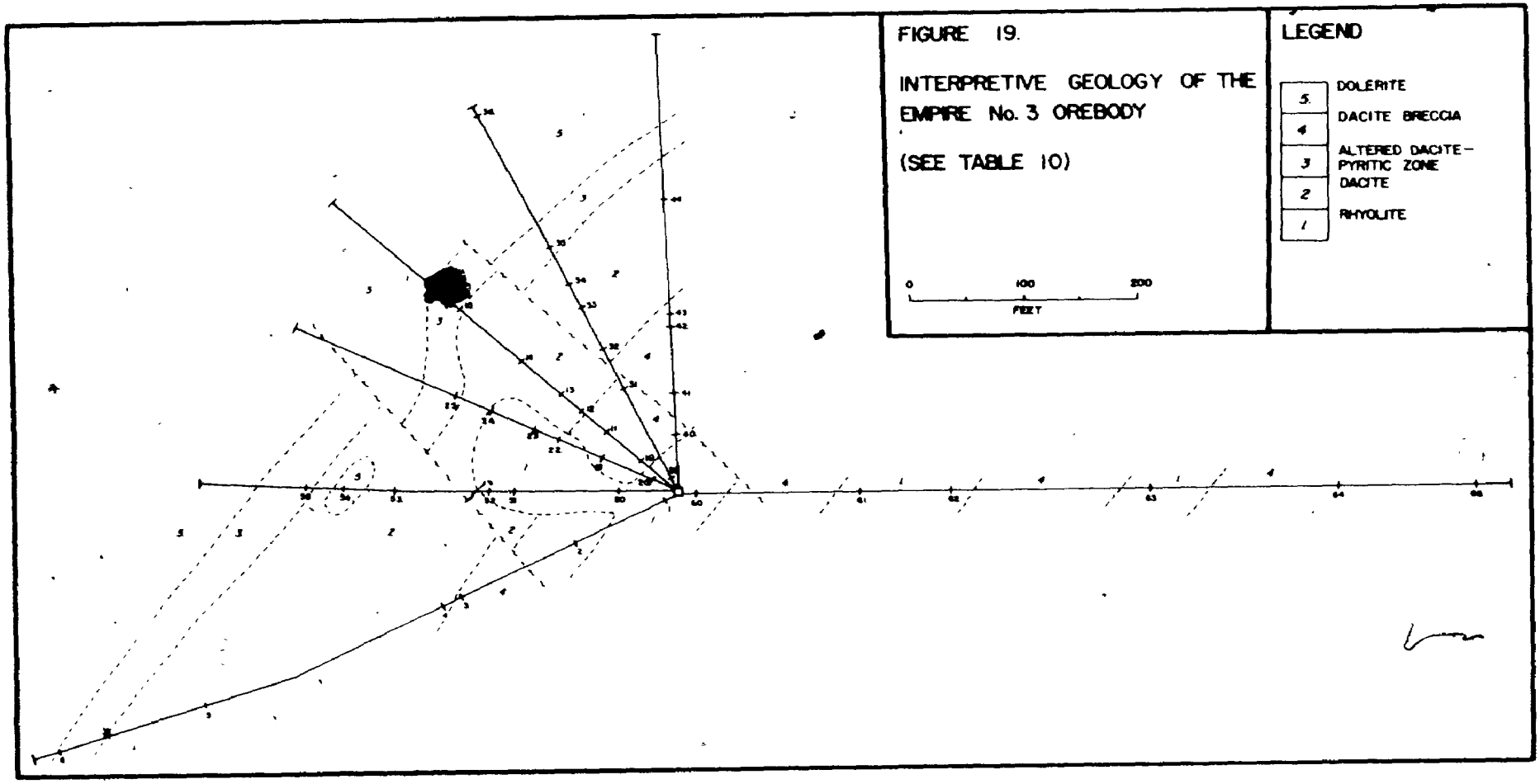
FIGURE 19.
INTERPRETIVE GEOLOGY OF THE EMPIRE No. 3 OREBODY
(SEE TABLE 10)
0
100
200
FEET
LEGEND
5. DOLERITE
4 DACITE BRECCIA
3 ALTERED DACITE – PYRITIC ZONE
2 DACITE
1 RHYOLITE

Sample 54 shows characteristics of the dolerite, but sample 55 is dacitic; faulting has caused repetition of the pyritic zone sequence.

The area around the orebody is less easy to interpret. Drill hole 8-402 (Fig. 18) is the only one in this section to intersect massive chalcopyrite; in this drill hole and in the two mine cross-sections 100' to the northeast and southwest of this cross-section the orebody lies close to the dacite-breccia contact. Drill holes 8-403 and 8-378 do not intersect the same sequence as those adjacent to them; they intersect a thick sequence of rhyolite which appears to be of limited lateral extent and is not present in the sections 100' to the northeast and southwest. Without more drill cores or underground exposure it is impossible to determine if this is an original volcanic feature or the result of complex faulting; its shape and contacts make the first possibility more probable.

No strong alteration effects are definable optically, even in the immediate vicinity of the orebody. Sample 12 contains a higher percentage of chlorite than surrounding samples, and sample 13 contains stringers of chalcopyrite.

The units within this section generally form a regular sequence, except in the proximity of the orebody. It is possible that the presence of the orebody is related to the irregularities in the volcanic sequence about it, but insufficient information is available to investigate this further. This type of irregularity is not a characteristic feature of other vein-type orebodies. The orebody therefore lies within dacite, immediately above the contact with breccia and on the margin of a dome shaped pile of rhyolite about 100' in diameter.

2. Chemistry and Alteration

The study of the chemistry of the rocks around the No. 3 orebody

was carried out to investigate the possibility of chemically definable alteration, not definable by optical study. A listing of the analytical data is presented in Appendix IV.

Data were plotted on graphs and cross-sections similar to those of the No. 4 orebody and studied in the same manner. Lateral variation of units around the orebody made interpretation of the data on cross-section more complex. Comparison of absolute percentage values is less significant if individual units are not continuous laterally; the contact between the dome of rhyolite and surrounding rocks is delineated in most chemical cross-sections. An attempt was therefore made to plot variation relative to expected values for each rock type. Offsets due to faulting further complicated the cross-section distribution patterns. Only those diagrams which were considered of greatest significance are included; they are presented in Appendix IV as Appendix figures 16-22.

The majority of distribution patterns were consistent with the stratigraphic distribution of samples; plotted against SiO_2 the oxides showed distribution similar to those of the surface samples.

SiO_2 has a distribution pattern consistent with the stratigraphy, although distorted about the dome of rhyolite (Appendix fig. 16). No significant change in SiO_2 content occurs around the orebody; SiO_2 decreases as the pyritic zone is approached.

TiO_2, Al_2O_3, MnO and MgO all have distributions similar to the surface samples when plotted against SiO_2, and patterns similar to the stratigraphy on section. Al_2O_3 shows a generally wider spread of values. The more mafic samples are lower in MgO than the surface samples, as are the mafic samples from the No. 4 orebody (Appendix fig. 5). FeO and

Fe_2O_3 also have distribution patterns consistent with the stratigraphy. FeO and $FeO:Fe_2O_3$ increase as the pyritic zone is approached and $FeO:Fe_2O_3$ ratios are high in the immediate vicinity of the orebody (Appendix fig. 17).

CaO, Na_2O and K_2O plotted individually against SiO_2 show distributions similar to the surface samples. The Na_2O+CaO vs. SiO_2 graph, most significant for the No. 4 orebody samples, shows the No. 3 orebody samples evenly distributed about the surface sample averages (Appendix fig. 18). CaO tends to be lower than expected in those samples close to the pyritic zone. No additional consistent variations of these oxides was found. CO_2 however shows generally low values at the stratigraphic level of the orebody (Appendix fig. 19).

P_2O_5 values show the greatest variation from the expected trend; plotted against SiO_2, almost half the samples have values considerably higher than their surface sample equivalents. Plotted on section, either as relative enrichment or absolute percentage (Appendix fig. 20), a narrow zone of enrichment is evident transecting the stratigraphic units from below the orebody to and widening towards the pyritic zone. Values are also high along the dacite-breccia contact.

Copper, lead, zinc, nickel and cobalt all show slight increases in the immediate proximity of the orebody; copper shows the greatest increase (Appendix fig. 21). With the exception of lead, these elements also increase as the pyritic zone is approached and decrease into the dolerite. In other parts of the section values are similar to the surface sample averages.

Lithium and barium values are similar to those of the surface samples. Boron distribution was particularly distinctive around the No. 4 orebody

(Appendix fig. 6) but in this section values for each sample are similar to or slightly higher than expected relative to the surface samples (Appendix fig. 22).

Neither chemically nor mineralogically does there appear to be any significant variation in these rocks which might be correlated with the presence of the two sulphide concentrations. Chemical distributions are similar to those expected from the stratigraphic location of each sample; only in the immediate vicinity of the orebody or the pyritic zone are anomalous values found. P_2O_5 is the only oxide which has a distribution which appears to be controlled by factors other than stratigraphic location of samples. CaO, Na_2O and boron, which were most strongly affected around the No. 4 orebody, do not appear to be significantly affected in this section. The complexity of the stratigraphy and structural deformation added to the difficulty of data interpretation. This part of the study has therefore not produced any positive results which might bear upon interpretation of sulphide genesis.

D. The Dolerite

The dolerite has been mentioned at three stages in the preceding text, but its overall characteristics have not been fully described. In and around Temagami Island it was originally mapped as basaltic (Moorhouse, 1946) and therefore part of the volcanic sequence. In later mapping of the area (Simony, 1964) it was depicted as two units, the lower (Southeastern) part a "Pre-Algoman diorite" intrusion, the upper part an andesitic flow. Geologists associated with the mine have interpreted it as a single unit in detailed mapping of the Temagami Island, although they have subdivided it into lower dioritic and upper gabbroic

phases (depicted as "metadiorite", fig. 4). The writer considers it to be a single unit because of the characteristic altered plagioclase and leucoxene phenocrysts present throughout it.

The dolerite is generally assumed to have intruded the volcanic rocks, although there is no conclusive evidence to support this hypothesis; the coarse grained nature of the remnant phenocrysts is put forward as evidence of its intrusive nature. The lower contact with volcanic rocks has been described and is not definable as either a volcanic or an intrusive contact. The upper contact of the dolerite with volcanic rocks is either water or drift covered, or overlain by Gowganda conglomerate. This contact has been transected by diamond drilling; a thick, carbonate-rich shear zone was intersected between dolerite and volcanic rocks. The writer has examined an outcrop which may include the upper contact; this outcrop is on the west side of Ogama Island (Fig. 4) and is exposed only when the lake level is low. It lies within a small fault block which has been displaced over 1000' to the northwest. The interpreted contact with the overlying andesite is sharp. Within the 5' section below the contact tuffaceous bands are present; below this large blocks of dolerite, up to 3' in diameter, are present within a doleritic matrix; approximately 20' below the contact massive dolerite is encountered. These features are similar to those encountered at some volcanic flow tops. The sequence may represent a blocky flow top followed by a period of quiescence in which the tuffaceous beds were deposited, prior to renewal of volcanic activity in which the andesite was deposited. This single outcrop in itself is not sufficient evidence to prove that the dolerite is a thick basaltic flow or series of flows; it does however show that this possibility cannot be rejected.

There is considerable variation in the chemistry of the dolerite although it is characterised by its low silica content. Samples from the upper part of the dolerite have high Na_2O, K_2O and CaO contents, possibly indicative of a higher original feldspar content; samples taken from close to its base have higher FeO and MgO contents, possibly indicative of higher original olivine-pyroxene content. Insufficient sampling within the dolerite prohibits the definition of any differentiation sequence. The overall chemistry of the dolerite is similar to that of average dolerite (Nockolds, 1954).

The dolerite is composed of chlorite, albite, quartz, epidote, carbonate and sericite; this secondary mineralogy is similar to that of the volcanic rocks of the southwestern portion of the greenstone belt, indicating that the dolerite and the volcanic rocks have been subjected to similar metamorphic conditions. CO_2 and H_2O contents are high, even relative to the surrounding volcanic rocks; these volatile constituents may have been introduced during either hydrothermal alteration or metamorphism. If this unit is a sill intrusion then introduction of volatiles from the surrounding volcanic rocks could have taken place during metamorphism; if it was a volcanic flow then volatile introduction could also have taken place by synvolcanic hydrothermal alteration. If the dolerite represents a sill, its altered state indicates that it was intruded during the volcanic activity, and therefore post-dated its enclosing volcanic rocks by a short time period.

Franklin (1967) concluded from his study of the dolerite and the pyritic zone that the pyritic zone was formed by separation and rapid settling of an immiscible sulphur-rich liquid within the intrusive dolerite silicate magma. Franklin's evidence for this hypothesis is the textural

relationship between sulphide and silicate near the pyritic zone; rounded blebs of silicate occur within sulphide masses and also the converse of sulphide within the silicate. The sulphide concentration decreases rapidly into the dolerite above the pyritic zone. This process requires complete sulphurization to pyrite of the pyrrhotite formed from this liquid. A high-sulphide mineral content, relative to the dolerite, is present throughout the pyritic zone. This evidence is however not conclusive in defining the source of the pyritic zone; Franklin could not find evidence of a genetic relationship between the pyritic zone and the orebodies.

CHAPTER V

DISCUSSION OF SULPHIDE CONCENTRATION AND WALLROCK ALTERATION

A. Introduction

This chapter is primarily concerned with the interpretation of the processes which resulted in the concentration of sulphides within the rocks of the Temagami Mine. The significance of the geological and geochemical features which have been described are discussed first. It is shown that hydrothermal activity affecting the freshly deposited volcanic rocks may have produced many of the alteration features. It is initially assumed that the sulphide deposition is related to this hydrothermal alteration; the assumption is justified in later sections. The mechanisms of operation of hydrothermal systems are then considered and discussed in relation to the Temagami volcanic rocks. The chemical conditions of hydrothermal alteration are also discussed in relation to the observed chemical alteration and element redistribution within these rocks. Lastly, the Temagami Mine is compared with other areas of sulphide concentrations, particularly those which are associated with wallrock alteration.

B. Discussion of Alteration Within the Temagami Mine

1. Pod-type orebodies

The idealized alteration pattern around the No. 4 orebody is shown

in figure 17 and the chemical variations within the altered zone are summarized in Table 9. This alteration zone can be interpreted as a pipe-like structure enclosing the No. 4 orebody, formed as the result of a hydrothermal fluid which transected the volcanic rock sequence following its deposition.

The alteration features characteristic of this pipe are not found in the dolerite immediately overlying the pipe (Table 9), which indicates that the dolerite was not affected by this alteration. The dolerite therefore either did not pre-date this hydrothermal activity or acted as an impermeable barrier to it. The second possibility is considered unlikely as the dolerite is itself extensively hydrated and altered from its original igneous state. The emplacement or deposition of the dolerite must therefore have been synchronous with or post-dated the alteration.

Rose (1966a) proposed that the orebodies were deposited from a hot fluid derived from the dolerite at the time of its emplacement as a sill. Rose, however, had no knowledge of the alteration zones around the orebodies and his theory is not consistent with the alteration pattern, particularly the high boron values. The emplacement or deposition of the dolerite probably post-dated the alteration.

It has been suggested (Chapter IV) that the base of the pyrite zone represents an original volcanic surface. There is a pronounced change in volcanic type across this plane, whether to a doleritic flow or to the fine grained mafic flows overlying it. The shape of the alteration zone leading up to and widening towards this plane (Fig. 17) suggests that it was formed while this plane was a volcanic surface. The dolerite was therefore intruded along the plane of contact between the felsic and overlying mafic volcanic rocks, or was deposited on top

of the felsic volcanic rocks and did not transect the alteration pipe. It is not essential to this line of reasoning to differentiate between these two possibilities although the second is considered more probable.

Reconstructing the volcanic rocks to their original horizontal attitude, the No. 4 orebody lies 200' below the volcanic surface and the alteration pipe is near vertical. No evidence has been found for a break in volcanic activity at the level of the No. 4 orebody and, in addition, the alteration zone is continuous around the orebody both above and below it. It is therefore probable that the No. 4 orebody was deposited below the volcanic surface during the final stage of ascent of the hydrothermal fluid. There is evidence for bulk rock removal around the No. 4 orebody (Table 9) and it is probable that the sulphide minerals were deposited in open spaces created by fracturing, solution or explosive volcanic or hydrothermal activity.

Although other pod-type orebodies have not been studied in detail, they do have characteristic tourmaline mineralization associated with them. It is therefore reasonable to assume that each of these is located on a separate channelway of hydrothermal fluid ascent, similar to that of the No. 4 orebody. The large number and apparent random distribution of the orebodies are comparable with the large number of individual vents present in recent geyser basins. The northeastern part of the mine may therefore have been a centre of hydrothermal activity.

2. Vein-type orebodies

The history of formation of the vein-type orebodies cannot be so readily interpreted and neither can it be assumed to be the same as that of the pod-type orebodies. Although they lie at a distance below the base of the pyritic zone similar to that of the pod-type orebodies,

their location appears to be, at least in part, stratigraphically controlled by the dacite-dacite breccia contact (Fig. 14). Little tourmaline mineralization is associated with these orebodies, and in the detailed chemical and mineralogical study around the Empire No. 3 orebody no clearly defined alteration pattern was found. The close spatial relationship between the two orebody types and their similar mineralogy and location suggest that they are genetically related and were formed during the same phase of hydrothermal activity. The genesis of the vein-type orebodies will be considered in relation to the model proposed for the pod-type orebodies in section C of this chapter.

3. The pyritic zone

The pyritic zone has been considered by all previous workers to have been derived from the dolerite. The uniqueness of sulphide concentrations within the Temagami greenstone belt and the close, regular spatial relationship between the pyritic zone and the orebodies requires investigation of the possibility that these two zones of sulphide concentration are genetically related and that their occurrence is not coincidental.

The importance of the location of the pyritic zone at the base of a mafic intrusion has been stressed by previous workers, but its location upon a volcanic surface which was exposed during hydrothermal activity has not been previously considered. It is possible therefore that the pyritic zone was deposited on this surface from the hydrothermal fluid as it was discharged. The regular lateral thinning and change in sulphide trace element content of the pyritic zone may be related to distance from the centre of hydrothermal activity and cannot be readily explained

by a hypothesis of immiscible liquid settling from the dolerite. Later deposition of the dolerite upon or intrusion along this surface causing metamorphism and remobilization of the sulphide-rich sedimentary deposit would have destroyed original sedimentary textures and have produced the apparent immiscible liquid relationship.

4. Environment of volcanism

Before attempting to determine the nature of the hydrothermal alteration affecting these rocks it is necessary to interpret their environment of deposition. No positive evidence of this has been found for the felsic volcanic and pyroclastic rocks in the immediate vicinity of the mine. In this sequence tuffaceous sedimentary beds might be formed during short breaks in submarine volcanic activity. Banded tuffaceous or cherty beds are however rare and, where present, irregular with short lateral extent (Plate 12). Pillows have been found in the mafic rocks both stratigraphically below the mine and in the northern portion of the greenstone belt, indicative of submarine deposition. In addition the extensive banded iron formations of the central part of the greenstone belt are also indicative of submarine deposition. The assumption must therefore be made that the rocks of the Temagami greenstone belt were deposited in a submarine environment although no estimate of water depth can be made. The possibility cannot be excluded that shallow water or sub-aerial deposition may have taken place due to rapid build up of the felsic portion of the pile followed by later subsidence.

C. The Physical and Chemical Conditions of Hydrothermal Alteration

In this section an attempt is made to interpret the source of the proposed hydrothermal fluid and in general terms to investigate the

ability of such a fluid to have brought about the observed alteration and sulphide deposition.

In an active submarine environment the fluid may be derived from either a sea water or a magmatic source. It will be shown that on the basis of the limited geological and geochemical data available from the Temagami Mine that no distinction can be made between the possible effects of these two fluids. It has however been suggested that a more widespread alteration has affected the rocks of the southwestern portion of the greenstone belt, evidenced by extensive hydration, carbonatization and chemical redistribution (Chapter III). If this alteration may be attributed to hydrothermal activity and related to that localized within the mine, then such widespread alteration cannot be readily explained as having been the result of a magma-derived fluid. Much of this section is therefore concerned with the development of a comprehensive model of convective sea water circulation within the rocks of the southwestern portion of the greenstone belt shortly following their deposition, which is both mechanically and chemically feasible. The possibility that the sulphide deposition was from a magma-derived hydrothermal fluid cannot be discounted, and it will be shown that some of the observed features may be as readily explained as being the result of such a fluid. The significance of a distinction between the relative roles of these two possible fluid types is minimal in relation to a consideration of the overall factors which have influenced sulphide localization and concentration.

1. Mechanisms of hydrothermal systems

The study of the mechanisms of submarine hydrothermal activity is hampered by the inaccessibility of recent, active systems. A certain

amount of information can, however, be inferred from recent submarine volcanic areas and also from active terrestrial geothermal areas.

Sea floor dredges from mid-oceanic ridge areas contain not only fresh tholeiitic basalt (Engel et al., 1965) but also a variable percentage of metamorphosed basalts and gabbros (Miashiro et al., 1971) which are present on the sea floor due to extensive normal and rift faulting. Metamorphic grade is normally greenschist facies, but ranges from zeolite to amphibolite facies. Although there is not universal agreement on their origin, metamorphosed volcanic and intrusive rocks are generally considered to constitute most of the oceanic crust (Barrett and Aumento, 1970; Cann, 1970; Miashiro et al., 1971).

These rocks have a wide range of chemical composition and therefore, as they are thought to have been derived from a tholeiitic basalt magma, considerable chemical redistribution must have occurred (Vallance, 1960; Hyndman, 1972). The most widely accepted theory of their origin is that they were formed as a result of prograde burial metamorphism in this area of high geothermal gradient (Cann, 1969, 1970). Heat may also have been supplied by subsequent overlying volcanic flows (Cann, 1969) and by dyke intrusion (Hyndman, 1972). Metamorphism took place in the presence of a partially mobile fluid phase, considered to be derived dominantly from sea water (Cann, 1969) but which may contain a juvenile water component (Melson and VonAndel, 1966; Melson et al., 1965; Aumento and Loubat, 1970).

Spooner and Fyfe (1973) have proposed a model for sub-sea floor metamorphism in which the mobile hydrous phase is not merely incidental to prograde metamorphism but is the principal medium of heat transfer

and therefore the cause of metamorphism by wallrock reaction, thereby allowing extensive solution transportation. Their study is based on terrestrial ophiolitic complexes which are considered to be sections of oceanic crust and upper mantle tectonically emplaced with a minimum of deformation (Gass, 1968; Coleman, 1971; Dewey and Bird, 1971). These complexes have undergone pre-emplacement metamorphism and therefore submarine metamorphism to lower greenschist facies (Spooner et al., in press). More intense alteration is localized in fracture zones which were originally near vertical. Intensity of alteration decreases with distance from these fracture zones, an effect which has also been noted in low grade Keweenawan metabasalts (Jolly and Smith, 1972; Jolly, 1972). A metamorphic temperature range of 180°-400°C is inferred from the mineral assemblage and maximum temperatures may have occurred as little as 1000' below the original rock-water interface (Spooner and Fyfe, 1973). Oxygen isotope data indicates that a large volume of fluid has passed through these rocks (Spooner et al., in press) and that it was sea water in origin (Muehlenbachs and Clayton, 1972).

Several geophysical studies across mid-oceanic ridges show heat flow values lower than those expected in active volcanic areas (Talwani et al., 1971; Bodvorsson and Lowell, 1972; Hyndman and Rankin, 1972; Lister, 1972). The interpretation of these data is that sea water circulation is the principal mechanism of heat transfer within these rocks and that downward movement of sea water in most areas causes the low heat flow values. Hot fluid discharge is therefore localized in relatively small areas which may be analogous to the numerous red sea brine discharge pools (Degens and Ross, 1969; Backer and Schoele, 1972) or the

seventeen active Icelandic geothermal zones (Bodvasson, 1961). The generalized model for convective sea water circulation in most of the oceanic crust near active ridge crests proposed by Lister (1972) is shown in figure 20a. He suggested that the form of the system would be affected by sea floor topography and also that a relatively thin impermeable sedimentary cover would limit discharge and cause recirculation such that the heat flow readings in these areas are close to normal values for active volcanic areas.

Elder (1965) proposed a well-defined model of terrestiral convective circulation of meteoric water based on observations of the Wairakei geothermal zone, New Zealand (Fig. 20b). He showed that, with increased discharge, recirculation and therefore the volume of the high level isotherm "mushroom" would decrease. Based on their study of ophiolitic complexes combined with Elder's data, Spooner and Fyfe (1973) proposed a model for submarine convective circulation (Fig. 20c). In these more massive rocks, fluid ascent is focused in the narrow, highly altered fracture zones, and discharge is virtually complete; the isotherm "mushroom" caused by recirculation is absent. In each of these models the greater volume of rock is subject to downward moving cool fluid, increasing in temperature with depth, which is not inconsistent with, and may be complimentary to, the hypothesis of prograde burial metamorphism (Cann, 1969, 1970).

Experiments have been performed and calculations made to determine the limiting conditions for initiation of convective hydrothermal circulation (Elder, 1965; Palmerson, 1967; Deffreys, 1970; Lister, 1972). Provided that there is a sufficient heat source, convective circulation is dependent largely on rock permeability. In the mid-oceanic ridge

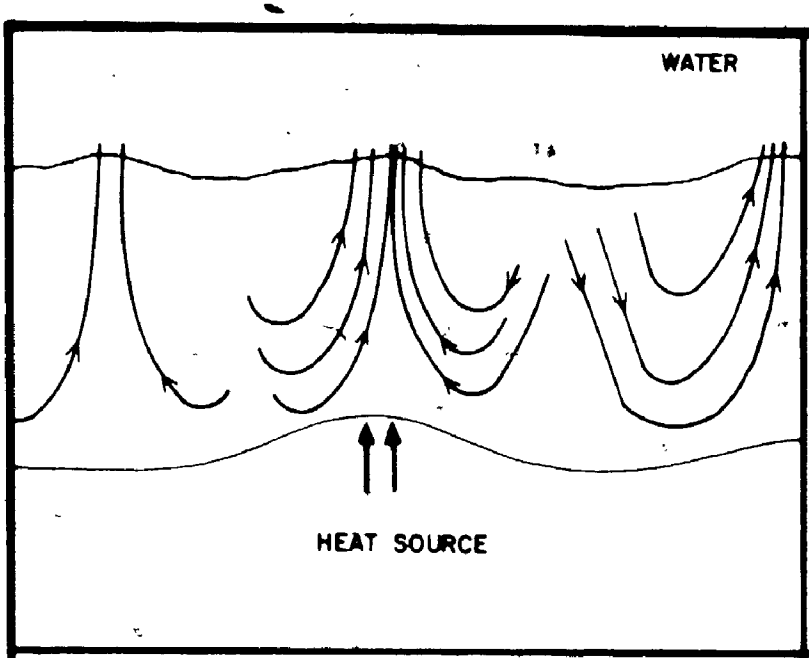

FIGURE 20a

HYDROTHERMAL CONVECTIVE CIRCULATION PATTERN EXPECTED NEAR A RIDGE CREST.

(AFTER LISTER, 1972)

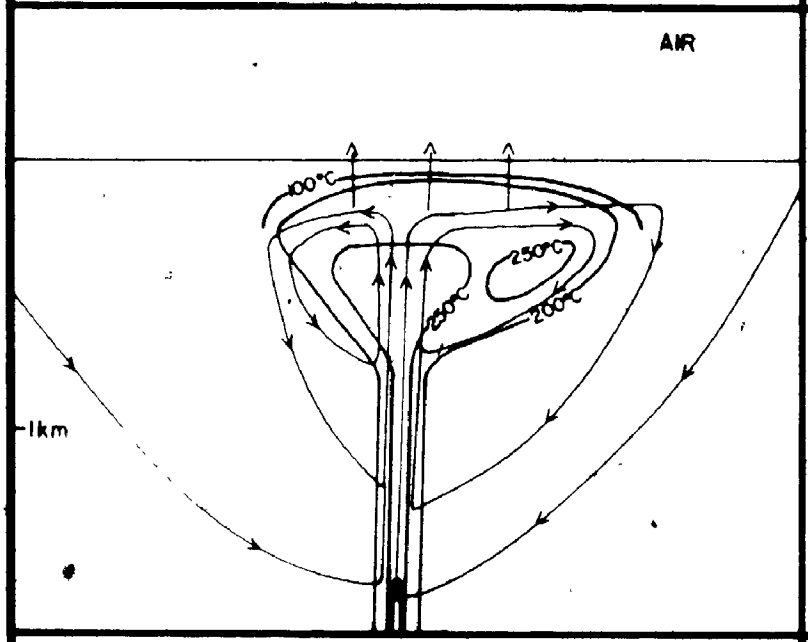

FIGURE 20b

ISOTHERM AND FLOW LINE DISTRIBUTION IN THE WAIRAKEI GEOTHERMAL SYSTEM.

(AFTER ELDER, 1965)

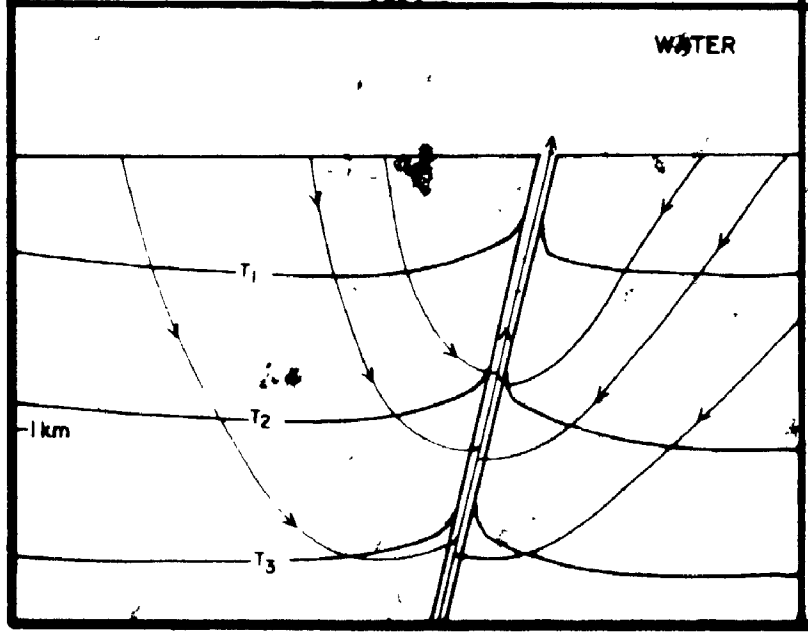

FIGURE 20c.

POSSIBLE SUB-SEA FLOOR GEOTHERMAL SYSTEM — DISCHARGE FRACTURE FOCUSSED.

(AFTER SPOONER AND FYFE, 1973)

environment heat may be supplied by basaltic hypabyssal intrusions which on cooling and crystallization can heat three times their volume of sea water to 300°C (Spooner and Fyfe, 1973). Even allowing for limited permeability in microfractures it appears not only that convective circulation is possible in these rocks but unlikely that it would not occur (Deffreys, 1970).

The application of such systems to the rocks of the Temagami greenstone belt requires that certain assumptions be made as these rocks have undergone a complex geological history and detailed knowledge of them is restricted to the immediate vicinity of the mine. In addition these rocks were probably deposited in a different tectonic setting and represent a different style of volcanism from recent mid-oceanic ridge volcanic rocks; however the limiting physical conditions of hydrothermal alteration may equally well be applied to the Temagami volcanic rocks. The permeability of the Temagami volcanic rocks may be assumed to have been considerably higher than the minimum required for fluid circulation as the pile is largely pyroclastic in nature and also extensive fracturing may have taken place during explosive felsic volcanism. Heat may have been supplied by the cooling of the volcanic rocks following rapid build-up of the felsic portion of the pile or by hypabyssal intrusions into the underlying mafic volcanic rocks, now covered by sedimentary rocks (Fig. 1). A positive heat source which is exposed is the proposed felsic synvolcanic hypabyssal intrusion which lies approximately 3000' stratigraphically below the mine (Fig. 1). It is interesting to note that the pyritic zone is well developed outside the mine area only where underlain by the Iceland Lake pluton (Fig. 1), parts of which may also have been emplaced during volcanic activity.

The proposed convective hydrothermal circulatory system for the area around the mine is shown in figure 21. Less permeable units near surface prevented complete discharge, causing recirculation and formation of a high temperature zone under much of the mine, although smaller than that of the Wairekei system (Elder, 1965; Fig. 20b). Maximum temperatures would be controlled by hydrostatic pressure and it is therefore unlikely that boiling would occur in a submarine environment except under shallow water cover and close to the rock-water interface. Isotherm T1 may therefore be in the order of 100°C and incremental increases 50C°.

Fluid was discharged from the system through numerous individual fracture-controlled channelways in the more permeable rocks. Sulphide deposition took place from the cooling fluid as it approached surface to form the pod-type orebodies and as it emerged on surface to form the pyritic zone. The massive dacite was less permeable and therefore prevented free fluid ascent. The ascending fluid would therefore be delayed at its base prior to ascent through localized fracture zones or recirculation. Cooling of the fluid during its residence time at the base of the dacite caused deposition of the planar vein-type orebodies. The surrounding volume of rocks would be affected by a downward moving fluid and therefore the intensity of alteration would be dependent on fluid volume, and composition and also temperature, which would be largely depth controlled. The Temagami Mine therefore represents approximately one quarter of the original geothermal zone.

The effects produced by an ascending magma-derived fluid may be equated with those in the localized ascent zone of a sea water-derived fluid. Such a fluid may also be equated with the proposed heat source,

FIGURE 21 POSSIBLE MODEL FOR CONVECTIVE SEA-WATER CIRCULATION AT THE TEMAGAMI MINE.

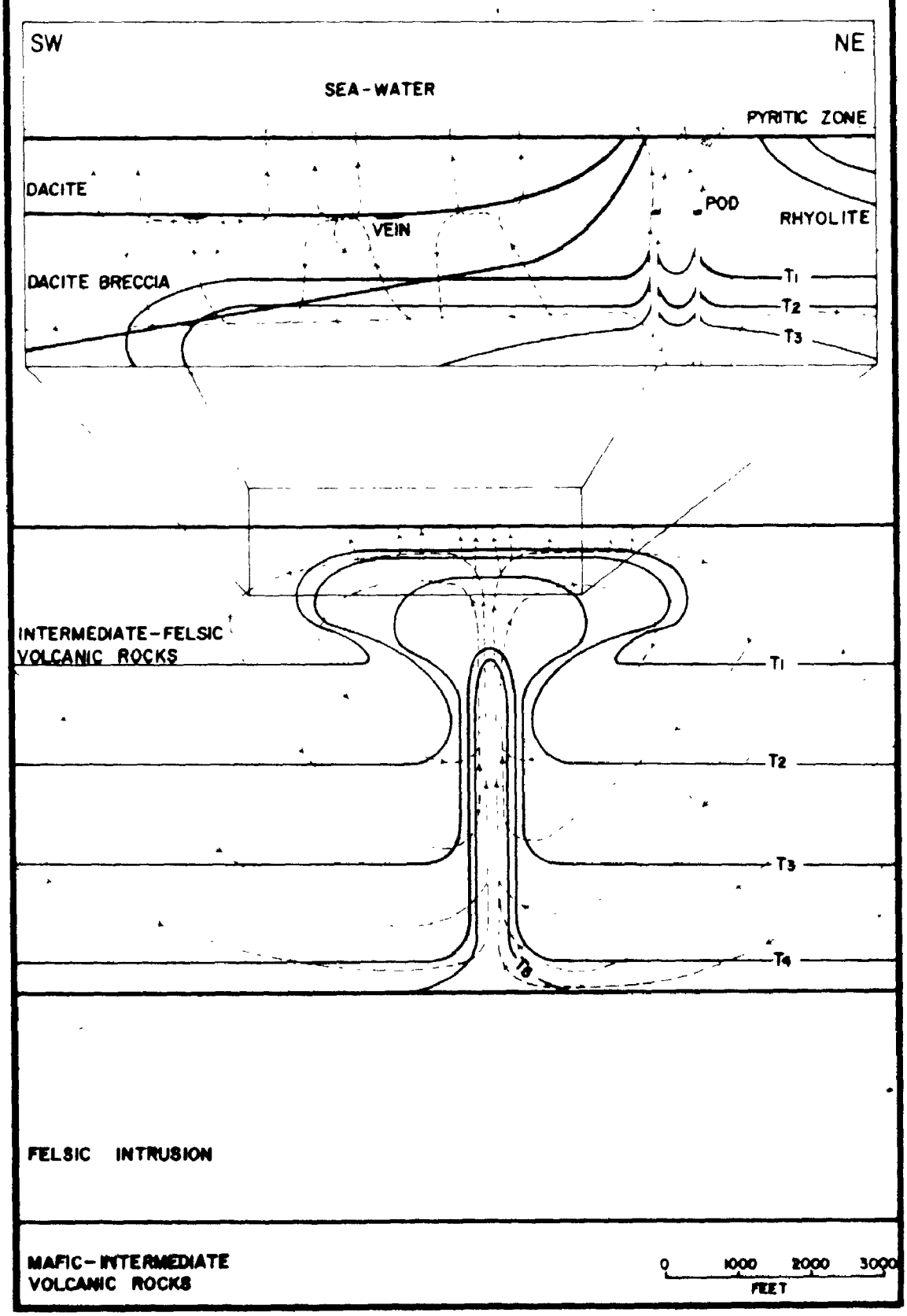

incorporating a connate water component during its ascent and thereby initiating convective circulation of connate and sea water. Distinction between these two systems is therefore dependent merely on interpretation of the relative importance of intrusions and magma-derived fluid as heat sources and the proportions of magma and sea water-derived components in the ascending fluid.

2. Chemistry of hydrothermal alteration

Zen and Thompson (in press) have summarized the difficulties of determining the chemical conditions of low grade metamorphism involving a fluid phase containing one or more volatile components. They show that laboratory results can be applied to these reactions only if the relationship between total pressure and the activity of all the components is known. They suggest that for ancient metamorphic rocks such relationships can be ascertained "only with difficulty" and that fluid inclusion studies may be the only way to define the composition of the fluid phase.

The rocks of the Temagami greenstone belt have undergone a later regional metamorphism, the effect of which may only have been to recrystallize the hydrothermally produced mineral assemblage in response to prevailing metamorphic conditions. As a result of this, however, detailed study of individual minerals cannot be used as an indication of hydrothermal fluid composition (Meyer and Hemley, 1967). These rocks have been affected by a mobile hydrous phase which has undergone progressive compositional change in irreversible hydration reactions with the silicate wallrock (Helgeson, 1969) and with temperature and pressure variations. In addition, the rocks under study form an inhomogeneous volcanic pile, highly variable in composition, and therefore buffering of volatile

components by mineral reactions would not be constant as is the case in more homogeneous rock suites (Helgeson, 1968a; Spooner and Fyfe, 1973). It has also been shown that no significant conclusions can be drawn from the trace element and isotopic sulphur content of the sulphide minerals (Chapter IV).

It is therefore impossible to define accurately the hydrothermal fluid composition or the transitions affected by the direct application of experimentally derived relationships. The evidence of chemical redistribution within these rocks can, however, be compared with the observed effects in recent hydrothermal systems in which fluid compositions have been determined. It is only by this approach that the feasibility of the proposed model (Fig. 21) can be evaluated in general terms and the cause of sulphide localization and concentration be explained. The similarity between the effects expected in this and a magma-derived fluid model are again noted.

The Reykjanes geothermal system of Iceland is not actively concentrating large quantities of sulphide minerals, but in many respects may be considered similar to the hydrothermal convective system proposed for the Temagami Mine. The circulatory fluid phase in the Pleistocene to recent basalts and tuffs of the Reykjanes geothermal zone is derived dominantly from sea water (Tamasson and Kristmannsdottir, 1972). Almost complete discharge takes place at surface such that there is a minimum of recirculation and the narrow pipe of fluid ascent is effectively isolated from the zone of dispersed sea water descent at higher levels. Figure 22 shows the isotherms and idealized flow lines for this system, enrichment or depletion of fluid relative to sea water composition and the

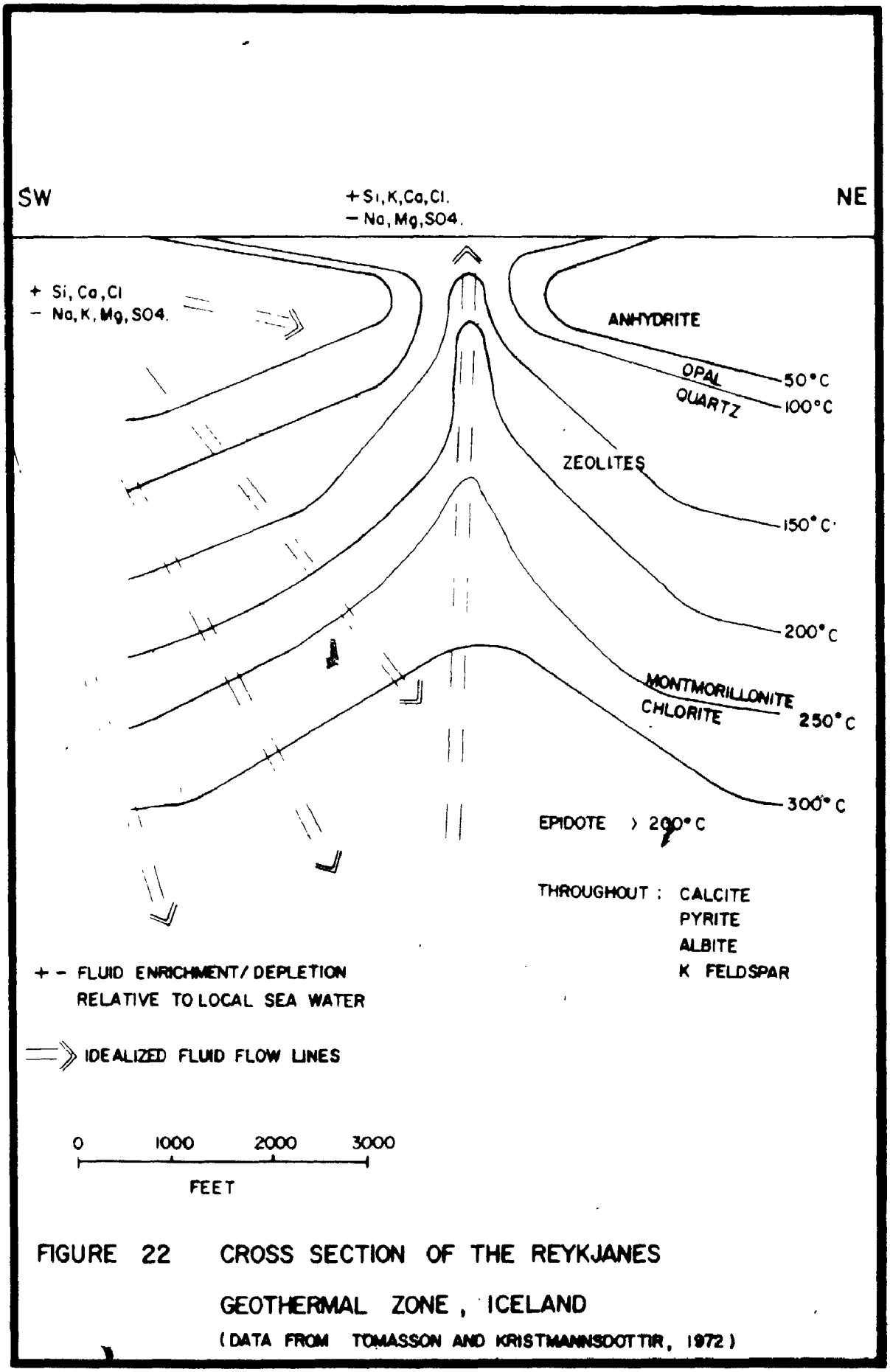

FIGURE 22 CROSS SECTION OF THE REYKJANES GEOTHERMAL ZONE, ICELAND

(DATA FROM TOMASSON AND KRISTMANNSDOTTIR, 1972)

approximate distribution of hydrothermally formed minerals.

Progressive reduction of the fluid takes place due to fixation of HCO_3^-, CO_3^{2-} and SO_4^{2-} in calcite and anhydrite which decrease in solubility with increasing temperature (Holland, 1967). Na^+ is removed progressively from the fluid by feldspar albitization and Ca^{2+} and K^+ contents vary. Similar effects of progressive fluid change, related to hydrothermal mineral assemblage and variations in temperature and pressure, have been observed in several hydrothermal systems involving meteoric water circulation (Sigvaldason, 1962; Honda and Muffler, 1970; Browne and Ellis, 1970; Browne, 1970, 1973).

In addition to progressive reduction of the Reykjanes fluid, slight Cl^- enrichment and considerable heavy metal enrichment are found (Bjornsson et al., 1970). Relatively large quantities of these metals may be carried in solution in a fluid of this composition at elevated temperatures, as chloride complexes (Barton, 1957; Helgeson, 1964, 1969, 1970). Mn^{2+}, Fe^{2+} and Mg^{2+} may pass into solution although their concentration is dependent on mineral reactions, particularly the formation of montmorillonite, chlorite and magnesian carbonate. Base and precious metals are not normally involved in silicate mineral formation reactions and therefore show progressive enrichment in solution. Heavy metal enrichment in solution has been noted in the Red Sea brine pools (Degens and Ross, 1969), the Salton sea brines (Helgeson, 1968b; Muffler and White, 1969) and in several less Cl^--enriched meteoric water geothermal systems (Lebedev, 1967; Browne, 1969, 1971; Browne and Lovering, 1973). In these systems the fluid appears to be an efficient leaching and transporting agent for heavy metals, but in most instances is undersaturated with respect to

them at elevated temperatures. Heavy metal concentration in most instances appears to be a function of possible supply, that is concentration in the rocks undergoing hydrothermal alteration. Although sulphur content of the fluid may be depleted relative to sea water it is probable that it was in excess of that required for sulphide deposition (Barnes and Czamanske, 1967).

Before comparing these results with the observations made on the rocks around the Temagami Mine it is necessary to consider the possible composition of Archean sea water. There is little positive evidence to define this although Holland (1972) suggested that sea water has remained within narrow compositional limits throughout geological time. There is some evidence, however, that Archean sea water had lower O_2 and higher CO_2 content and possibly lower SO_4^{2-}:HS^- ratio (Cloud, 1968, 1972; Glikson, 1972; Roscoe, 1973) and was therefore more reducing than present day sea water.

The consideration of the alteration of the Temagami rocks is subdivided into two parts, that related to the area of widespread fluid descent and that of localized fluid ascent. In the area of descent the chemically observable changes are H_2O and CO_2 enrichment and Na_2O and CaO redistribution. The mineral reactions have been discussed (Table 5) and the present mineralogy is consistent with that produced by a fluid of the proposed composition. The high CO_2 content of the fluid has produced large quantities of calcitic and dolomitic carbonate throughout these rocks. Ca^{2+} mobility would have been dependent on carbonate solubility. No extensive sulphate mineralization has been recognised, but SO_4^{2-} reduction may have taken place by reaction with iron-bearing

silicate minerals to form magnetite and pyrite which are present throughout. The wide range of Na_2O contents (Appendix Fig. 1j) suggests limited introduction and removal, but extensive redistribution, dependent largely on feldspar albitization reactions. The extent of heavy metal removal cannot be accurately estimated, but the present concentrations probably represent depleted values particularly that of Cu (Descarreaux, 1973). Contents of these metals were however sufficient to have produced the concentrations found within the mine; for example, the amount of Cu now contained in less than one half of one cubic mile of these volcanic rocks, averaging 40 ppm. Cu, is greater than that concentrated within the mine.

The relative changes in chemical composition of the rocks in the alteration pipe through the No. 4 orebody have been summarised (Table 9). The mineralogy and chemistry of these rocks may be related to the proposed composition of the hotter, more reducing fluid which has affected them. CO_2 content is low and therefore CaO has been removed. Feldspars have been extensively altered and sericitized but little albitization has occurred and therefore Na_2O has been removed. The other major elements which do not appear to have been extensively removed are constituents of the hydrothermal mineral assemblage. MgO, MnO and to a lesser extent FeO may be related to Al_2O_3 content and the observed chlorite distribution. The original high SiO_2 content of these rocks would mask detection of enrichment.

The sulphide enrichment is however not evenly distributed throughout the alteration zone, but tends to be localized in specific areas. This may be explained partially by the ability of sulphide minerals to precipitate directly from a hydrous fluid without the necessity for silicate

wallrock reaction (Barton et al., 1963).

As the pyritic zone was deposited directly on the sea floor its concentration is more readily explainable. Rapid cooling of the fluid on discharge and possible reaction with sea water caused precipitation of the sulphide minerals. Deposition and concentration of the chloritic matrix to the pyritic zone also took place, in the form of a colloidal or montmorillonitic deposit. Allowing sufficient hydrothermal fluid residence time for mineral nucleation and formation (Barton et al., 1963), the lateral extent of the pyritic zone would be dependent on sea floor topography and would decrease in thickness with distance from the discharge point (Sato, 1972).

The pod-type orebodies represent sub-surface open space fillings, deposited from the cooling fluid as it approached surface. The regular subsurface depth of these orebodies is less readily explainable. An extremely high geothermal gradient was present across the upper few hundred feet of the volcanic pile (Fig. 21) and chalcopyrite deposition was largely in response to decreasing solubility of metal-chloride complexes with decreasing temperature. Fluid ascent delayed in cavities would allow cooling and therefore deposition to take place at that level. Partition of volatile components into a vapour phase due to high level boiling under shallow sea water cover would cause rapid chemical change of the remnant liquid phase (Mahon, 1962; Browne and Ellis, 1970). Ridge (1973), however, shows that this process would be unlikely to cause sulphide deposition. High-level mixing of cool sea water with the hydrothermal fluid would cause rapid temperature decrease and chemical change within the fluid thereby initiating sulphide deposition. This

process is however not consistent with the observed alteration pattern.

The principal cause of sulphide localization in the pod-type orebodies was temperature decrease, which was dependent on several factors; the relative importance of change in fluid composition due to wallrock reaction at this level cannot be assessed. The physical and chemical conditions within the geothermal system may have remained fairly constant throughout much of its life. This system is in effect self-refining such that the effects of fluctuations would be later erased, accounting for the effective partitioning of chalcopyrite and pyrite between the orebodies and the pyritic zone respectively.

The vein-type orebodies have also been explained as the result of deposition from the cooling hydrothermal fluid, delayed at the base of the dacite. A high geothermal gradient was also present across the dacite (Fig. 21), in which heat transfer would have been largely conductive. Convective heat transfer was restricted to localized fracture zones of fluid ascent; intense wallrock alteration was also restricted to these zones, which would not necessarily be spatially related to the orebodies and would not be detected by the detailed chemical and mineralogical study around the Empire No. 3 orebody. Hydrothermal fluid flow in the underlying breccia would not be restricted to zones, as found around the pod-type orebodies and therefore alteration would be less intense and more pervasive throughout this unit and not readily detectable.

Boron is concentrated in the fluid phase on interaction of heated sea water with silicate rocks (Thompson and Melson, 1970). It is therefore enriched in a manner similar to the heavy metals and is deposited as tourmaline as a result of decreasing temperature and wallrock reaction above the pod-type orebodies.

A narrow temperature range of chalcopyrite deposition and wider range of pyrite deposition principally at lower temperature is consistent with the paragenetic scheme proposed by Park and MacDiarmid (1970, p. 167). Zn concentration is low relative to that of Cu, although the average Zn content of the surrounding rocks is 80 ppm., double that of Cu. It is probable that Zn was not significantly enriched in the hydrothermal fluid, possibly due to fixation in carbonates caused by the high CO_2 content of the descending fluid. The more dispersed Zn distribution around the orebodies (Appendix fig. 8) and also its concentration in the pyritic zone are consistent with its lower temperature of deposition. Ni enrichment in the fluid may have occurred as a result of leaching from the more mafic volcanic rocks, and its depositional pattern is similar to that of pyrite. It is possible that Ni was added to the pyritic zone by sulphurization of olivines during intrusion or deposition of the dolerite. Melting and remobilization of the pyritic zone must have occurred and this would explain the apparent magma-derived nickeloan pyrite. No significant Ni addition from the dolerite into the underlying volcanic rocks has occurred (Appendix fig. 9).

A model involving a magma-derived fluid may also be developed to explain many of the observed features. The feasibility of such a model cannot be tested so readily in relation to recent systems. Metal concentration by volcanic processes offers "a particularly attractive possibility because the mechanisms of volcanic action are so little understood that hypotheses regarding it cannot easily be refuted" (Krauskopf, 1967, p. 17).

The composition of a hydrous phase which may separate from a volcanic

magma can therefore only be inferred from fluid inclusion studies or its resultant composition measured on discharge in active volcanic areas. Such a fluid would in general terms be equivalent to the ascending fluid produced in the sea water convective model. It would be reducing and may also be S, Cl and heavy metal enriched (White and Waring, 1963; Hewett et al., 1963; Krauskopf, 1967; Park and MacDiarmid, 1970). Sulphide deposition and associated alteration could also be produced by this fluid in its final stages of ascent.

The source of metals concentrated in the mine is therefore the volcanic magma either by primary hydrothermal fluid separation and exhalation or by secondary leaching. Sulphur may be both sea water and magma-derived. Corliss (1971) has shown that a magma-derived hydrous fluid deposited with the volcanic rocks would remain as a separate phase and be subject to preferential leaching by circulating hydrous fluid. Thus the distinction between a primary and secondary hydrothermal fluid is further minimised.

The sulphide concentrations in the Temagami Mine were therefore deposited from a hydrothermal fluid as it approached and was discharged on the sea floor. A comprehensive model involving convective circulation of sea water can be defined and appears to be capable of producing the alteration effects associated with and more distant from the orebodies. Metals were derived by leaching of the volcanic rocks and sulphur was derived largely from sea water. The hydrothermal fluid may have contained a magma-derived hydrous fluid component.

D. Discussion of the Temagami Mine in Relation to Mineral Deposits Geology and Metallogenesis

In this section the Temagami Mine is compared with other mineral

deposits, particularly base metal massive sulphide types which are associated with wallrock alteration. Although a large amount of useful information is contained in studies of these deposits, consideration of it and related interpretations at an earlier stage would have of necessity biased the interpretation of the Temagami Mine; the limited coverage of these studies is therefore not an attempt to minimise the importance of their contribution to mineral deposits geology. The Temagami Mine is also discussed in the more general context of metallogenic models.

1. Comparison with other deposits

Within the Archean of Canada the Abitibi greenstone belt and related mineral deposits have been subjected to intensive study. The base metal massive sulphide deposits of the belt occur within the differentiated, intermediate-felsic portion of a volcanic pile, which is chemically calc-alkaline in nature (Goodwin and Ridler, 1971; Descarreaux, 1973). This relationship is similar to that found in greenstone belts throughout the Archean of Canada (Wilson et al., 1965) including the Temagami belt. The deposits normally lie within a pyroclastic unit at the top of a felsic volcanic pile, underlying a basaltic sequence. In a regional geochemical study, Descarreaux (1973) has shown MgO enrichment and Na_2O depletion in the felsic volcanic rocks in the proximity of many of the deposits.

More detailed studies have been performed on individual deposits, the most comprehensive chemical study being that of Sakrison (1966) on the Lake Dufault (Norbec) Mine of the Noranda area. The Norbec orebody is typical of these deposits, consisting of massive stratiform pyrite, sphalerite and chalcopyrite which grades laterally into a banded cherty

tuff horizon. Underlying the orebody is a zone containing a network of stringer sulphides, chalcopyrite- and, marginally, sphalerite-rich. Underlying this stringer zone, several hundred feet below the stratiform body, lenses of massive chalcopyrite up to 3" in thickness occur paralleling the plane of the stratigraphy (personal observation, 1971).

An extensive alteration zone underlies the orebody in the form of a pipe, cross-cutting the stratigraphic units including the stringer sulphide zone. Cu, Zn, Sn, Pb, Co, Fe, Mn and Mg are all enriched in this zone and Na and Ca depleted (Sakrison, 1966). The alteration pipe does not continue into the overlying basaltic rocks, but widens towards the top of the felsic pile; the marginal tuffaceous beds are enriched in several of the metallic elements.

Sakrison (1966) has interpreted the alteration and sulphide deposition to be the result of a hydrothermal fluid ascending through the felsic pile to a rock-water interface during a period of volcanic quiescence prior to deposition of the overlying basaltic sequence; on deposition onto the sulphide-rich surface deposit the base of the basaltic sequence was "contaminated with ore elements" (Sakrison, 1966, p. 121). The movement of the hydrothermal fluid appears to have been controlled by local channelways (Sakrison, 1966), probably original fracture zones developed within the volcanic rocks. The original chlorite-sericite mineralogy of the alteration pipe has later been thermally metamorphosed to the distinctive cordierite-anthophyllite (dalmationite) assemblage (Sakrison, 1966; Rosen-Spence, 1969).

Similar geological relationships, mineralogy and alteration pipes have been documented for the Amulet, Waite, Vauze, Millenbach and

Delbridge deposits of the Noranda area (Boldy, 1968; Sharpe, 1967; Simmons, 1973; Spence, 1970) and for the Mattagami Lake Mine (Roberts, 1966). The relationship of the alteration zone to the orebody has in each instance resulted in a similar interpretation of synvolcanic hydrothermal exhalative origin for these deposits.

The nature and source of the hydrothermal fluid has not been specified, but the close genetic relationship between these deposits and volcanic activity has been stressed and a volcanic source for metals suggested. Sakrison (1966) considers the possibility that a residual hydrous fluid phase was produced as a result of differentiation of basaltic magma to produce the intermediate and felsic magmas.

In addition to the similarities between these deposits and the Temagami Mine, the relationship of mineralization to volcanic and hydrothermal activity, several significant differences may be noted. The alteration at the Temagami Mine is not characterised by Mg-enriched chloritic alteration pipes. The sulphide mineralization is in two distinct zones, not in the form of a massive top with underlying stringer zone. Zn content is low and Ni content high relative to the Quebec deposits. It is possible to explain these differences, in part at least, in a discussion of some other sulphide deposits throughout the world.

Examination of many of the Japanese "Kuroko" deposits is facilitated by their occurrence in rocks which have undergone little deformation and metamorphism (Matsukuma and Horikoshi, 1970). The deposits occur within a series of submarine-deposited calc-alkaline intermediate-felsic volcanic rocks at the top of a rhyolitic sequence within a tuff breccia unit, which may have been formed by hydrothermal steam explosion (Horikoshi and Sato, 1970). The stratiform lenses of sulphide consist largely of

Kuroko ore, which is predominantly sphalerite with pyrite, chalcopyrite, galena and barite; it is underlain by lesser amounts of Oko, chalcopyritic ore and Ryukako, pyritic ore (Kajiwara, 1970). The massive sulphide zone at the Shakanai Mine is underlain by a pipe-like mineralized stringer zone, which shows zonation, pyrite-chalcopyrite-sphalerite upwards within the zone and laterally from it. The mineral zonation may be correlated with zonation of intensity of wallrock alteration, with quartz-sericite alteration in the central and lower parts and sericite-chlorite in the outer and upper parts.

Similar alteration zonation has been noted for cupriferous pyrite deposits in Cyprus in which the alteration zone underlying the massive bodies is characterised by a quartz illite core and chlorite-quartz marginal zone (Hutchinson and Searle, 1971).

There appears to be a clear relationship between intensity of alteration and type of sulphide mineralization, which may in part be equated with temperature of alteration. A similar paragenetic scheme has been proposed by Park and MacDiarmid (1970, p. 167), shown for the Japanese deposits (Horikoshi and Sato, 1970, p. 189) and long recognised within the Canadian Archean deposits.

The quartz-sericite alteration pipe through the No. 4 orebody of the Temagami Mine is therefore representative of more intense, higher temperature alteration, associated with pyrite-chalcopyrite mineralization. The lower temperature chloritic alteration is not recognised laterally from the main alteration zone, but is present above it as the highly chloritic matrix to the pyritic zone; the chloritic halo around some vein-type orebodies (Franklin, 1967), not specifically recognised by the

writer, may be indicative of less intense, lower temperature alteration. The chloritic alteration characteristic of the Noranda orebodies is therefore also indicative of generally less intense lower temperature alteration; more intense quartz-sericite alteration has not been recognised in the areas studied. Such alteration is associated with the dominantly chalcopyritic orebodies of the Horne Mine (G. G. Suffel, personal communication, 1974). Higher temperatures at near-surface levels are produced in the convective hydrothermal model proposed for the Temagami Mine (Fig. 21) and therefore more intense alteration may be expected; fluid discharge is restricted to narrow channelways and therefore extensive alteration laterally would not be expected. More intense alteration might be expected in the zone of recirculation (Fig. 21), but this area was not covered in the sampled sections. Almost complete hydrothermal discharge in the Quebec orebodies would explain their lower temperature alteration assemblage at high levels.

Similar alteration and mineral zonation is characteristic of many porphyry deposits. Typical alteration (Lowell and Guilbert, 1970; Hutchinson and Hodder, 1971) is from a potassic core, through phyllic and argillic zones to a propylitic margin. The phyllic, quartz-sericite-pyrite and the propylitic, chlorite-epidote-calcite-pyrite zones may be equated with the higher and lower temperature alteration zones respectively proposed for the massive sulphide deposits; the argillic zone is intermediate between these two and the central, highest temperature, potassic zone not present in the massive sulphide environment. The phyllic-potassic zone boundary is associated with chalcopyrite mineralization and the propylitic zone with chalcopyrite, sphalerite, galena

mineralization (Hutchinson and Hodder, 1971). Tourmaline mineralization has been described associated with phyllic alteration around porphyries (Lowell and Guilbert, 1970) and associated breccia pipes (Sillitoe and Sawkins, 1971).

The alteration and mineral zonation is therefore consistent with generalised schemes proposed for massive sulphide and porphyry deposits. Chalcopyrite is deposited over a higher relatively narrow, temperature range, which accounts for its subsurface deposition in the more intense quartz-sericite alteration zone. Pyrite has a much wider temperature range of deposition and is found throughout the mine, but principally in the lower temperature surface environment associated with chloritic "alteration". Variation in alteration and deposit form between the Temagami Mine and other Archean massive sulphide deposits may be explained by the localized near surface physical conditions which restricted hydrothermal fluid flow at the Temagami Mine.

Differences in content of other sulphide minerals cannot be so readily explained. It is possible to consider zinc, in similar terms, as being deposited at lower temperatures in the paragenetic sequence. In this higher temperature system it may have been carried through and not deposited in the area studied. The relatively low Zn concentration in the pyritic zone and marginal to the alteration zone suggests, however, that it was not extensively concentrated in the hydrothermal fluid, as discussed previously, and this cannot be satisfactorily explained beyond being a result of the chemical composition of the hydrothermal fluid.

It has been suggested previously that the relative concentration

of nickel within the Temagami Mine is partly the result of leaching of basaltic and andesitic fragments in the underlying breccias. This theory may be tested by comparison with cupriferous pyrite deposits of Cyprus which overly basaltic rocks. These deposits lie within the basaltic portion of an ophiolitic complex (Chapter V, Section B) and have been extensively described (Johnson, 1970; Hutchinson and Searle, 1971; Govett and Pantazis, 1971; Constantinou and Govett, 1972; Searle, 1972). These deposits and their underlying intensely altered brecciated and mineralized zones have been interpreted by these writers to have been formed by an ascending hydrothermal fluid of magma, connate or sea water origin and have been used by Spooner and Fyfe (1973) as a typical example of deposits formed according to their sea water convective model.

Nickel is not generally enriched in the sulphide zones (Govett and Pantazis, 1971) and it has been suggested that this is due to the separation of a nickel-rich liquid at an earlier stage of basaltic magma development (Hutchinson and Searle, 1971). Johnson (1970) has however shown by a detailed study of the nickel content of pyrites from these deposits that nickel may be significantly enriched, which he associates with nickel depletion in and therefore leaching from surrounding basaltic rocks.

It therefore appears probable that the relative nickel concentration at the Temagami Mine was in part the result of leaching from the surrounding rocks as part of hydrothermal system proposed for sulphide concentration. The extent of this concentration cannot be readily assessed as nickel addition to the pyritic zone from the dolerite is also considered a possibility.

2. Discussion in Relation to Metallogenesis

Throughout the history of mineral deposits geology schemes have been devised for the classification of ore deposits. Beyond the simple schemes, based on factors such as morphology or metal and mineral type, these are essentially genetic classification schemes, although in some instances they are not proffered as such. Their formulation is therefore, not merely an exercise in systematics, but an attempt to define the most significant variables which control the nature of mineral deposits.

From the interpretations made as to genesis of the Temagami Mine it is possible to allocate it to a grouping in each of the major classification schemes. It could be classified as a "xenothermal, hydrothermal" deposit on the basis of its process of concentration (Lindgren, 1933; Buddington, 1935; Park and MacDiarmid, 1970), a "stratiform sulphide deposit of marine-volcanic association" on the basis of its form, rock association and environment of formation (Stanton, 1972) and an "early" deposit on the basis of its tectonic setting (Bilibin, 1955). The relationship between these three classification schemes is readily apparent; the second is based on the association of processes with the formation of particular rock types, the third on the association of rock types and therefore processes with stages of the tectonic cycle.

Hutchinson (1973) has summarized the relationships between rock type, tectonic setting, age and processes of concentration for this grouping of deposits, which he terms "volcanogenic sulphide deposits", and considers further subdivision within the grouping. Of primary importance in this paper (Hutchinson, 1973) is the recognition not of the general similarities between these deposits, but of the differences

between them and the uniqueness of each. The Temagami copper-gold deposit which carries minor zinc and nickel may therefore in general terms be considered as an intermediate between nickel-copper deposits of mafic-ultramafic association and zinc-copper deposits of felsic dome association (Hutchinson et al., 1971), or as an end member of a linear progression scheme of volcanogenic deposits (Gilmour, 1971). The deposit is certainly associated not only with felsic but also with mafic and intermediate rocks of early stages of Archean tectonic development.

Classification in terms of a linear progression (Gilmour, 1971), however, assumes that a single variable is dominant in controlling the mineral deposit type. It has been shown that the exact nature of the Temagami deposit is the resultant of several variables, for example extent and intensity of hydrothermal activity, localized permeability conditions and the chemistry of the hydrothermal fluid. In addition the observed geological and geochemical features observed are not "typical" of the "volcanogenic" group of deposits. The relative importance and combination of these variables must be unique for each individual deposit, and although one may be dominant, the others cannot be ignored.

The Temagami Mine is consistent in general terms with overall metallogenic schemes and with subdivisions of the volcanogenic sulphide group (Hutchinson, 1973). It is only in detailed consideration of this deposit that inconsistencies with these schemes can be found. Rather than detracting from these schemes, a consideration of these inconsistencies adds to the understanding of the processes of metallogenesis.

CHAPTER VI

SUMMARY AND CONCLUSIONS

The purpose of this study as outlined in Chapter I was to investigate the nature of the orebodies in the Temagami Mine - specifically their relationships with their host rocks - and to interpret the cause of sulphide localization and concentration. A summary of the conclusions reached is presented below. Definitive, interpretative and speculative conclusions are included. The basis for each of these conclusions has been discussed at length in the preceding text and is not repeated at this stage.

1. The rocks of the southwestern portion of the Temagami greenstone belt represent a differentiated volcanic suite. The mafic portions may be categorised chemically as tholeiitic, the intermediate and felsic portions as calc-alkaline. These rocks were probably deposited in a submarine environment.

2. The volcanic rocks underwent regional metamorphism, possibly during the Kenoran orogeny, to form a uniform greenschist facies assemblage.

3. Petrographic and geochemical investigations indicate a primary burial metamorphism which involved extensive hydration, carbonatization, and albitization. Chemical redistribution indicates the presence of a

mobile hydrous phase during this metamorphism. Metamorphic grade attained within some of these rocks during this episode may have been greenschist facies.

4. The rocks within the mine are generally similar to and part of the same volcanic sequence as those of the surrounding greenstone belt.

5. The mine is at the top of an intermediate to felsic volcanic sequence. The northeastern part of the mine may have been a centre of volcanic activity. The top of this sequence may have been exposed for a period of time prior to renewed mafic volcanic activity.

6. The pipe-like zone of intense alteration around the No. 4 orebody was formed by an ascending hydrothermal fluid. This activity took place following deposition of the felsic portion of the volcanic pile, prior to renewed volcanism.

7. The pod-type orebodies were deposited as subsurface cavity fillings from the cooling fluid as it approached surface. Alteration took place by reaction of the fluid with the silicate wallrocks.

8. The sulphides and chloritic matrix of the pyritic zone were deposited on surface on discharge of the fluid, due to its cooling and mixing with sea water. The variable thickness of the pyritic zone is the result of original sea floor topography. The pyritic zone thickness decreases with distances from the area of greatest discharge in the northeastern part of the mine.

9. The vein-type orebodies were deposited as subsurface replacement or cavity fillings due to cooling of the ascending fluid while delayed at the base of the relatively impermeable dacitic unit. The rocks around these orebodies are not intensely altered in recognisable zones.

10. The dolerite unit may have been a thick mafic flow deposited on top of the pyritic zone. Its deposition or emplacement caused melting and remobilization of the pyritic zone to form the observed immiscible liquid textures.

11. The data obtained for isotopic contents of sulphide minerals are inconclusive. The source of sulphur may have been either juvenile magmatic or sea water. Indicated temperatures of mineral formation are indicative of recrystallization during regional metamorphism.

12. The hydrothermal fluid almost certainly contained components of both magmatic water and sea-connate water. While the proposed model of convective circulation of sea water is largely speculative it is forwarded because the alteration effects expected from such a system are those observed not only within the mine but also within the surrounding volcanic rocks. In this model metals were derived by leaching from the volcanic rocks and sulphur dominantly from sea water.

13. The energy source for the convective hydrothermal system may have been a hypabyssal felsic intrusion which was emplaced during volcanic activity.

14. The nickel concentration and lack of zinc concentration relative to other Archean massive sulphide deposits has not been satisfactorily explained. It may be due in part to the nature of the host and underlying volcanic rocks and the chemical composition of the hydrothermal fluid.

15. The metals were derived from the same magmatic source as the volcanic rocks. Concentration was due either to the separation of a residual hydrous phase during magmatic differentiation or leaching of the volcanic rocks following their deposition.

APPENDIX I

Petrography and mineral chemistry

The petrographic description of the samples (Tables 2, 8, 10) was based largely on optical determinations. X-ray diffraction patterns of samples were examined and shown to confirm the optically determined mineralogy. Selected samples of chlorite and tourmaline group minerals were analysed in order to determine their exact composition within their respective groups. Mineral analysis was by electron microprobe using polished thin sections cut from the same samples as those used for petrographic thin sectioning.

The chlorite analyses shown below are representative of the major surface sample groupings (Table 2). All samples may be classified as ripidolite (Deer et al., 1963, v. 3, p. 137). FeO and MgO values show an inverse relationship but vary within narrow limits. The lower Al_2O_3 value (Sample 20) may be correlated with a high FeO value.

Analyses of tourmaline grains from the No. 4 orebody cross-section are also shown below; sample locations are shown in figure 16. All samples lie in the dravite-schorl solid solution series (Deer et al., 1963, v. 1, p. 300). Variations can be seen both between samples and within individual grains. MgO, FeO, CaO and to a lesser extent Na and Ti, show the most prominent variations. Al_2O_3 is noticeably low in the

cores of grains adjacent to the orebody. As each of these elements has been considered mobile within the proposed hydrothermal system, variations may be indicative of changes in hydrothermal fluid composition. Uncertainty as to the effects of metamorphic recrystallization, and lack of experimental data limit the usage of these results.

Lastly a series of photographs and photomicrographs are presented of several of the more interesting features which have been referred to in the preceding text.

CHLORITE ANALYSES - SURFACE SAMPLES (wt. %)

		MgO	SiO_2	FeO (Total)	Al_2O_3	CaO	MnO	Total
4.	Rhyolite	12.60	23.91	26.32	23.22	0.01	0.23	86.29
13.	Rhyodacite-dacite	13.62	23.54	25.98	23.08	0.01	0.13	86.36
22.	Rhyolite breccia	15.34	24.82	23.60	21.22	0.01	0.05	85.06
8.	Dacite breccia	13.61	24.11	24.55	22.85	0.03	0.01	85.15
20.	Dacitic tuff	8.26	24.63	33.19	18.04	0.06	0.69	84.87
21.	Dacite-andesite	10.62	23.28	29.10	20.23	0.01	0.00	83.25
17.	Andesite-basalt	15.22	25.37	23.97	20.02	0.03	0.00	84.61
5.	Rhyodacite-dacite porphyry	13.39	24.37	26.02	22.26	0.08	0.01	86.14
56.	Dolerite	11.97	22.70	28.18	22.97	0.00	0.01	85.84

TOURMALINE ANALYSES - NO. 4 OREBODY CROSS-SECTION (wt. %)

	Sample	MgO	SiO_2	FeO (Total)	Al_2O_3	CaO	Na_2O	K_2O	TiO_2	MnO	Total
50-1	Core	6.40	35.02	9.90	32.54	1.81	1.76	0.07	0.31	0.19	88.00
	Intermediate	6.86	34.50	9.38	32.42	1.99	1.82	0.08	0.63	0.37	88.06
	Inner Rim	6.95	34.87	8.78	32.64	1.32	2.13	0.06	0.74	0.37	87.86
	Rim	6.79	33.99	9.53	32.54	2.21	2.43	0.08	0.53	0.31	88.41
	Outer Rim	9.89	36.50	5.96	30.23	2.13	2.01	0.03	0.35	0.09	87.17
50-2	Core	5.33	33.75	11.42	32.44	2.02	1.70	0.09	0.57	0.28	87.60
	Rim	8.62	36.88	4.70	32.75	1.26	2.09	0.02	0.22	0.00	86.53
104-1	Core	9.18	35.30	4.10	31.82	1.97	1.99	0.08	1.03	0.63	86.38
	Intermediate	9.64	35.53	3.36	31.78	2.07	1.46	0.05	1.16	0.95	86.03
	Rim	6.58	36.64	7.73	32.57	0.39	2.25	0.01	0.67	0.89	87.73
	Core	9.44	35.94	4.16	32.09	1.96	1.61	0.04	1.14	0.51	86.96
	Intermediate	8.80	35.61	4.61	32.49	1.52	1.97	0.05	1.09	0.22	86.35
	Rim	6.50	36.44	7.39	32.68	0.16	1.99	0.00	0.62	0.35	86.14
	Outer Rim	6.55	36.87	8.54	32.84	0.36	1.90	0.01	0.75	0.42	88.25
157-1	Core	8.39	33.49	2.21	36.20	2.14	1.47	0.06	0.89	1.57	86.46
	Intermediate	8.85	33.40	2.73	34.58	2.18	1.42	0.07	1.16	1.46	85.85
	Rim	9.73	34.30	2.59	33.48	2.12	1.67	0.09	0.61	1.28	85.87
	Outer Rim	8.47	36.07	4.31	33.56	0.84	2.27	0.04	0.23	1.41	87.20
157-2		8.21	35.13	2.48	36.02	1.37	1.97	0.07	0.54	1.20	86.98
10-1		9.28	34.52	8.49	26.63	3.57	0.89	0.08	2.15	0.15	85.75
10-2	Core	9.30	34.85	8.55	27.72	3.63	0.67	0.07	1.29	0.01	86.10
	Intermediate	9.32	34.44	8.57	26.88	3.83	0.58	0.07	1.33	0.12	85.15
	Rim	0.50	36.51	10.05	32.96	0.20	1.33	0.03	0.00	0.02	86.61

	Sample	MgO	SiO_2	FeO (Total)	Al_2O_3	CaO	Na_2O	K_2O	TiO_2	MnO	Total
8-1		10.83	34.91	6.46	25.74	4.28	0.49	0.06	3.50	0.25	86.50
8-2	Core	11.78	35.33	5.89	26.19	4.43	0.33	0.05	2.19	0.15	86.33
	Intermediate	11.72	36.42	4.76	27.96	4.10	0.54	0.04	1.22	0.11	86.86
	Rim	5.12	36.77	8.16	34.70	0.02	1.76	0.00	0.10	0.00	86.63
1-1		8.67	33.49	11.00	27.05	3.88	0.76	0.07	0.19	0.66	85.76
1-2	Core	9.28	34.15	12.96	23.16	4.62	0.51	0.05	0.54	0.00	85.25
	Core	9.54	34.55	10.70	24.80	4.06	0.36	0.05	0.69	0.00	84.75
	Rim	5.43	35.94	7.71	34.12	0.03	2.02	0.00	0.23	0.21	85.69
5-1	Core	11.31	35.59	10.70	24.07	4.04	0.78	0.08	1.62	0.00	87.19
	Rim	6.37	37.14	6.66	34.30	0.07	1.54	0.00	0.08	0.00	86.16
5-2	Core	9.77	35.30	11.16	25.07	4.07	0.98	0.06	2.11	0.00	88.51
	Intermediate	11.14	36.66	8.32	28.00	3.15	1.23	0.06	1.20	0.00	88.76
	Rim	5.79	37.31	7.96	34.50	0.14	1.86	0.01	0.37	0.00	87.94

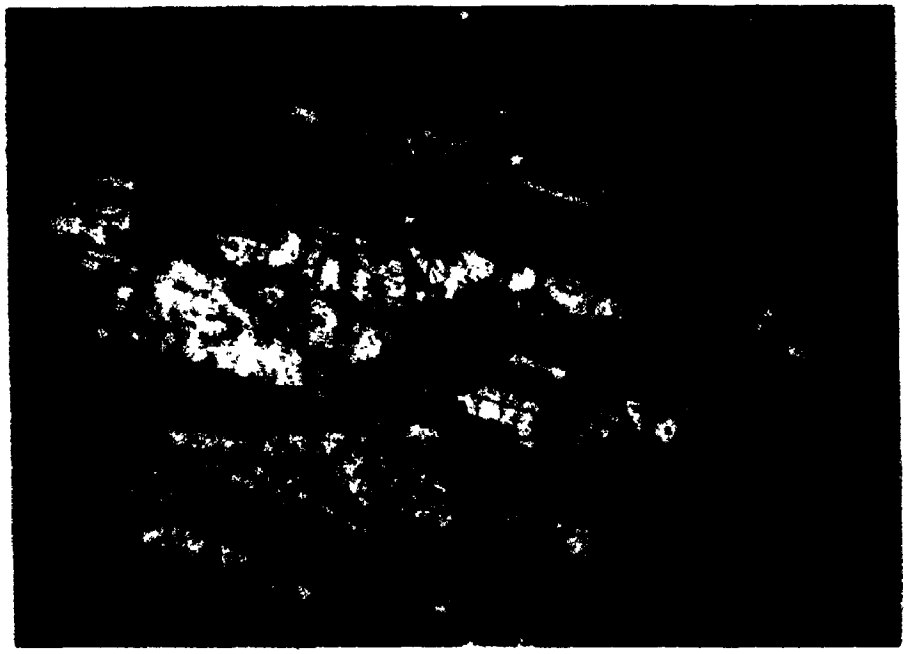

Plate 1. Large albitized feldspar phenocryst in fine grained quartz-sericite-chlorite-carbonate matrix.
Sample D.27 Rhyodacite-dacite porphyry.
(x-nicols).

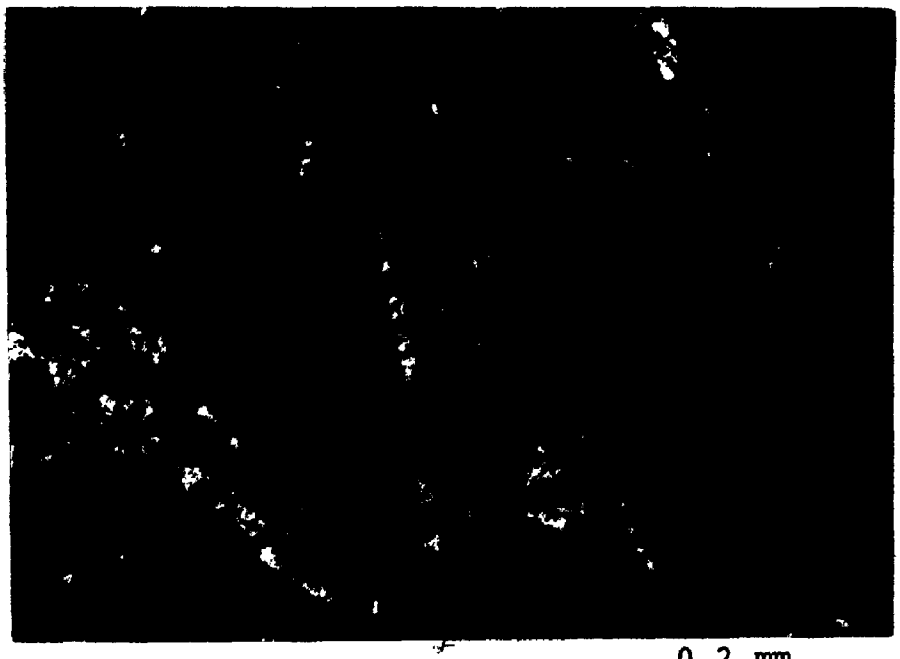

Plate 2. Fine grained albitic laths in chlorite-carbonate-epidote matrix.
Sample D.27 Andesite-basalt.
(x-nicols).

1.0 mm

Plate 3. Highly sericitized and carbonitized feldspar phenocryst in fine grained quartz-chlorite-sericite matrix.
Sample 14 Rhyodacite-dacite. Below No. 4 orebody.
(x-nicols).

0.2 mm

Plate 4. Euhedral clinozoisite grains with chlorite and carbonate.
Sample D.20 Dacitic tuff.
(x-nicols).

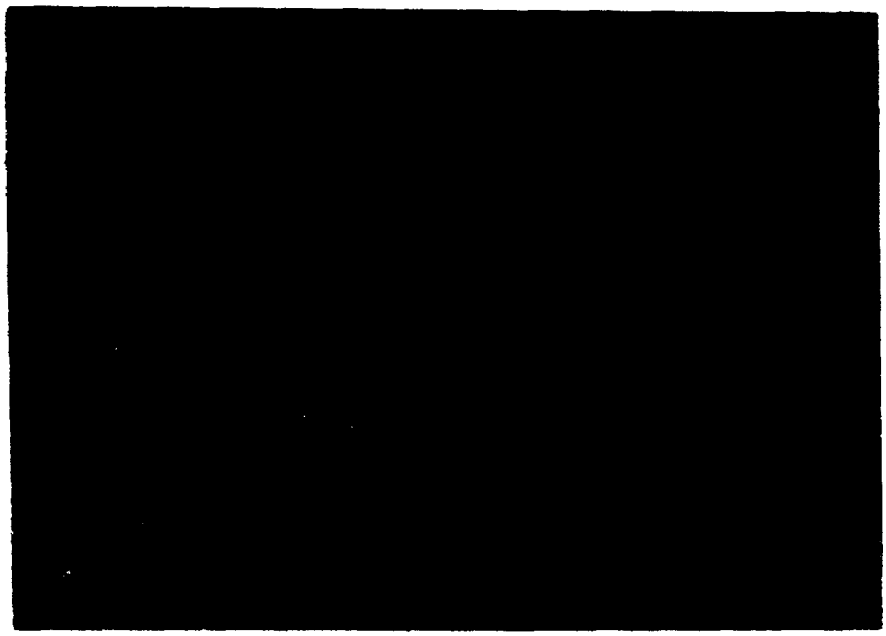

0.2 mm

Plate 5. Radiating sheaths of chlorite and sericite around quartz-carbonate grains.
Sample D.9 Rhyolite breccia.
(x-nicols).

1.0 mm

Plate 6. Chlorite around margins of pyrite grains.
Sample 43 Rhyolite. Below pyritic zone.
(x-nicols).

1.0 mm

Plate 7. Large tourmaline grain poikioblastically enclosing small quartz grains.
Sample 30 Rhyolite. Above No. 4 orebody.
(x-nicols).

1.0 mm

Plate 8. Large skeletal leucoxene grain with remnant ilmenite exsolution lamellae.
Sample 188 Dolerite. Above pyritic zone.
(plane polarized light).

Plate 9. Lower contact of vein-type orebody with dacite breccia. Massive chalcopyrite with pyrite at contact.
14-44 stope.
(Photograph courtesy of R. J. Graham).

Plate 10. Upper contact of massive chalcopyrite vein-type orebody with dacite. Quartz-carbonate vein cross-cutting rocks above orebody.
12-44 stope.
(Photograph courtesy of R. J. Graham).

Plate 11. Cellular pyritic nodule in cavity in massive chalcopyrite. (Location unknown).

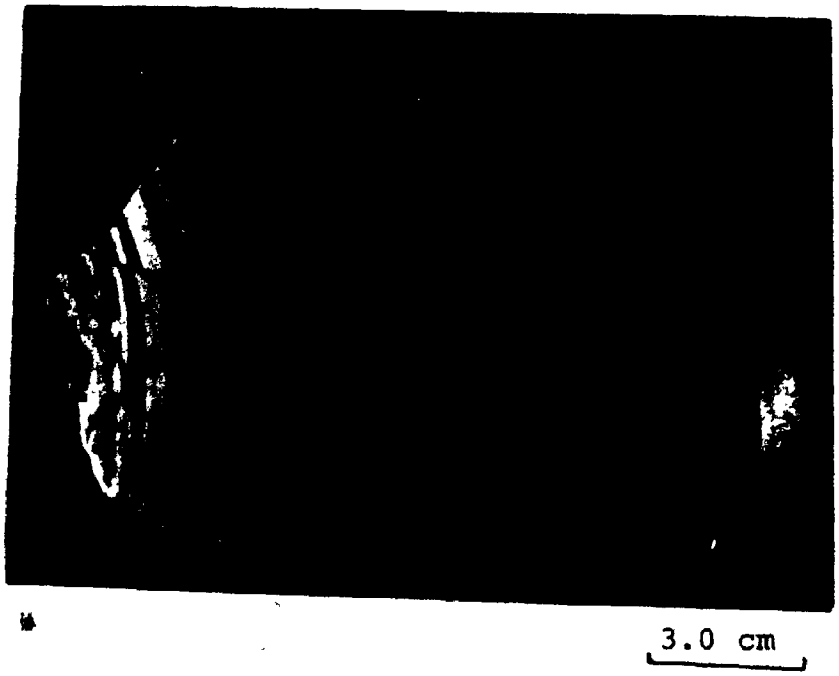

Plate 12. Banded cherty-tuffaceous material with andesitic pyroclastic "dropstone".
(Location unknown).

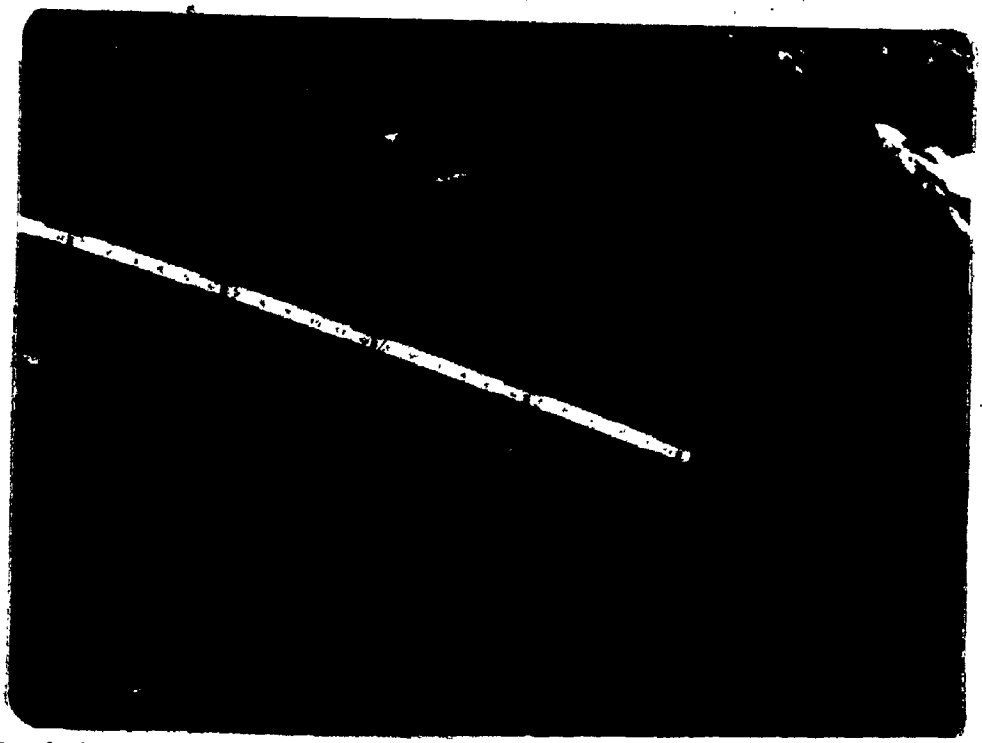

Plate 13. Dacitic breccia. Large andesitic fragments in dacitic matrix. Approximately 600' stratigraphically below the No. 4 orebody.

Appendix II

Sample collection, preparation and analytical techniques

Surface samples were collected using a portable diamond drill capable of core recovery of up to 18". Systematic grid sampling was not possible due to lake and overburden cover, but an attempt was made to sample throughout the southwestern portion of the greenstone belt and to collect a representative suite of the volcanic rocks present. Several core lengths were extracted from single outcrops, within approximately 10' spacing, in order to obtain sufficient bulk for sample analysis.

Inhomogeneous samples were discarded except in fragmental units. Samples with well developed schistosity were also discarded. Surface and fracture weathering and quartz-carbonate veinlets were removed using a diamond saw. Cores were split lengthwise using a diamond saw, examined and a portion removed for thin sectioning; the remainder was sent for chemical analysis.

The mine samples were collected exclusively from diamond drill core which had been split lengthwise using a diamond saw. Analytical samples consisted of one half of 5' lengths of split core. Sampling pattern was such that all of the main rock units were represented and the areas around the orebodies were covered in greatest detail. Samples

were not taken across rock contacts and more schistose portions and zones of quartz-carbonate veining were excluded. Smaller quartz-carbonate veinlets were removed using a diamond saw.

Major elements were analysed by K. Ramlal at the University of Manitoba. The analytical techniques used have been described previously (Wilson et al., 1965). Minor and trace elements were analysed by the Mineral Research Branch of the Ontario Division of Mines under the supervision of D. A. Moddle. Cu, Pb, Zn, Ni, Co, Li and Ba were analysed by atomic absorption, B, Cr, Ga, Sr, V and Zr by emission spectrography.

APPENDIX III

Surface sample analytical data and figures

Firstly, the analytical data are presented in the format:

Sample Number.

SiO_2 TiO_2 Al_2O_3 Fe_2O_3 FeO MnO MgO CaO Na_2O K_2O P_2O_5 CO_2 H_2O

Cu Pb Zn Ni Co Li Ba B Cr Ga Sr V Zr

The major oxides are in weight percent units, the minor and trace elements in parts per million units. "-1" indicates that the content of that element in the sample is below the detectable limits of the analytical technique; "-2" indicates that the element was not analysed in the sample. Surface samples are prefixed by "D" for identification; this prefix is not used in the preceding text, specifically figure 4 and Table 2.

Secondly, the major oxides and more significant ratios are plotted against SiO_2 (Appendix figs. 1a-p); dolerite samples are indicated by solid black squares. Two lines enclosing over 75% of the volcanic rock samples are shown on these figures, where possible, to clarify the distribution trends and to facilitate their discussion (Chapters III and IV); these lines have no statistical validity.

Thirdly, a listing is given of the sample numbers with their

equivalent coding for the thin section collection of the Geology Department of the University of Western Ontario.

SAMPLE D1												
63.90	.46	14.92	1.10	2.96	.08	2.72	3.15	.82	2.91	.16	4.31	2.57
6	-1	50	28	7	6	450	40	-2	-2	-2	-2	-2
SAMPLE D2												
65.50	.39	13.64	.78	1.80	.10	2.23	3.76	1.05	2.49	.14	5.89	1.98
12	-1	35	26	7	4	480	30	-2	-2	-2	-2	-2
SAMPLE D3												
61.35	.46	15.12	.93	2.48	.07	2.33	4.31	1.24	2.68	.16	5.97	2.29
6	-1	50	30	7	4	360	20	-2	-2	-2	-2	-2
SAMPLE D4												
65.85	.39	14.21	.87	1.54	.08	1.85	4.38	1.13	2.71	.14	5.71	1.98
26	-1	35	29	6	4	465	30	-2	-2	-2	-2	-2
SAMPLE D5												
64.55	.41	14.40	.68	3.44	.07	2.03	2.64	5.57	.61	.20	3.24	1.76
12	-1	65	49	8	10	105	10	-2	-2	-2	-2	-2
SAMPLE D6												
65.15	.36	13.76	1.07	3.24	.19	2.47	3.31	3.17	1.57	.17	3.85	2.88
29	-1	65	41	10	6	180	10	-2	-2	-2	-2	-2
SAMPLE D7												
41.25	1.62	11.52	2.56	13.64	.10	5.45	9.84	.89	.14	.14	7.57	5.11
78	-1	110	89	42	12	-2	-1	-2	-2	-2	-2	-2
SAMPLE D8												
68.85	.52	11.58	1.05	3.96	.09	4.28	5.06	3.42	.98	.28	7.11	1.66
11	-1	95	102	30	8	165	10	-2	-2	-2	-2	-2
SAMPLE D9												
64.65	.43	14.84	1.11	2.32	.08	2.49	3.36	2.62	2.52	.15	2.53	2.39
48	-1	120	40	11	4	380	10	-2	-2	-2	-2	-2
SAMPLE D10												
67.20	.27	14.16	.92	1.20	.04	1.57	3.48	1.87	2.98	.16	3.96	1.76
12	-1	20	12	6	1	375	150	-2	-2	-2	-2	-2
SAMPLE D11												
68.10	.29	14.37	.91	1.39	.17	1.52	2.64	2.16	2.99	.18	3.51	1.64
5	-1	20	15	-1	2	420	10	-2	-2	-2	-2	-2
SAMPLE D12												
61.90	.45	15.37	2.22	1.44	.17	1.80	3.56	2.09	3.81	.24	4.91	1.90
22	-1	15	18	7	2	315	15	-2	-2	-2	-2	-2
SAMPLE D13												
63.80	.42	14.56	1.19	2.32	.13	1.45	4.31	1.84	2.89	.25	4.55	2.03
13	-1	40	24	-1	6	390	40	-2	-2	-2	-2	-2
SAMPLE D14												
39.60	.45	7.33	1.82	7.26	.19	13.58	10.61	.17	.12	.19	15.06	4.11
12	-1	95	728	.56	15	30	-1	-2	-2	-2	-2	-2
SAMPLE D15												
53.10	.51	14.18	1.40	5.28	.13	5.02	6.55	3.63	1.19	.17	5.14	3.18
29	-1	75	172	25	5	180	-1	-2	-2	-2	-2	-2
SAMPLE D16												
64.40	.49	11.34	2.86	10.92	.06	2.15	1.28	.88	.38	.41	0.00	3.74
550	-1	105	212	75	A	75	30	-2	-2	-2	-2	-2
SAMPLE D17												
46.25	.79	12.62	2.23	9.08	.18	6.09	8.35	2.89	.09	.15	6.41	4.31
130	-1	110	104	44	A	-2	-1	-2	-2	-2	-2	-2
SAMPLE D18												
58.45	1.04	14.44	3.70	8.62	.21	6.08	8.04	3.31	.10	.12	4.39	3.23
55	-1	90	110	38	3	15	-1	-2	-2	-2	-2	-2
SAMPLE D19												
48.10	.95	13.12	1.97	7.90	.19	5.38	8.26	1.74	.89	.10	6.69	4.28
134	-1	110	98	48	10	120	10	-2	-2	-2	-2	-2
SAMPLE D20												
63.15	.64	14.31	1.26	4.84	.22	1.53	5.14	3.92	2.71	.13	1.37	1.61
54	-1	155	76	20	5	285	10	-2	-2	-2	-2	-2

SAMPLE D21
58.05 .65 15.36 2.03 6.32 .11 3.38 2.49 4.01 1.23 .20 3.23 2.78
18 55 88 66 26 6 135 20 -2 -2 -2 -2 -2

SAMPLE D22
62.25 .49 14.69 1.22 3.40 .16 2.73 3.58 2.87 2.31 .13 2.92 2.71
18 -1 118 37 10 4 300 20 -2 -2 -2 -2 -2

SAMPLE D23
62.88 .61 15.29 1.45 4.84 .11 2.58 3.22 1.38 2.51 .18 3.64 3.13
3 -1 82 52 10 4 465 30 -2 -2 -2 -2 -2

SAMPLE D24
61.85 .47 15.12 .96 2.96 .16 2.49 3.52 3.04 2.09 .19 4.97 1.88
16 -1 80 39 6 2 300 20 -2 -2 -2 -2 -2

SAMPLE D25
62.60 .52 14.43 1.16 2.84 .14 2.85 3.27 3.42 1.58 .15 4.55 1.92
28 -1 57 37 6 4 480 15 -2 -2 -2 -2 -2

SAMPLE D26
65.35 .54 14.62 1.11 2.41 .17 2.37 2.57 2.87 2.15 .23 3.12 2.17
12 -1 61 20 -1 4 405 10 -2 -2 -2 -2 -2

SAMPLE D27
68.05 .61 14.16 .93 3.58 .09 3.20 4.98 3.02 1.49 .19 4.51 2.53
24 -1 82 66 10 8 285 10 -2 -2 -2 -2 -2

SAMPLE D28
52.65 1.26 14.57 1.94 7.96 .20 4.65 6.19 4.29 .32 .11 2.02 3.58
124 -1 116 95 40 10 30 10 -2 -2 -2 -2 -2

SAMPLE D29
67.10 .44 17.02 .99 1.64 .03 1.55 1.84 1.29 4.10 .16 1.22 2.65
10 -1 36 28 -1 6 465 30 -2 -2 -2 -2 -2

SAMPLE D30
68.25 .59 14.58 .98 3.76 .11 4.43 4.05 4.32 .81 .20 2.61 2.87
6 -1 78 75 14 7 150 10 -2 -2 -2 -2 -2

SAMPLE D31
68.70 .57 14.21 1.25 4.36 .25 3.77 4.14 2.26 1.79 .21 3.32 3.12
4 -1 58 42 10 4 180 15 -2 -2 -2 -2 -2

SAMPLE D32
65.80 .36 14.74 .88 2.04 .10 1.75 3.76 3.41 1.98 .13 2.58 2.08
15 -1 84 21 10 5 300 20 -2 -2 -2 -2 -2

SAMPLE D33
66.95 .40 15.02 1.03 2.01 .10 1.40 3.14 3.32 2.21 .13 2.81 2.85
8 -1 45 17 8 4 375 20 -2 -2 -2 -2 -2

SAMPLE D34
58.65 .89 15.02 1.27 3.96 .13 4.63 4.78 2.85 1.27 .47 2.92 3.37
6 -1 68 48 6 4 135 10 -2 -2 -2 -2 -2

SAMPLE D35
60.70 .71 14.28 1.26 2.35 .10 3.78 5.31 5.05 .51 .29 3.01 2.34
12 -1 68 77 6 7 135 50 -2 -2 -2 -2 -2

SAMPLE D36
53.65 .55 10.49 1.97 7.88 .16 8.78 8.59 3.86 .71 .16 1.81 1.98
338 -1 56 480 22 4 150 10 -2 -2 -2 -2 -2

SAMPLE D37
58.08 .79 14.89 1.75 6.44 .21 4.67 5.96 1.84 .93 .23 .44 3.56
79 -1 38 82 27 16 165 20 -2 -2 -2 -2 -2

SAMPLE D38
67.60 .39 13.33 .73 1.41 .17 1.89 3.84 1.27 2.26 .19 5.13 1.83
18 -1 21 11 -1 4 360 50 -2 -2 -2 -2 -2

SAMPLE D39
51.45 1.35 18.56 3.55 6.68 .19 4.75 8.23 3.88 .28 .14 .45 3.10
91 -1 116 82 27 4 45 10 -2 -2 -2 -2 -2

SAMPLE D40
46.38 1.14 12.21 1.42 11.02 .21 5.62 8.43 1.73 .12 .17 6.68 4.75
129 -1 175 38 32 18 45 10 -2 -2 -2 -2 -2

SAMPLE D41
48.25 .77 11.84 4.56 8.12 .27 7.63 5.95 3.28 .08 .28 4.31 4.29
11 34 162 220 36 10 45 -1 -2 -2 -2 -2 -2

SAMPLE D42
47.70 .79 12.82 4.69 10.21 .44 7.42 7.15 .73 .11 .10 2.42 5.33
58 -1 122 98 30 16 45 -1 -2 -2 -2 -2 -2

SAMPLE D43
64.10 .49 13.69 1.27 2.88 .08 2.60 3.91 3.47 1.84 .19 3.19 2.18
46 -1 68 51 12 8 330 20 -2 -2 -2 -2 -2

SAMPLE D44
74.05 .51 11.29 1.20 3.72 .11 1.48 .82 1.21 2.38 .17 .89 2.23
26 -1 42 38 9 5 225 10 -2 -2 -2 -2 -2

SAMPLE D45
46.20 1.01 12.78 2.24 10.04 .19 6.40 8.05 1.73 .23 .15 6.85 4.89
12 -1 136 76 39 28 45 -1 -2 -2 -2 -2 -2

SAMPLE D46
63.85 .46 13.62 1.44 2.41 .08 1.89 4.97 1.09 2.18 .19 5.33 2.38
8 -1 56 38 15 10 345 20 -2 -2 -2 -2 -2

SAMPLE D47
46.30 1.96 11.53 3.76 13.56 .29 5.35 8.84 1.84 .25 .27 2.04 3.49
138 -1 120 56 46 15 135 10 -2 -2 -2 -2 -2

SAMPLE D48
61.85 .61 15.84 1 78 4.41 .08 3.93 1.90 3.74 2.08 .20 2.31 2.74
43 -1 92 86 23 4 240 15 -2 -2 -2 -2 -2

SAMPLE D49
44.15 1.19 11.66 4.44 8.16 .22 8.15 10.82 1.52 .11 .15 5.07 4.09
138 -1 105 68 47 18 30 10 -2 -2 -2 -2 -2

SAMPLE D50
58.30 .63 15.06 1.19 6.28 .06 7.65 .52 4.62 .19 .17 .25 4.32
16 -1 108 101 27 20 60 18 -2 -2 -2 -2 -2

SAMPLE D51
69.90 .47 15.46 1.77 1.72 .06 1.75 1.56 3.64 2.25 .89 .72 .55
10 -1 69 44 7 4 345 18 -2 -2 -2 -2 -2

SAMPLE D52
67.65 .41 15.13 1.60 1.48 .09 1.76 2.58 2.89 3.22 .13 1.82 2.51
68 -1 82 24 7 4 480 10 -2 -2 -2 -2 -2

SAMPLE D53
68.15 .42 15.15 1.62 1.60 .07 1.55 2.28 4.19 1.81 .14 1.85 1.83
8 -1 80 22 8 4 285 10 -2 -2 -2 -2 -2

SAMPLE D54
63.10 .68 14.66 1.78 2.68 .15 2.97 3.56 3.84 1.68 .27 1.96 2.40
95 -1 248 43 13 7 180 10 -2 -2 -2 -2 -2

SAMPLE D55
69.05 .41 14.51 1.18 1.52 .10 2.88 2.31 5.36 .98 .11 .91 1.47
16 -1 116 22 6 5 75 10 -2 -2 -2 -2 -2

SAMPLE D56
39.70 .67 17.41 3.74 7.16 .16 3.70 10.71 4.35 .28 .06 7.71 3.93
7 -1 75 40 25 21 45 18 -2 -2 -2 -2 -2

SAMPLE D57
44.75 .96 18.18 2.16 7.76 .13 4.22 7.64 4.03 1.25 .21 5.81 2.91
18 -1 86 51 30 16 210 15 -2 -2 -2 -2 -2

SAMPLE D58
43.25 .49 16.78 1.71 7.40 .16 4.17 9.39 3.98 1.23 .07 7.29 3.70
4 -1 80 86 33 18 210 10 -2 -2 -2 -2 -2

SAMPLE D59
42.65 .49 15.54 1.61 7.88 .17 4.60 10.11 2.91 1.32 .07 7.96 4.31
18 -1 90 99 40 23 240 10 -2 -2 -2 -2 -2

SAMPLE D60
54.85 .74 16.07 1.71 6.64 .08 5.43 2.78 4.15 .82 .25 1.94 4.08
4 -1 84 89 26 12 105 -1 -2 -2 -2 -2 -2

APPENDIX FIGURE 1a

TiO2 vs SiO2 wt %

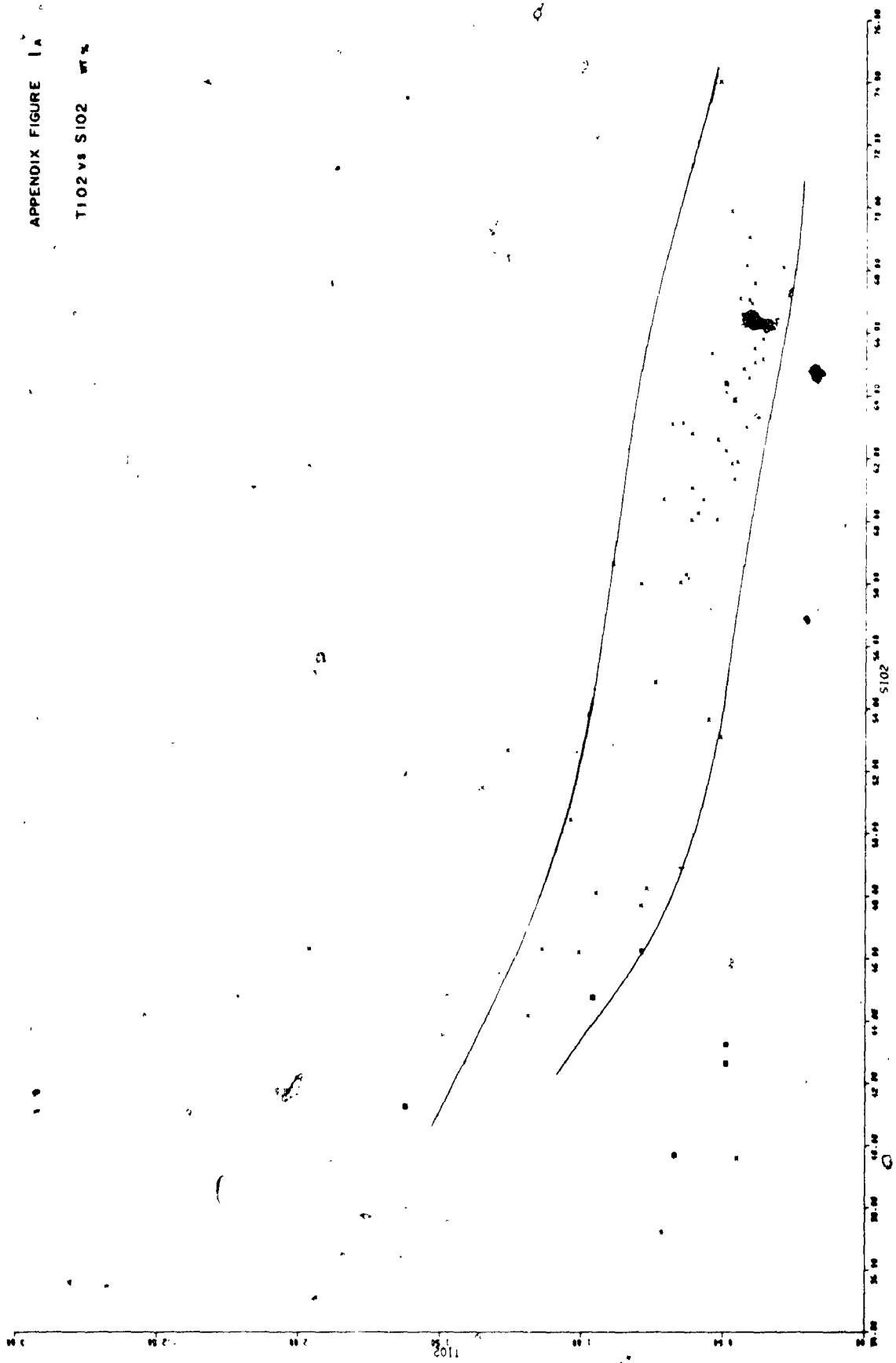

APPENDIX FIGURE 1a

AL203 vs SIO2 WT %

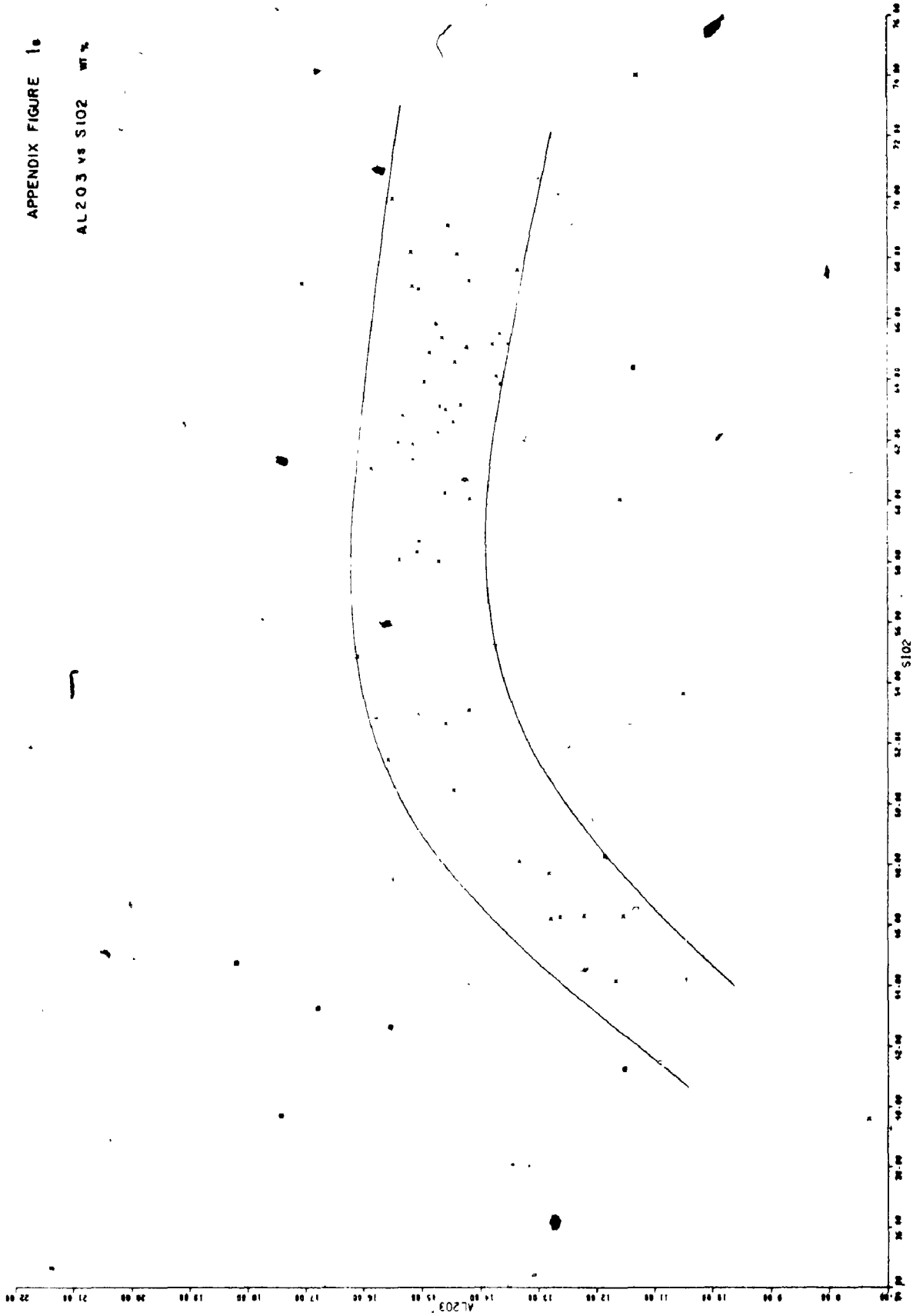

APPENDIX FIGURE 1c

FE2 O3 vs SIO2 WT %

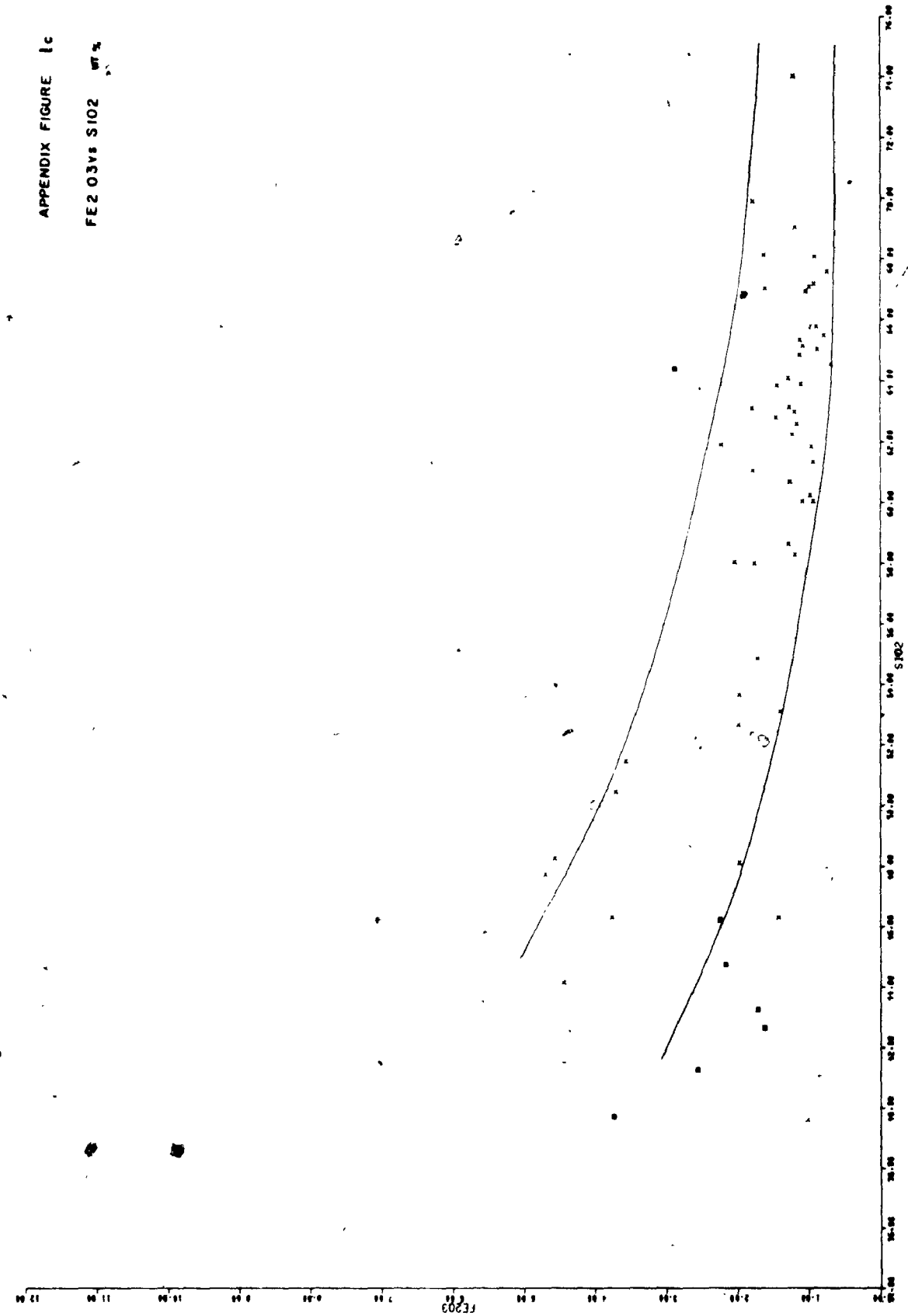

APPENDIX FIGURE 1b

FEO vs SIO2 WT %

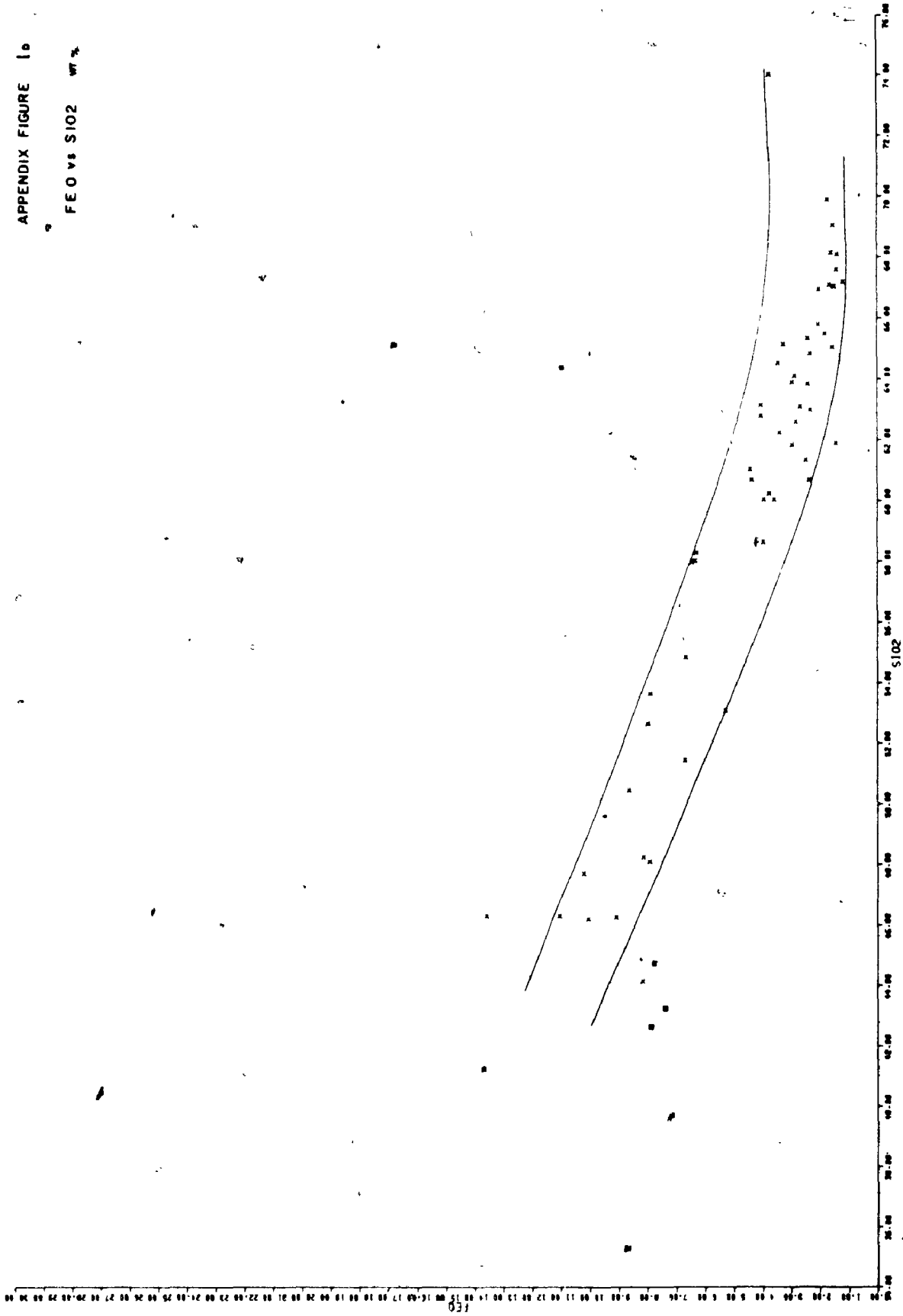

APPENDIX FIGURE 1e.

FEO/FE2O3 vs SIO2 wt %

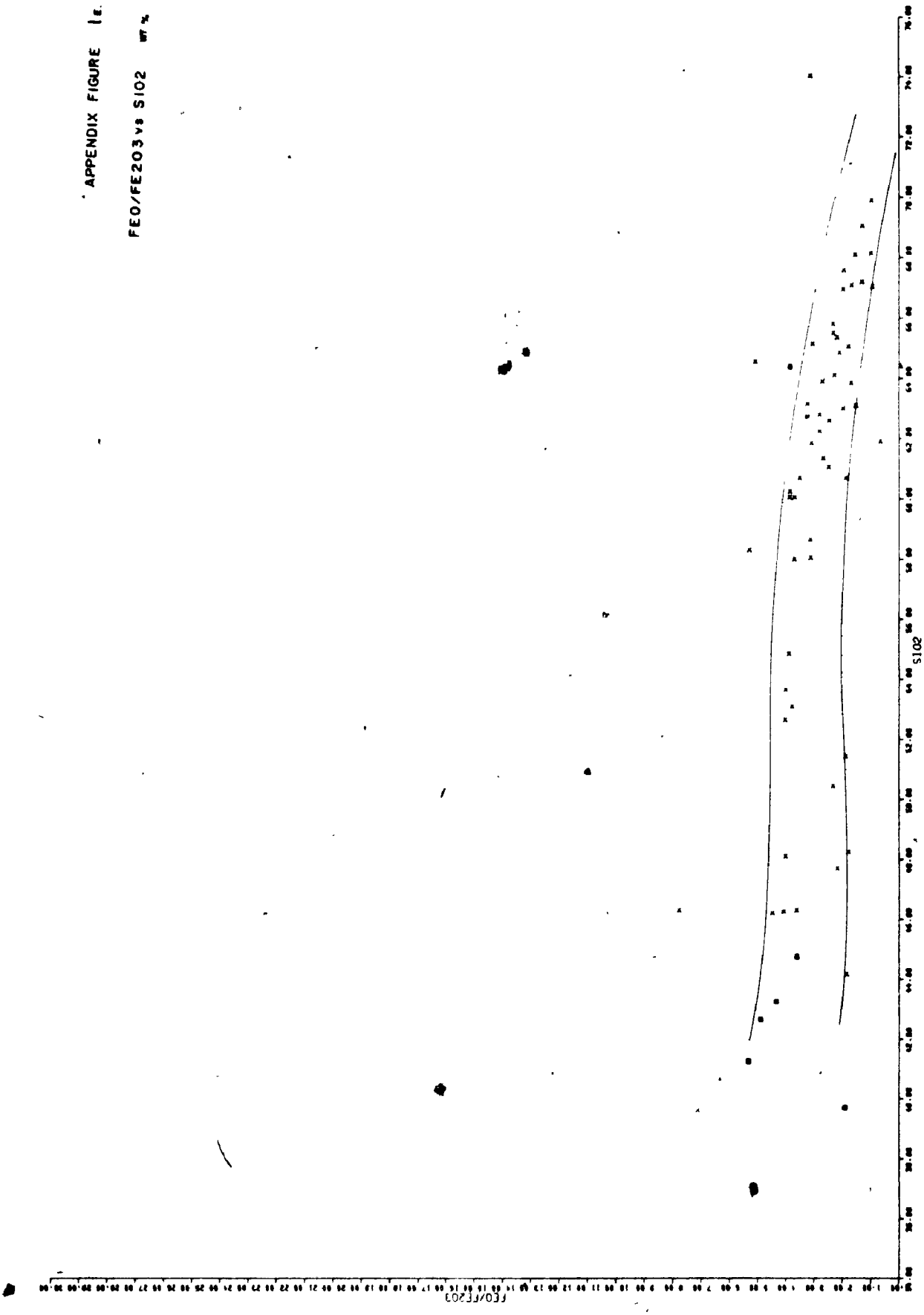

APPENDIX FIGURE 1r

FEO + FE2O3 vs SIO2 wt %

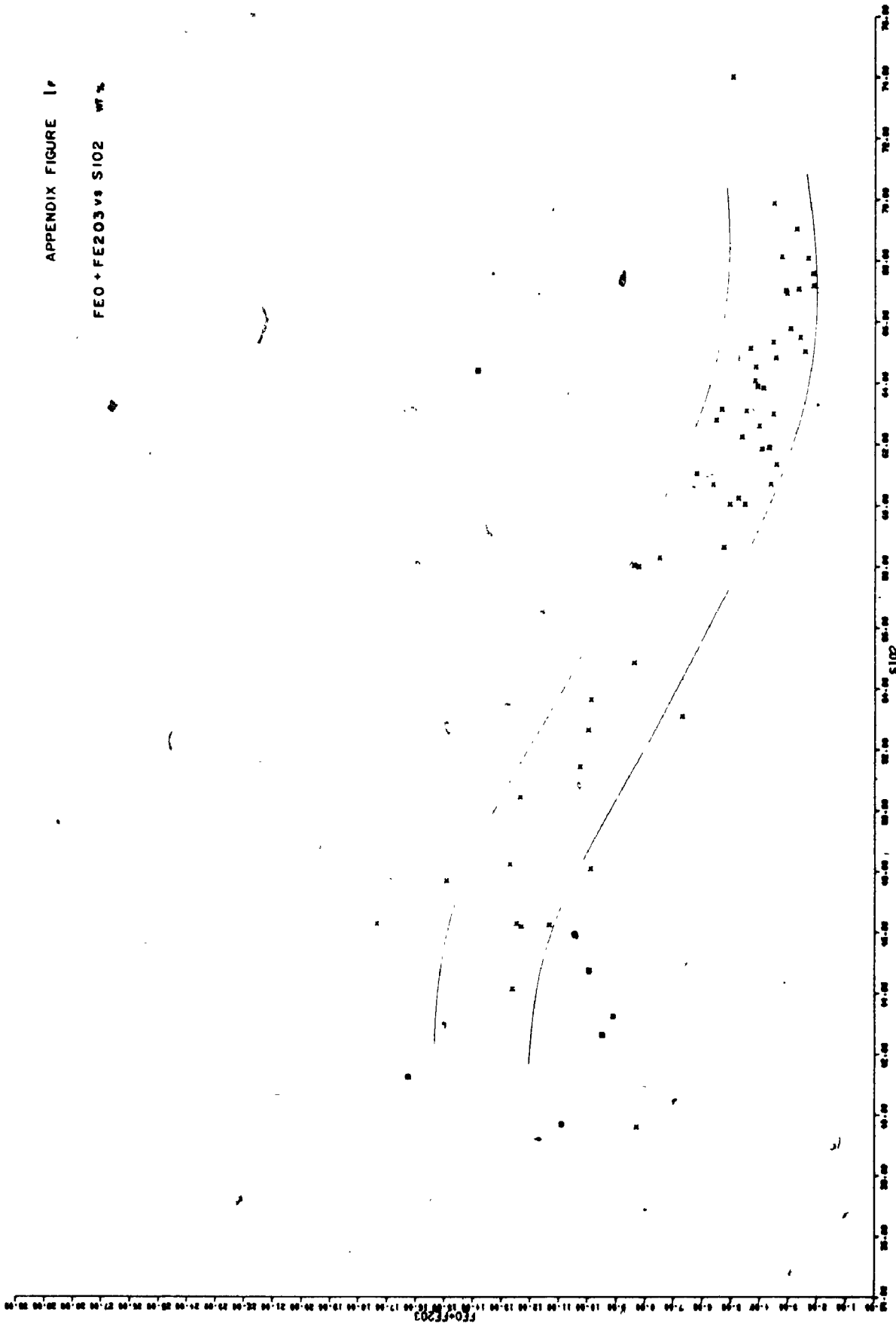

APPENDIX FIGURE 1a.

MnO vs SiO2 wt %

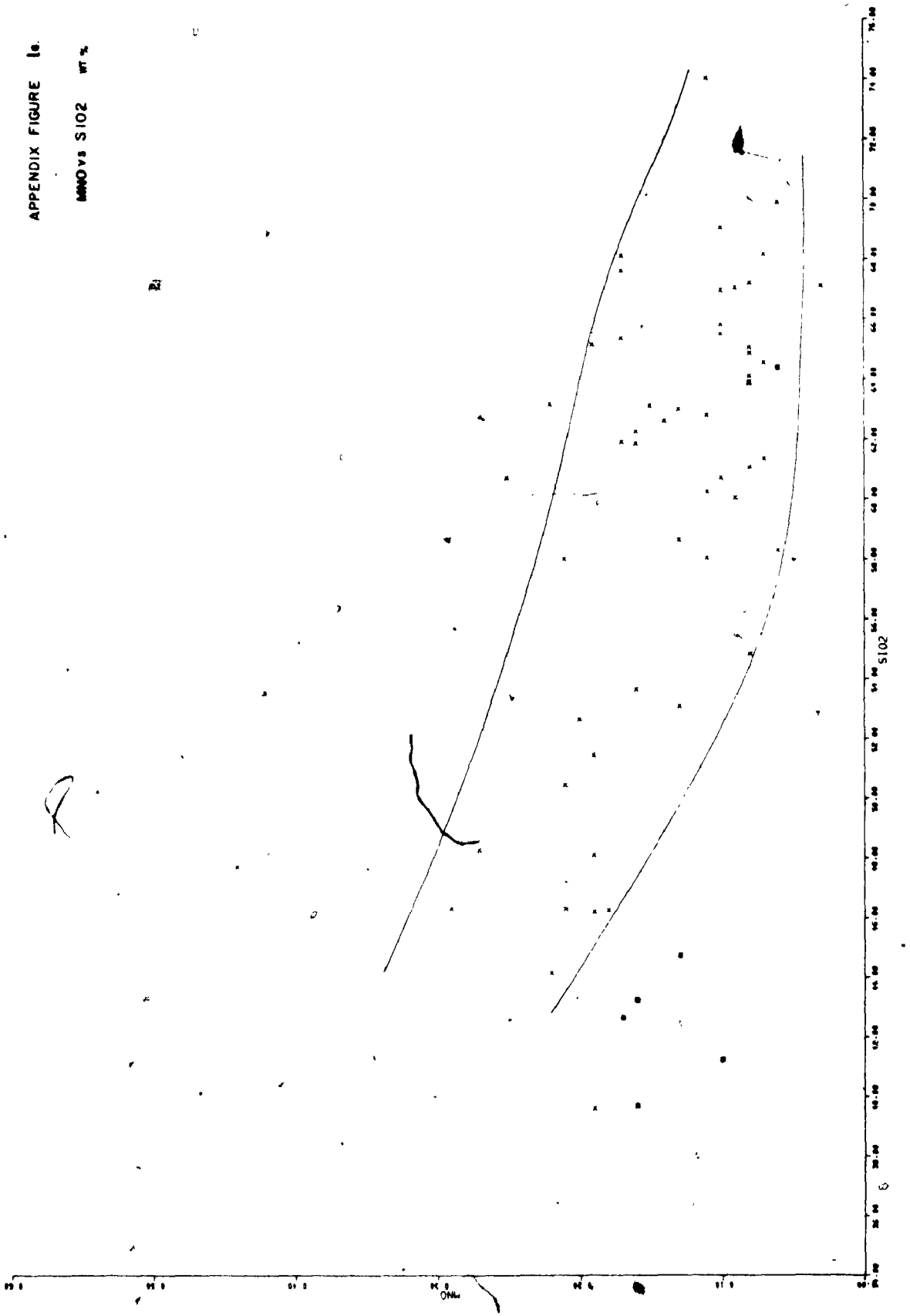

APPENDIX FIGURE 1m.

MGOvs SIO2 wt%

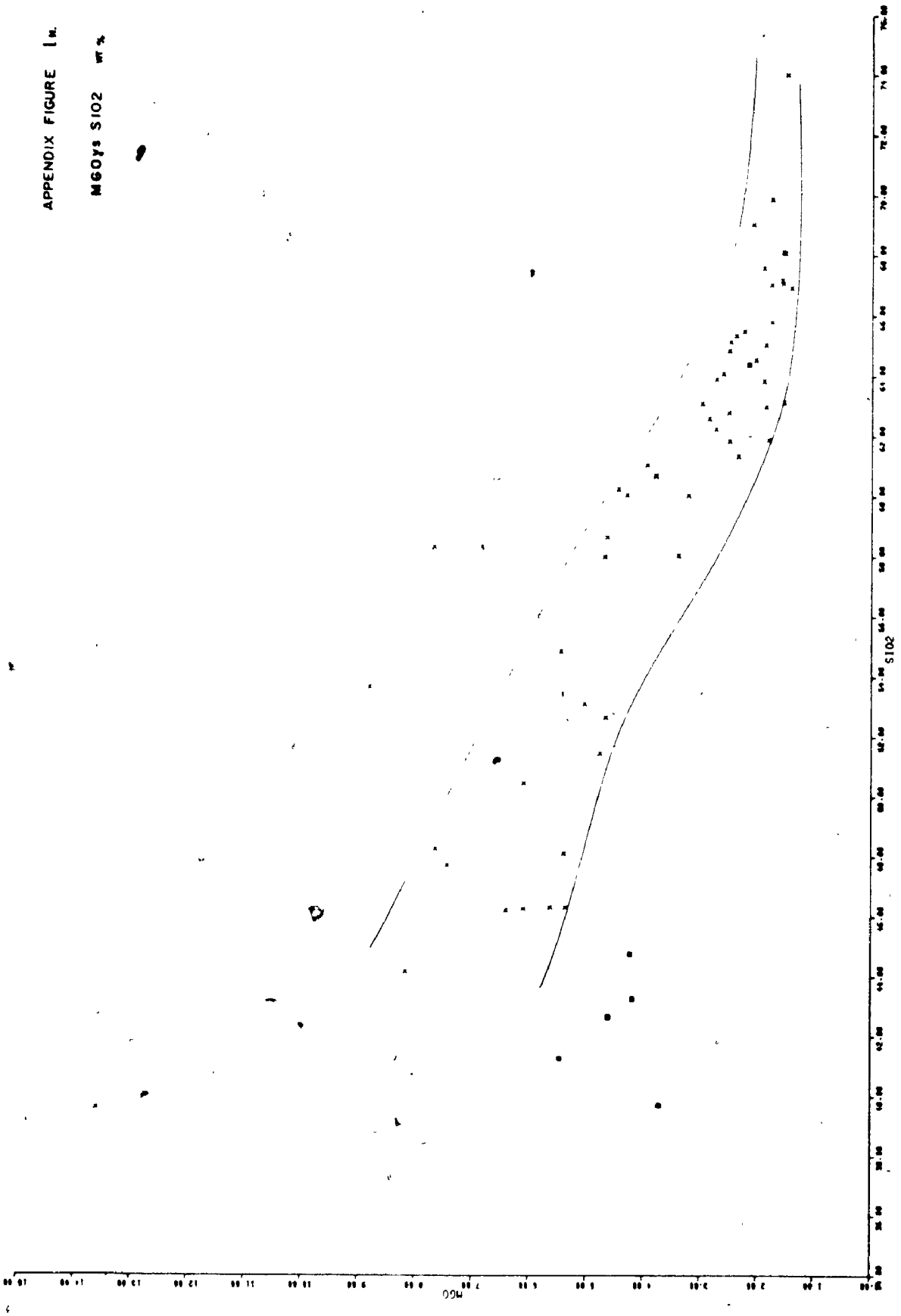

APPENDIX FIGURE 11.

CAO vs SIO2 WT %

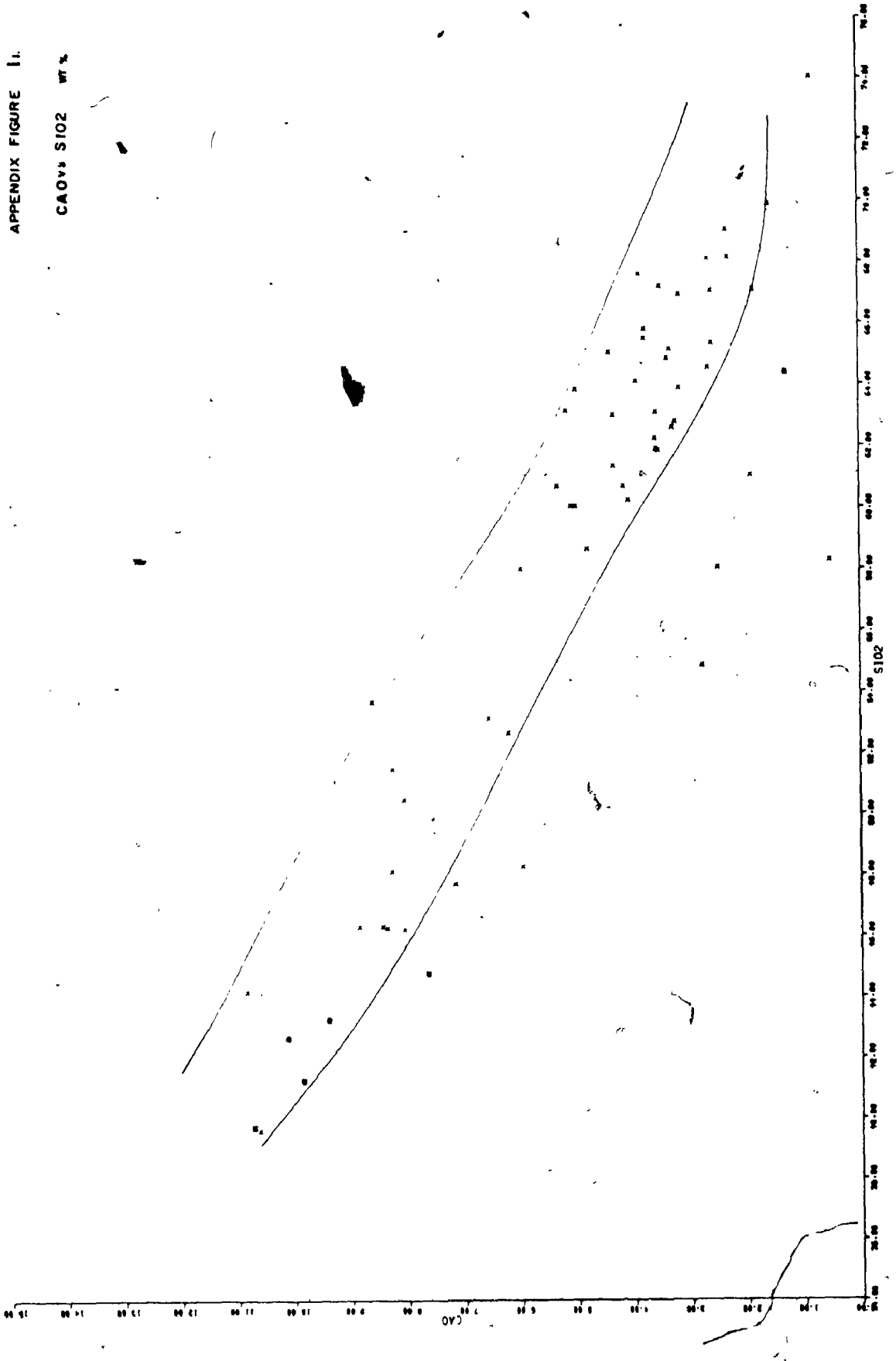

APPENDIX FIGURE 1.

NA2O vs SIO2 WT %

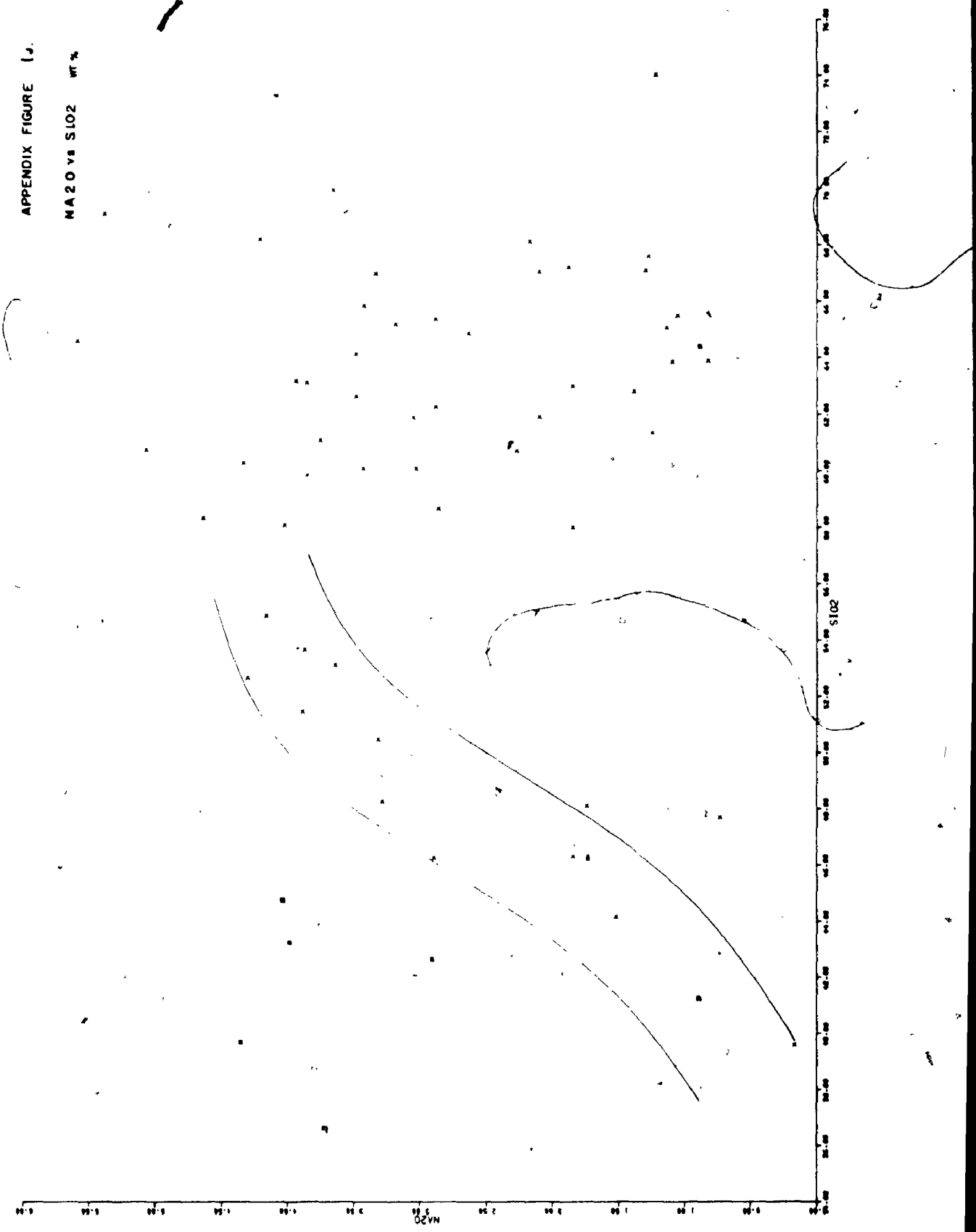

APPENDIX FIGURE 1x

K2Ovs SIO2 wt %

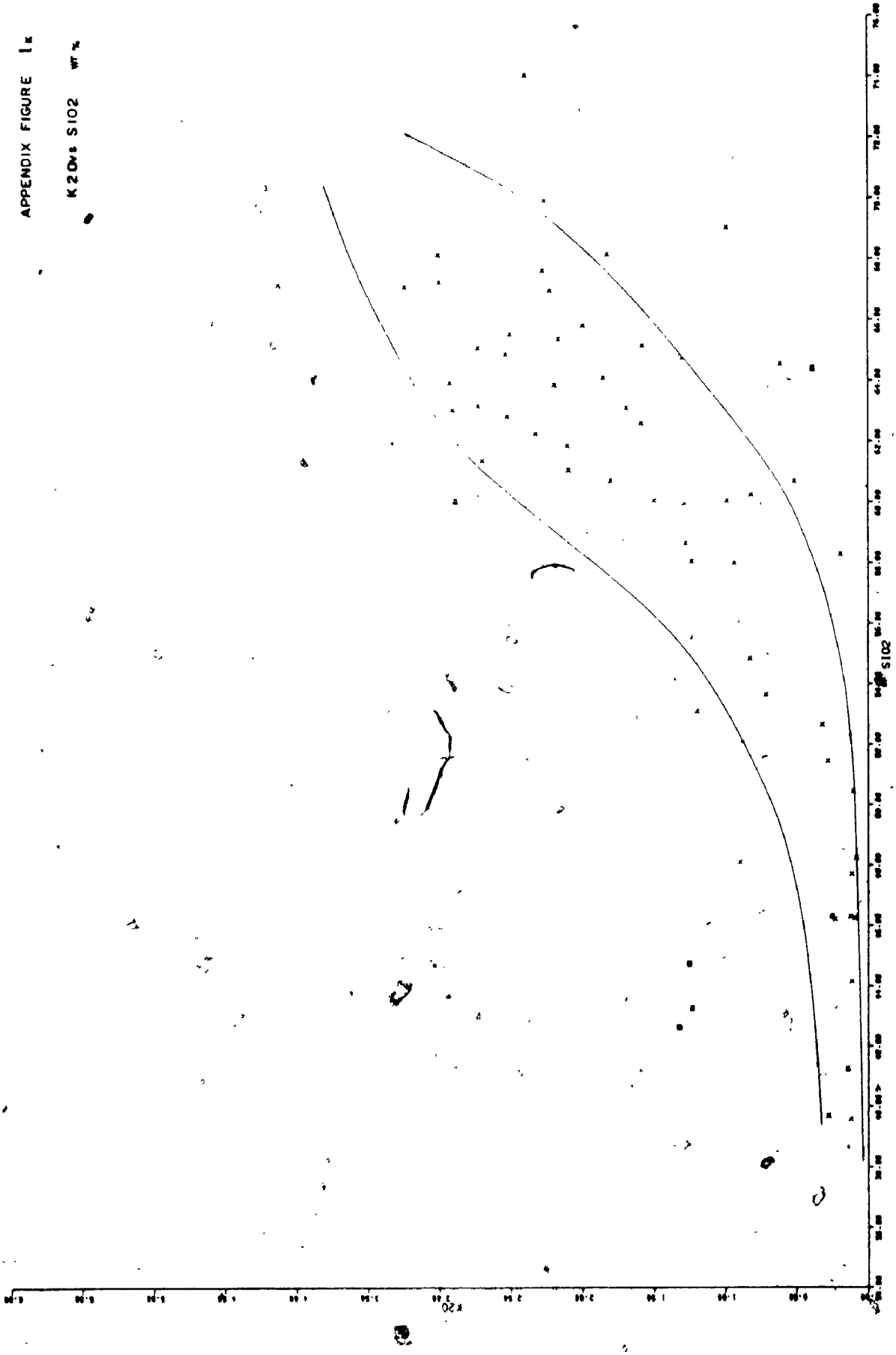

APPENDIX FIGURE 11.

NA2O+K2O vs SIO2 - wt %

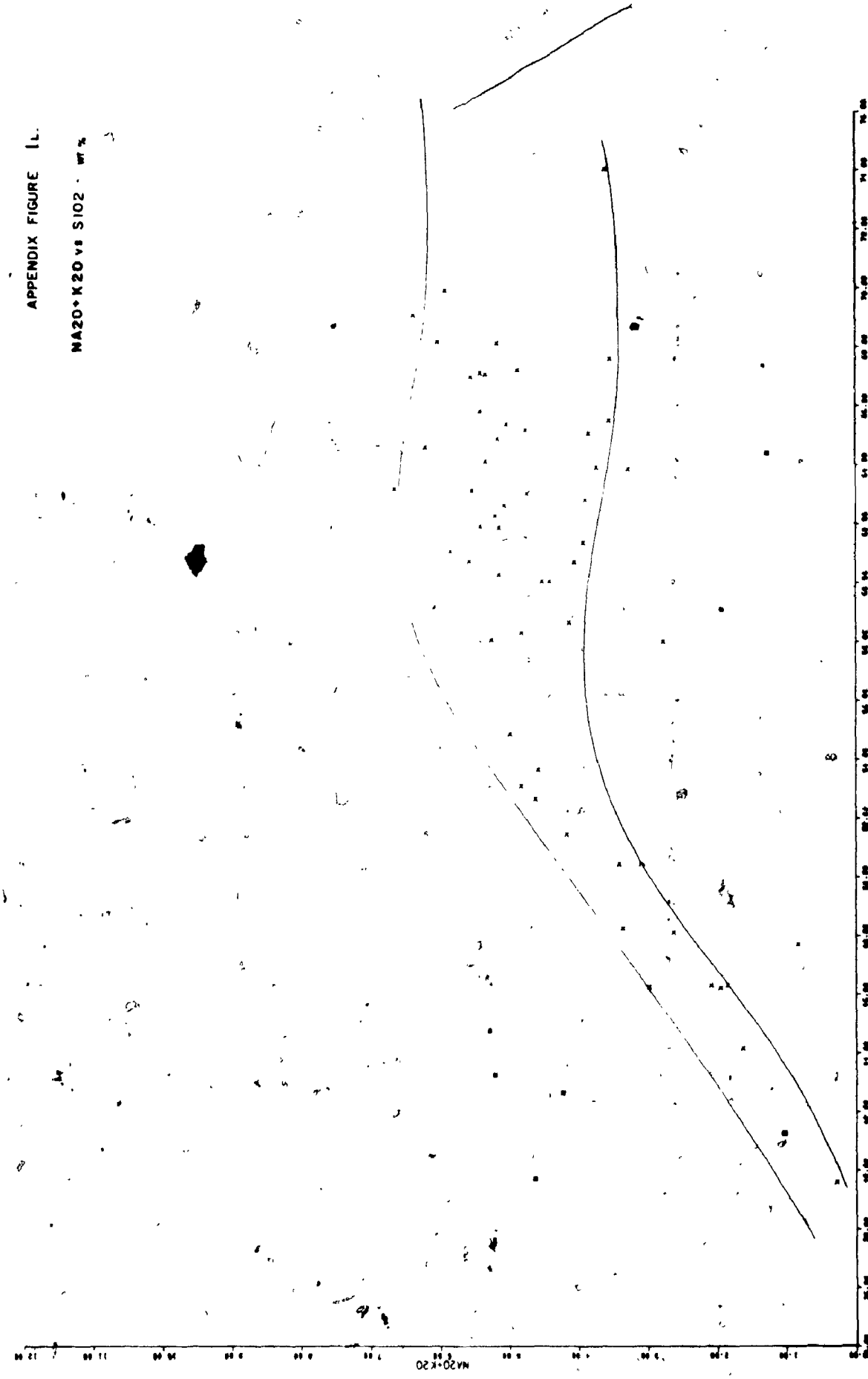

APPENDIX FIGURE 1a.

CAO+NA2O+K2O vs SIO2 wt %

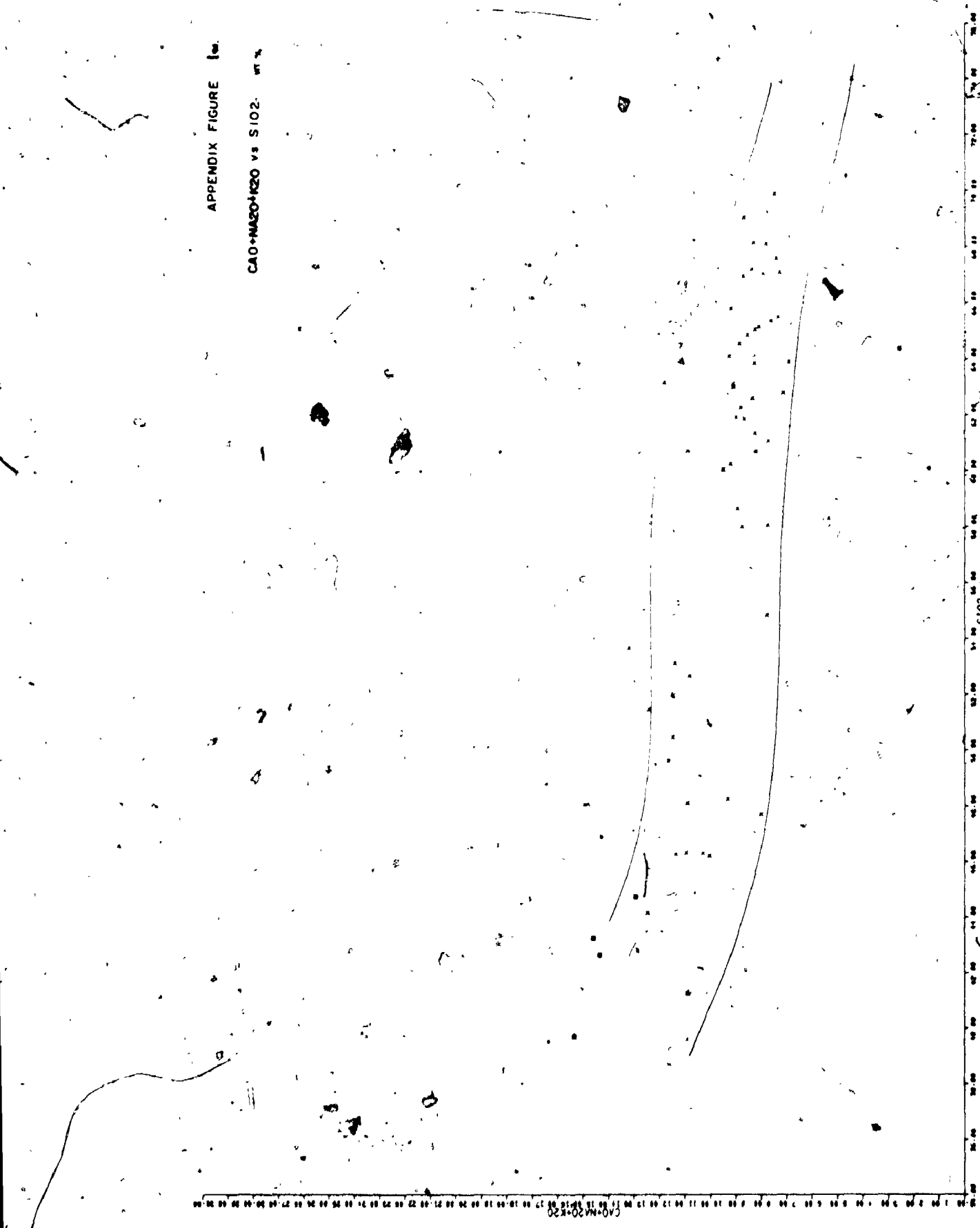

APPENDIX FIGURE 1a.

P2O5 vs SIO2 wt %

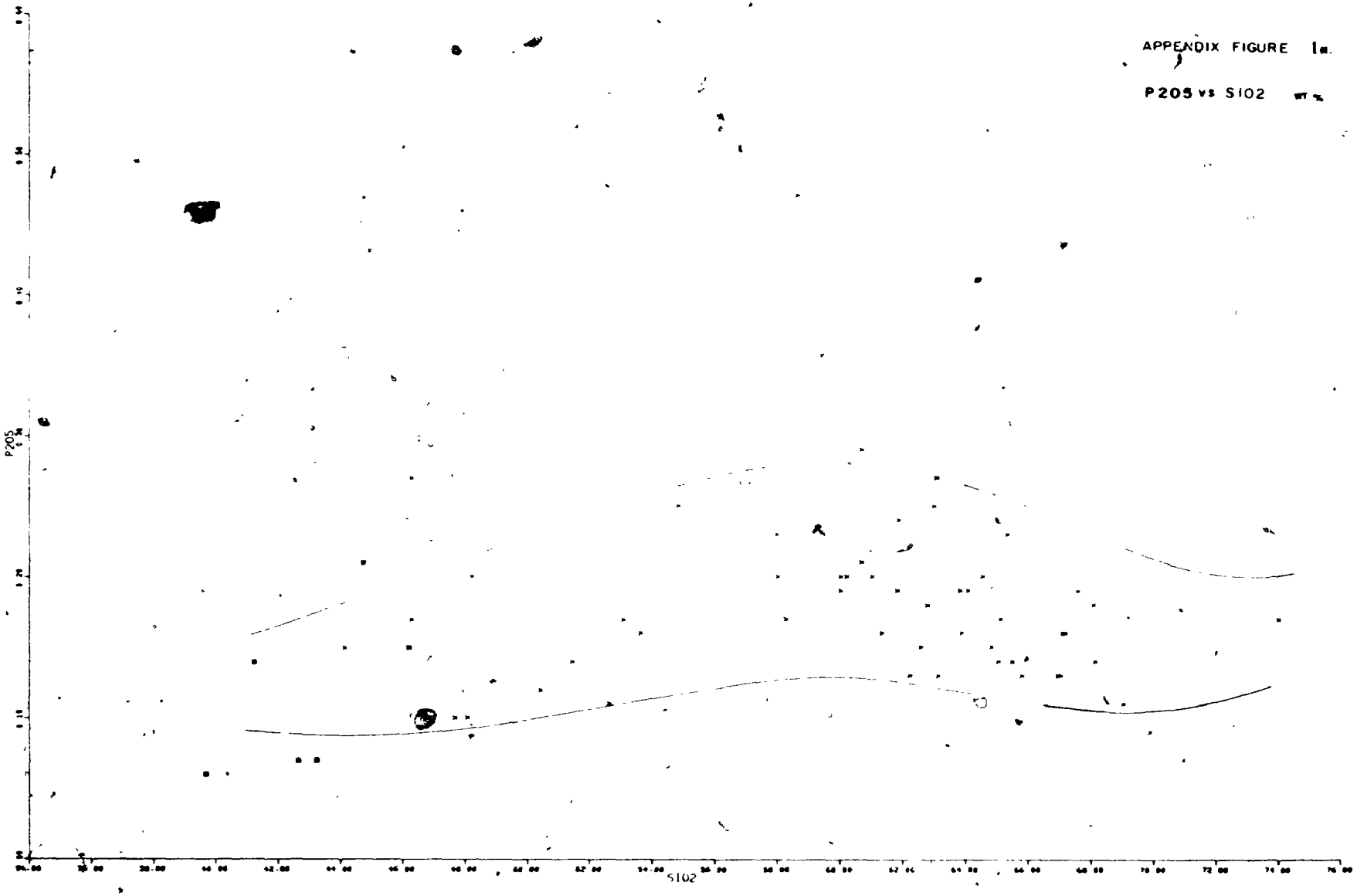

APPENDIX FIGURE 1a.

C02 vs. SiO2 wt %

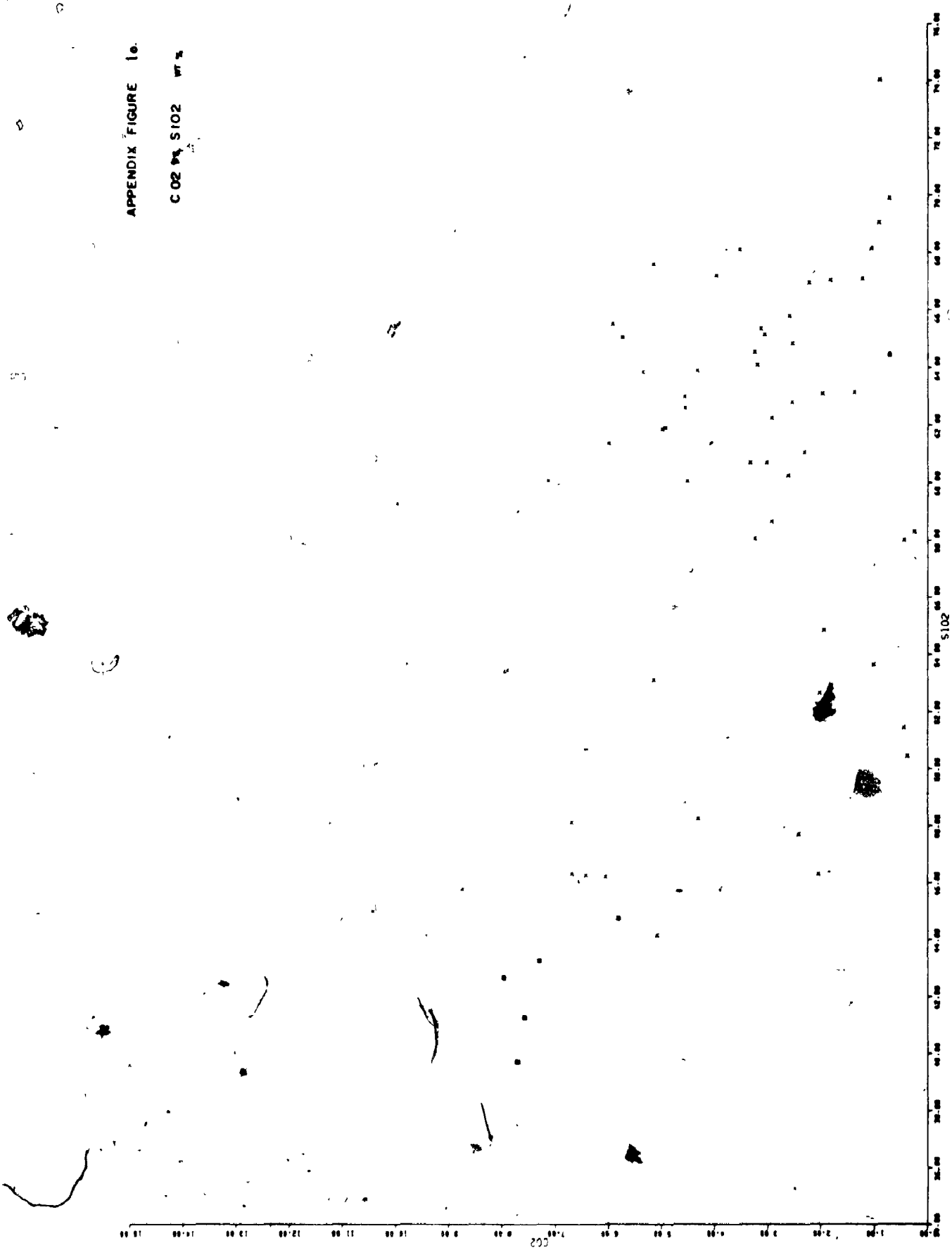

APPENDIX FIGURE 1.

H2O vs SIO2 WT %

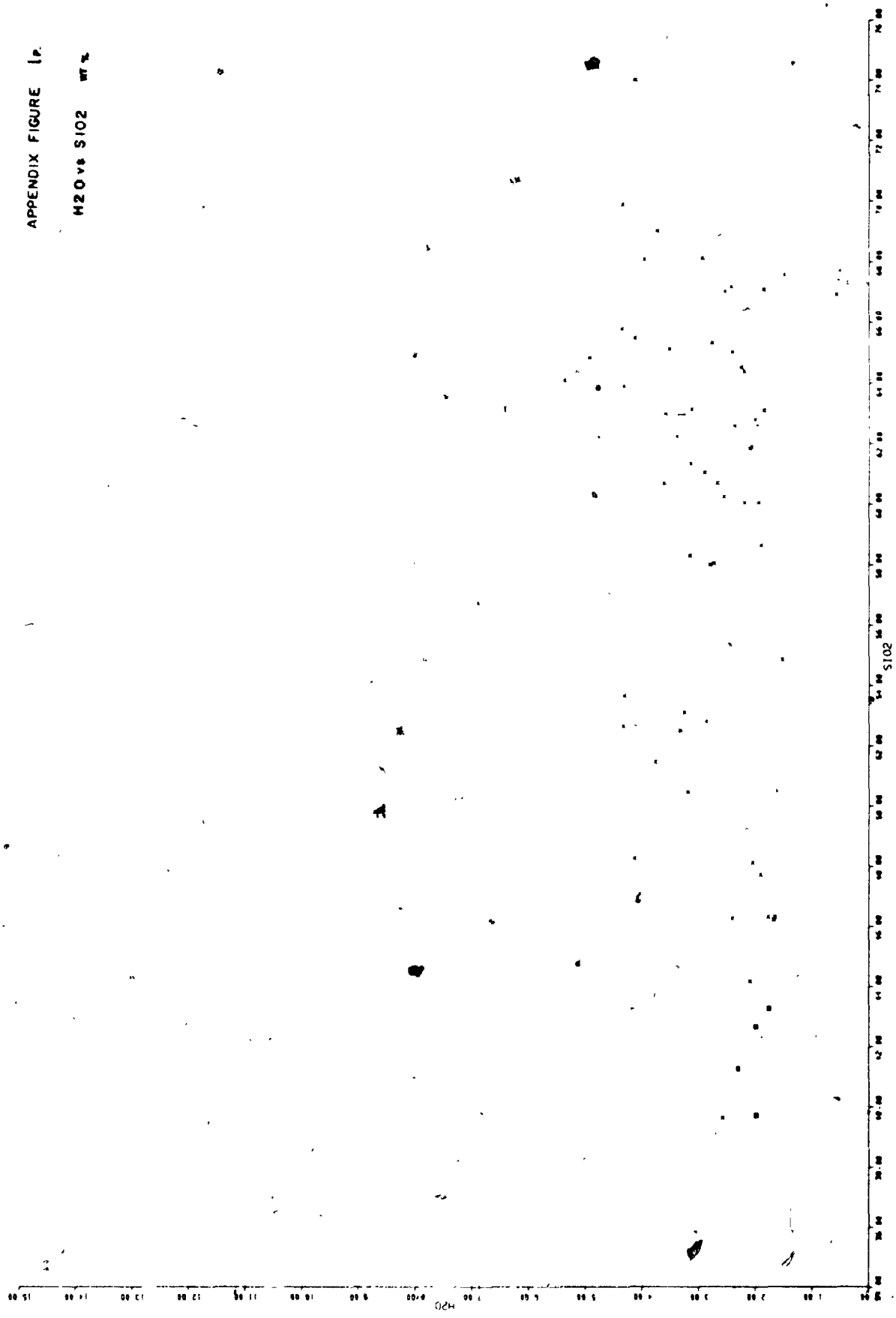

Sample Number	Equivalent Coding	Sample Number	Equivalent Coding	Sample Number	Equivalent Coding
D 1	1803	D21	1823	D41	1843
D 2	1804	D22	1824	D42	1844
D 3	1805	D23	1825	D43	1845
D 4	1806	D24	1826	D44	1846
D 5	1807	D25	1827	D45	1847
D 6	1808	D26	1828	D46	1848
D 7	1809	D27	1829	D47	1849
D 8	1810	D28	1830	D48	1850
D 9	1811	D29	1831	D49	1851
D10	1812	D30	1832	D50	1852
D11	1813	D31	1833	D51	1853
D12	1814	D32	1834	D52	1854
D13	1815	D33	1835	D53	1855
D14	1816	D34	1836	D54	1856
D15	1817	D35	1837	D55	1857
D16	1818	D36	1838	D56	1858
D17	1819	D37	1839	D57	1859
D18	1820	D38	1840	D58	1860
D19	1821	D39	1841	D59	1861
D20	1822	D40	1842	D60	1862

APPENDIX IV

Mine sample analytical data and figures

Firstly, the analytical data are presented for the samples from the two orebody cross-sections, in the same format as that for the surface samples (Appendix III). Empire No. 3 orebody samples are prefixed by "E" for identification; this prefix is not used in the preceding text, specifically figure 19 and Table 10. No. 4 orebody samples are not prefixed.

Secondly, cross-sections showing contoured distribution of selected oxides, elements and combinations of these are presented for the No. 4 orebody (Appendix figs. 2-12 and 15). Contouring was performed by multiple triangle resolution. The triangular base was constructed such that it contained a maximum number of triangles, excluding those with apices on the same drill hole; the same base was used for all sections. Contours are not rounded, but relate directly to the points involved in their calculation. Individual relatively high or low values have the effect of overemphasising their field of influence, beyond that expected from geological evidence, specifically Cu around the orebody (Appendix fig. 7); this effect would be emphasised by contour rounding.

Thirdly, cross-sections showing contoured distribution are presented for the Empire No. 3 orebody cross-section (Appendix figs. 16, 17, 19-22). Values were contoured in a similar manner to those of the No. 4 orebody. Samples 6, 61, 62, 63, 64 and 65 (Fig. 19) were excluded for ease of presentation, although these were included in initial examination. Sample 30 was excluded due to its exceptionally high CO_2 content (14.14%) which invalidated its direct comparison with other samples.

Lastly, a listing is given of the sample numbers with their equivalent coding for the thin section collection of the Geology Department of the University of Western Ontario.

SAMPLE 30												
69.50	.12	17.00	1.37	1.81	.04	1.15	.54	.95	2.62	.09	1.10	2.77
700	15	80	40	10	8	875	400	30	15	200	10	80
SAMPLE 25												
72.10	.09	15.90	1.29	1.74	.02	.84	.07	.80	2.78	.09	.24	2.55
70	15	100	40	20	8	900	250	15	20	150	15	100
SAMPLE 10												
58.80	.60	17.00	2.00	4.34	.15	2.64	2.84	.80	1.84	.19	3.62	3.26
6600	50	240	240	30	8	650	5000	30	15	150	40	100
SAMPLE 8												
60.60	.59	17.90	1.96	4.55	.08	2.26	1.68	.74	2.80	.17	1.45	3.20
6200	50	260	500	20	8	725	4000	80	20	200	50	150
SAMPLE 1												
54.00	.25	17.70	1.13	6.73	.13	2.33	2.04	.61	1.89	.18	2.08	3.46
12200	40	460	880	20	12	700	3000	70	15	150	40	100
SAMPLE 7												
61.20	.18	17.20	2.38	4.62	.04	1.70	1.05	.76	1.93	.14	.97	3.17
22400	100	480	800	15	10	775	3000	15	15	150	40	200
SAMPLE 5												
54.70	.38	12.90	1.53	4.70	.20	3.44	6.92	.75	1.35	.25	10.00	2.54
1240	50	480	120	30	10	900	1000	150	15	200	50	150
SAMPLE 14												
61.90	.48	15.80	1.57	4.34	.16	2.00	2.98	1.05	1.48	.21	4.18	3.28
900	30	170	100	30	14	700	400	40	20	200	60	300
SAMPLE 16												
55.60	.90	20.50	1.03	5.06	.08	2.40	2.35	1.62	1.87	.19	2.88	4.58
60	15	200	100	20	19	525	100	350	20	200	200	200
SAMPLE 19												
51.00	.49	15.10	1.15	8.96	.20	4.86	5.11	.79	1.10	.06	8.10	4.24
40	10	260	80	20	21	725	50	250	20	150	150	200
SAMPLE 38												
51.80	.56	14.19	5.05	5.98	.11	3.26	4.61	2.05	1.01	.33	5.66	3.80
1100	-1	156	143	117	24	240	150	80	10	150	60	200
SAMPLE 41												
52.80	.39	16.30	1.93	6.22	.11	3.16	4.58	1.77	1.04	.32	6.66	3.56
640	20	120	60	60	19	250	150	50	15	200	60	200
SAMPLE 50												
65.45	.14	15.44	4.54	3.86	.05	2.58	1.15	.63	1.44	.09	.54	2.64
3675	-1	190	605	52	14	360	2500	80	-1	30	15	100
SAMPLE 52												
72.05	.24	14.64	.98	2.02	.05	1.80	1.18	.76	2.44	.09	1.18	2.63
810	-1	155	48	10	12	555	800	80	-1	60	20	150
SAMPLE 55												
61.55	.42	14.09	1.07	2.82	.22	2.73	4.44	1.02	2.47	.19	6.36	2.35
59	25	135	58	15	8	720	50	100	10	100	50	150
SAMPLE 59												
72.40	.04	14.76	1.36	1.94	.03	1.33	.81	1.43	2.10	.18	.26	2.54
310	-1	105	60	20	12	540	50	80	110	100	50	150
SAMPLE 60												
64.30	.42	13.90	2.07	3.02	.14	2.45	3.66	1.09	1.77	.20	3.51	2.43
256	-1	135	52	18	12	555	600	80	10	80	50	200
SAMPLE 65												
49.65	.67	16.26	3.27	3.41	.19	3.88	8.07	1.77	1.98	.23	6.97	2.71
186	-1	170	140	36	10	375	250	250	10	150	70	150
SAMPLE 70												
51.20	.53	14.34	2.81	3.90	.19	3.70	9.24	2.18	1.44	.20	7.68	2.56
530	75	540	174	50	15	465	150	200	15	100	60	200
SAMPLE 73												
56.55	.59	14.27	1.43	3.94	.13	4.22	4.56	3.68	1.06	.25	6.22	2.47
61	35	210	168	20	14	330	40	250	10	100	70	200

SAMPLE 76												
51.35	.58	13.93	1.02	5.45	.20	4.57	6.77	2.96	1.54	.24	9.46	2.55
184	-1	215	140	30	13	285	40	200	15	100	60	200
SAMPLE 79												
61.90	.42	14.26	.89	3.53	.13	2.43	5.17	1.13	1.36	.17	4.87	2.68
165	25	125	50	15	17	405	50	50	15	200	50	250
SAMPLE 200												
49.70	.52	17.20	3.15	14.50	.14	3.17	1.82	.21	1.22	.21	1.24	6.40
580	10	760	280	30	22	310	30	10	15	30	100	300
SAMPLE 205												
62.10	.48	16.00	1.25	3.40	.14	1.60	3.64	1.01	2.25	.17	4.54	2.56
90	30	220	70	20	8	700	40	40	15	40	40	15
SAMPLE 215												
65.20	.32	16.30	.77	3.11	.11	1.44	2.98	.94	2.14	.10	3.78	2.87
30	30	150	50	10	10	675	50	40	20	150	40	100
SAMPLE 220												
59.20	.46	15.70	1.04	3.90	.15	2.24	4.70	1.28	1.79	.16	5.46	3.01
100	30	110	50	10	10	550	100	50	20	200	50	100
SAMPLE 225												
58.30	.46	16.20	1.06	3.98	.17	1.93	4.66	2.21	1.50	.21	5.64	2.90
70	20	110	80	20	12	375	80	150	20	200	70	150
SAMPLE 232												
54.60	.48	19.10	.89	4.41	.12	2.25	3.88	3.56	1.29	.16	5.38	2.76
30	15	50	50	10	9	450	40	200	20	200	150	150
SAMPLE 43												
68.35	.21	12.55	3.82	3.26	.04	1.66	1.58	1.03	1.91	.15	1.06	3.07
2160	208	154	478	55	16	600	150	100	15	100	30	200
SAMPLE 101												
61.90	.39	14.81	3.58	4.74	.05	2.94	1.42	1.08	2.13	.18	1.76	3.96
2070	30	235	450	50	-2	-2	100	100	20	60	40	200
SAMPLE 104												
60.55	.19	14.16	1.98	2.09	.07	1.43	1.78	1.19	2.57	.13	2.10	2.90
1720	-1	145	84	15	-2	-2	400	80	15	80	20	200
SAMPLE 107												
72.35	.18	14.53	1.24	1.94	.04	.99	.98	1.08	2.58	.13	.68	2.84
157	-1	280	106	15	-2	-2	150	50	10	40	10	200
SAMPLE 116												
48.40	.36	11.20	9.04	17.76	.07	2.97	1.34	.31	.46	.25	.65	4.80
50000	95	590	1600	35	-2	-2	3000	100	10	15	100	250
SAMPLE 121												
61.15	.24	11.10	3.14	7.78	.17	2.76	4.39	1.01	1.57	.14	5.60	2.85
1690	54	310	260	44	-2	-2	800	80	10	50	30	150
SAMPLE 126												
47.75	.82	14.44	1.52	4.28	.20	3.07	5.98	3.04	2.21	.18	8.18	3.77
73	124	125	136	24	-2	-2	100	300	20	100	150	200
SAMPLE 154												
66.05	.33	14.37	3.49	3.52	.05	1.41	1.95	1.16	2.32	.19	1.81	3.48
207	28	245	106	28	8	540	50	50	10	60	20	150
SAMPLE 157												
68.75	.32	13.88	2.48	4.27	.04	1.93	.81	.97	1.76	.14	.55	3.68
385	14	235	101	34	16	480	1500	80	15	50	40	150
SAMPLE 164												
69.45	.27	14.41	1.33	1.58	.07	1.21	1.76	1.73	2.36	.09	2.24	2.94
63	-1	160	40	15	6	870	500	50	10	60	85	100
SAMPLE 170												
57.45	.47	15.02	2.17	3.52	.15	2.34	4.16	1.81	2.29	.33	5.94	3.05
30	35	490	66	19	6	630	200	40	15	60	40	150
SAMPLE 178												
63.30	.39	14.44	2.14	2.78	.12	1.77	3.13	2.26	1.92	.15	4.26	2.78
153	-1	93	55	23	10	600	200	150	10	100	40	200

SAMPLE 181												
55.30	.63	14.36	2.41	6.96	.13	2.74	4.98	2.08	1.14	.25	4.86	4.89
125	-1	230	70	20	25	240	30	200	10	100	60	200
SAMPLE 182												
51.40	.66	14.18	2.19	5.46	.19	3.28	6.49	2.17	1.34	.19	8.87	3.27
61	-1	140	62	21	16	240	30	200	15	100	60	200
SAMPLE 187												
58.58	.71	15.38	4.16	4.22	.06	1.96	2.86	2.68	1.07	.22	3.12	3.70
537	38	130	126	103	21	195	80	40	10	150	60	150
SAMPLE 201												
61.15	.43	14.43	1.85	3.86	.10	1.77	4.98	.51	2.78	.16	4.03	3.85
284	150	220	96	14	12	645	150	150	-	50	50	150
SAMPLE 229												
50.65	.79	15.69	2.20	6.02	.17	3.29	5.60	4.02	1.03	.20	6.75	3.61
10	-1	120	36	12	-2	-2	50	20	15	100	150	150
SAMPLE 250												
60.25	.48	13.76	3.10	4.66	.09	2.68	3.17	1.48	1.16	.15	4.12	3.35
705	25	735	134	35	-2	-2	1500	70	10	80	100	200
SAMPLE 255												
57.05	.44	12.21	3.51	4.26	.17	2.93	4.89	1.31	2.02	.29	6.46	3.06
915	62	595	110	45	-2	-2	200	100	15	100	80	150
SAMPLE 259												
49.85	.76	17.10	1.75	5.06	.15	3.37	5.63	2.62	1.91	.18	7.64	4.04
54	-1	165	145	22	-2	-2	50	300	15	100	150	150
SAMPLE 261												
59.15	.49	15.17	3.48	3.18	.12	1.82	3.41	1.48	2.41	.21	4.45	2.88
3200	32	150	260	25	-2	-2	1500	60	10	80	40	150
SAMPLE 272												
72.85	.19	13.48	1.44	2.18	.06	1.27	1.46	1.11	2.17	.11	.38	2.82
236	-1	360	48	14	-2	-2	1500	80	10	60	30	150
SAMPLE 276												
68.60	.15	13.02	2.52	4.62	.05	2.03	1.18	.67	1.85	.11	1.16	3.36
290	-1	340	93	30	-2	-2	150	50	-1	60	20	200
SAMPLE 279												
55.80	.76	14.18	5.32	11.62	.07	3.05	1.12	.38	.86	.21	.84	5.45
370	-1	460	340	20	-2	-2	30	60	-1	10	200	250
SAMPLE 48												
42.40	.43	14.62	5.57	11.64	.18	6.28	5.94	1.49	.49	.07	4.81	5.40
1490	50	360	750	162	33	90	-1	-2	-2	-2	-2	-2
SAMPLE 128												
40.90	.36	14.58	2.68	11.08	.18	6.87	8.46	1.71	.57	.10	6.51	5.46
1530	28	290	600	73	30	150	-1	-2	-2	-2	-2	-2
SAMPLE 188												
40.35	.35	13.82	3.04	11.96	.14	7.98	8.37	1.18	.23	.10	6.33	5.86
2030	78	390	850	112	28	60	-1	-2	-2	-2	-2	-2
SAMPLE E1												
72.40	.19	14.53	1.04	1.16	.09	1.03	1.41	1.82	1.97	.08	2.04	2.07
12	-1	24	20	-1	12	285	60	-2	-2	-2	-2	-2
SAMPLE E2												
52.05	.87	18.97	1.87	5.48	.14	2.89	4.30	2.44	2.51	.25	3.94	3.85
52	-1	66	68	26	15	285	100	-2	-2	-2	-2	-2
SAMPLE E3												
60.65	.69	14.69	1.07	4.32	.11	2.90	4.16	2.85	1.27	.27	3.81	2.74
150	-1	72	400	33	11	210	50	-2	-2	-2	-2	-2
SAMPLE E4												
56.45	.67	14.63	1.24	4.88	.21	4.15	5.17	3.99	1.09	.32	6.58	2.38
15	-1	70	148	24	10	210	20	-2	-2	-2	-2	-2
SAMPLE E5												
57.10	.57	13.74	1.39	5.24	.15	3.18	6.61	2.27	.83	.30	5.52	3.19
2310	-1	97	550	17	15	195	30	-2	-2	-2	-2	-2

SAMPLE E6												
54.85	.45	14.94	2.14	7.40	.14	3.10	4.91	3.44	.38	.17	4.31	3.51
298	-1	139	440	46	14	185	20	-2	-2	-2	-2	-2
SAMPLE E10												
60.65	.61	16.04	1.68	4.60	.08	2.13	2.96	2.97	1.77	.37	2.82	3.39
14	-1	70	45	18	12	345	20	-2	-2	-2	-2	-2
SAMPLE E11												
55.60	.73	16.31	1.46	5.58	.13	2.27	5.03	3.71	1.71	.47	3.73	3.04
9	-1	79	25	16	13	330	15	-2	-2	-2	-2	-2
SAMPLE E12												
55.30	.69	14.68	1.68	7.20	.15	2.87	5.36	2.57	1.23	.46	3.90	3.49
85	-1	108	74	28	19	210	10	-2	-2	-2	-2	-2
SAMPLE E13												
59.55	.69	15.48	.37	6.96	.11	1.97	3.64	3.78	1.38	.46	2.56	2.99
1800	-1	87	230	25	13	285	10	-2	-2	-2	-2	-2
SAMPLE E14												
57.05	.65	14.74	2.82	5.76	.15	2.35	4.74	2.90	.91	.44	3.73	3.44
48	-1	96	110	28	18	165	10	-2	-2	-2	-2	-2
SAMPLE E15												
51.65	.78	14.42	2.25	7.28	.11	5.23	4.02	4.39	.53	.49	5.10	3.31
220	-1	98	390	54	16	75	-1	-2	-2	-2	-2	-2
SAMPLE E16												
42.60	.81	14.32	3.99	9.44	.19	5.58	7.44	2.96	.38	.18	6.54	4.69
940	-1	129	740	116	22	60	-1	-2	-2	-2	-2	-2
SAMPLE E17												
43.50	1.11	15.55	1.72	9.60	.18	6.18	7.36	3.93	.33	.09	5.47	4.73
80	-1	83	116	43	20	30	-1	-2	-2	-2	-2	-2
SAMPLE E20												
69.75	.23	14.42	1.29	1.88	.11	1.57	1.94	1.82	2.01	.08	2.77	2.04
14	63	41	30	11	10	345	30	-2	-2	-2	-2	-2
SAMPLE E21												
55.90	.73	17.03	1.52	4.20	.15	2.12	5.38	2.53	2.49	.44	4.42	2.98
9	39	66	24	15	12	390	20	-2	-2	-2	-2	-2
SAMPLE E22												
66.05	.42	14.94	.92	2.16	.10	1.58	3.46	1.54	2.21	.13	3.51	2.38
34	-1	35	29	8	12	420	40	-2	-2	-2	-2	-2
SAMPLE E23												
73.40	.17	14.39	.79	1.32	.06	.72	1.89	1.17	2.16	.08	1.64	2.15
20	25	25	23	6	10	465	40	-2	-2	-2	-2	-2
SAMPLE E24												
68.25	.25	14.98	1.08	3.72	.08	1.50	2.47	1.15	1.71	.11	1.91	2.97
22	-1	55	42	11	16	345	50	-2	-2	-2	-2	-2
SAMPLE E25												
51.05	.78	15.82	1.19	6.96	.16	5.05	6.01	3.37	1.25	.40	4.35	3.47
121	-1	91	81	20	17	210	20	-2	-2	-2	-2	-2
SAMPLE E30												
42.45	.23	10.36	1.69	6.40	.29	5.87	13.02	.63	1.26	.16	14.14	2.93
2550	44	78	82	25	17	210	80	-2	-2	-2	-2	-2
SAMPLE E31												
57.80	.39	12.45	1.38	6.60	.11	5.87	3.79	.58	1.36	.18	5.67	3.70
420	50	103	104	34	20	225	20	-2	-2	-2	-2	-2
SAMPLE E32												
61.65	.65	17.12	1.45	4.32	.06	2.20	1.59	4.67	1.24	.35	1.33	2.79
26	378	74	55	18	12	180	20	-2	-2	-2	-2	-2
SAMPLE E33												
57.10	.68	16.17	1.43	5.48	.12	1.93	4.47	4.46	1.18	.48	3.19	2.81
39	-1	63	66	28	15	165	10	-2	-2	-2	-2	-2
SAMPLE E34												
55.20	.78	16.28	1.58	6.84	.12	2.45	4.14	3.66	1.29	.46	7.86	3.47
58	-1	67	50	26	19	225	10	-2	-2	-2	-2	-2

SAMPLE E35												
53.80	.76	16.45	2.74	12.04	.08	4.90	.67	1.04	.43	.35	.29	5.81
111	-1	124	298	35	42	75	40	-2	-2	-2	-2	-2
SAMPLE E36												
44.95	1.23	16.14	3.73	7.76	.17	6.07	9.35	2.47	.04	.08	2.78	4.39
75	25	78	109	42	15	45	10	-2	-2	-2	-2	-2
SAMPLE E40												
61.05	.51	16.11	1.08	3.96	.13	1.95	4.29	2.13	1.98	.24	3.64	2.71
154	-1	52	54	19	17	300	40	-2	-2	-2	-2	-2
SAMPLE E41												
62.10	.59	15.24	3.32	4.24	.09	2.03	2.53	3.25	1.53	.23	2.45	2.51
16	-1	58	49	16	8	150	15	-2	-2	-2	-2	-2
SAMPLE E42												
57.35	.77	15.86	1.45	5.04	.13	2.22	4.71	3.26	1.73	.46	3.43	3.12
4	-1	58	20	12	8	210	15	-2	-2	-2	-2	-2
SAMPLE E43												
53.90	.74	15.91	1.73	5.92	.16	2.55	5.76	3.59	1.27	.45	4.23	3.32
5	-1	72	33	16	12	225	15	-2	-2	-2	-2	-2
SAMPLE E44												
58.85	.76	14.72	1.43	6.52	.06	4.73	2.86	1.35	.79	.34	3.03	4.01
105	-1	74	54	20	14	105	80	-2	-2	-2	-2	-2
SAMPLE E50												
73.85	.29	14.82	.95	1.28	.04	.90	.86	1.54	2.01	.13	.94	2.23
5	-1	20	20	5	10	300	80	-2	-2	-2	-2	-2
SAMPLE E51												
70.50	.26	14.71	1.45	1.48	.06	1.07	2.11	1.21	2.18	.10	1.85	2.47
42	-1	30	55	5	9	375	200	-2	-2	-2	-2	-2
SAMPLE E52												
65.20	.27	13.23	1.27	3.72	.12	2.03	4.16	1.06	1.92	.11	3.90	2.71
140	-1	56	51	12	13	300	40	-2	-2	-2	-2	-2
SAMPLE E53												
53.05	.63	16.30	1.36	6.44	.14	2.55	6.61	2.57	1.27	.33	4.97	3.56
58	-1	105	128	19	12	135	40	-2	-2	-2	-2	-2
SAMPLE E54												
34.30	.57	11.61	7.56	14.04	.12	9.90	5.06	.06	.85	.15	9.82	6.10
4270	-1	260	1960	199	30	30	-1	-2	-2	-2	-2	-2
SAMPLE E55												
51.75	.67	15.29	1.18	6.44	.14	3.25	7.08	2.70	.96	.30	6.59	3.62
200	-1	107	240	32	14	135	30	-2	-2	-2	-2	-2
SAMPLE E60												
71.05	.34	15.11	.87	1.98	.06	1.10	1.76	1.71	1.80	.14	1.82	2.25
31	-1	30	37	8	12	255	80	-2	-2	-2	-2	-2
SAMPLE E61												
69.90	.24	13.91	.78	2.36	.10	1.35	2.49	1.88	1.13	.11	3.01	2.24
124	-1	38	76	10	15	135	100	-2	-2	-2	-2	-2
SAMPLE E62												
71.15	.24	14.19	.62	2.04	.06	1.27	1.96	2.45	1.26	.11	2.05	2.12
35	-1	32	32	5	12	150	100	-2	-2	-2	-2	-2
SAMPLE E63												
72.70	.19	13.82	.49	1.56	.07	.95	1.98	2.89	1.22	.08	2.46	1.67
21	-1	22	23	5	13	165	100	-2	-2	-2	-2	-2
SAMPLE E64												
51.95	.51	19.97	1.07	8.72	.27	4.48	7.06	.96	1.04	.25	7.93	3.58
3630	-1	96	62	18	18	185	40	-2	-2	-2	-2	-2
SAMPLE E65												
54.15	.63	14.34	1.08	5.24	.15	4.73	4.71	2.63	1.88	.28	6.74	2.84
28	-1	59	94	19	12	150	80	-2	-2	-2	-2	-2

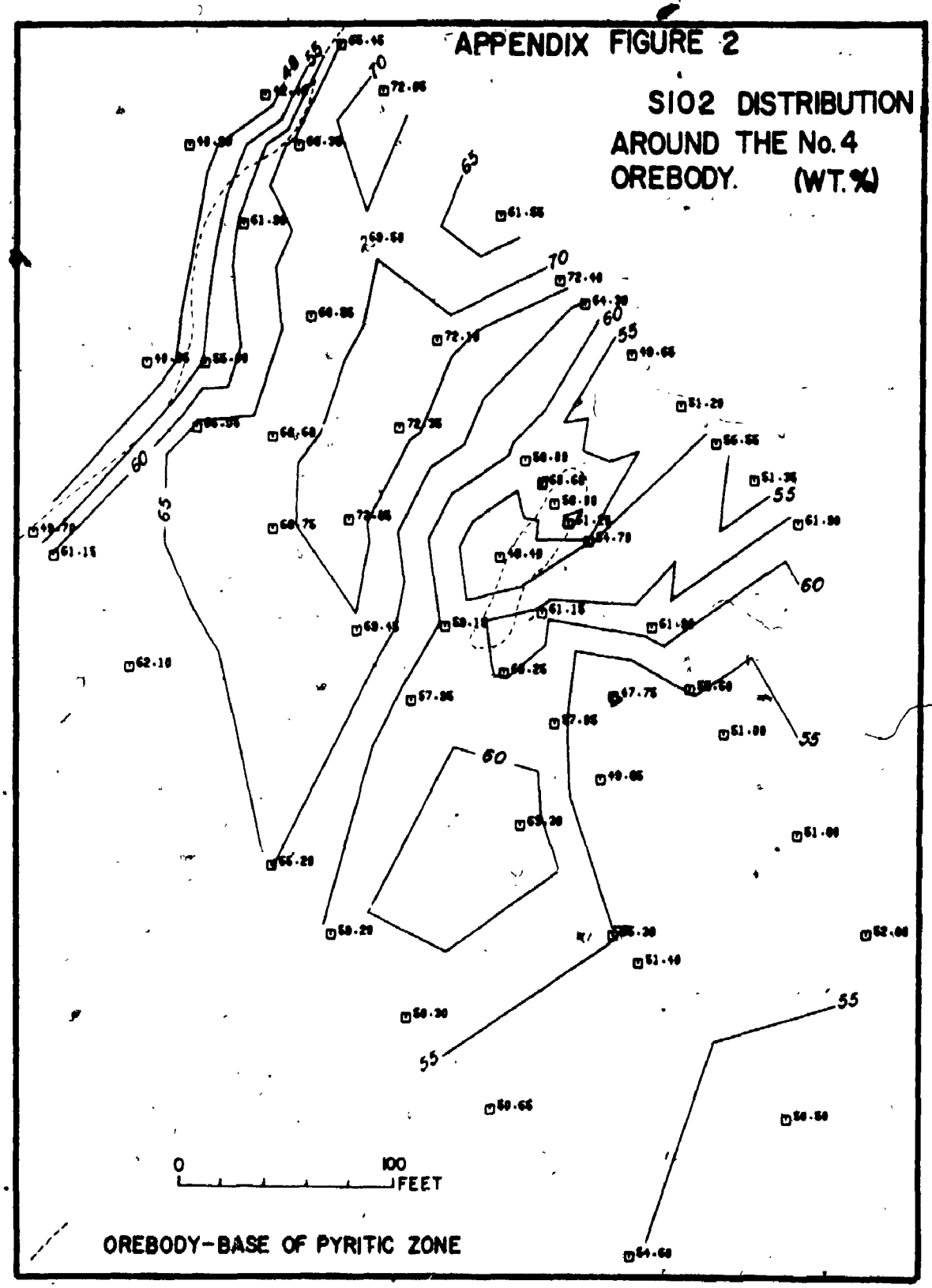
APPENDIX FIGURE 2
SIO2 DISTRIBUTION AROUND THE No. 4 OREBODY. (WT.%)
0
100
FEET
OREBODY-BASE OF PYRITIC ZONE

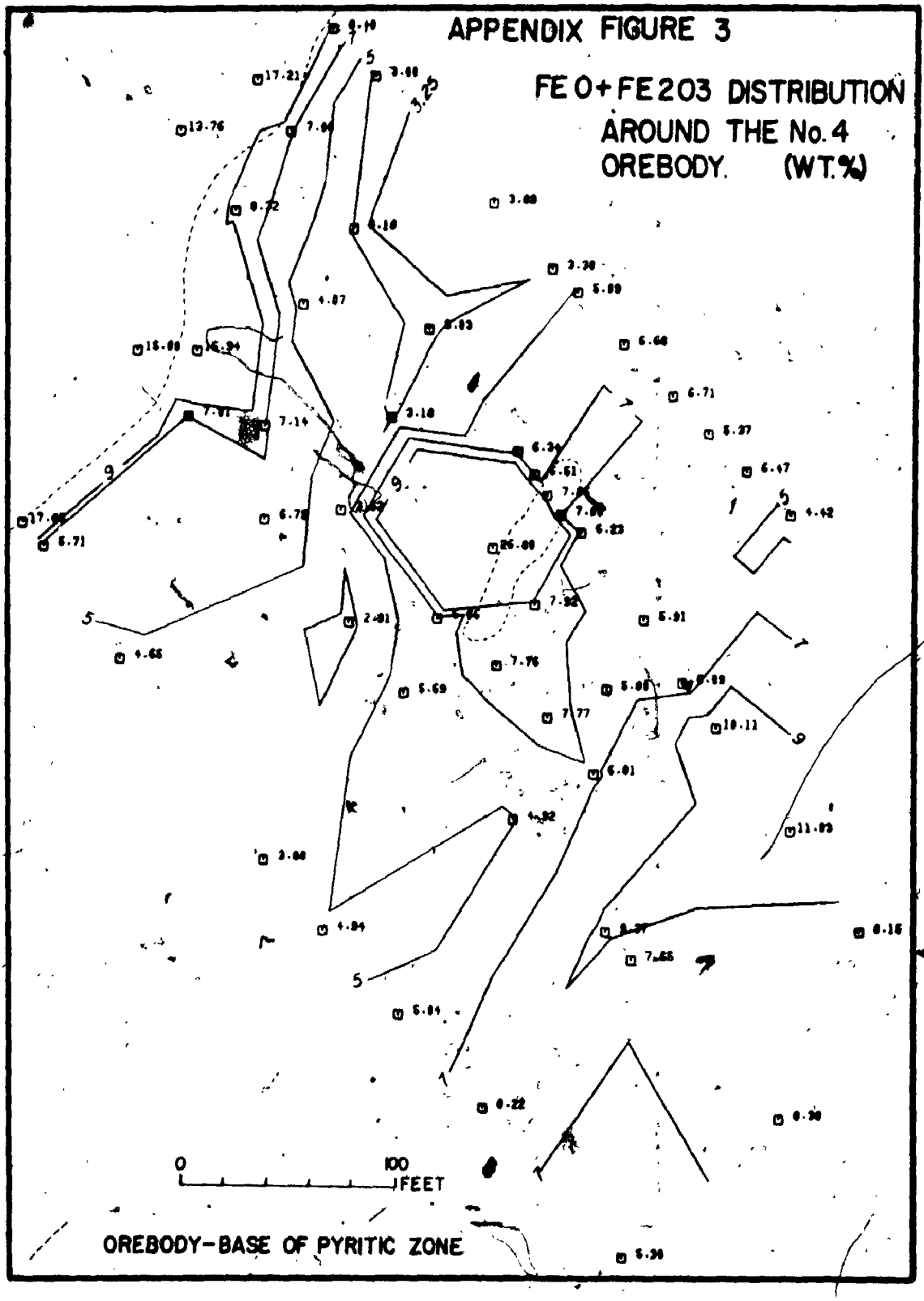
APPENDIX FIGURE 3
FE O+FE 203 DISTRIBUTION AROUND THE No. 4 OREBODY. (WT.%)
0
100
FEET
OREBODY-BASE OF PYRITIC ZONE

3 3

OF/DE

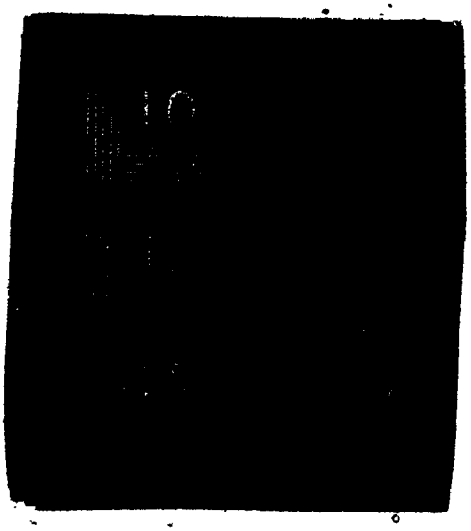

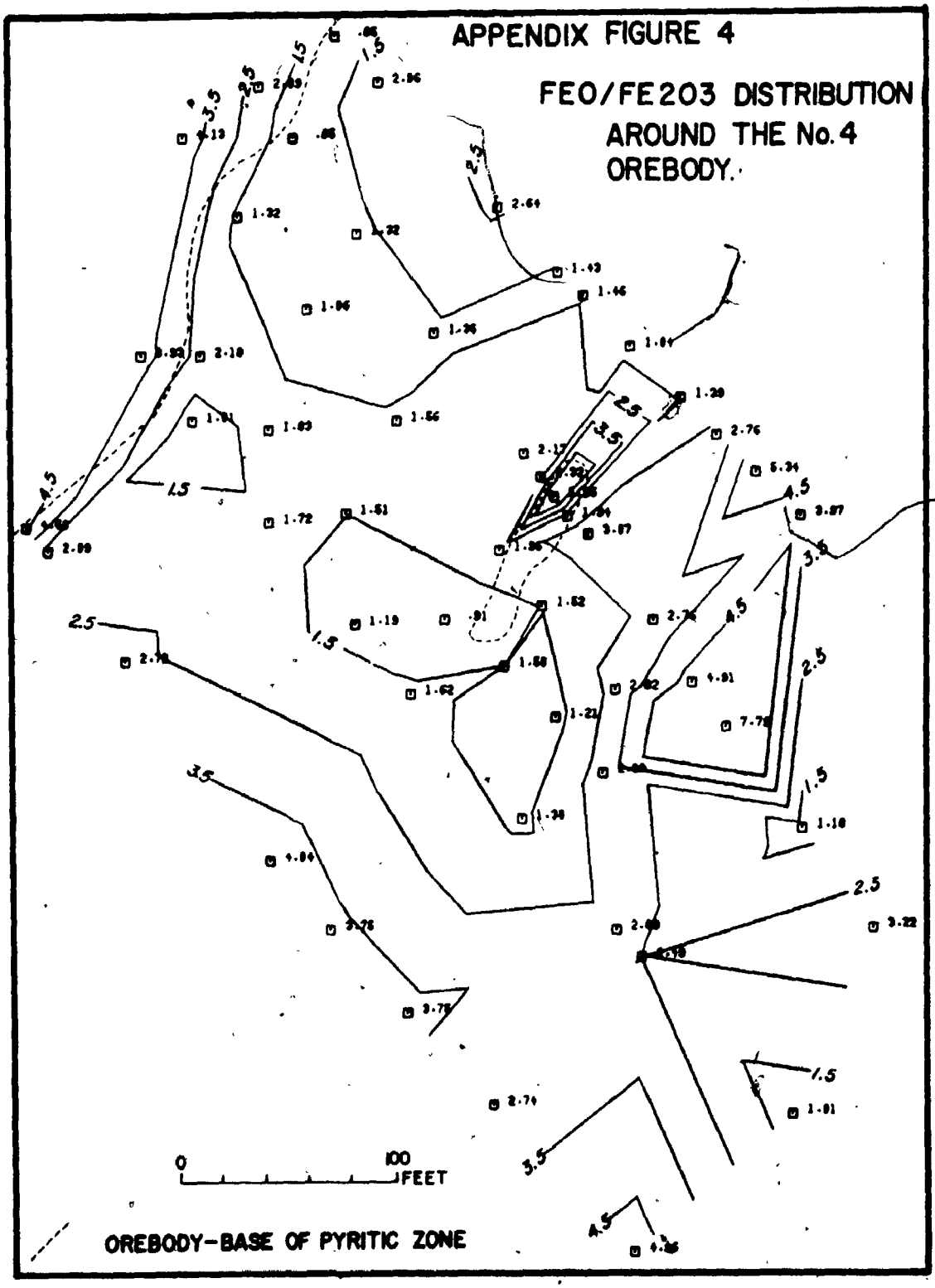
APPENDIX FIGURE 4
FEO/FE203 DISTRIBUTION AROUND THE No. 4 OREBODY.
0
100
FEET
OREBODY-BASE OF PYRITIC ZONE

APPENDIX FIGURE 5

MGO vs. SIO2 No.4 OREBODY SAMPLES (wt.%)

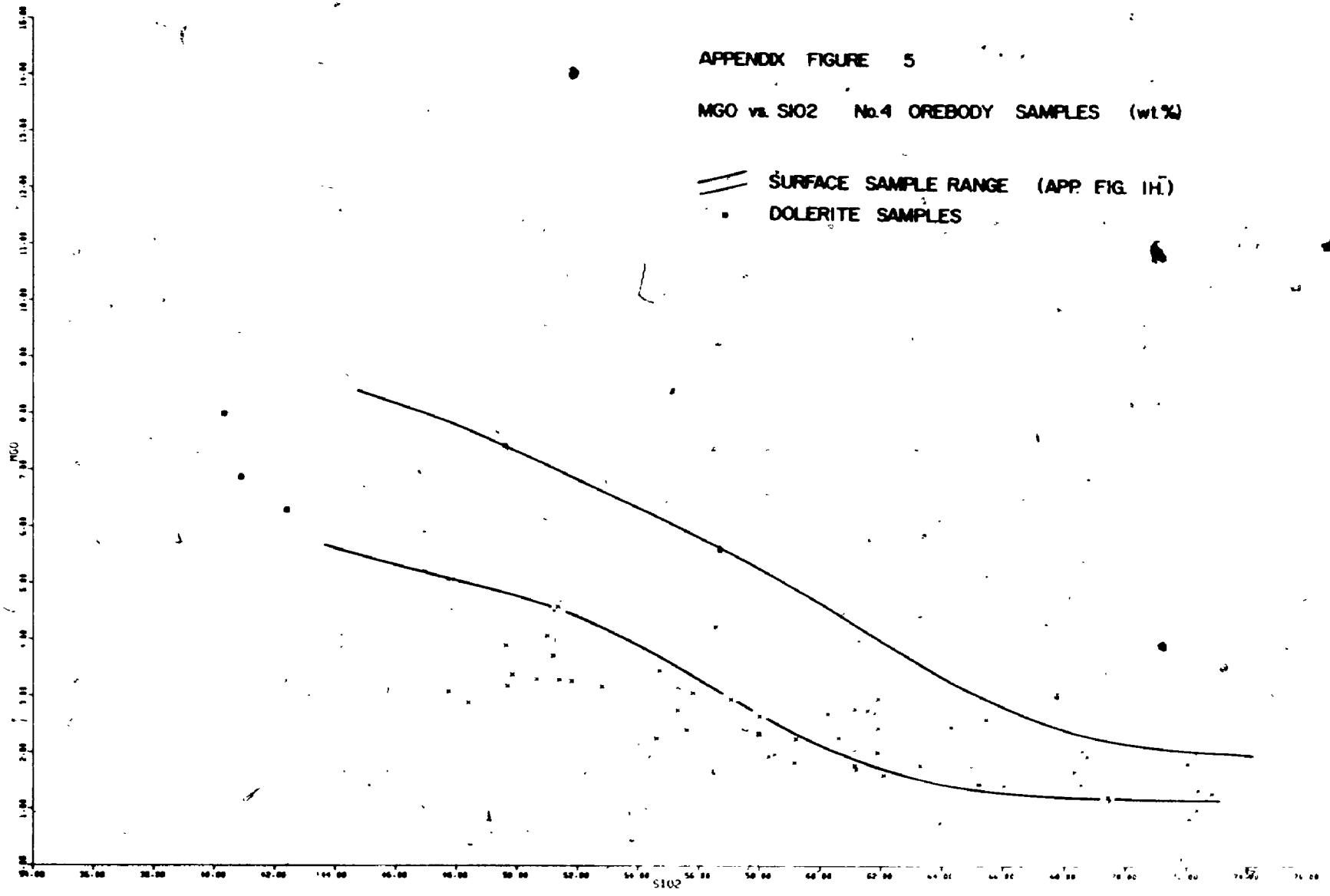

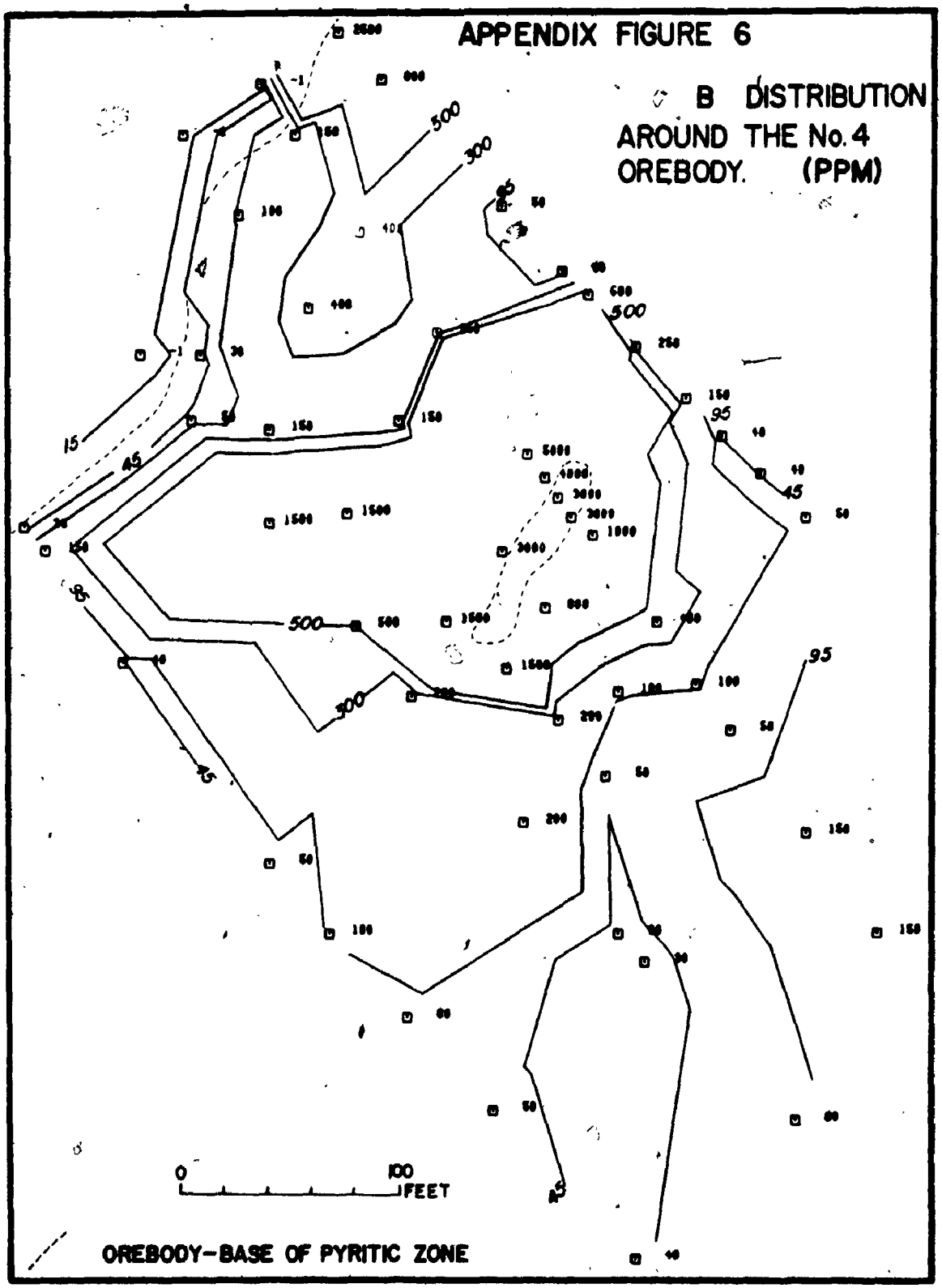
APPENDIX FIGURE 6
B DISTRIBUTION AROUND THE No. 4 OREBODY. (PPM)
0
100
FEET
OREBODY-BASE OF PYRITIC ZONE

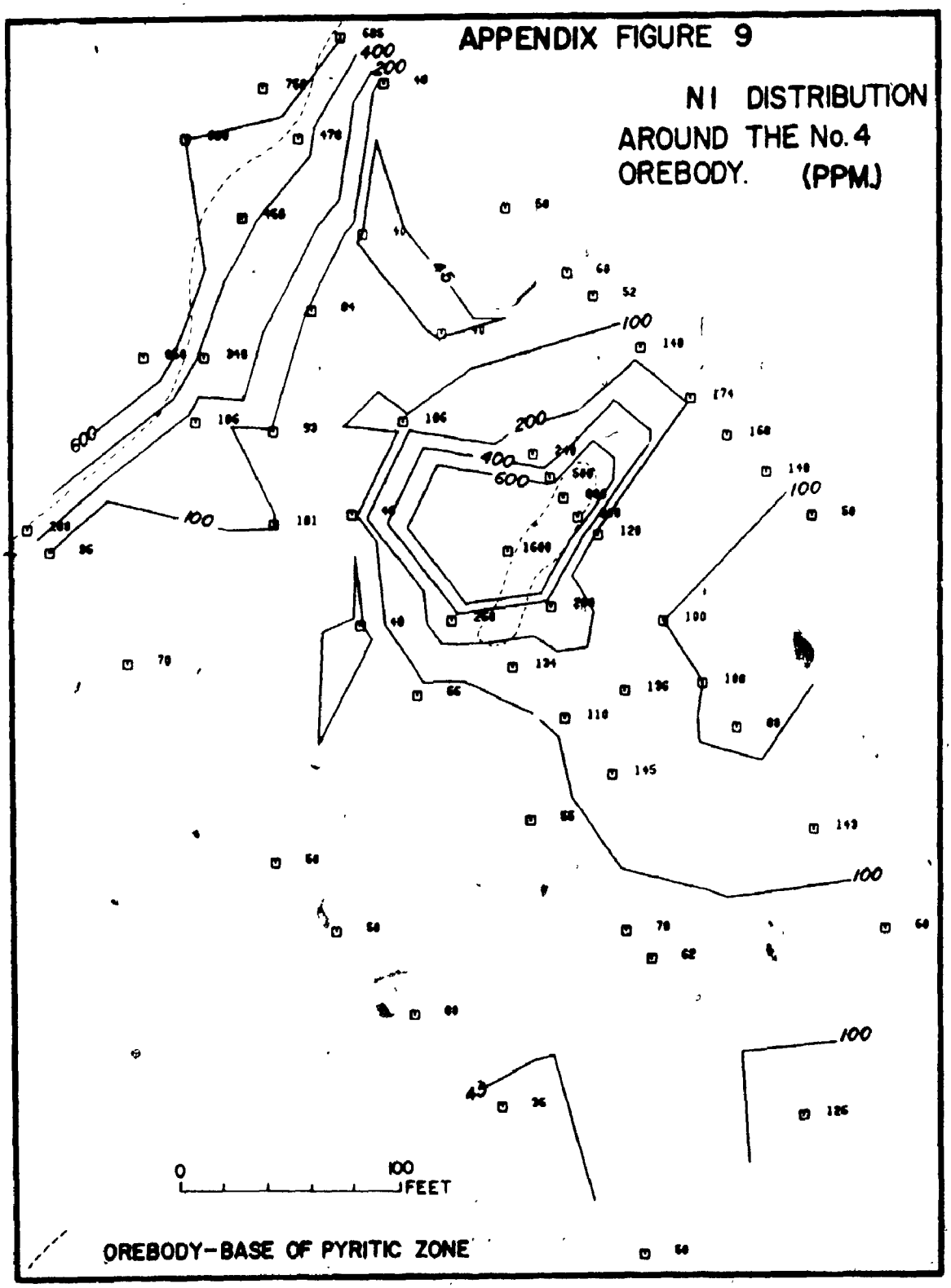
APPENDIX FIGURE 9
NI DISTRIBUTION AROUND THE No. 4 OREBODY. (PPM.)
100
200
400
600
0
100
FEET
OREBODY-BASE OF PYRITIC ZONE

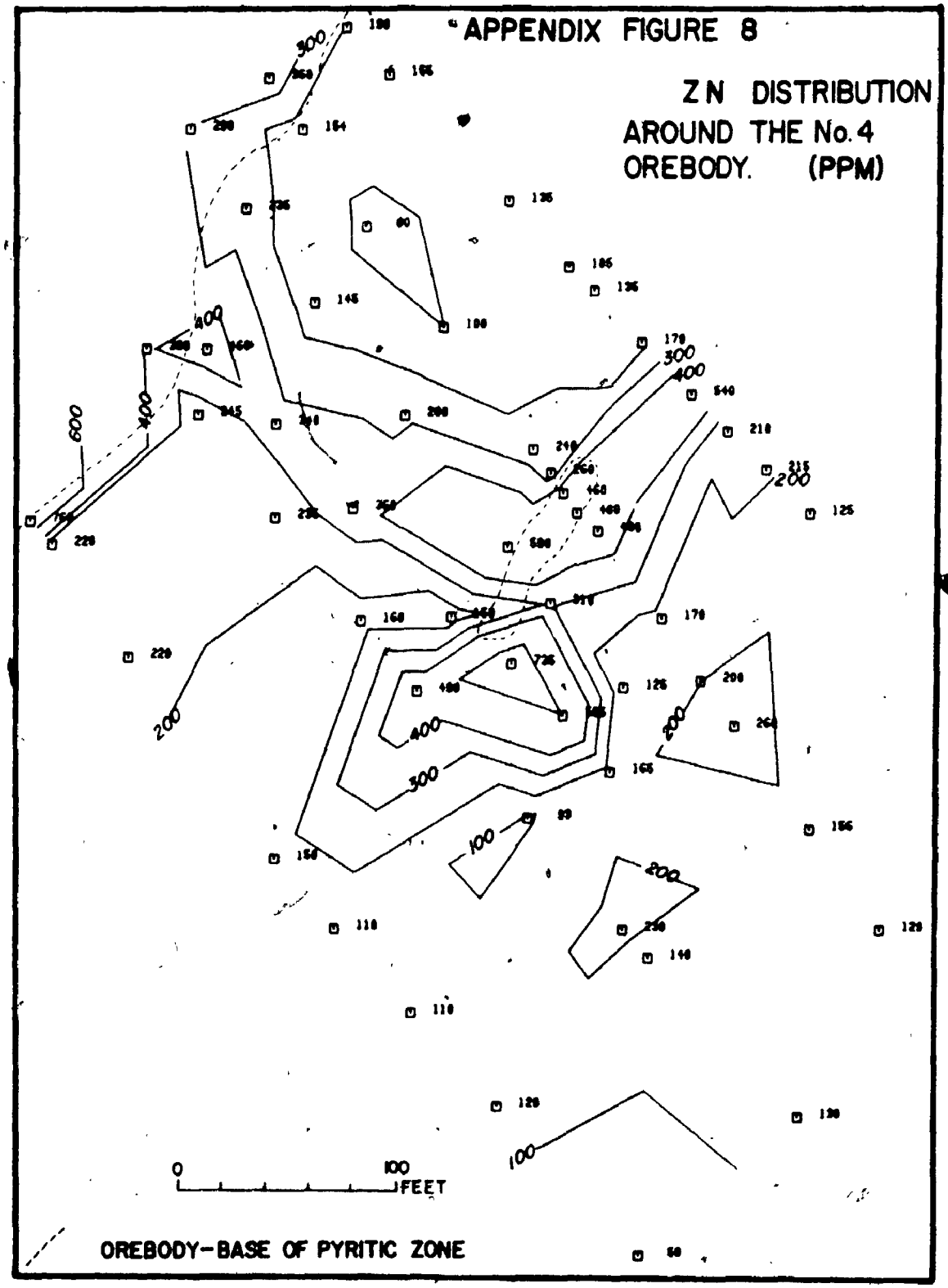
APPENDIX FIGURE 8
ZN DISTRIBUTION AROUND THE No. 4 OREBODY. (PPM)
0
100
FEET
OREBODY-BASE OF PYRITIC ZONE

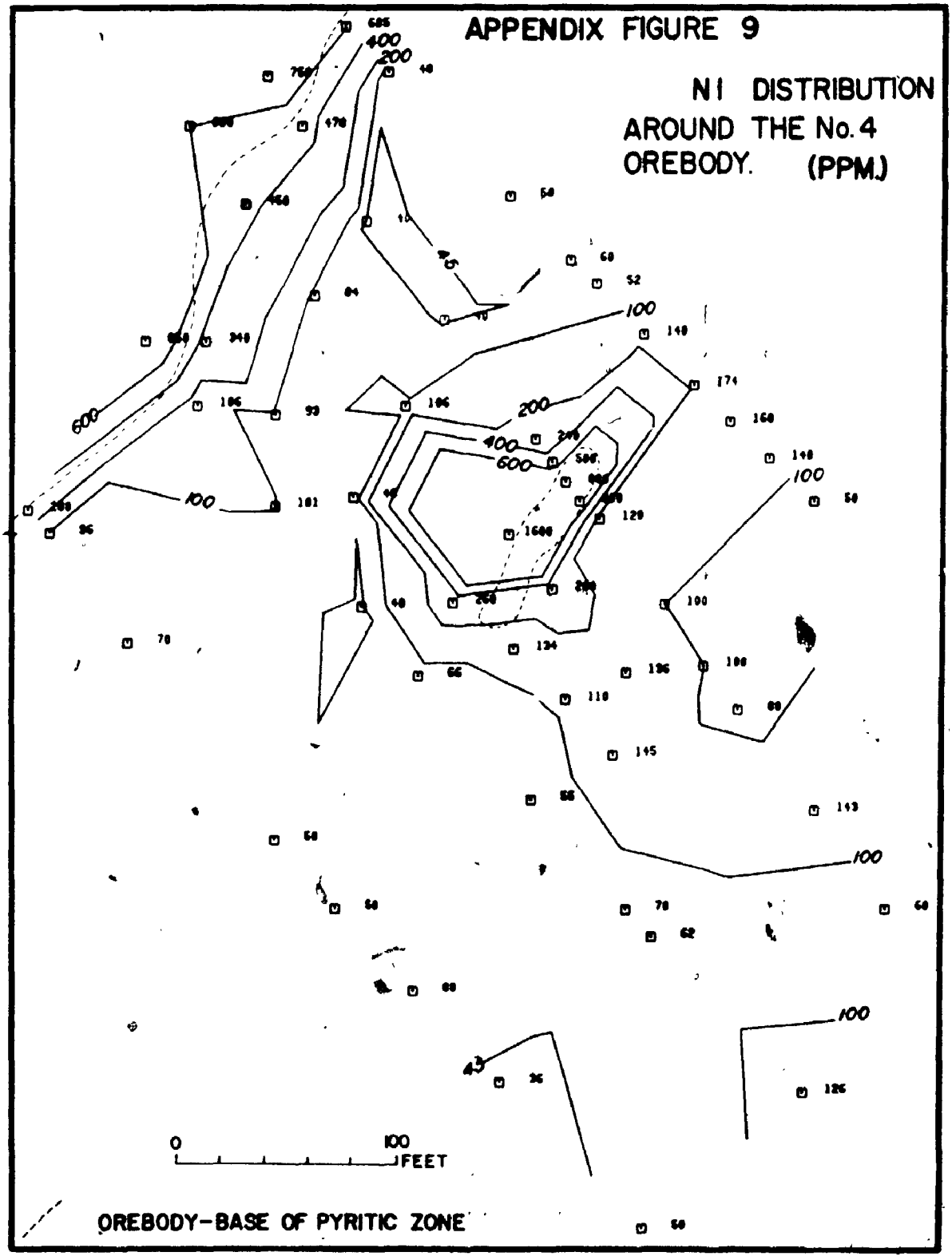
APPENDIX FIGURE 9
NI DISTRIBUTION AROUND THE No. 4 OREBODY. (PPM.)
100
200
400
600
0
100
FEET
OREBODY-BASE OF PYRITIC ZONE

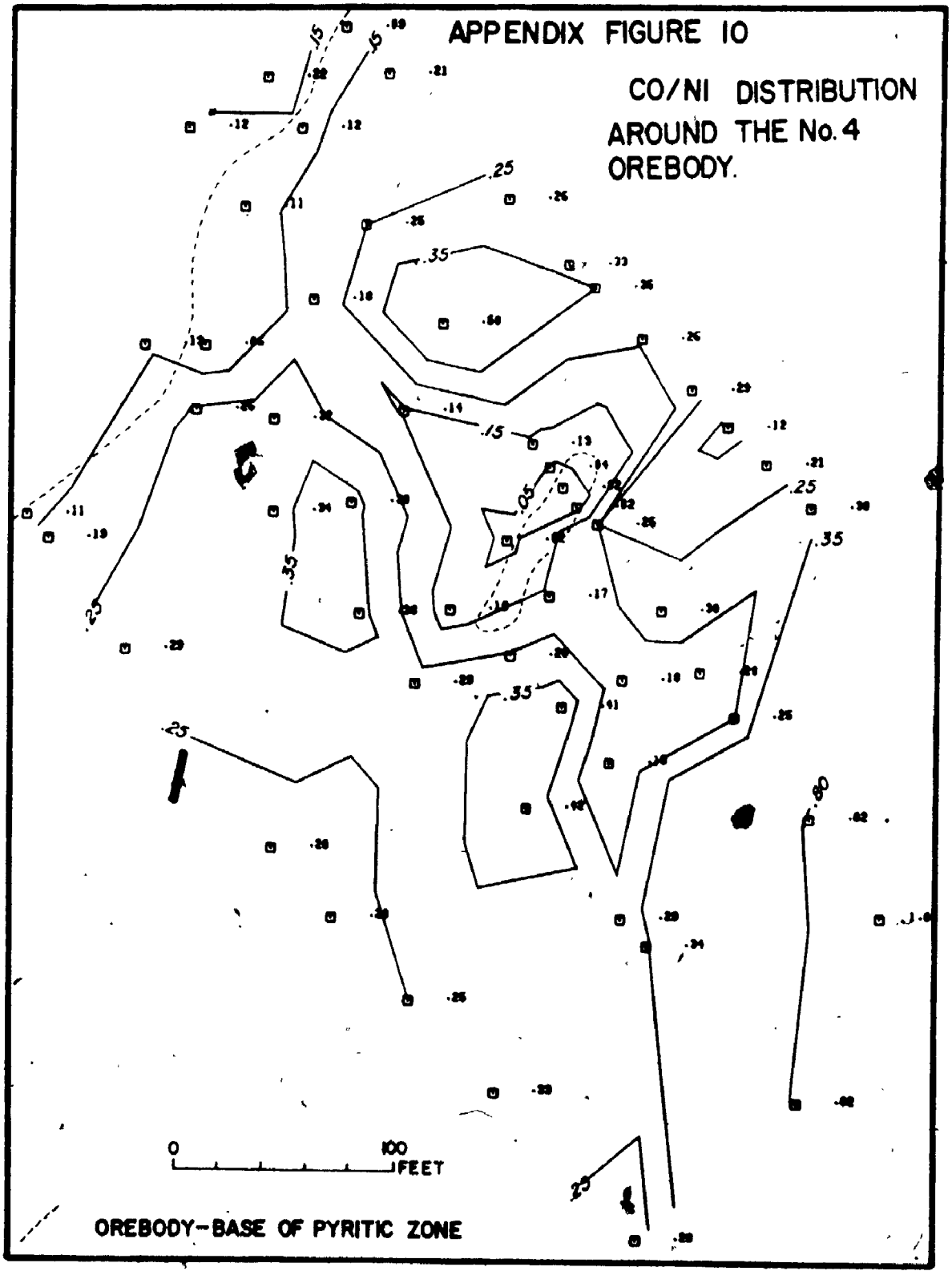
APPENDIX FIGURE 10
CO/NI DISTRIBUTION AROUND THE No. 4 OREBODY.
0
100
FEET
OREBODY-BASE OF PYRITIC ZONE

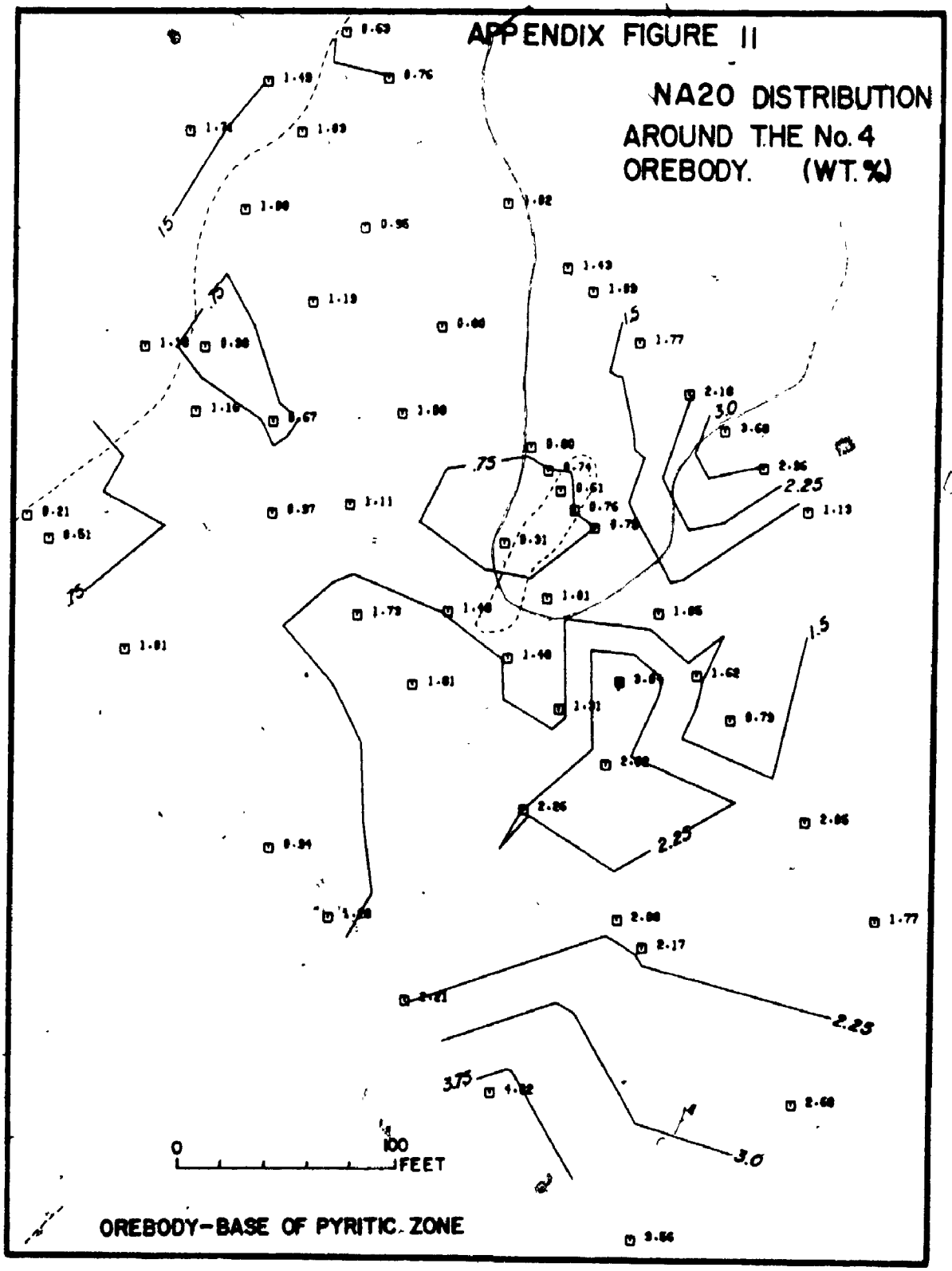
APPENDIX FIGURE 11
NA2O DISTRIBUTION AROUND THE No. 4 OREBODY. (WT.%)
0
100
FEET
OREBODY-BASE OF PYRITIC ZONE

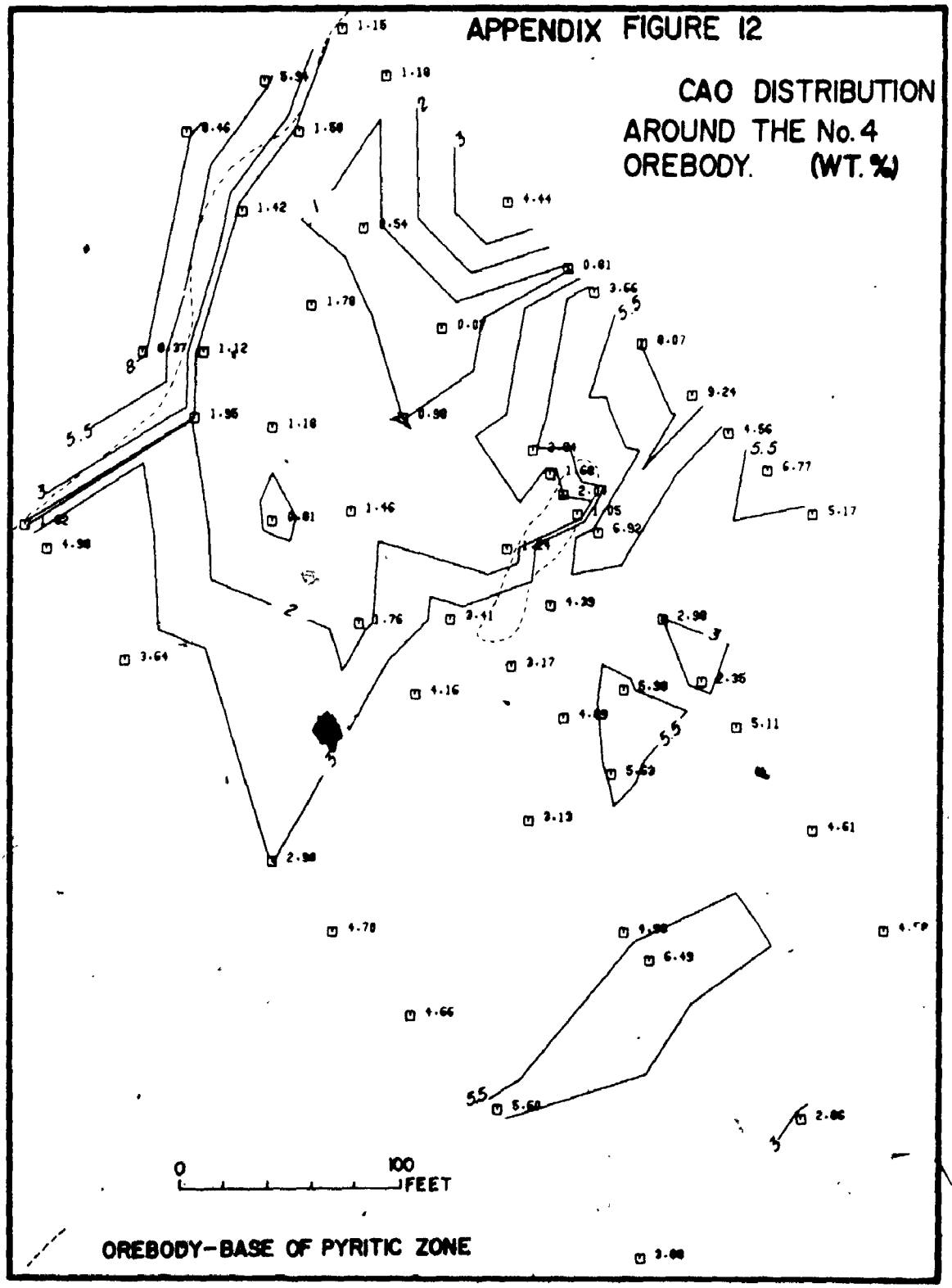
APPENDIX FIGURE 12
CAO DISTRIBUTION AROUND THE No. 4 OREBODY. (WT. %)
0
100
FEET
OREBODY-BASE OF PYRITIC ZONE

APPENDIX FIGURE 13

Na_2O+CaO vs SiO_2 SURFACE SAMPLES (wt%)

VOLCANIC AVERAGE JOIN

DOLERITE SAMPLES

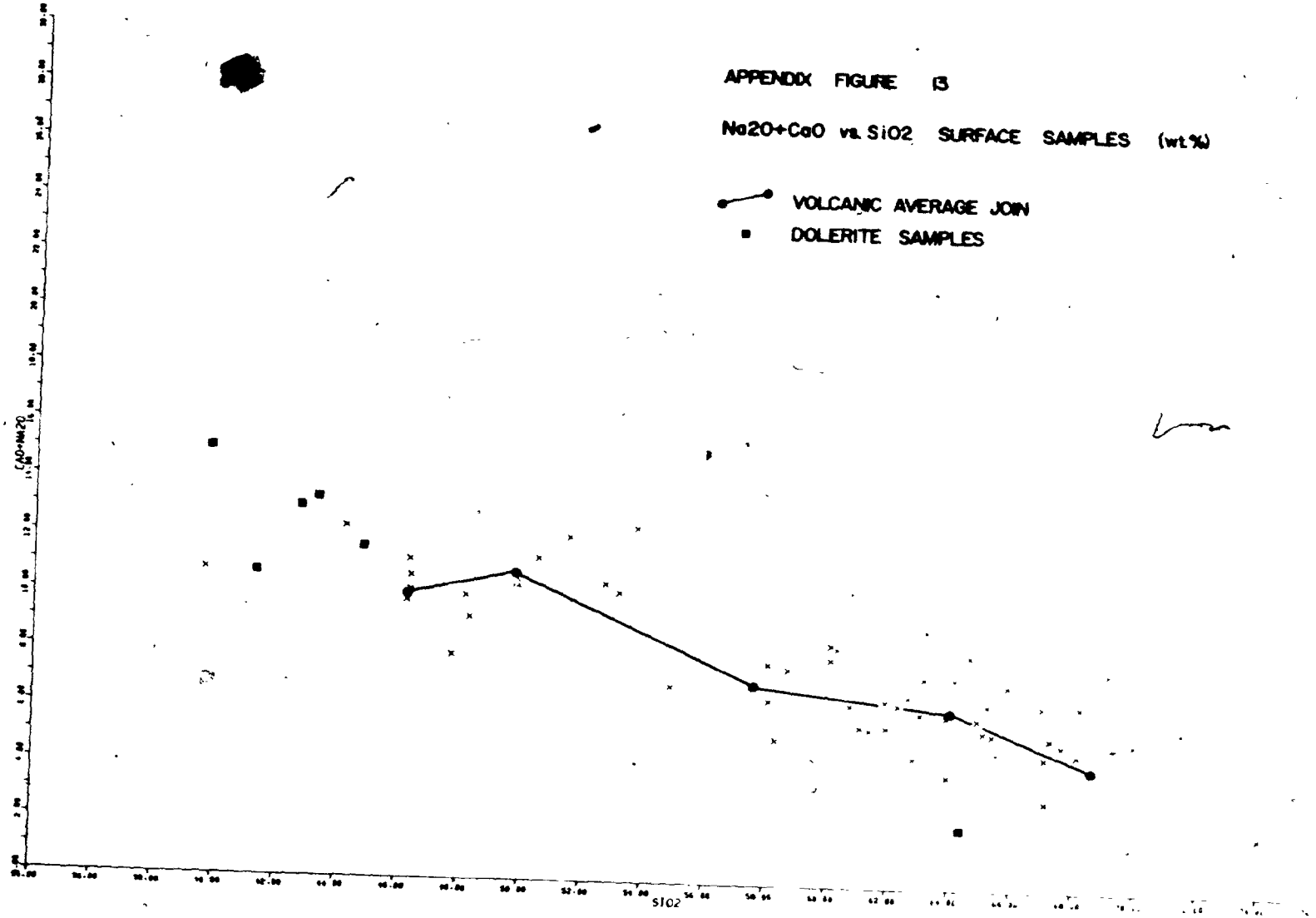

APPENDIX FIGURE 14

Na_2O+CoO vs. SiO_2 No.4 OREBODY SAMPLES (wt.%)

VOLCANIC AVERAGE JOIN (APP FIG 13)

DOLERITE SAMPLES

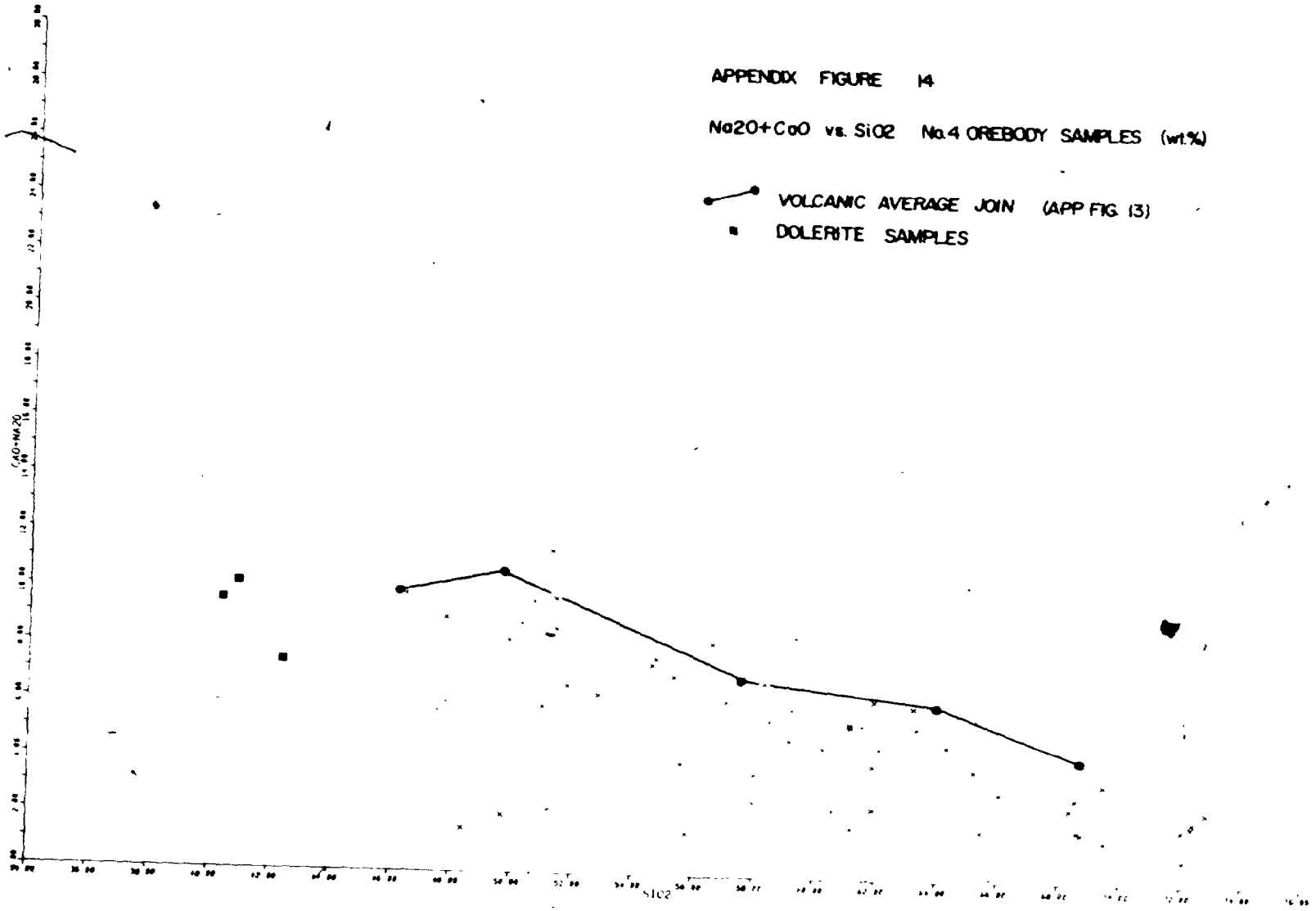

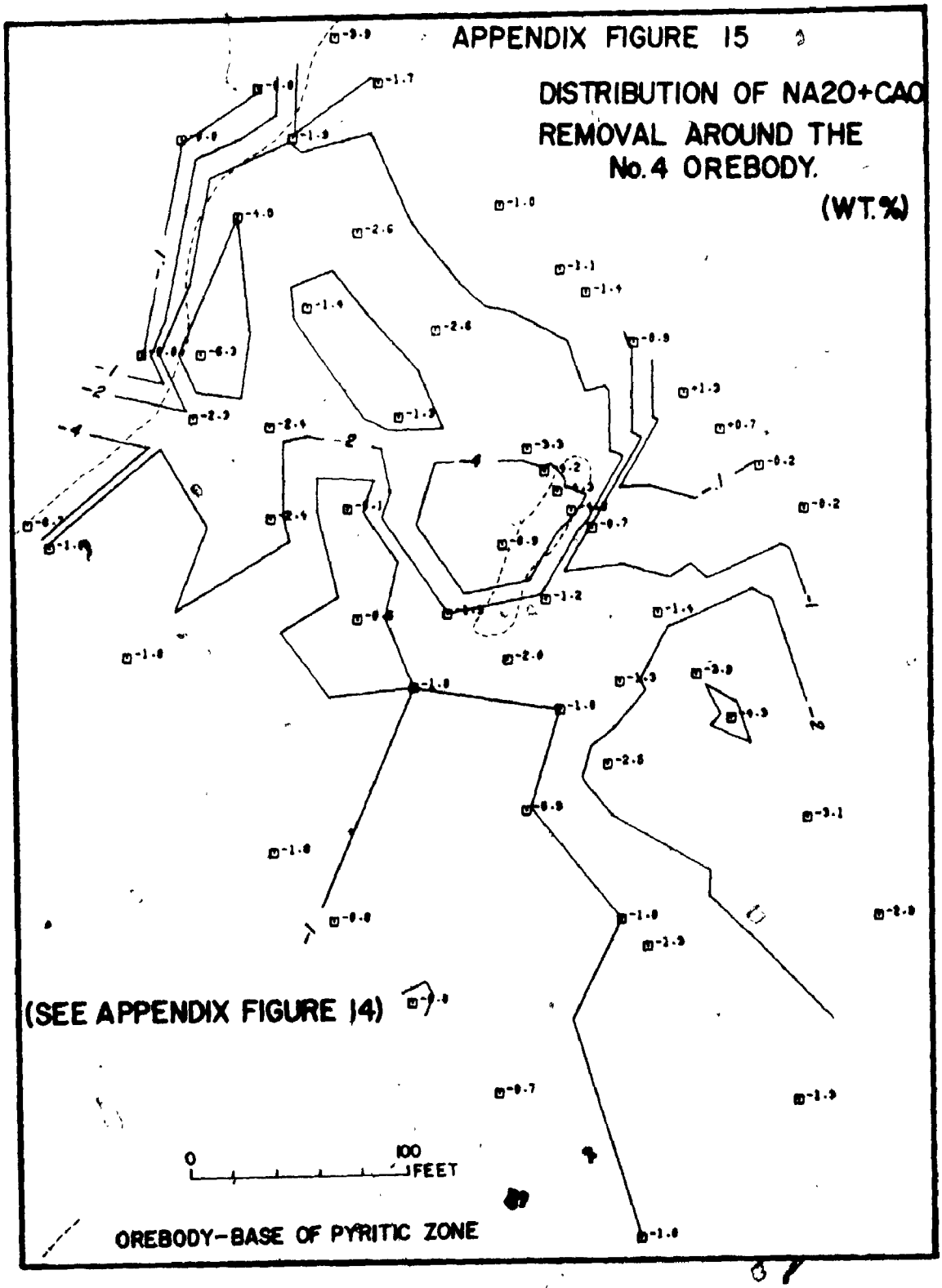
APPENDIX FIGURE 15
DISTRIBUTION OF NA2O+CAO REMOVAL AROUND THE No. 4 OREBODY.
(WT.%)
(SEE APPENDIX FIGURE 14)
0
100
FEET
OREBODY-BASE OF PYRITIC ZONE

APPENDIX FIGURE 16

SIO2 DISTRIBUTION AROUND THE No. 3 OREBODY. (WT.%)

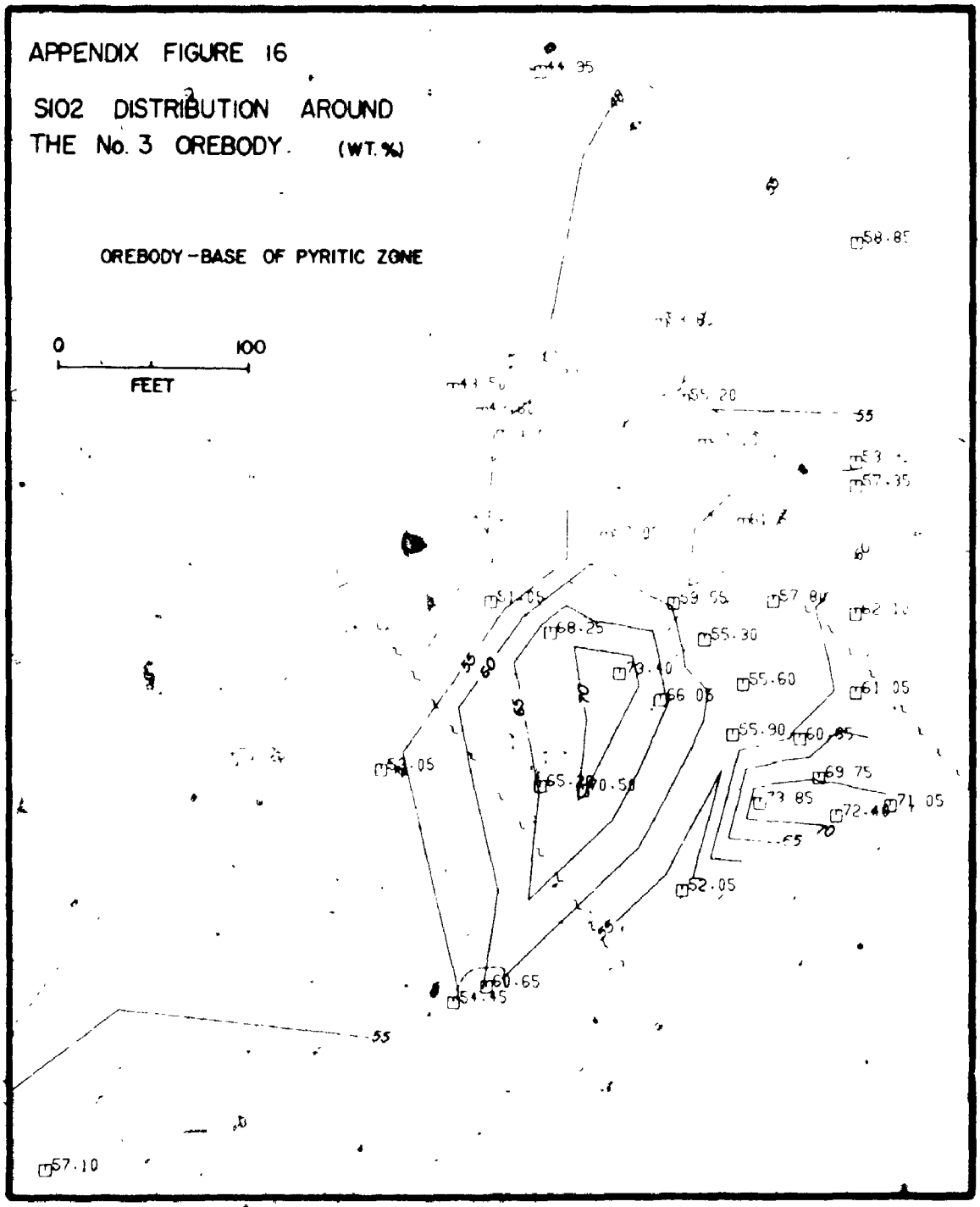

APPENDIX FIGURE 17

FEO / FE203 DISTRIBUTION AROUND THE No. 3 OREBODY

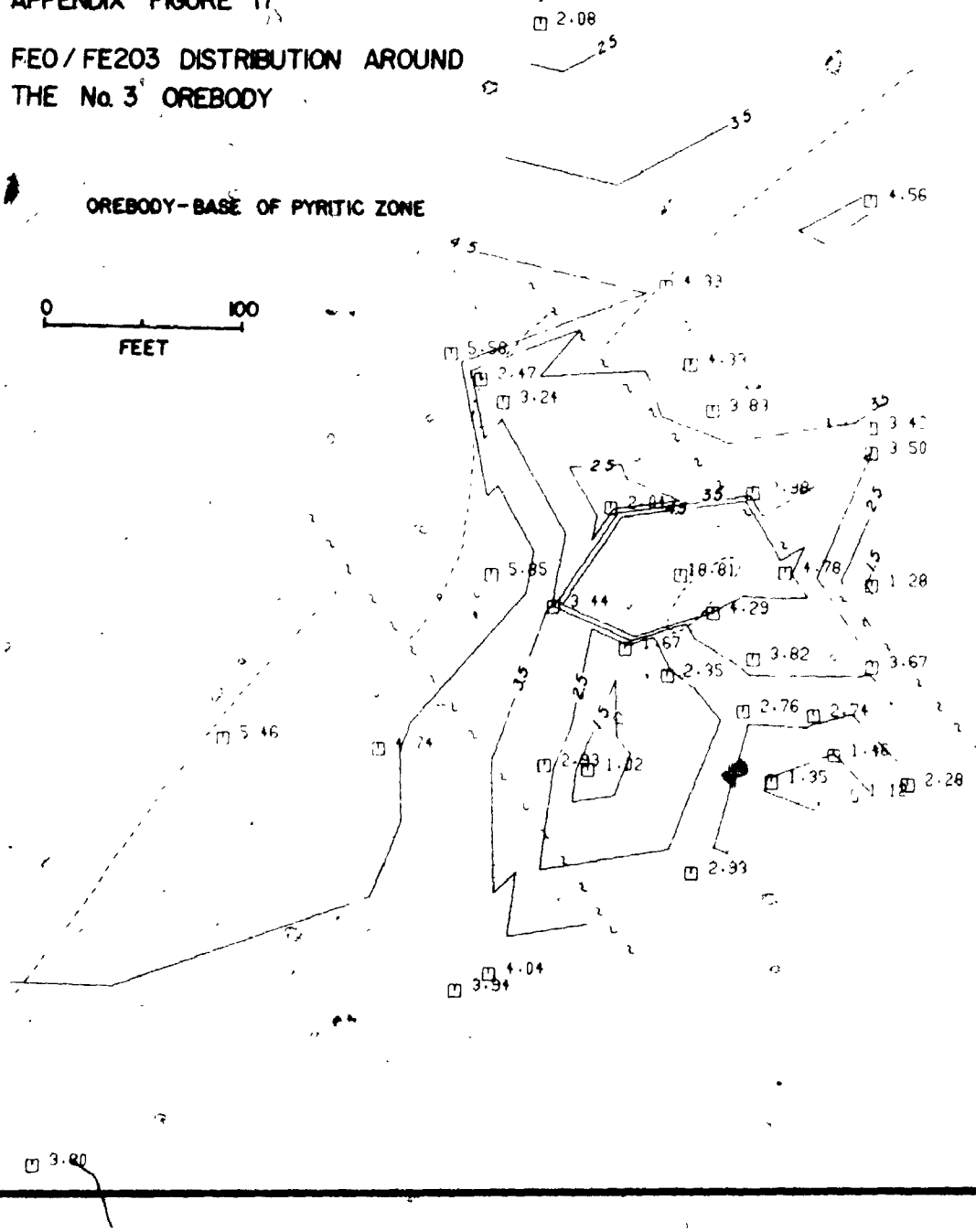

APPENDIX FIGURE 18

Na2O+CaO vs. SiO2 No3 OREBODY SAMPLES (wt%)

VOLCANIC AVERAGE JOIN (APP FIG 13)

DOLERITE SAMPLES

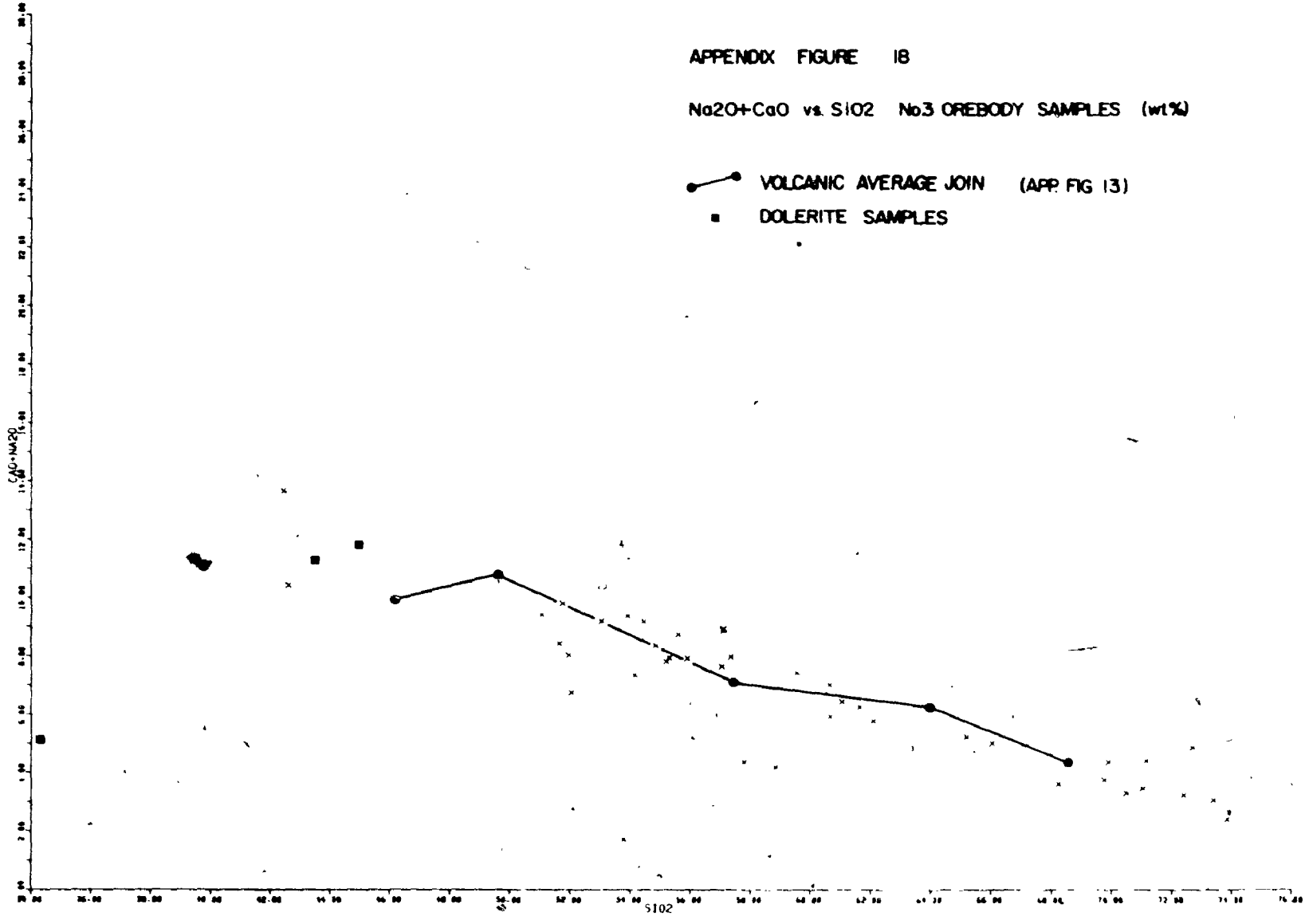

APPENDIX FIGURE 19

CO2 DISTRIBUTION AROUND THE No. 3 OREBODY (WT.%)

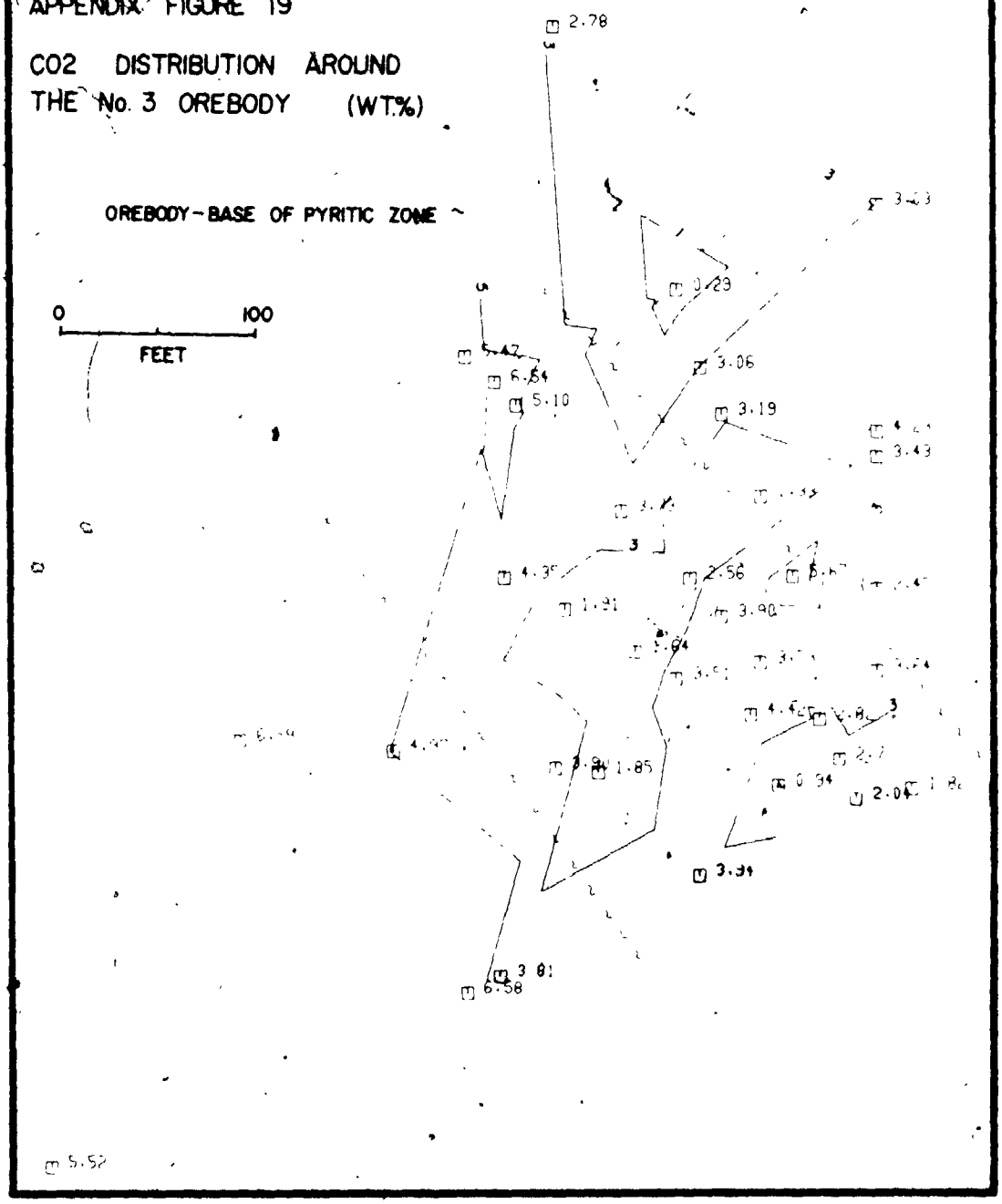

APPENDIX FIGURE 20

P205, DISTRIBUTION AROUND THE No. 3 OREBODY (WT.%)

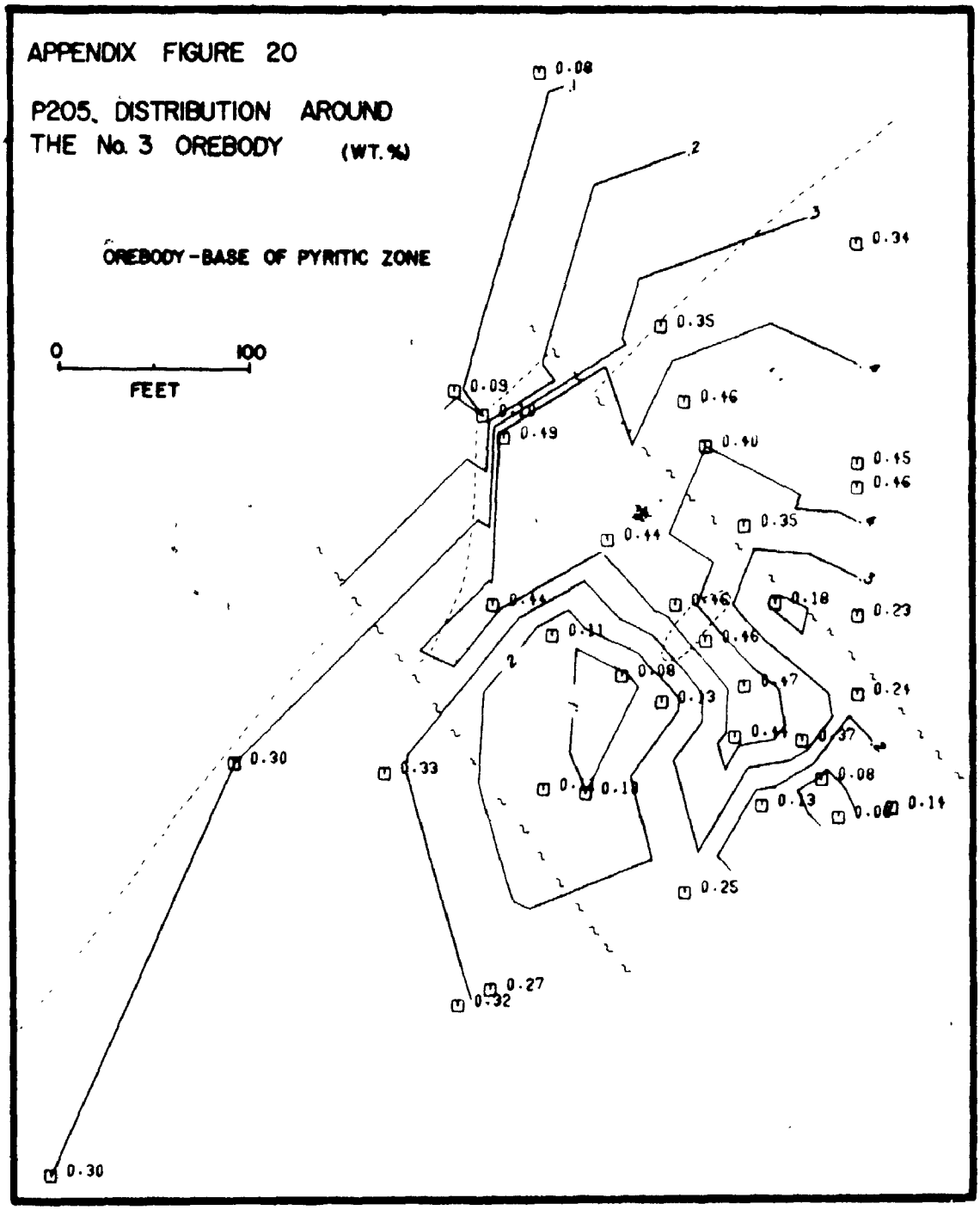

APPENDIX FIGURE 21

CU DISTRIBUTION AROUND THE No. 3 OREBODY (PPM.)

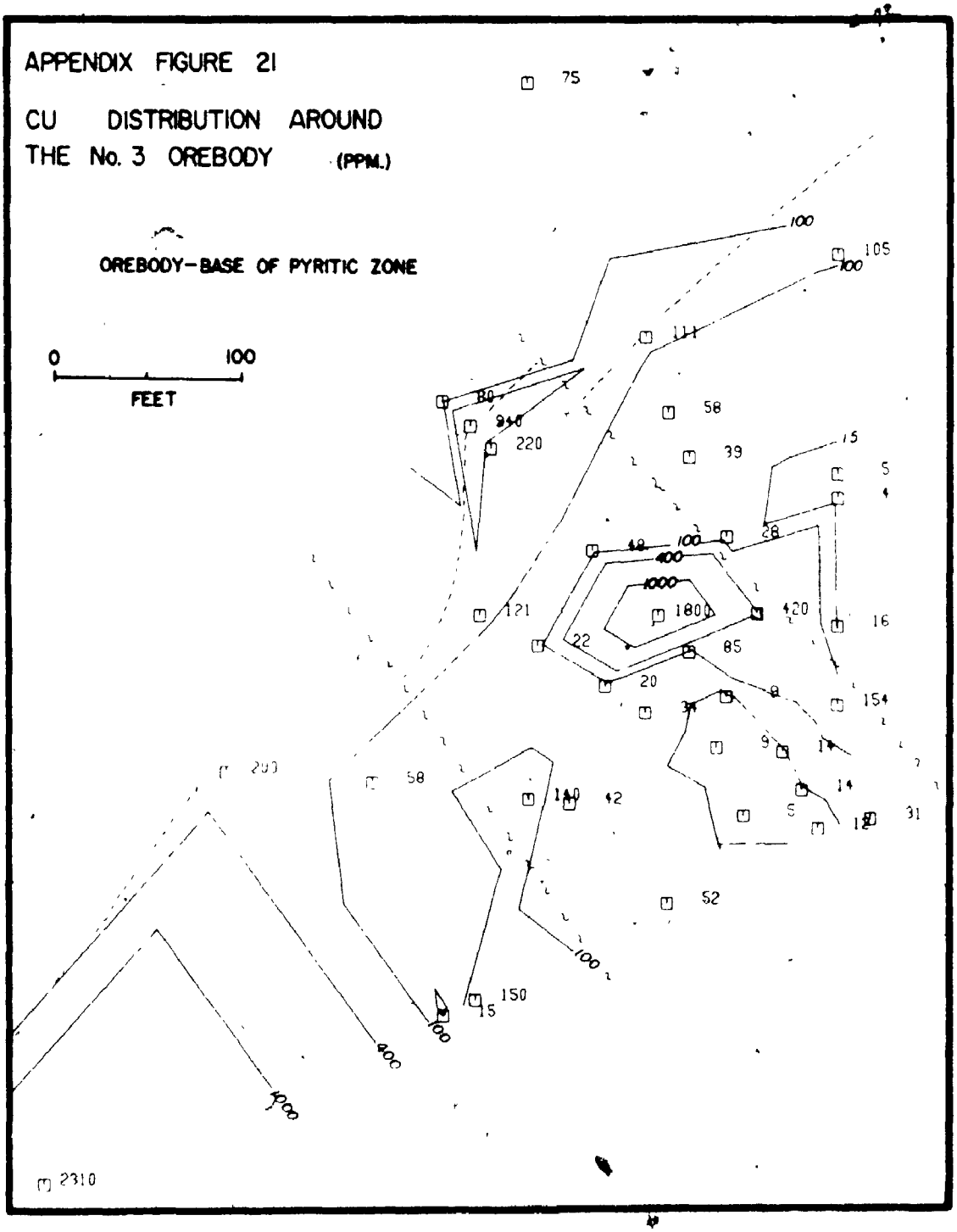

APPENDIX FIGURE 22

B DISTRIBUTION AROUND THE No. 3 OREBODY (PPM)

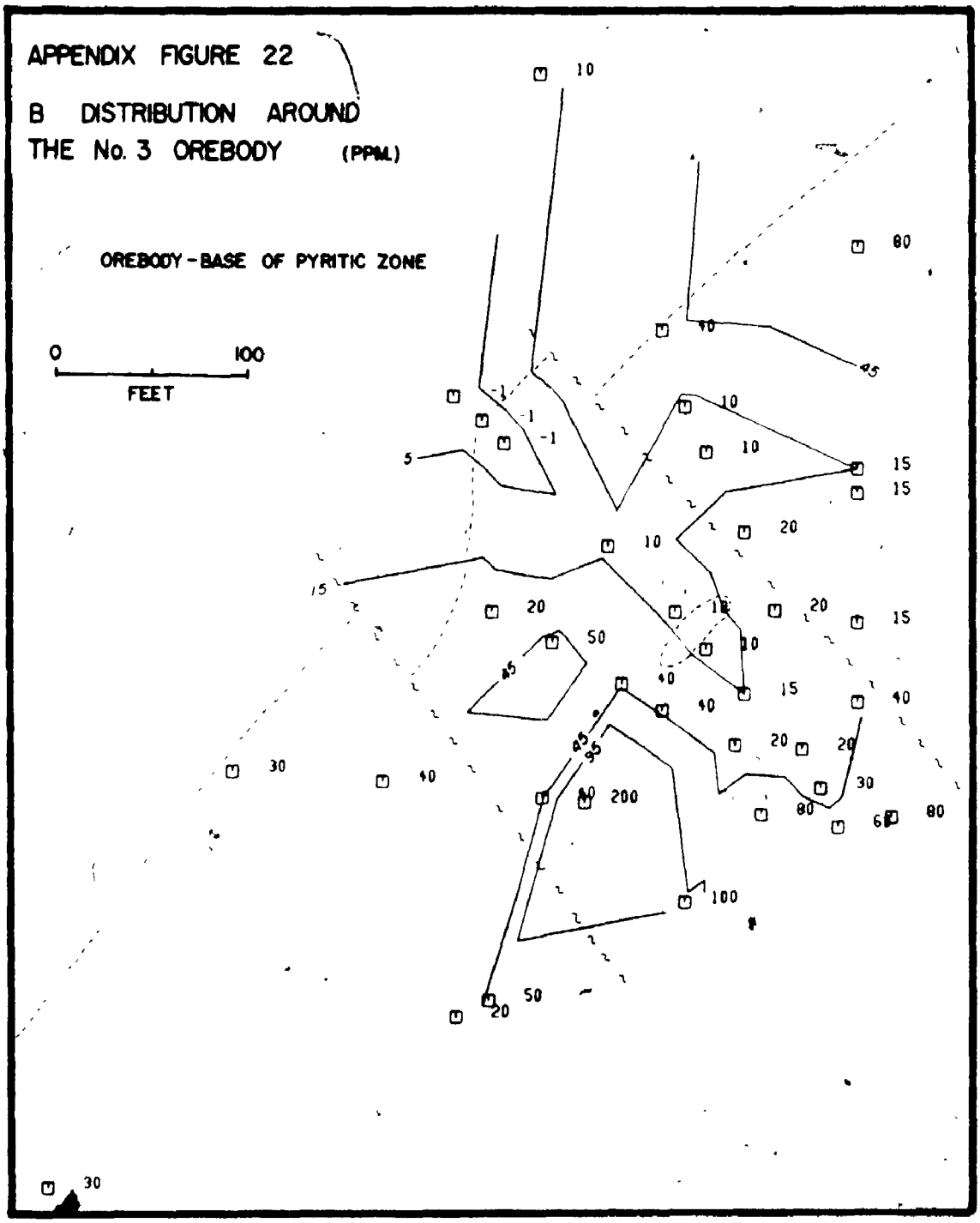

Sample Number	Equivalent Coding	Sample Number	Equivalent Coding	Sample Number	Equivalent Coding
E 1	1863	E22	1879	E50	1895
E 2	1864	E23	1880	E51	1896
E 3	1865	E24	1881	E52	1897
E 4	1866	E25	1882	E53	1898
E 5	1867	E30	1883	E54	1899
E 6	1868	E31	1884	E55	1900
E10	1869	E32	1885	E60	1901
E11	1870	E33	1886	E61	1902
E12	1871	E34	1887	E62	1903
E13	1872	E35	1888	E63	1904
E14	1873	E36	1889	E64	1905
E15	1874	E40	1890	E65	1906
E16	1875	E41	1891	48	1907
E17	1876	E42	1892	128	1908
E20	1877	E43	1893	188	1909
E21	1878	E44	1894		

APPENDIX V

Sulphur isotope data

Samples were selected from drill core through one pod-type and ore vein-type orebody and from the pyritic zone immediately adjacent to these. Only in three samples was sufficient separate of both pyrite and chalcopyrite obtained for analysis. Sample preparation and analytical techniques have been described previously (Schwarcz, 1973). Analyses were performed by H. Schwarcz at McMaster University.

	$S^{34}Py(^{o}/_{oo})$	$S^{34}Cp(^{o}/_{oo})$
Pod-Type:		
Lower	-1.21	-1.06
Upper		+0.15
Pyritic zone	+0.17	
Vein-Type:		
Lower	+1.84	+0.57
Upper	+0.67	+0.03
Pyritic zone	+0.59	

REFERENCES

Aumento, F. and Loubat, H. (1971). The Mid-Atlantic Ridge near 45°N. XVI. Serpentinized ultramafic intrusions. Can. J. Earth Sci., v. 8, p. 631-663.

Barker, H. and Schoell, M. (1972). New deeps with brines and metalliferous sediments in the Red Sea. Nature Phys. Sci., v. 240, p. 153-158.

Baragar, W. R. A. and Goodwin, A. M. (1969). Andesite and volcanism of the Canadian Shield. Oreg. Dept. Geol. Miner. Ind. Bull., v. 65, p. 121-141.

Barnes, W. L. and Czamanske, G. K. (1967). Solubilities and transport of ore minerals. In Geochemistry of hydrothermal ore deposits. H. L. Barnes, ed., p. 334-381. New York: Holt, Rinehart and Winston.

Barrett, D. L. and Aumento, F. (1970). The Mid-Atlantic Ridge near 45°N. XI. Seismic velocity, density and layering of the crust. Can. J. Earth Sci., v. 7, p. 1117-1124.

Barton, P. B. (1957). Some limitations on the possible composition of the ore-forming fluid. Econ. Geol., v. 52, p. 333-353.

_____, Bethke, P. M. and Toulmin, P. (1963). Equilibrium in ore deposits. Mineral. Soc. Amer. Spec. Paper 1, p. 171-185.

Bennett, G. (1970). Briggs and Strathcona Townships. Ont. Dept. of Mines Prelim. Geol. Maps P595, P596.

_____ (1971). Chambers and Strathy Townships. Ont. Dept. of Mines Prelim. Geol. Maps P666, P667.

Bergey, W. R., Clark, A. R., Frantz, J. C., Keevil, N. B. and Smith, F. G. (1957). Discovery of copper-nickel orebodies at the Temagami Mine, Ontario. Mining and case histories in mining geophysics, v. 4, p. 168-175.

Bilibin, Y. A. (1955). Metallogenic provinces and eras Gosgeoltekizdat, Moscow.

Björnsson, S., Arnorsson, S., Tamasson, J. (1970). Exploration of the Reykjanes brine area. Geothermics Spec. Issue 2, p. 1-25.

Bödvarsson, G. (1961). Physical characteristics of natural heat resources in Iceland. Jökull, v. 11, p. 29-38.

_____ and Lowell, R. P. (1972). On heat flow and the circulation of interstitial waters. J. Geophys. Res., v. 77, p. 4472-4475.

Boldy, J. (1968). Geological observations on the Delbridge massive sulphide deposits. CIM Bull., p. 1045-1052.

Boyum, B. H. and Hartviksen, R. E. (1970). General geology and ore grade control at Sherman Mine, Temagami, Ont. Mine Report, unpublished, Sherman Mine.

Browne, P. R. L. (1969). Sulfide mineralization in a Broadlands geothermal drill hole, Taupo volcanic zone, New Zealand. Econ. Geol., v. 64, p. 151-159.

_____ (1970). Hydrothermal alteration as an aid in investigating geothermal fields. Geothermics Spec. Issue 2, p. 564-570.

Browne, P. R. L. (1971). Mineralization in the Broadlands geothermal field, Taupo volcanic zone, New Zealand. Soc. Mining Geologists Japan Spec. Issue 2, p. 64-75.

_____ (1973). Geology, mineralogy and geothermometry of the Broadlands geothermal field, Taupo volcanic zone, New Zealand. Unpubl. Ph.D. thesis, Univ. of Wellington, N. Z.

_____ and Ellis, A. J. (1970). The Ohaki-Broadlands hydrothermal area, New Zealand: mineralogy and related geochemistry. Am. J. Sci., v. 269, p. 97-131.

_____ and Lovering, J. E. (1973). Composition of sphalerites from the Broadlands geothermal field and their significance to sphalerite geothermometry and geobarometry. Econ. Geol., v. 68, p. 381-387.

Buddington, A. F. (1935). High-temperature mineral association at shallow to moderate depths. Econ. Geol., v. 30, p. 205-222.

Cann, J. R. (1969). Spilites from the Carlsberg Ridge, Indian Ocean. J. Petrol., v. 10, p. 1-19.

_____ (1970). A new model for the structure of the ocean crust. Nature, v. 226, p. 928-930.

Chayes, F. (1964a). Alkaline and subalkaline basalts. Amer. J. Sci., v. 264, p. 128-145.

_____ (1964b). A petrographic distinction between Cenozoic volcanics in and around the open oceans. J. Geophys. Res., v. 69, p. 1573-1988.

_____ (1964c). Variance-covariance relations in some published harker diagrams of volcanic rock suites. J. Petrol., v. 5, p. 219-237.

Cloud, P. (1968). Atmospheric and hydrospheric evolution on the primitive earth. Science, v. 180, p. 729-736.

_____ (1972). A working model for the primitive earth. Am. J. Sci., v. 272, p. 537-548.

Coleman, R. G. (1971). Plate tectonic emplacement of Upper Mantle peridotites along continental edges. J. Geophys. Res., v. 76, p. 1212-1222.

Constantinou, G. and Govett, G. J. S. (1972). Genesis of sulphide deposits, ochre and umber of Cyprus. Trans. I.M.M./Sect. B, v. 81, p. B34-46.

Corliss, J. B. (1971). Origin of metal bearing hydrothermal solutions, J. Geophys. Res., v. 76, p. 8128-8138.

Deer, W. A., Howie, R. A. and Zussman, J. (1963). Rock forming minerals. Longmans, London.

Deffeyes, K. S. (1972). The axial valley: a steady state feature of the terrain. In Megatectonics of continents and oceans. Rutgers Univ. Press, p. 194-222.

Degens, E. T. and Ross, O. A. (1969). Hot brines and recent heavy metal deposits in the Red Sea. Springer-Verlag: Berlin-Heidelberg-New York.

Descarreaux, J. (1973). A petrochemical study of the Abitibi volcanic belt and its bearing on the occurrences of massive sulphide ores. C.I.M. Bull., v. 66, p. 61-69.

Dewey, J. F. and Bird, J. M. (1971). Origin and emplacement of the ophiolite suite: Appalachian ophiolites in Newfoundland. J. Geophys. Res., v. 26, p. 3179-3206.

Elder, J. W. (1965). Physical processes in geothermal areas. Am. Geophys. Union Geophys. Mon., v. 8, p. 211-239.

Engel, A. J., Engel, C. G. and Havens, R. G. (1965). Chemical characteristics of oceanic basalts and the upper mantle. Bull. Geol. Soc. Amer., v. 67, p. 719-734.

Fahrig, W. F., Gaucher, E. H. and Larochelle, A. (1965). Paleomagnetism of diabase dykes of the Canadian shield. Can. Jour. Earth Sci., v. 2, p. 278-298.

Franklin, J. McW. (1967). The pyrite zone of the Temagami mine of Copperfields Mining Company, Timagami, Ontario. M.Sc. thesis, unpubl., Carleton Univ.

Gass, I. G. (1968). Is the Troodos massif of Cyprus a fragment of Mesozoic ocean floor? Nature, v. 220, p. 39-42.

Gates, T. M. and Hurley, P. M. (1973). Evaluation of Rb-Sr dating methods applied to the Matachewan, Abitibi, Mackenzie and Sudbury dike swarms in Canada. Can. J. Earth Sci., v. 10, p. 900-919.

Gilmour, P. (1971). Strata-bound massive sulphide deposits - a review. Econ. Geol., v. 66, p. 1239-1244.

Glikson, A. Y. (1972). Early Precambrian evidence of a primitive ocean crust and island nuclei of sodic granite. Bull. Geol. Soc. Am., v. 83, p. 3323-3344.

Goodwin, A. M. (1968). Archean protocontinental growth and early crustal history of the Canadian shield. XXIII International Geol. Congress, v. 1, p. 69-89.

_____ and Ridler, R. H. (1971). The Abitibi orogenic belt. In Symposium on precambrian basins and geosynclines. Geol. Surv. Can. Paper 70-40.

Govett, G. J. S. and Pantazio, T. M. (1971). Distribution of Cu, Zn, Ni and Co in the Troodos pillow lava series, Cyprus. Trans. I.M.M./ Sect. B, v. 80, p. B27-46.

Grant, J. A. (1964). The geology of the Vogt-Hobbs area. Ont. Dept. of Mines Geol. Rept. 22.

Gruner, J. W. (1942). Conditfons for the formation of paragonite. Am. Mineral., v. 27, p. 131.

Hawley, J. E. (1962). The Sudbury ores: their mineralogy and origin. Can. Mineral., v. 7, pt. 1.

_____ and Nichol, I. (1961). Trace elements in pyrite, pyrrhotite and chalcopyrite of different ores. Econ. Geol., v. 56, p. 467-487.

Helgeson, H. C. (1964). Complexing and hydrothermal ore deposition. New York: Pergamon Press.

_____ (1968a). Evaluation of irreversible reactions in geochemical processes involving minerals and aqueous solutions. I. Thermodynamic relations. Geochim. et Cosmochim. Acta, v. 32, p. 853-877.

_____ (1968b). Geologic and thermodynamic characteristics of the Salton Sea geothermal system. Am. J. Sci., v. 266, p. 129-166.

_____ (1969). Thermodynamics of hydrothermal systems at elevated temperatures and pressures. Am. J. Sci., v. 267, p. 729-804.

_____ (1970). A chemical and thermodynamic model of ore deposition in hydrothermal systems. Mineral. Soc. Amer. Spec. Paper 3, p. 155-186.

Hewitt, D. F., Fleischer, M. and Conklin, N. (1963). Deposits of the manganese oxides, supplement. Econ. Geol., v. 58, p. 1-51.

Holland, H. D. (1967). Gangue minerals in hydrothermal systems. In Geochemistry of hydrothermal ore deposits. H. L. Barnes, ed., p. 382-436. New York: Holt, Rinehart and Winston.

_____ (1972). The geologic history of sea water - an attempt to solve the problem. Geochim. et Cosmochim. Acta, v. 36, p. 637-651.

Honda, S. and Muffler, L. J. P. (1970). Hydrothermal alteration in core from research drill hole Y1, Upper Geyser basin, Yellowstone National Park, Wyoming. Amer. Mineral., v. 55, p. 1714-1737.

Horikoshi, E. and Sato, T. (1970). Volcanic activity and ore deposition in the Kosaka Mine. In Volcanism and ore genesis. T. Tatsumi, ed., p. 181-195. Tokyo: Univ. Tokyo Press.

Hutchinson, R. W. and Searle, D. L. (1971). Stratabound pyrite deposits in Cyprus and relations to other sulphide ores. Soc. Mining Geologists Japan, Spec. Issue 3, p. 198-205.

_____ and Hodder, R. W. (1971). Possible tectonic and metallogenic relationships between porphyry copper and massive sulphide deposits. CIMM Bull., v. 85, p. 34-40.

_____, Ridler, R. H. and Suffel, G. G. (1971). Metallogenic relationships in the Abitibi belt, Canada. A model for Archean metallogeny. CIMM Bull., v. 74, p. 106-115.

Hyndman, D. W. (1972). Petrology of igneous and metamorphic rocks. McGraw-Hill, New York.

Hyndman, R. D. and Rankin, D. S. (1972). The Mid-Atlantic ridge near 45°N. XVIII. Heat flow measurements. Can. J. Earth Sci., v. 9, p. 664-678.

Irvine, T. N. and Baragar, W. R. A. (1971). A guide to chemical classification of the common volcanic rocks. Can. J. Earth Sci., v. 8, p. 523-548.

Jensen, M. L. (1967). Sulphur isotope and mineral genesis. In Geochemistry of hydrothermal ore deposits. H. L. Barnes, ed. New York: Holt, Rinehart and Winston.

_____ and Nakai, N. (1963). Sulphur isotope meteorite standards results and recommendations in biogeochemistry of sulphur isotopes. Proc. of a Nat'l. Sci. Found. Symp., Yale Univ., p. 30-35.

Johnson, A. E. (1970). Textural and geochemical investigations of Cyprus pyrite deposits. Unpubl. Ph.D. thesis, Univ. Western Ontario.

Johnston, W. G. Q. (1954). Geology of the Temiskaming-Grenville contact southeast of Lake Temagami, northern Ontario, Canada. Bull. Geol. Soc. Am., v. 65, p. 1047-1074.

Jolly, W. T. (1972). Degradation (hydration)-aggradation (dehydration) and low rank metamorphism of mafic sequences. 24th Int. Geol. Congress Sect. 2, p. 11-18.

_____ and Smith, R. E. (1972). Degradation and metamorphic differentiation of the Keweenawan tholeiitic lavas of northern Michigan. J. Petrol., v. 13, p. 273-309.

Kajiwara, Y. (1970). Syngenetic features of the Kuroko ore from the Shakanai Mine. In Volcanism and ore genesis. T. Tatsumi, ed., p. 197-206. Tokyo: Univ. Tokyo Press.

_____ and Krouse, H. R. (1971). Sulfur isotope partitioning in metallic sulphide systems. Can. J. Earth Sci., v. 8, p. 1397-1408.

Krauskopf, K. B. (1967). Source rocks for metal-bearing fluids. In Geochemistry of hydrothermal ore deposits. H. L. Barnes, ed. New York: Holt, Rinehart and Winston.

Kuno, H. (1967). Differentiation of basaltic magmas. In Basalts. H. H. Hess and A. Poldervaart, eds., v. 2, p. 623-688. Interscience, J. Wiley and Son, New York.

Lebedev, L. M. (1968). Modern growth of sphalerite. Dokl. Akad. Nauk SSSR, v. 174, p. 173-176.

Lindgren, W. (1933). Mineral deposits. McGraw-Hill, New York.

Lister, C. R. B. (1972). On the thermal balance of a mid-ocean ridge. Geophys. J. R. Astr. Soc., v. 26, p. 515-535.

Loftus-Hills, G. and Solomon, M. (1967). Cobalt, nickel and selenium in Sulphides as indicators of ore genesis. Mineralium Deposita, v. 2, p. 228-242.

Lovell, H. L. (1970). Kirkland Lake district. In Ont. Dept. of Mines Misc. Paper 46. G. R. Guillet, ed.

Lowell, J. D. and Guilbert, J. M. (1970). Lateral and vertical alteration-mineralization zoning in porphyry ore deposits. Econ. Geol., v. 65, p. 373-408.

McDonald, G. A. (1968). Composition and origin of Hawaiian lavas. Geol. Soc. Amer. Mem. 116, p. 477-522.

Mahon, W. A. J. (1962). The carbon dioxide and hydrogen sulphide content of steam from drillholes at Wairakei, New Zealand. N. Z. J. Sci., v. 5, p. 85-98.

Manson, V. (1967). Geochemistry of basaltic rocks: major elements. In Basalts. H. H. Hess and A. Poldervaart, eds., v. 1, p. 215-269. Interscience, J. Wiley and Son, New York.

Matsukuma, T. and Horikoshi, E. (1970). Kuroko deposits in Japan, a review. In Volcanism and ore genesis. T. Tatsumi, ed., p. 153-180. Tokyo: Univ. Tokyo Press.

Melson, W. G. and Van Andel, Tj. H. (1966). Metamorphism in the mid-Atlantic ridge, 22°N latitude. Marine Geol., v. 4, p. 165-186.

_____, Thompson, G. and Van Andel, Tj. H. (1968). Metamorphism in the mid-Atlantic ridge, 22°N latitude. J. Geophys. Res., v. 73, p. 5925-5941.

Meyer, C. and Hemley, J. J. (1967). Wallrock alteration. In Geochemistry of hydrothermal ore deposits. H. L. Barnes, ed., p. 166-235. New York: Holt, Rinehart and Winston.

Miyashiro, A., Shido, F. and Ewing, M. (1971). Metamorphism in the mid-Atlantic ridge near 24°N and 30°N. Phil. Trans. Roy. Soc. London Ser. A, v. 268, p. 589-603.

Moorhouse, W. W. (1942). Northeastern portion of the Temagami Lake area. Ont. Dept. of Mines Ann. Rept., v. 51, pt. 6.

Muehlenbacks, K. and Clayton, R. N. (1972). Oxygen isotope geochemistry of submarine greenstones. Can. J. Earth Sci., v. 9, p. 471-478.

Muffler, L. J. P. and White, D. E. (1969). Active metamorphism of upper Cenozoic sediments in the Salton Sea geothermal field and the Salton trough, southeastern California. Bull. Geol. Soc. Amer., v. 80, p. 157-182.

Nockolds, S. R. (1954). Average chemical compositions of some igneous rocks. Bull. Geol. Soc. Amer., v. 65, p. 1007-1032.

Ohmoto, H. (1972). Systematics of sulfur and carbon isotopes in hydrothermal ore deposits. Econ. Geol., v. 67, p. 551-578.

Palmason, G. (1967). On heat flow in Iceland in relation to the mid-Atlantic Ridge. In Iceland and mid-ocean ridges. S. Bjornsson, ed., v. 38, p. 111-127. Soc. Sci. Icelandica.

Park, C. F. jr. and MacDiarmid, R. A. (1970). Ore deposits. San Francisco, W. H. Freeman.

Patrick, T. O. H. (1966). Temagami chalcopyrite: syngenetic or hydrothermal. Unpubl. mine report.

Peacock, M. A. (1931). Classification of igneous rocks. J. Geol., v. 39, p. 54-67.

Pearce, T. H. (1968). A contribution to the theory of variation diagrams. Contr. Mineral. and Petrol., v. 19, p. 142-157.

Ridge, J. D. (1973). Volcanic exhalations and ore deposition in the vicinity of the sea floor. Mineralium Deposita, v. 8, p. 332-348.

Roberts, R. G. (1966). Geology of the Mattagami Lake mine, Galinee township, Quebec. Unpubl. Ph.D. thesis, McGill Univ.

Rosen-Spence, A. (1969). Genese des roches a cordierite-anthophyllite des gisements cupro-zinciferes de la region de Rouyn-Noranda, Quebec, Canada. Can. J. Earth Sci., v. 6, p. 1339-1345.

Roedder, E. (1967). Fluid inclusion as samples of ore fluids. In Geochemistry of hydrothermal ore deposits. H. L. Barnes, ed. New York: Holt, Rinehart and Winston.

Roscoe, S. M. (1965). Geochemical and isotopic studies, Noranda and Mattagami areas. CIMM Bull., v. 58, p. 965-971.

Rose, E. R. (1966a). The copper-nickel deposits of Timagami Island, Ontario. Econ. Geol., v. 61, p. 27-43.

Rose, E. R. (1966b). Pyrite nodules of the Temagami copper-nickel deposit. Can. Mineral., p. 317-324.

Sakrison, H. C. (1966). Chemical studies of the host rocks of the Lake Dufault Mine, Quebec. Unpubl. Ph.D. thesis, McGill Univ.

Sato, T. (1972). Behaviour of ore-forming solutions in sea water. Mining Geol., v. 22, p. 31-42.

Schwarcz, H. P. (1973). Sulfur isotope analyses of some Sudbury, Ontario, ores. Can. J. Earth Sci., v. 10, p. 1444-1459.

Scott, S. A. (1969). Trace element study of sulphides from the Temagami Mine, Ontario. Unpubl. M.Sc. thesis, McGill Univ.

Searle, D. L. (1972). Mode of occurrence of the cupriferous pyrite deposits of Cyprus. Trans. I.M.M./Sect. B., v. 81, p. B189-197.

Sharpe, J. I. (1967). Metallographic portrait of the Noranda area. CIM Centennial Field Excursion, Northwestern Quebec and Northern Ontario, p. 62-63.

Sigvaldason, G. E. (1962). Epidote and related minerals in two deep geothermal drill holes, Reykjavik and Hveragendi, Iceland. U. S. Geol. Surv. Profess. Papers 450-E, p. 77-79.

Sillitoe, R. H. and Sawkins, F. J. (1971). Geologic, mineralogic and fluid inclusion studies relating to the origin of copper-bearing tourmaline breccia pipes, Chile. Econ. Geol., v. 66, p. 1028-1041.

Simmons, B. D. (1973). Geology of the Millenbach massive sulphide deposit Noranda, Quebec, Canada. Presented 75th Ann. General Meeting of the CIM, Vancouver, B. C.

Simony, P. S. (1964). Geology of northwestern Temagami area. Ont. Dept. of Mines Geol. Rept. 28.

Smith, F. G. (1957). Copper-nickel mineralization at Lake Temagami. Unpubl. Mine Report.

Smith, R. E. (1968). Redistribution of major elements in the alteration of some basic lavas during burial metamorphism. J. Petrol., v. 9, p. 191-219.

Spence, C. D. (1967). The Noranda area. In CIM Centennial Field Excursion, Northwestern Quebec and Northern Ontario, p. 36-39.

Spooner, E. T. C. and Fyfe, W. S. (1973). Sub sea floor metamorphism. Contr. Mineral. and Petrol., v. 43, p. 287-304.

_____, Beckinsdale, R. D., Fyfe, W. S. and Smewing, J. D. (in press). ^{18}O enriched ophiolitic metabasic rocks from E. Ligura (Italy), Pindo (Greece) and Troodos (Cyprus).

Stanton, R. L. (1972). Ore petrology. McGraw Hill, New York.

Talwani, M., Windish, C. C. and Langseth, M. G. Jr. (1971). Reykjanes ridge crest: a detailed physical study. J. Geophys. Res., v. 76, p. 473-517.

Thompson, G. and Melson, W. G. (1970). Boron contents of serpentinites and metabasalts in oceanic crust: implication for the boron cycle in the oceans. Earth and Planetary Sci. Letters, v. 8, p. 61-65.

Tomasson, J. and Kristmannsdottir, H. (1972). High temperature alteration minerals and thermal brines, Reykjanes, Iceland. Cont. to Mineral. and Petrol., v. 36, p. 123-134.

Turner, F. J. (1958). Mineral assemblages of individual metamorphic facies. In Metamorphic reactions and metamorphic facies. W. S. Fyfe, F. J. Turner and J. Verhoogen. Geol. Soc. Am. Mem. 73, p. 199-237.

Turner, F. J. and Verhoogen, J. (1960). Igneous and metamorphic petrology. McGraw Hill, New York.

Vallance, T. G. (1960). Concerning spilites. Proc. Linn. Soc. New South Wales, v. 85, p. 8-52.

Wass, S. Y. (1973). Plagioclase-spinel intergrowths in alkali basaltic rocks from the southern highlands, N.S.W. Contr. Mineral. and Petrol., v. 38, p. 167-175.

White, D. E. and Waring, G. A. (1963). Data of geochemistry. 6th ed. Chap. II. Volcanic emanations. U. S. Geol. Surv. Prof. Paper 440K, p. 29.

Wilson, H. D. B., Andrews, P., Moxham, R. L. and Ramlal, K. (1965). Archean volcanism of the Canadian Shield. Can. J. Earth Sci., v. 2, p. 161-175.

Zen, E-an and Thompson, A. B. (in press). Annual review of earth and planetary science. F. A. Donath, ed., v. 2.